UNIVERSITÈ DE MONTREAL

FACULTÈ DES ÈTUDES SUPÈRIEURES

Cette thèse intitulèe :

<< Physiological model based determination of the interspecies toxicokinetic uncertainty factors for organic chemicals >>

présentée par

Michael Pelekis

a été évaluée par un jury composé des personnes suivantes:

Jules Brodeur, président-rapporteur

Kannan Krishnan, directeur de recherche

Robert Tardif, membre du jury

Laurie Chan, examinateur externe

Thése acceptée le: 28 mai 1998

SOMMAIRE

L'objectif général de cette thèse est d'estimer pour des substances organiques le facteur d'incertitude animal-humain relatif à la toxicocinétique ($UF_{AH\text{-}TK}$) sur la base des mécanismes biologiques, ceci en utilisant une approche de modélisation à base physiologique. En premier lieu, le $UF_{AH\text{-}TK}$ sera estimé à partir d'un modèle toxicocinétique à base physiologique (PBTK) développé chez le rat et l'humain, ceci pour un pesticide de la famille des carbamates: l'aldicarb (ALD). Par la suite, cette méthodologie sera appliquée pour estimer le $UF_{AH\text{-}TK}$ d'autres substances chimiques. Subséquemment, le modèle PBTK sera simplifié en des expressions algébriques pour ainsi identifier les facteurs mécanistiques qui influencent le $UF_{AH\text{-}TK}$ lorsque l'état d'équilibre est atteint dans l'organisme.

Cette thèse comprend quatre chapitres. Le chapitre 1 présente les différentes théories et les méthodologies utilisées pour déterminer le $UF_{AH\text{-}TK}$ lors de l'analyse d'un risque toxicologique. Dans ce cas, on y discutera de la démarche de l'analyse du risque toxicologique des substances non cancérigènes et de la façon conventionnelle de déterminer le $UF_{AH\text{-}TK}$. Ensuite, les défauts de cette approche conventionnelle seront discutés en détail. A la fin du chapitre 1, on discute de la modélisation à base physiologique et de ses applications scientifiques, plus particulièrement son application en toxicologie pour l'estimation des facteurs d'incertitude.

Dans le chapitre 2, on retrouve trois publications dans lesquelles on traite de l'utilisation des modèles physiologiques pour déterminer le UF_{AH-TK}. Dans la première publication, on démontre une nouvelle façon de conceptualiser un modèle PBTK dans le but de permettre la prédiction des coefficients de partage tissu:sang lors des simulations. En se basant sur une récente étude, les compartiments (tissus) d'un modèle PBTK peuvent être représentés comme étant un mélange de lipides neutres, de phospholipides et d'eau; à partir de la valeur de la solubilité dans l'eau et dans l'huile pour chacune des substances chimiques, la valeur des coefficients de partage tissu:sang peut être calculée automatiquement durant la simulation. Cette façon de calculer les coefficients de partage a été validée à l'aide d'un modèle PBTK développé chez l'humain pour le dichlorométhane. Par la suite, la valeur des coefficients de partage tissu:sang de l'ALD a été calculée de la même manière.

Dans les deux autres publications du chapitre 2, l' on traite de la modélisation toxicocinétique de l'ALD chez le rat et l'humain, ainsi que de la détermination du UF_{AH-TK}. Pour commencer, on y retrouve la méthodologie utilisée pour mesurer la valeur des constantes métaboliques de l'ALD. La vitesse d'oxydation de l'ALD a été déterminée par la mesure de la quantité de d'aldicarb sulfoxide (ALX) produite suite à l'incubation de l'ALD avec des microsomes hépatiques, rénaux et pulmonaires. Les valeurs de la vitesse maximale (mg/kg/hr) pour l'oxydation de l'ALD sont de 718, 587 et 5.26 respectivement dans le foie, les reins et les poumons chez le rat. Les valeurs correspondantes

de la constante de Michaelis-Menten (mg/L) chez le rat pour ces trois tissus sont 35, 200 et 36, respectivement. Par comparaison, chez l'humain, la valeur de la vitesse maximale (μmoles/min/mg protéine) et celle de la constante de Michaelis-Menten (μM) pour l'oxydation de l'ALD suite à l'incubation avec des microsomes hépatiques sont de 3497 et 1318, respectivement. Sous des conditions expérimentales *in vitro* telles qu' utilisées dans cette étude, l'ALX est le seul métabolite généré; ainsi les voies d'oxydation subséquentes ont été négligées (p.ex., l'ALX en aldicarb sulfone).

Après le travail sur la prédiction de la valeur des paramètres physico-chimiques et la mesure de la valeur expérimentale des constantes métaboliques, un modèle PBTK chez le rat et l'humain a été développé pour l'ALD et l'ALX. Les simulations avec le modèle ont été obtenues suite à l'incorporation de la valeur de chacun des paramètres (physiologiques, physico-chimiques, biochimiques) dans les équations différentielles décrivant les divers processus toxicocinétiques de l'ALD et de l'ALX, et suite à la résolution de ces équations par intégration numérique à l'aide d'un logiciel de simulation basé sur le language Fortran (ASCL®, Advanced Continuous Simulation Language, MGA, Concord, MA). Le modèle PBTK de l'ALD pour le rat a été validé en comparant les valeurs simulées de la concentration de l'ALX dans les différents tissus en fonction du temps avec des valeurs obtenues sous des conditions *in vivo* suite à une administration intra-veineuse (0.1 et 0.4 mg/kg de ALD). A cause de l'absence de données chez l'humain et du fait que l'éthique ne permet pas l'expérimentation

avec des sujets humains, la validation du modèle PBTK à été effectuée à partir de valeurs de la littérature portant sur l'inhibition de l'acétylcholinestérase (AChE) par l'ALD. Dans ce cas, le mécanisme de l'inhibition de l'AChE a été décrit dans le modèle PBTK humain, lequel a ensuite été validé avec des valeurs expérimentales. Ce même exercice de validation pour l'inhibition de l'AChE a été effectué en utilisant un modèle PBTK développé chez le rat.

Suite à la validation du modèle PBTK chez le rat et l'humain, la concentration tissulaire et sanguine de l'ALD et l'ALX a été simulée chez l'une et l'autre espèce sous des scénarios d'exposition comparables; les valeurs obtenues ont été utilisées pour calculer le $UF_{AH\text{-}TK}$. Les résultats indiquent que pour une dose équivalente d'exposition à l'ALD, les concentrations sanguine et cérébrale sont 9.5 fois plus petites chez le rat que chez l'humain et 17 fois plus petites lorsque la cinétique du métabolite est considérée. En d'autres mots, pour avoir une équivalence de la toxicocinétique entre l'humain et le rat pour les concentrations sanguine et cérébrale, l'humain doit être exposé à une dose 9.5 fois plus petite que celle chez le rat. En se basant sur cet exercice de modélisation, le $UF_{AH\text{-}TK}$ utilisé par défaut (= 3.16) ne semble pas adéquat pour tenir compte de la différence inter-espèce observée avec l'ALD et l'ALX (i.e., 9 et 17). Or, l'ALD est rapidement éliminé de l'organisme, et il contribue peu à l'inhibition de l'AChE contrairement à l'ALX; par conséquent, on devrait considérer le facteur 17 comme étant le $UF_{AH\text{-}TK}$ le plus approprié.

Dans le troisième chapitre qui traite de la quatrième publication, on présente les résultats du $UF_{AH\text{-}Tk}$ pour onze substances chimiques. Le $UF_{AH\text{-}TK}$ de ces onze substances a été calculé avec un modèle PBTK de la même manière que pour l'ALD et l'ALX, pour ainsi le comparer avec le $UF_{AH\text{-}TK}$ de 3.16 qui est présentement utilisé par défaut. Les modèles PBTK validés antérieurement chez l'animal et l'humain pour le dichlorométhane (DCM), le tétrachloroéthylène (TETRA), le 1,4-dioxane (DIOX), le toluène (TOL), le m-xylène (XYL), le styrène (STY), le tétrachlorure de carbone (CATE), l'éthyl benzène (ETBE), le chloroforme (CHLO), le trichloroéthylène (TRI) et le chlorure de vinyle (VICH) ont été utilisés pour estimer les concentrations tissulaire et sanguine de la substance-mère et de ses métabolites pour des scénarios d'exposition comparables. Les résultats indiquent que pour ces substances chimiques le $UF_{AH\text{-}TK}$ déterminé avec ces modèles PBTK varie de 0.06 à 1.45, indiquant que le $UF_{AH\text{-}TK}$ (= 3.16) utilisé par défaut n'est pas adéquat. En plus, ces résultats réfutent l'opinion que la vitesse des processus régissant la clairance physiologique est toujours plus petite chez l'humain que chez les animaux de laboratoire.

La méthodologie utilisée dans la présente recherche pour estimer le $UF_{AH\text{-}TK}$ pourrait aussi être utilisée pour comprendre et estimer les facteurs responsables de la variabilité entre les espèces lors d'expositions chroniques, lorsque l'état d'équilibre est atteint. Dans la cinquième publication, l'on présente des expressions algébriques simples qui permettent d'estimer la concentration

d'une substance chimique dans les tissus et le sang, à l'état d'équilibre. De ces expressions algébriques, on note que des 17 paramètres utilisés dans le modèle PBTK pour prédire la toxicocinétique des substances chimiques, seuls la vitesse du métabolisme (VMAX), la constante de Michaelis-Menten (KM), la fraction du débit cardiaque qui passe par le foie (QLC), le coefficient de partage sang:air (PB) et les coefficients de partage tissu:sang (PT) sont des paramètres critiques pour la prédiction de la toxicocinétique à l'état d'équilibre. Dans la sixième publication, en se basant sur les expressions algébriques qui sont présentées dans la cinquième publication, l'on à déterminé l'impact de chacun des paramètres sur le $UF_{AH\text{-}TK}$. Il est important de noter que le $UF_{AH\text{-}TK}$ calculé avec le modèle PBTK et les expressions algébriques est identique, ce qui a été vérifié pour plusieurs substances chimiques. Dans le dernier chapitre, l'on retrouve une discussion générale portant sur les résultats contenus dans la thèse et sur l'impact d'une telle recherche en toxicologie.

La méthodologie développée dans cette étude pour calculer un $UF_{AH\text{-}TK}$ spécifique à chaque substance pourrait remplacer l'approche traditionnelle et améliorer le caractère scientifique de la démarche de l'analyse d'un risque toxicologique.

ABSTRACT

The overall objective of this dissertation is to elucidate the magnitude and mechanistic basis of animal-human toxicokinetic uncertainty factor ($UF_{AH\text{-}TK}$), using a physiological modeling approach. Initially the $UF_{AH\text{-}TK}$ for the carbamate pesticide aldicarb (ALD) is determined by developing rat and human physiologically-based toxicokinetic (pharmacokinetic) PBTK (PBPK) models. This is accomplished by incorporating the values of the mechanistic parameters, i.e., physiological, physicochemical and metabolic parameters, into differential equations that describe the toxicokinetics of ALD and ALX in blood, liver, kidney, lungs, brain, fat and rest of the body tissue compartments. The values for the rat and human physiological parameters are obtained from the literature, and the estimation of the partition coefficients (PCs) is based on a new modeling framework that involves the description of each tissue compartment as a mixture of neutral lipids, phospholipids, and water, and data on oil and water solubility of the chemical. The rate of sulfoxidation of ALD in rat hepatic, renal and pulmonary microsomes is determined by quantitating the levels of aldicarb sulfoxide (ALX) produced during incubations. The average maximal velocity (mg/kg/hr) for the sulfoxidation of ALD, based on measurements of product formation, in liver, kidney and lung microsomes is 718, 587, and 5.26, respectively. The corresponding values for the Michaelis constant (mg/L) are 35, 200 and 36 respectively. The average maximal velocity (μmoles/min/mg protein) and the Michaelis constant (μM) for the sulfoxidation of ALD in human liver was 3497 and 1318 respectively. Under *in vitro*

experimental conditions used in the present study, ALX was the only metabolite produced, and further metabolism of ALX to aldicarb sulfone was negligible.

Solutions of the equations that describe the toxicokinetics of ALD in the tissues are obtained by numerical integration with the aid of a Fortran-based simulation software (ASCL®, Advanced Continuous Simulation Language, MGA, Concord, MA). The adequacy of the rat PBTK model is assessed by comparing the model simulations of the metabolite ALX time-course with those obtained from in vivo intravenous administration of ALD (0.1 and 0.4 mg/kg), while the validation of the human model is based on available data that describe profile of the ALD-caused acetylcholinesterase (AChE) inhibition in human blood. This necessitated the expansion of the PBTK model to include the description of the ALD-induced AChE inhibition. The validated rat and human PBTK models are run under the same exposure scenario and the interspecies toxicokinetic uncertainty factor for ALD was calculated from the respective blood and brain concentrations. The results indicate that with respect to the parent chemical, equivalent applied doses in rats and humans result in a 9.5-fold difference in the effective dose in the blood and brain concentration in the two species, and 17-fold difference with respect to the concentration of the metabolite in blood and brain. In other words, in order to have toxicokinetic equivalence in the blood and brain concentrations in the rat and human, the former must be exposed to a dose that is 9.5 and 17 times higher than the human with respect to the parent chemical and the metabolite

respectively. This means that the default $UF_{AH\text{-}TK}$ (=3.16) is not sufficient to correct the interspecies differences.

In order to gain a better understanding of the accuracy of the currently used $UF_{AH\text{-}TK}$, the same methodology is applied in the determination of the $UF_{AH\text{-}TK}$ for eleven other chemicals commonly encountered in the environment. Validated animal and human PBTK models of dichloromethane (DCM), tetrachloroethylene (TETRA), 1,4-dioxane, (DIOX), toluene (TOL), m-xylene (XYL), styrene (STY), carbon tetrachloride (CATE), ethyl benzene (ETBE), chloroform (CHLO), trichloroethylene (TRI) and vinyl chloride (VICH) are run under the same exposure scenarios to estimate the total dose received, blood and tissue concentrations of the parent compound, and concentrations of the metabolite in animals and humans. The results indicate that for the chemicals used in the present study the $UF_{AH\text{-}TK}$ varies between 0.06 and 1.45, thus indicating that the use of the default $UF_{AH\text{-}TK}$ (3.16) overestimates the derived exposure limits, by a factor as large as 3, and refute the unidirectionality of the $UF_{AH\text{-}TK}$.

With the applicability of PBTK models in the estimation of $UF_{AH\text{-}TK}$ established, the unanswered question pertains to the specificity and nature of the factors that contribute to the toxicokinetic variability across species. To answer this question, PBTK model-based mathematical equations that make possible the estimation of blood and tissue concentration of chemicals at steady-state are

developed. The results show that, of the 17 parameters used in conventional PBTK models to predict the toxicokinetic behavior of chemicals only the maximum metabolic rate, Vmax, the Michaelis-Menten constant, Km, the fraction of cardiac output reaching the liver, QLC, the blood:air partition coefficient, PB and tissue:blood partition coefficients, PT, are critical to the prediction of steady-state kinetics. By incorporating the values of these mechanistic factors into analytical equations one can obtain estimates of the $UF_{AH\text{-}TK}$ that are identical to those determined with the PBTK models.

The methodology developed in this dissertation can replace the currently used empirical default approaches to provide the chemical-specific $UF_{AH\text{-}TK}$ and thus improve the scientific basis of the risk assessment process.

TABLE OF CONTENTS

LIST OF FIGURES

FIGURE No PAGE

INTRODUCTION

ARTICLE 1

ARTICLE 2

ARTICLE 3

ARTICLE 4

ARTICLE 5

LIST OF TABLES

TABLE No PAGE

INTRODUCTION

ARTICLE 1

ARTICLE 3

ARTICLE 4

ARTICLE 5

ARTICLE 6

LIST OF SIGNS AND ABBREVIATIONS

α	Allometric Proportionality Coefficient
AChE	Acetylcholinesterase
ACSL®	Advanced Continuous Simulation Language®
AEU	Amount of Chemical Excreted in Urine
ALD	Aldicarb
ALU	Aldicarb Sulfone
ALX	Aldicarb Sulfoxide
A_{met}	Amount of Chemical Metabolized
AT	Amount of Chemical in Tissue
AUC	Area Under the Curve
β	Allometric Exponent
BMD	Benchmark Dose
BW	Body Weight
^0C	Degrees Celsius
CA	Concentration of Chemical in Arterial Blood
CA_{SS}	Concentration of Chemical in Arterial Blood at Steady-State
Calv	Concentration of Chemical in Alveolar Air
CATE	Carbon Tetrachloride
CF	Concentration of Chemical in Fat Tissue

CF_{SS}	Concentration of Chemical in Fat Tissue at Steady-State
CINH	Concentration of Chemical in Inhaled Air
CHLO	Chloroform
CL_h	Hepatic Clearance
CL_{int}	Intrinsic Clearance
CL	Concentration of Chemical in Liver
CL_{SS}	Concentration of Chemical in Liver at Steady-State
CM	Concentration of Metabolite
Cp	Concentration of Protein in Microsomes
cpm	Counts Per Minute
CR	Concentration of Chemical in Richly Perfused Tissues
CR_{SS}	Concentration of Chemical in Richly Perfused Tissues at Steady-State
CS	Concentration of Chemical in Slowly Perfused Tissues
CS_{SS}	Concentration of Chemical in Slowly Perfused Tissues at Steady-State
.CSL	Continuous Simulation Language file; Model File in ACSL®
CVF	Concentration of Chemical in Venous Blood Exiting the Fat tissue
CVL	Concentration of Chemical in Venous Blood Exiting Liver
CVL_{SS}	Concentration of Chemical in Venous Blood Exiting Liver at Steady-State
CVR	Concentration of Chemical in Venous Blood Exiting the Richly Perfused Tissues

CVS	Concentration of Chemical in Venous Blood Exiting the Slowly Perfused Tissues
CVT	Concentration of Chemical in Venous Blood Exiting Tissue T
CVT_{SS}	Concentration of Chemical in Venous Blood Exiting Tissue T at Steady-State
DCM	Dichloromethane
dCT/dt	Rate of Change in the Tissue Concentration
DIOX	1,4-Dioxane
DNA	Deoxyribonucleic Acid
E	Extraction Ratio
EDTA	Ethylene Diamine Tetraacetic Acid
ETBE	Ethyl Benzene
FMO	Flavin Monooxygenase
FNL_B	Fraction of Neutral Lipid in Blood
FNL_T	Fraction of Neutral Lipid in Tissue
FPL_B	Fraction of Phospholipid in Blood
FPL_T	Fraction of Phospholipid in Tissue
Ft	Volume Fraction of Tissue
FW_B	Fraction of Water in Blood
FW_T	Fraction of Water in Tissue

GSH	Reduced Form of Glutathione
HPLC	High Performance Liquid Chromatography
κ_L	Similarity Constant
κ	Transfer Constant
K_2	Carbamylation Constant
K_3	Decarbamylation Constant
Ka	Affinity Constant
Ki	Inhibition Constant
KF	First Order Metabolic Rate Constant
KFC	Allometric First Order Metabolic Rate Constant
kg	Kilogram
KH	Hydrolysis Rate Constant
Ko	Oral Absorption Rate Constant
KM	Michaelis Constant
KOW	Vegetable Oil:Water Partition Coefficient
KUE	Urinary Excretion Rate Constant
L	Liter
L_I	the ith Side of a Geometric Object
LC	Liquid Chromatography
LD50	Lethal Dose of Chemical that Results in 50% Mortality

LOAEL	Lowest Observed Adverse Effect Level
M_R	Metabolic Rate
MBDE	Mass Balance Differential Equation
MF	Modifying Factor
mg	Milligram
min	Minute
μM	Micromolar
μmol	Micromole
NADPH	Reduced Form of Nicotinamide Adenine Diphosphate
NL	Neutral Lipid Content in Liver Tissue Compartment
NOAEL	No Observed Adverse Effect Level
$NOAEL_{HEC}$	Human Equivalent No Observed Adverse Effect
OPA	*o*-Phthalaldehyde
P	n-Octanol:Water Partition Coefficient
PB	Blood:Air Partition Coefficient
PB_{APP}	Apparent Blood:Air Partition Coefficient
PBPK	Physiologically-Based Pharmacokinetic
PBTK	Physiologically-Based Toxicokinetic
PC	Partition Coefficient

PDF	Probability Density Function
PF	Fat:Blood Partition Coefficient
PL	Liver:Blood Partition Coefficient
PLA	Liver:Air Partition Coefficient
ppm	Parts Per Million
PPO	5-Phenyl-2-Oxazolyl Benzene
POPOP	1,4-Bis(5-Phenyl-2-Oxazolyl Benzene)
PR	Richly Perfused Tissue:Blood Partition Coefficient
PS	Slowly Perfused Tissue:Blood Partition Coefficient
PT	Tissue:Blood Partition Coefficient
$P_{T:W}$	Tissue:Water Partition Coefficient
QC	Cardiac Output
QCC	Cardiac Output Scaled to an Animal of 1 kg Body Weight
QF	Blood Flow Rate to Fat Tissue Compartment
QFC	Blood Flow Rate Constant to Fat Tissue Compartment, % of Cardiac Output
QL	Blood Flow Rate to Liver Tissue Compartment
QLC	Blood Flow Rate Constant to Liver Tissue Compartment, % of Cardiac Output
QP	Pulmonary Ventilation
QPC	Pulmonary Ventilation Scaled to an Animal of 1 kg Body Weight
QR	Blood Flow Rate to Richly Perfused Tissue Compartment

QRC	Blood Flow Rate Constant to Richly Perfused Tissue Compartment, % of Cardiac Output
QS	Blood Flow Rate to Slowly Perfused Tissue Compartment
QSAR	Quantitative Structure Activity Relationship
QSC	Blood Flow Rate Constant to Slowly Perfused Tissue Compartment, % of Cardiac Output
QT	Blood Flow to a Tissue Compartment
RAM	Rate of the Amount Metabolized
RfC	Reference Concentration
RfD	Reference Dose
SA	Saturable Vapor Concentration of Chemical
SO	Solubility of Chemical in Oil or n-Octanol
SS	Steady State
STY	Styrene
SW	Solubility of Chemical in Water
TETRA	Tetrachloroethylene
TD	Toxicodynamic
TK	Toxicokinetic
TOL	Toluene
TRI	Trichloroethylene

TRIS-HCL	Trizma Hydrochloride
UF	Uncertainty Factor
UF_{AH}	Interspecies (Animal-Human) Uncertainty Factor
UF_{AH-TK}	Toxicokinetic Interspecies (Animal-Human) Uncertainty Factor
$UF_{AH-TK-ABS}$	Toxicokinetic Interspecies (Animal-Human) Uncertainty Factor-Absorption
$UF_{AH-TK-DIS}$	Toxicokinetic Interspecies (Animal-Human) Uncertainty Factor-Distribution
$UF_{AH-TK-MET}$	Toxicokinetic Interspecies (Animal-Human) Uncertainty Factor-Metabolism
$UF_{AH-TK-TOT}$	Overall Toxicokinetic Interspecies (Animal-Human) Uncertainty Factor
UF_{HH}	Intraspecies (Human-Human) Uncertainty factor
V	Volume
VICH	Vinyl Chloride
VF	Volume of Fat Tissue Compartment
Vi	Volume of Compartment i
VFC	Volume of Fat Tissue Compartment as % of Body Weight
VL	Volume of Liver Tissue Compartment
VLC	Volume of Liver Tissue Compartment as % of Body Weight
VMAX	Maximum Metabolic Rate

VMAXC	Maximum Metabolic Rate Constant
VOC	Volatile Organic Chemical
VR	Volume of Richly Perfused Tissue Compartment
VRC	Volume of Richly Perfused Tissue Compartment as % of Body Weight
VS	Volume of Slowly Perfused Tissue Compartment
VSC	Volume of Slowly Perfused Tissue Compartment as % of Body Weight
VT	Volume of Tissue
v/v	Dilution on a per Volume Basis
WL	Water Content in Liver Tissue Compartment
X	Allometric Predictor
XYL	m-Xylene
Y	Allometric Parameter

ACKNOWLEDGEMENTS

Many people helped me during my studies at the Université de Montréal. I would like to thank Dr. Kannan Krishnan, Dr. Jules Brodeur, Dr. Stephanie Padilla, Pierrette Gagnon, Diane Talbot, Lucette Merineau, and Chantal Belisle for making this dissertation possible. Financial support from the Natural Sciences and Engineering Research Council of Canada (NSERC) and the Canadian Network of Toxicology Centres (CNTC) is gratefully appreciated.

To my Mother

CHAPTER 1

GENERAL INTRODUCTION

1.1. INTRODUCTION TO RISK ASSESSMENT

The term "risk" has different meanings in different situations. In everyday life it is used to describe a situation characterized by uncertainty, danger or an adverse outcome. In a business venture, where the adverse outcome is material loss, it is seen as an opportunity for increased reward. In the public health domain risk is used as a technical term that is characterized within carefully selected and calibrated scientific means. It is defined as the probability that an individual will develop a particular adverse effect under specified exposure conditions. It may be described either in qualitative terms (high or low risk) or quantitatively taking values from zero to one. Quantitative risk assessment is the use of scientific data to define the risk. It is a formal, analytical process of estimating the probability and magnitude of an adverse outcome in individuals or populations from some environmental hazard or practice, such as a toxic substance or a construction project (Covello and Merkhofer 1993).

1.1.1. Overview of the risk assessment process

The process of human health risk assessment involves the qualitative and quantitative characterization of potential health effects of human exposure to environmental hazard (National Research Council, 1983). It is performed in

four steps: i) hazard identification, ii) exposure assessment, iii) dose-response assessment and iv) risk characterization. Once the toxic effects of a chemical are identified (hazard identification), the risks associated with exposure are characterized (risk characterization) by combining quantitative information on exposure levels (exposure assessment) and on the dose-response relationship for the critical toxicological endpoint (dose-response assessment).

1.1.2. Default approach of dose-response assessment of systemic toxicants

Non-cancer risk assessment is currently conducted with the Reference Dose/Concentration (RfD/RfC) or Benchmark Dose (BMD) methodology. The United States Environmental Protection Agency (USEPA) has chosen the RfD[1] methodology to estimate of "safe exposure limits" (USEPA, 1985). Other agencies also use the same method although with a different name (ADI, acceptable daily intake, Food and Drug Administration, FDA; PEL, permissible exposure level Occupational Safety and Health Administration, OSHA; TDI, tolerable daily intake, Health Canada). The RfD is defined as:

"a lifetime daily dose of a substance that would not result in an observable increase in adverse effects in a well conducted study of a sub-population of humans sensitive to the substance"

[1] The approach and discussion presented here apply to both the RfD and RfC, but for ease of reading, the RfD will be used throughout this thesis, except in cases we are dealing exclusively with volatiles.

Doses at or below the RfD are considered to be without a noncancer risk, while doses above the RfD are assumed to have some unknown probability of causing adverse effects. The RfD method represents one component of the risk assessment process and the RfD estimate must be compared against an exposure estimate in order to characterize risk. Its estimation requires the identification of the highest experimental dose that is not associated with an increase in any adverse effect above background, and then division by uncertainty factors and a modifying factor. Typically, the RfD is expressed in mg/kg of body weight/day, and is estimated by dividing the NOAEL (derived usually from animal studies) by arbitrary uncertainty factors as follows: (USEPA, 1991):

$$RfD = \frac{NOAEL\ (LOAEL)}{UF_{(s)} * MF}$$

where:

- NOAEL (no observable adverse effect level)=the highest exposure level at which there are no statistically or biologically significant increases in the frequency of adverse effects between the exposed population and its appropriate control,
- LOAEL (lowest observable adverse effect level)=lowest exposure level at which there is statistically significant increase in the frequency of adverse effects between the exposed population and its appropriate control,

- $UF_{(s)}$=uncertainty or safety factor(s), and
- MF=modifying factor that addresses the adequacy and quality of the toxicologic database used in the derivation of the RfDs.

The Benchmark Dose approach, advocates the use of an alternative to the NOAEL, called benchmark dose, BMD, which is calculated by fitting a dose-response model to the experimental data. The BMD is the dose that is associated with a pre-determined response (benchmark response, BMR). Then an RfD is estimated by dividing the BMD with the appropriate uncertainty factors, similar to the NOAEL-based approach (Crump, 1984; USEPA, 1991).

1.1.3. Uncertainty factors

In conducting health risk assessment of chemicals human data are preferred (USEPA, 1991). However, since they are often unavailable or inadequate and ethical considerations prevent experimentation with humans, risk assessors are forced to use data obtained in animal studies to derive RfD. The use of animal data for human health risk assessment is based on the assumption that there is:

- a qualitative similarity in effects in different species, and

- a quantitative equivalence in the tissue chemical exposure required to produce an equivalent intensity of biological effect in various species (Andersen, 1987).

The validity of these assumptions has been attributed to the evolutionary relationships and the phylogenetic continuity of animal species including man and the principle of extrapolation of animal data to humans has been widely accepted in the scientific and regulatory communities. Thus, at least among some mammalian species, the basic anatomical, physiological and biochemical parameters are similar across species (USEPA, 1985). Despite the fact that the general principle of inferring effects in humans from effects in experimental animals is well founded, there have been examples where these assumptions are known to be inaccurate and this has led risk assessors to question their validity (Davidson *et al.* 1989). In general the use of animal data to estimate safe levels for humans introduces several uncertainties, which are due to:

- The qualitative and quantitative differences between the animals and humans. For example, if the toxicity observed in animals is due to an enzyme that is not present at all or it is present at lower concentrations in humans, then the particular experimental data are irrelevant for humans.
- Uncertainties associated with the extrapolation from high experimental dose to low dose typical of human exposures. Since most animal studies

are conducted at doses that are much higher than the expected human exposure levels, quantitative dose-response models are needed to interpolate/ extrapolate from high doses to lower doses.

- The issue of whether equivalent doses of a chemical are equitoxic given the variability in toxic responses among different species.

The RfD methodology employs uncertainty factors (UFs) to get around all the above concerns (Dourson and Stara, 1983). The requirement for UFs stems in part from the belief that humans could be more sensitive to the toxic effects of a chemical than laboratory animals and the belief that variations in sensitivity are likely to exist within the human population (National Research Council, 1980). Those beliefs are plausible, but the magnitude of interspecies and intraspecies differences for every chemical and every toxic end point are not known. The uncertainty factor used in noncancer risk assessment has been defined by the National Academy of Sciences as (NAS, 1977):

"a number that reflects the degree or amount of uncertainty that must be considered when experimental data in animals are extrapolated to man"

The types of uncertainty factors used in the RfD methodology and their default values in brackets are shown below:

- Human heterogeneity [10]: account for differences in sensitivity among individuals in the human population.
- Animal to human extrapolation [10]: account for species differences in the extrapolation from animals to humans in long-term studies.
- Subchronic to chronic extrapolation [10]: account for differences between animals and humans, if animal exposures are less than lifetime or otherwise deficient, due to such variables as accumulation and recovery.
- LOAEL to NOAEL extrapolation [10]: account for uncertainty in establishing the relationship between the observed adverse effect level and the presumed threshold.

1.2. EMPIRICAL FOUNDATION OF THE UNCERTAINTY FACTORS AND THE DEFAULT APPROACHES USED IN THE INTERSPECIES EXTRAPOLATION OF TOXICOLOGICAL DATA

1.2.1. Introduction to allometry

Allometry is based on the concept of isometry which was advanced along with Euclidean geometry 2000 years ago (Schmidt-Nielsen, 1984). Two objects, e.g., triangles (Figure 1), are said to be geometrically similar or isometric [iso=equal] if the following relationship is observed:

$$L_2 = \kappa_L * L_1 \quad \text{or}$$

$$L_2/L_1 = \kappa_L \qquad [1\text{-}2\text{-}1]$$

where:

L_1 =side 1 of the object

L_2 =side 2 of the object

κ_L =similarity constant

The constant κ_L is called similarity constant and relates all linear properties of similar objects, such as height, angles, etc., and is true for all two-dimensional bodies.

Similarly, geometric considerations dictate that the surface areas of two isometric three-dimensional bodies are not related linearly, but rather

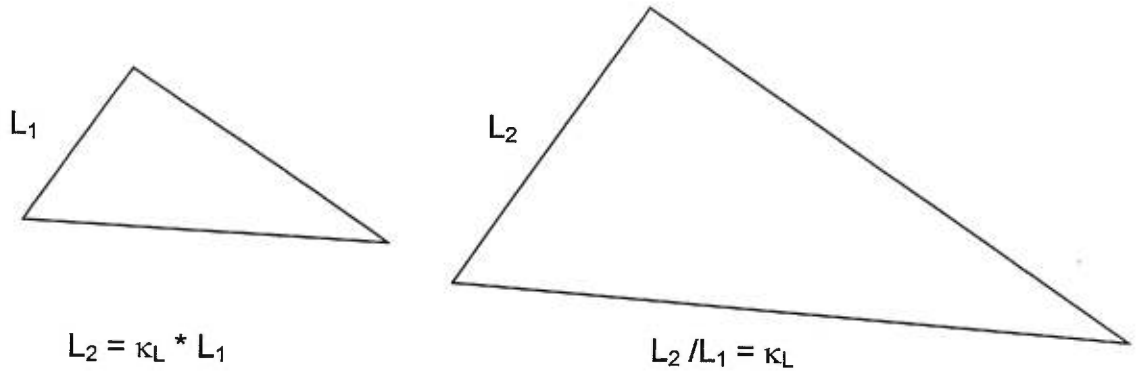

Figure 1. Linear dimensions in isometric triangles

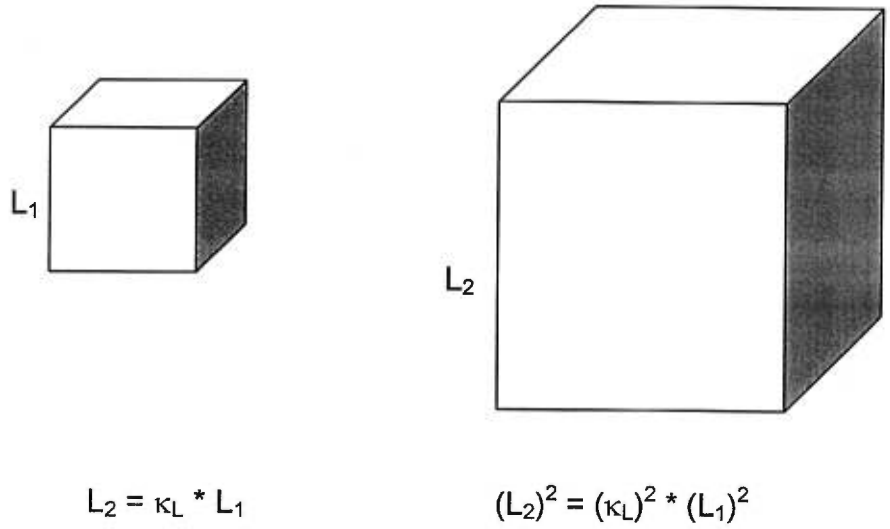

Figure 2. Surfaces in isometric bodies

with the square of the linear ratio, while their volume is proportional to the third power of their linear dimensions (Figure 2).

$$L_2^2 = \kappa_L^2 * L_1^2$$

$$\text{Surface}_2 = \kappa_L^2 * (\text{Length}_1)^2 \qquad [1\text{-}2\text{-}2]$$

$$L_2^3 = \kappa_L^3 * L_1^3$$

$$\text{Volume}_2 = \kappa_L^3 * (\text{Length}_1)^3 \qquad [1\text{-}2\text{-}3]$$

From Eqns [1-2-2] and [1-2-3] Eqn [1-2-4] is obtained, which states that, the increase in the surface of a three-dimensional body does not increase linearly with its volume but rather to the 2/3 power of its volume.

$$\text{Surface} = \kappa_L * V^{2/3} \qquad [1\text{-}2\text{-}4]$$

These equations hold true for all isometric three-dimensional objects regardless of their shape, and have been extended to describe the relationship of volume and surfaces among animals. However, since biological organisms are not truly geometric and certain proportions change in a regular fashion, the term allometric [allo=different] is used to describe any scaling or extrapolation process that is applied to biological variables.

The general form of allometric equations is the following:

$$Y = \alpha * X^{\beta} \quad \text{or}$$

$$\log Y = \log\alpha + \beta * \log X \qquad [1\text{-}2\text{-}5]$$

where:

Y =parameter of interest

X =predictor (usually body weight)

α =an empirically derived proportionality coefficient

β =an empirically derived exponent

Thus, when one plots two variables, X and Y, on logarithmic scales a straight line results with slope β. The intercept of the straight line, i.e., the proportionality coefficient α, relates information about the differences between two variables of two groups, while the slope, i.e., the exponent β describes the variation with respect to the predictor. Let us, for example, assume that the allometric equation that describes the variation of metabolic rate among birds and mammals, with respect to body weight, has α=1 and β=0.75. That means that both birds and mammals have the same rate of metabolism, which varies with respect to the ¾ power of the body weight. If on the other hand, α=0.6 and β=1, that would have meant that birds have a lower metabolic rate than mammals which varies with changing body weight in the same way in birds and mammals.

1.2.1.1. Extrapolations based on surface body area

The first quantitative use of allometry was made by Rubner in 1883 who studied basal metabolic rate (measured as oxygen consumption) in dogs of various sizes. He found that when body weight was the predictor, the

metabolic rate increased as the weight of the animal decreased. However, when basal metabolic rate was calculated per body surface area, the ratio was constant regardless of body weight. The work of Moore (1909) also suggested that extrapolation based on body surface area was appropriate. The work of Rubner and Moore led to the formulation of "the surface law" which states that there is a direct proportionality between metabolic rate and body surface area in mammals. Since the surface area in almost all vertebrates is a function of $BW^{0.67}$ (Hemmingsen, 1950), this was established as a metric for interspecies extrapolations. The surface law gained momentum from the work of Crawford *et al.* (1950), Pinkel (1958) and Freireich *et al.* (1966). Their argument is essentially based on Eqns [1-2-2 - 1-2-4]; they argued that if surface area is proportional to the square of linear dimension of size, and body weight (or volume) is proportional to the cube of the dimension, then body surface area is proportional to the two-thirds power of body weight. Since the two-thirds power is a reasonable approximation of many allometric physiologic correlations (Adolph, 1949), and in agreement with the data of a large number of antineoplastic drugs, which they tested in experimental animals and humans, the surface law seemed to be a reasonable way to extrapolate. What is significant about the work of Crawford *et al.* (1950), Pinkel (1958) and Freireich *et al.* (1966) is that they used body surface area to extrapolate toxicity data, and not just metabolic determinants like the earlier researchers did.

1.2.1.2. Extrapolations based on body weight

Body weight, perhaps because it can easily and accurately be measured, has been used more frequently for interspecies extrapolation. Kleiber (1932) analyzing the metabolic rates in a variety of animals ranging in size from rats to steers (0.15 kg-679 kg) came up with the following allometric equation to describe metabolic rate (M_R) as a function of body weight (kg):

$$M_R = 73.3 * BW^{0.74} \qquad [1\text{-}2\text{-}6]$$

Later on Brody *et al.* (1934) expanded the work of Kleiber and included a larger number of animals with a wider range of body weight. He concluded that the slope of the regression line, β was 0.734. In 1934 Benedict studied the metabolism of birds and mammals and found that β was 0.76. The results of these studies were the first indication regarding deviations from the surface law, which at that time had been in use for almost a century, and used unquestionably for extrapolations. Eventually, these observations led to the acceptance of extrapolation based on body weight.

1.2.1.3. Linear extrapolations based on body weight

A third type of extrapolation, is called body weight equivalence or linear body weight extrapolation. It assumes that metabolic and/or physiological parameters are related linearly to body weight in all species. In other words, it is assumed that the exponent in the allometric equation is 1.

Of the three methods presented, this is the least explained and least frequently used one (Vocci and Farber, 1988).

1.2.2. Interspecies extrapolation of toxicological data

1.2.2.1. The allometric approach

The extensive use of allometric equations to extrapolate the physiological and biochemical parameters that determine toxicity across species (Boxenbaum 1982b; Mordenti, 1986b), has led toxicologists and risk assessors to use it for dose extrapolation across species. If toxicity Y is a function of dose X, and Y is allometrically related to body weight by the usual allometric equation, then the following equation is true:

$$Y = f(X) = f(\alpha * BW^{\beta}) \qquad [1\text{-}2\text{-}7]$$

Therefore, when the dose in the experimental animal is X_A the equivalent dose in human, X_H will be:

$$\frac{X_H}{X_A} = \frac{\alpha * (\text{human body weight, } BW_H^{\beta})}{\alpha * (\text{animal body weight, } BW_A^{\beta})} \qquad \text{or}$$

$$\text{Equivalent human dose} = X_H = (BW_H / BW_A)^{\beta} * X_A \qquad [1\text{-}2\text{-}8]$$

With the equation in hand, the risk assessor has to decide which type of extrapolation he will use. The type of extrapolation used depends on individual choice. Some people argue against body weight extrapolation ($BW^{0.75}$) claiming that the number of data used by Kleiber was insufficient (Davidson *et al.* 1986, Travis *et al.* 1990, Dedrick 1992), while others argue

against surface extrapolation claiming that mammals are not isometric bodies, and thus the use of $BW^{0.67}$ is inappropriate.

1.2.2.2. The Interspecies uncertainty factor – UF_{AH}

The use of interspecies uncertainty factor, UF_{AH}, was initiated by Lehman and Fitzhugh in 1954 who advocated the derivation of the Acceptable Daily Intake (ADI) from chronic animal NOAEL (mg/kg) (Lehman and Fitzhugh, 1954). Initially they proposed the use of a 100-fold uncertainty factor, to account for what they called "several sources of variability" and later clarified as uncertainty due to interspecies and intraspecies variation. The National Academy of Science (1977) and regulatory agencies (WHO, FAO, EPA, Food Safety Council) (Food Safety Safety Council, 1982; Hill and Wands, 1989) adopted and expanded these guidelines, but provided no evidence to support it. Later on, the 100-fold factor was divided into two 10-fold factors in order to distinguish and account separately for inter- and intra-species variation (Bigwood, 1973; Klaasen and Doull, 1980).

Recently, EPA in the redefined RfC methodology reduced the magnitude of the interspecies uncertainty factor from 10 to 3.16 (USEPA, 1989). The RfCs for inhaled compounds now incorporate dosimetric adjustments to account for species-specific relationships of exposure concentrations to deposited/delivered doses, and the rationale for the reduction is based on the following two premises. First, the various species

used in inhalation studies do not receive identical doses in comparable respiratory tract regions, mainly the extrathoracic, tracheobronchial and pulmonary areas, when exposed to the same toxicant. Second, the adverse toxic effect may be more directly related to the quantitative pattern of deposition within the respiratory tract than to the exposure concentration, because the regional deposition pattern determines not only the initial lung tissue dose, but also the specific pathways and rates by which the inhaled material is cleared and re-distributed (Schlesinger, 1985; Jarabek, 1994). Therefore, if it is assumed that the default UF_{AH} adjusts for both toxicokinetic and toxicodynamic differences among species, and if the dose has already been adjusted for toxicokinetic (dosimetric) differences, only half the correction, on a geometric scale, is necessary. The RfC methodology argues that the default UF_{Total} is equal to:

$$UF_{AH\text{-}Total} = (UF_{A\text{-}Toxicokinetics}) * (UF_{A\text{-}Toxicodynamics})$$
$$= (3.16) * (3.16)$$
$$= 10 \qquad [1\text{-}2\text{-}9]$$

Thus, when the delivered dose is the same in both species, $UF_{AH\text{-}TK}=1$ and the $UF_{AH\text{-}Total}=3.16$.

1.3. RESEARCH ISSUES

1.3.1. Deficiencies of the default approaches used in the interspecies extrapolation of doses

1.3.1.1. Allometric approach

The use of allometry in the interspecies extrapolation of toxicological doses is problematic for the following reasons:

- First, the magnitude of the extrapolation factor depends not only on the weight of the animal but also on the type of extrapolation used. Extrapolation from rat to human and mouse to human, based on linear body extrapolation ($BW^{1.0}$), result in uncertainty factors of 70/0.25=280 and 70/0.025=2333, respectively, while extrapolation based on $BW^{0.75}$, results in uncertainty factors of $(70/0.25)^{0.75}$=68.5 and $(70/0.03)^{0.75}$=335. If on the other hand, the extrapolation is based on body surface correction, the uncertainty factors are $(70/0.25)^{0.67}$= 43 and $(70/0.025)^{0.67}$=180. Thus, depending on the method of extrapolation used, there could be a 6.5-fold difference for rat to human extrapolation, and a 13-fold difference for mouse to human extrapolation (Table 1).
- Second, although the concept of surface area extrapolation explains why the metabolic rate per kilogram of small animals is greater than that of larger animals, no appropriate mechanism has been described and it has been through several cycles of acceptance and rejection. It has been criticized as being simply empirical and therefore should not be treated as

TABLE 1: INTERSPECIES UNCERTAINTY FACTORS DETERMINED BY ALLOMETRY

	$BW^{0.67}$	$BW^{0.75}$	$BW^{1.0}$	$\frac{BW^{0.75}}{BW^{0.67}}$	$\frac{BW^{1.0}}{BW^{0.67}}$	$\frac{BW^{1.0}}{BW^{0.75}}$
Rat to Human	43.6	68.5	280	1.57	6.42	4.09
Mouse to human	180	335	2333	1.86	13	8.36

though it is a scientific principle (Forbes, 1959). Regression analysis of the same data used by Freireich *et al.* (1966), which led to the wider acceptance of the surface law, has shown that the exponent was not constant and equal to 0.67, but that it varied from 0.60-0.87 (Mordenti, 1986c). Others suggested that the surface area/dosage is a semantic faux pas and proposed a more appropriate power exponent for the body weight, i.e., $BW^{0.75}$ (Done, 1964). Heusner (1982) has challenged the body weight extrapolation. His analysis of covariance of the data of Kleiber, Brody and Benedict showed that the exponent is 0.67, i.e., the surface law applied. Feldman and McMahon (1983) re-analyzed the same data and concluded that the exponent is 0.75. They also concluded that when extrapolating between children and adults of the same species the exponent varied between 0.612 and 0.728, while when extrapolating across species the exponent varied between 0.744 and 0.760. This has led to the suggestion that the surface law is appropriate for intraspecies extrapolation, and body weight extrapolation for interspecies extrapolation. It should be noted here, that none of the aforementioned allometric relationships are applicable for animals at different stages of growth. This deviation has been explained in terms of energy required by the developing animal to grow. In growing animals the metabolic rate initially rises quickly as a function of increasing mass and then drops with time and eventually, the metabolism of mature humans approaches the

general curve related to weight in mature animals of other species (Brody, 1945).

- Third, there is no similarity among the regulatory agencies in the type of extrapolation used. WHO considered and rejected the body surface extrapolation (Lu, 1985). The main reason was that the metabolism of chemicals does not necessarily correlate with the normal metabolic rate. The EPA has adopted the body surface approach ($BW^{0.67}$) for interspecies extrapolation of equivalent exposure doses. It has however been pointed out that this type of extrapolation is appropriate only if i) the parent compound is responsible for the toxic effects, and ii) total exposure is the appropriate correlate of toxicity (Gargas *et al.* 1989; Krishnan and Andersen, 1991). This is because the toxic effect of direct acting toxicants, is dependent on the clearance of the chemical, which at low concentrations is influenced by blood flow to the metabolizing organs, which in turn is related to body surface ($BW^{0.67}$). Linear body weight ($BW^{1.0}$). extrapolation is recommended for chemicals, which produce stable metabolites, because both metabolite production and elimination are likely to be related to body weight.

Despite the 150-year debate, controversy still exists about the relationship for energy metabolism and the value of the exponent, and in general about the usefulness of allometry in Toxicology. It has been argued that similarity analysis is difficult to apply in living organisms because of their

complexity, and therefore nothing can be proven mathematically (Gunther, 1975). Furthermore, the empirical nature of allometry and its inability to provide an understanding of underlying mechanisms make it even more difficult to accept its conclusions in an era dominated by mechanistic toxicology.

1.3.1.2. Uncertainty factor approach

Although the use of the UF_{AH} is widely practised, there is no conclusive experimental or theoretical justification for its magnitude, nor a strong scientific basis for using the same uncertainty factor for all situations (NRC, 1986). Bigwood (1973) tried to justify the 100-fold UF_{AH} on the basis of differences in the body size of experimental animals versus humans, differences in food requirements which vary with age, sex, differences in water balance exchange between the body and the environment among species, and differences in susceptibility to the toxic effect of a given chemical among species. The conclusion of his studies however, cannot be evaluated satisfactorily because of the limited data.

Dourson and Stara (1983) tried to justify the UF_{AH} of 10 on theoretical grounds. Based on the experimental work of Altman and Dittmer (1962) they calculated an UF_{AH} as the cube root of the average human body weight (70 kg) divided by the animal body weight (kg):

UF_{AH} = (Human body weight/Animal body weight)$^{1/3}$ [1-3-1]

This equation was hypothesized to adjust for dose differences (mg/kg BW/day) due to the different body surface areas between experimental animals and humans, and was based on the assumption that different species are equally sensitive to toxic effects on a dose per unit surface area. This assumption is based on the principles of allometry, which state that dose conversions based on body-surface area are thought to more accurately reflect differences among species in several biological parameters when compared to conversions based on mg per kilogram body weight. Thus the UF_{AH} can be thought as a reduction of the animal dose needed to estimate the equivalent human dose. The validity of this assumption has been questioned based on the following reasons:

- First, as was mentioned in section 1.3.1.1. depending on the animal used, the calculated UF_{AH} is not constant and varies depending on the weight of the animal. For a 0.25 kg rat the UF_{AH} is $(70/0.25)^{1/3}$= 6.5 while for a 0.025 kg mouse the is $(70/0.025)^{1/3}$=13. That means that a rat to human extrapolation using an UF_{AH} of 10 would overestimate the RfD by a factor of approximately 2, while a mouse to human extrapolation using an UF_{AH} of 10 will underestimate the RfD by a factor of between 1 and 2. It has been shown that in general with most experimental animals the UF_{AH} of 10 underestimates the RfD by a factor between 1 and 10. Also it has

been shown that upward extrapolation from small animal body weight to large human body weight results in larger error than downward extrapolation, because the variance in the measurement of small body weight is multiplied (Dourson and DeRosa, 1991).

- Second, the use of UF_{AH}s has not been validated with respect to particular adverse health effects, and that they may not adequately account for important sources of variability.

- Third, the unidirectionality of the UF_{AH} has been questioned since it has not been well established and the assumption that humans are more sensitive than most laboratory animals is debatable as evidenced by the many of experimental studies that show the opposite (Davidson *et al.* 1986).

- Fourth, the UF_{AH} will vary depending on whether it is the parent compound or a metabolite(s) that are responsible for the observed toxicity and whether the detoxification mechanisms are the same across all species. Since the metabolic rate of most experimental animals is higher than that of humans, if the detoxification mechanisms follow similar patterns in animals and humans, it would be expected that the susceptibility to the parent compound would be reduced in the animal species as compared to man due to the greater rate of detoxification. If,

however, the toxic moiety is the metabolite, this same higher metabolic rate would generally make the experimental animal more vulnerable than the human, again if the detoxification mechanism is similar (Dourson and DeRosa, 1991).

The RfC approach has improved the risk assessment process, in that what was previously implied is now explicitly stated; the default $UF_{AH\text{-}TOT}$ adjusts for differences in two processes:

- changes in toxicokinetics from one species to another, i.e., how the target tissue dose associated with exposure varies from one species to another, and,
- changes in sensitivity to tissue dose, i.e., how the tissue response to tissue dose varies among species.

The differentiation of the default $UF_{AH\text{-}TOT}$ into toxicokinetic and toxicodynamic components was never made clear in the early applications, and became increasingly apparent as the risk assessment of chemicals moved away from the correlation of exposure dose and response and began to incorporate knowledge on mechanism of toxicity and differentiate between tissue and exposure dose. Although, operationally the RfC is similar to the RfD in that NOAEL is divided by uncertainty factors, it differs from the latter in that the animal NOAEL is adjusted to derive a human equivalent NOAEL

($NOAEL_{HEC}$). More importantly, the RfC methodology recognizes the potential errors in equating exposure with tissue dose, and proceeds to improve this discrepancy by explicitly accounting for the interaction of physicochemical characteristics of the chemical and the quantitative patterns of deposition within the upper respiratory tract.

In spite of the fact that the RfC methodology represents an improvement in that it provides a justification - at least in part - based on mechanistic considerations for the use of UF_{AH}, there are several basic questions that have to be clarified. Why is $UF_{AH\text{-}TOTAL}$ equal to ten? Why are both $UF_{AH\text{-}TK}$ and $UF_{AH\text{-}TD}$ equal to 3.16? Is the UF_{AH} the same for all chemicals regardless of the toxic endpoint? Is it possible that the $UF_{AH\text{-}TOTAL}$ varies depending on each chemical and species?

There is a need to develop tools/approaches to determine the magnitude and mechanistic basis of the uncertainty factors in general, and of the interspecies uncertainty factors in particular. In the past, there was no quantitative tool that would permit either the estimation of the overall UF_{AH} or its components, and risk assessors were forced to use the default values. A relatively new tool has, however become available which may provide the answers to the questions raised above. This tool is called physiologically-based modeling and is described in the next section.

1.4. INTRODUCTION TO MODELING

Modeling is the art of creating mathematical descriptions of phenomena that appear in reality (Kheir, 1988). It is a means of capturing some aspects of a given reality, within the framework of a mathematical apparatus, and provides us with an instrument for exploring the properties of that reality (natural or man made). A model is a system of postulates, data and inferences presented in a mathematical description and is a representation of an entity or a state of affairs. Models are not reality, and no matter how complex, they are a representation of reality and should never be confused with it (Bekey, 1977).

Because reality cannot be studied in its entirety at the same time, the modeler must at the outset decide which part of reality he will study, i.e. he has to select a system. A system is a subjective entity that encompasses those items important to the objectives of the modeling exercise, and as such reflects the modeler's understanding of reality, its components and their interrelationships. Thus, modeling is grasping a central issue from reality and translating it into an abstract language such as a mathematical model, and it enables us to understand and/or describe reality, at least partially.

Understanding of reality is achieved by: synthesis: use of knowledge of inputs and outputs to infer system characteristics, analysis: use of

knowledge of the parts and their stimuli to account for the observed responses, instrumentation: design a system such that a specified output is the result of an input. Models as representations of reality can be used in each of these areas and when they are, they allow us to: (i) understand an existing physical system or a scientific theory, (ii) predict the future state of a physical system that is currently unknown, and (iii) control a system to produce a desirable condition (Haefner, 1996).

Systems that are modeled mathematically can be classified in several ways, some of which are based on the particular mathematical structure that is used, i.e., classification is based on the mathematical form of the equations. A continuous system is one for which the system variables change continuously with respect to time, whereas in a discrete system variables change only at distinct (specific) instants of time. A stochastic system is one in which the relationships between system variables are random and are described in a probabilistic fashion, whereas in a deterministic system they are described by known and unique mathematical equations. Static models describe a linear (or non-linear) relation between output and input of a function with the aid of algebraic equations, and are applicable for steady-state conditions. Dynamic models describe the behavior of the system in time with the aid of differential equations, and are based on the laws of conservation of energy, mass and momentum. Models that describe biological systems are classified as: compartmental: they

describe the flow of physical materials (e.g., water, blood, etc.,) between physical and biological compartments, transport: those that model transport material from point to point in physical space, and particle: they model the fate of individual particles moving in space. The classification of systems is not mutually exclusive, and a given model can contain elements of several of them. For example, a continuous atmospheric transport model may contain a compartmental model describing the effects of a volatile pollutant in humans.

Mathematical models can also be described or classified as empirical or mechanistic (Hopkins and Leipold, 1996). Empirical models comprise an arbitrary mathematical function and suitable parameter values that adequately describe the process being modeled. The model parameter values are generally obtained by an optimization procedure that adjusts the parameter values until the best fit of the model predictions to the experimental data is found. If no acceptable fit is possible, the arbitrary mathematical function underlying the model is modified or replaced and the optimization procedure is repeated. The end result is a mathematical function and a set of parameter values that adequately describe the process, but there is an implicit understanding that neither the nature of the function nor the parameter values have any fundamental physical significance. Mechanistic models, on the other hand, attempt to describe a system in terms of identifiable physical processes and parameters. With these models,

the parameters have fundamental physical significance, e.g., rate constants, equilibrium constants, initial concentrations, etc.

The process of mathematical modeling involves three steps: (i) identification and characterization of a system's individual elements (subsystems), (ii) identification and characterization of the interaction among the subsystems, and (iii) application of scientific laws (physical, biological, etc.) (Cannon, 1967; Shearer *et al.* 1967; Luenberger, 1979). This type of modeling involves deduction. Experimental modeling, on the other hand, is the selection of mathematical relationships (through induction) of an already existing system by fitting its observed input-output data.

When building models, the most important decision a modeler has to make concerns the choice of model. Since the same "reality" can be represented by several models each describing some aspects of it, of the very many models that can be applied to a specific part of reality only a few can be useful in illuminating the processes being under study. The success of modeling depends on the selection of only those characteristics, among the many that describe the system, that are necessary and sufficient to describe the process accurately enough to suit the objectives of the model and the modeler. It also depends on the constraints imposed in the model which in turn depend on the goal of the model. The model constraints include: realism: the degree to which the model structure mimics reality (in a

biological model one could describe all arteries and veins), precision: the accuracy of model predictions (in precise rat model, the percent inhibition of acetylcholinesterase is exactly the same as in the "real" rat), and generality: the number of systems and applications to which the model correctly applies (a physiological model that includes the gizzard as one of its compartment will only be applicable to birds and none of the mammals). In building models one cannot maximize all three properties. Each of these properties is traded off against each other, depending on the purpose of the model. In general, prediction requires more precision or reality and less generality, understanding needs more generality and less precision, while control needs a lot of precision and less generality (Levins, 1966)

The application of mathematical models in Toxicology serves four broad roles:

- First, a model proposed before experiments are actually done serves as an extended hypothesis that can aid in the experimental design.
- Second, a mathematical model can be used to correlate data.
- Third, by implying the quantitative relationship suggested by a mathematical model outcomes can be predicted at conditions where measurements were not made.
- Fourth, a mathematical model can be used for simulating observed toxicological phenomena in order to determine underlying mechanisms.

1.4.1. Physiological models

Physiologically-based modeling refers to the development of mathematical description of the processes that determine the toxicokinetic and toxicodynamic behavior of a chemical, as well as the quantitative interrelationships among the critical biological determinants of these processes (Leung, 1993; Krishnan and Andersen, 1994). These determinants include physicochemical (e.g., tissue:blood partition coefficients), biochemical (e.g., rate constants for metabolism and binding), physiological (e.g., tissue volumes, blood flow rates, breathing rates) and molecular (e.g., genetic regulation of enzyme activity) parameters.

1.4.2. Development of physiological models

The development of physiologically-based toxicokinetic (PBTK) models is performed in four steps: (i) model representation, (ii) model parameterization, (iii) model simulation and (iv) model validation (Figure 3).

1.4.2.1. Model representation is subdivided into three steps: (a) conceptual, (b) functional and (c) computational description of the model.

1.4.2.1.1. Conceptual representation involves the selection of the appropriate anatomical and physiological features of the animal, and the uptake and disposition pathways of the chemical. The organism i.e., the system is represented by a series of tissue compartments that are physiologically and

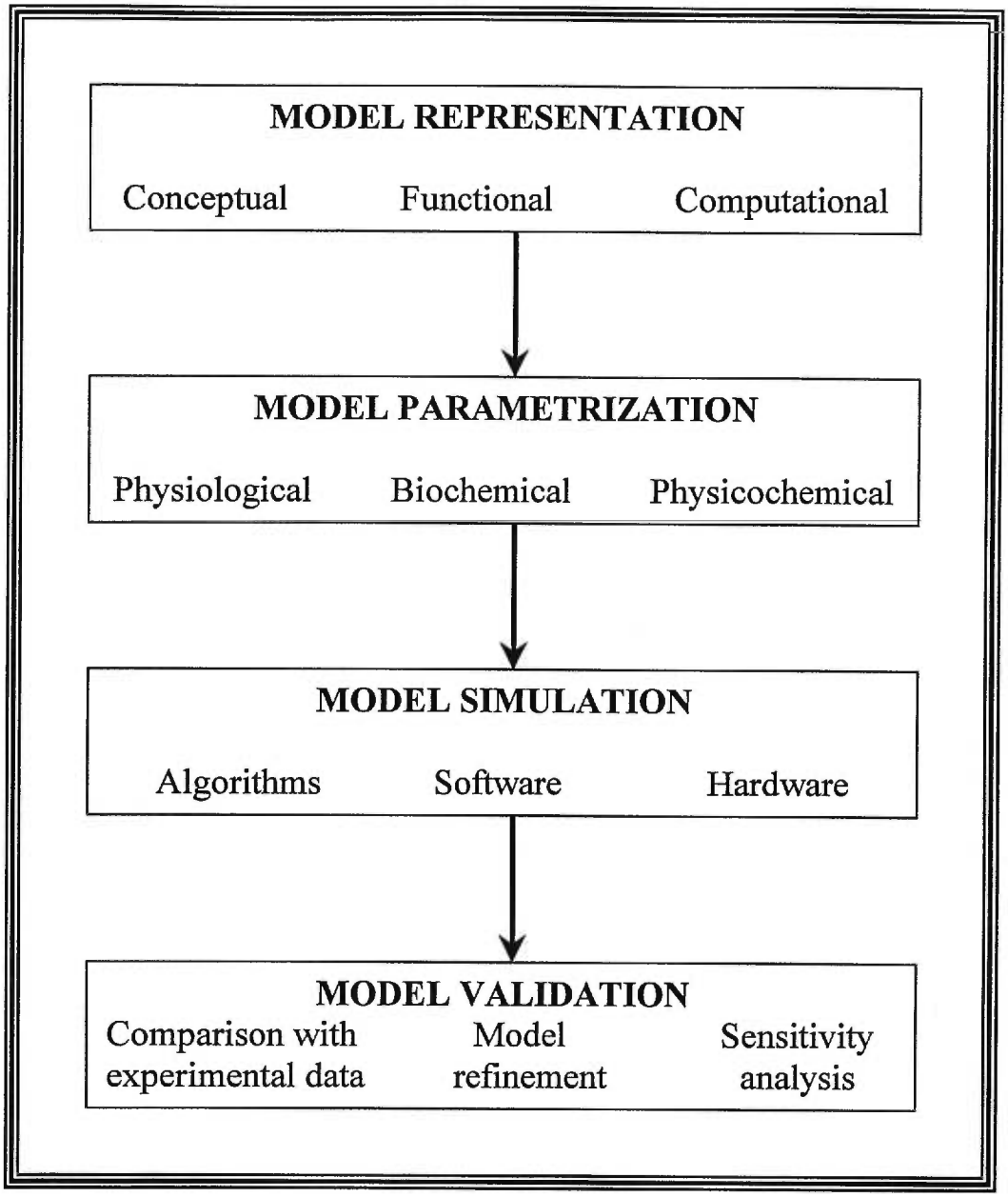

Figure 3: Development of Physiologically-based Toxicokinetic Models

anatomically correct and represent the actual body tissues. The number of tissue compartments depends on the chemical that is modeled, its toxic effects and the objective of the study. Each tissue can be represented as an individual compartment, or a number of tissues sharing the same characteristics (e.g., same rate of blood flow, same partition coefficient, same enzyme activity, etc.) can be lumped together. Additional factors that are taken into consideration when determining the number of compartments include: the site of administration (skin, lungs), the excretion site (urine, lungs), the target organ (brain, blood) and the ability of the chemical to bioaccumulate in specific tissue (fat, bone). Traditionally, only 91% of the actual body volume is modeled with the balance (9%, representing skeletal and structural components) being omitted because they do not play a significant role in the toxicokinetics of organic chemicals. Once the tissue compartments of the animal and pathways of disposition of the chemical are identified, the interrelationships among the critical biological determinants are characterized with a series of differential equations.

1.4.2.1.2. Functional representation involves the mathematical description of the processes that take place in the tissue compartments, the relationships among the mechanistic parameters that determine these processes as well as the relationships among the tissue compartments.

(i). Uptake of chemicals. Figure 4 represents a tissue compartment. The chemical enters the tissue via the arterial blood with concentration equal to CA and flow QT, and exits the tissue via the venous blood with concentration equal to CVT (concentration in venous blood exiting tissue T). The transport of chemicals through the membranes that separate blood from tissues or in the case of volatile compounds from the air across the alveolar spaces in the lungs most commonly occurs by simple diffusion. The uptake of chemical is driven by the difference in concentration on either side of the membrane in accordance to Fick's first law:

$$VT*(dCT/dt) = \kappa*dC \qquad [1\text{-}4\text{-}1]$$

where:

CT =the concentration of the chemical in the tissue

κ =the transfer constant

VT =the volume of the tissue compartment

dCT =the concentration gradient in the tissue

If the transfer is perfusion limited (i.e., blood flow limited), the transfer constant is the rate of blood flow to the compartment, and the following equation describes the rate of change in the amount of chemical in the tissue:

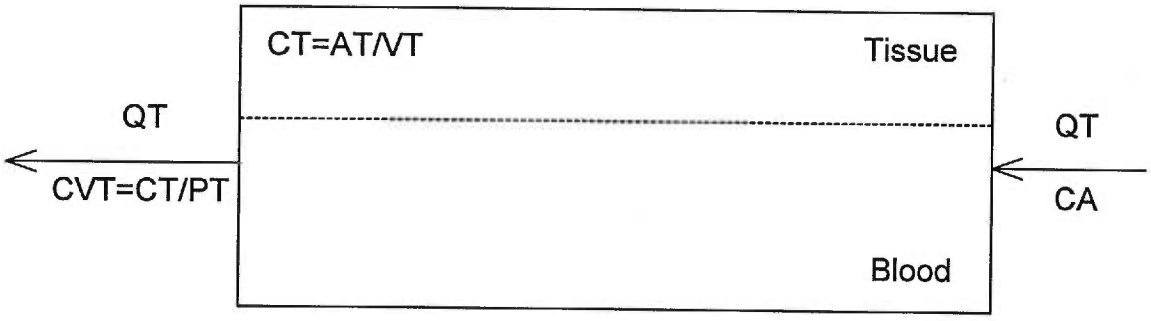

Figure 4. Functional representation of perfusion-limited uptake of chemicals. QT=Blood flow to the tissue, CT=Concentration of chemical in tissue, CA=Concentration of chemical in arterial blood, CVT=Concentration of chemical in the venous blood exiting the tissue, and PT= Tissue:blood partition coefficient.

Rate of change in the amount of chemical in the tissue =input - output

$$VT*(dCT/dt) = QT*(CA - CVT) \quad [1\text{-}4\text{-}2]$$

$$VT*(dCT/dt) = QT*(CA - CT/PT) \quad [1\text{-}4\text{-}3]$$

where:

QT =the blood flow to the tissue

CA =the concentration of chemical in arterial blood

CVT =the concentration of chemical in the venous blood exiting the tissue, and

PT = the tissue:blood partition coefficient.

(ii). Distribution of chemicals. The tissue compartments in a model are connected via the systemic circulation. The arterial circulation distributes the chemical to the tissues, and the venous blood exiting each tissue compartment is combined to yield the mixed venous blood concentration, which reaches the lung via the heart and the cycle restarts.

(iii). Metabolism of chemicals. For metabolizing tissues (e.g., liver) the equation that describes the amount in the tissue has to be modified to account for the amount of chemical being lost through metabolism. Metabolism is usually modeled as a saturable or as a non-saturable (first

order) process. The mass balance differential equation (MBDE) for a metabolizing tissue is as follows:

Rate of change in the amount of chemical In the tissue =input - output - rate of loss due to metabolism

$$VT*(dC/dt) = QT*(CA-CT/PT) - (VMAX*CT/PT)/(KM+CT/PT) \quad [1\text{-}4\text{-}4]$$

or

$$VT*(dC/dt) = QT*(CA-CT/PT) - KF*CVT*VT \quad [1\text{-}4\text{-}5]$$

where:

VMAX =the maximum velocity of metabolism

KM =the Michaelis constant, and

KF =the first order rate constant

(iv). Excretion of chemicals. The most common route of excretion, particularly for those that are volatile, is expired air and urine , and the following equations are used to describe them.

Urinary excretion:

Rate of amount of chemical excreted in urine =urinary excretion constant * concentration of chemical in arterial blood * volume of blood

$$dAEU/dt = KUE*CA*VB \quad [1\text{-}4\text{-}6]$$

where:

KUE =the urinary excretion constant, and

VB =the volume of arterial blood

Pulmonary excretion:

The concentration of chemical in exhaled air (CX) is given by the following equation.

$$CX = (0.7*CA/PB) + (0.3*CINH) \quad [1\text{-}4\text{-}7]$$

where:

PB =Blood:air partition coefficient, and

CINH =Concentration of chemical in inhaled air

1.4.2.1.3. Computational representation

Once the structure of the model has been outlined and each tissue compartment has been described mathematically, the differential equations that describe the model must be written in a programming language to be used for simulation. Examples of simulation languages commonly encounetered in PBPK modeling include ACSL®, SCOPE® and MATLAB®.

1.4.2.2. Model parameterization.

It deals with the estimation of the numerical values of the parameters of the system being modeled. In general, the more *a priori* information about the system is available, the "better" the model will be. Models that assume less *a priori* knowledge are not only less accurate but also more complex in terms of their functional representation and require more computational time than those with more prior knowledge (Kheir 1988). Three type of parameters are employed in physiological-based models, physiological, physicochemical and biochemical.

1.4.2.2.1. Physiological parameters such as breathing rates, blood flow rates and tissue volumes are generally measured directly in the animal species of interest or obtained from the literature. If the values of any of the parameters are not directly known, allometric extrapolation is employed for their estimation. Briefly, the parameters and the allometric equations that are used in estimating them are presented below (Leung, 1993; Krishnan and Andersen, 1994).

i) Organ volumes.

It is generally accepted that organ volumes can be scaled across species using the following allometric equation:

$$V_i = V_j * (BW)^{1.0} \qquad [1\text{-}4\text{-}8]$$

where:

V_j = is the species-independent allometric constant.

This has been based on the work of Stahl (1967), Schmidt-Nielsen (1984), and the recommendations of National Research Council (1986).

ii) Cardiac output

The work of Guyton (1971) showed that cardiac output is a function of basal metabolism. Based on body weight extrapolation the following allometric equation is derived and used to estimate the cardiac output, and its distribution to the different tissues:

$$QC_i = QC_j * (BW)^{0.74} \qquad [1\text{-}4\text{-}9]$$

where:

QC_j = is the species-independent allometric constant.

iii) Alveolar ventilation

According to Guyton (1947), Adolph (1949) and Stahl (1967), the fraction of ventilation volume available for gas exchange is a function of body weight and the following allometric equation is used:

$$Q_{alvi} = Q_{alvj} * (BW)^{0.74} \qquad [1\text{-}4\text{-}10]$$

where:

Q_{alvj} = is the species-independent allometric constant.

iv) Renal clearance

Adolph (1949) showed that the rate of elimination of insulin by the kidneys is a function of $BW^{0.74}$. This finding was corroborated by the studies of Brody (1945), Edwards (1975), Lindstedt and Calder (1981), Boxenbaum (1982a), Schmidt-Nielsen (1984) and Mordenti (1986a), and the following allometric equation is used:

$$K_i = K_j * (BW)^{0.74} \qquad [1\text{-}4\text{-}11]$$

where:

K_j = is the species-independent allometric constant.

1.4.2.2.2. Physicochemical parameters refer to partition coefficients, which describe the solubility of the chemical in tissues. The partition coefficient of a chemical between two media is defined as the ratio of the equilibrium chemical concentration in the first medium to the chemical concentration in the second medium. The most common measurements for volatile organics are blood/air and tissue/air partition coefficients with tissue/blood derived as the ratio of (tissue/air)/(blood/air). It is generally believed that tissue/air partition coefficients are constant across species, while blood/air partition coefficients are species-dependent (Gargas *et al.* 1989).

1.4.2.2.3. Biochemical parameters such as rates of absorption, biotransformation, binding and excretion are determined by conducting time-course *in vivo* or *in vitro* experiments. In the absence of experimental data, allometric extrapolation may be used. When metabolism is described as a saturable process the following equation is used to describe the rate of the amount metabolized (dA_{met}/dt):

$$\frac{dA_{met}}{dt} = \frac{VMAX * CVT}{KM + CVT} \qquad [1\text{-}4\text{-}12]$$

With respect to VMAX body weight extrapolation is the method most commonly used (Leung, 1993; Krishnan and Andersen, 1994).

$$VMAX_i = VMAX_j * (BW)^{0.74} \qquad [1\text{-}4\text{-}13]$$

where:

$VMAX_j$ = the species-independent allometric constant.

The Michaelis-Menten constant, KM, is assumed to be species-invariant and thus the same value is used when modeling the kinetics of the same toxicant in different species.

1.4.2.3. Model simulation

Simulation is the process of experimenting with a computerized system model such that the specific purpose of the study is achieved through observing the model's behavior under the assumptions defined by the experimenter. The computerized model is an operational computer program that implements a system's model and is used for:

- obtaining model responses in order to analyze and understand their dynamic behavior,
- comparison of alternatives model designs on the basis of some performance measures,
- retrospective and prospective analysis, and
- sensitivity analysis and parameter optimization studies.

Simulation is used when experiments with real systems is:

- impossible,
- expensive,
- too fast or too slow, and
- for extrapolation of measured data.

1.4.2.4. Model validation.

Model validation is defined as the substantiation that a computer model represents the system's model within specified limits of accuracy. It

requires comparison of its behavior, i.e., the simulation results, with that of the real system (observed data).

1.4.3. Theory of physiological toxicokinetic modeling

In the model shown in Figure 5, the following mass balance equations are applicable:

$$VF*(dCF/dt) = QF*(CA-CVF) \quad [1\text{-}4\text{-}14]$$

$$VS*(dCS/dt) = QS*(CA-CVS) \quad [1\text{-}4\text{-}15]$$

$$VR*(dCR/dt) = QR*(CA-CVR) \quad [1\text{-}4\text{-}16]$$

$$VL*(dCL/dt) = QL*(CA-CVL) - dA_{met}/dt \quad [1\text{-}4\text{-}17]$$

$$CA = (QP*CINH+QC*CV) / (QC+(QP/PB)) \quad [1\text{-}4\text{-}18]$$

$$CV = (QF*CVF + QL*CVL + QS*CVS + QR*CRV)/QC \quad [1\text{-}4\text{-}19]$$

where:

Vi =Volume of the ith tissue compartment

CINH =Concentration of the chemical in inhaled air

CV =Concentration of the chemical in venous blood

CA =Concentration of the chemical in arterial blood

CVi =Concentration of the chemical in the venous blood exiting the ith compartment

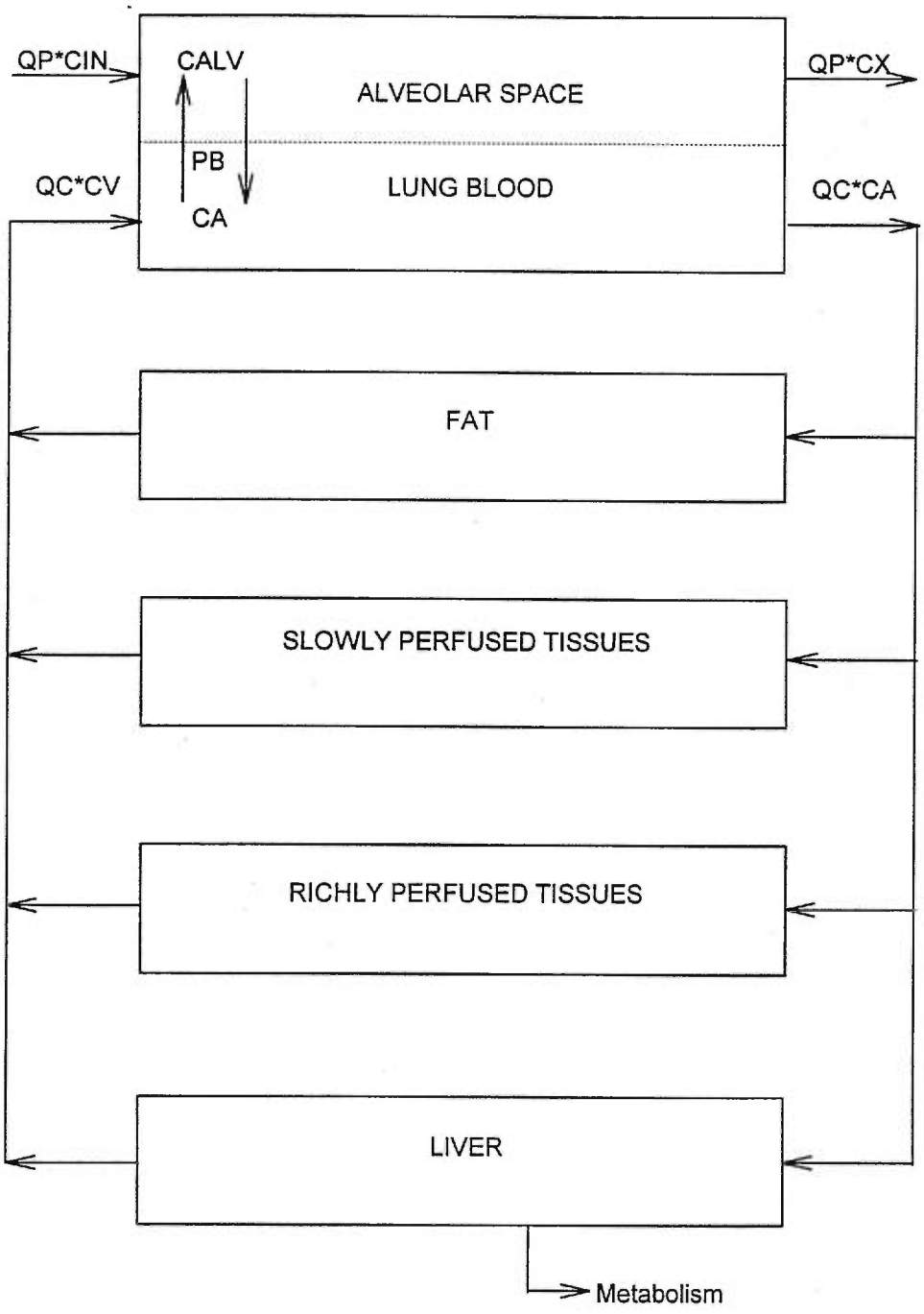

Figure 5: Conceptual Representation of a Physiologically-based Toxicokinetic Model

Ci =Concentration of the chemical in ith tissue compartment

QC =Cardiac output

Qi =Blood flow in the ith compartment

QP =Pulmonary ventilation

A_{met} =Amount metabolized, and

PB =Blood:air partition coefficient

The symbols F, S, R and L designate the fat, slowly perfused, richly perfused, and liver compartments respectively. It is assumed that the delivery of the chemical in the different tissue compartments is perfusion limited, and that there is no macromolecular binding of the chemical in blood or any of the tissues. In the above equations the terms that describe the volumes and flows of each compartment are considered known but the terms CF, CL, CS, CR, CV, CA, CVF, CVL, CVS and CVR are not. Thus, there are 6 equations and 10 unknown variables. In order to solve these equations the venous exit condition, which states that the blood flowing out of a tissue compartment has a chemical concentration proportional to the concentration of the chemical in the tissue compartment, is used (Perl, 1972).

$CVi = \gamma * Ci$ or

$CVi = 1/PCi * Ci$ or

$CVi = Ci/PCi$

where:

PCi =the ith tissue / blood partition coefficient

The coefficient γ may be thought as inversely proportional to partition coefficient. By using the venous exit condition (i.e., tissue:blood partition coefficients) and provided that the tissue:partition coefficients and metabolic constants are known, the number of variables is reduced to six, and the equations can be solved using numerical methods, thus providing estimates of tissue concentrations.

1.4.4. Application of Physiological Models in Risk Assessment and the Estimation of Interspecies Uncertainty Factors

Every adverse effect has a dose-response curve, the shape of which is determined by:

- the relationship between exposure and dose in the target tissue
- the relationship between the parent compound in the target tissue and its biologically active form, and
- the sequence of events triggered by the biologically active form, which produces the effect.

The goal of quantitative risk assessment is to accurately predict the shape of the dose-response curve in humans from animal studies, thereby allowing direct translation from exposure to risk of adverse effect. In this

section the application of allometry and physiological modeling in extrapolating animal data to humans will be discussed. The original National Academy of Science report used the expression "dose-response assessment to refer to the process of estimating the expected incidence of response for various exposure levels in animals and people (NRC 1983). Because tissue dose is not always proportional to exposure concentration and the need to clearly distinguish between the two concepts, the use of the more comprehensive expression "exposure-dose-response assessment has been promoted (Andersen *et al.* 1992). This expression refers to the determination of the quantitative relationship between exposure levels and target tissue dose, and further the relationship between tissue dose and observed response in animals and humans.

Physiological models may be used in non-cancer risk assessment to:

- convert exposure concentration or doses to internal dose for NOAEL determination in the critical study.
- allow integration and extrapolation using diverse data, and
- enable interspecies toxicokinetic and toxicodynamic comparisons

The most important property of physiological models in risk assessment is their ability to incorporate toxicokinetic information of both experimental animals and humans. The same model can be used to describe the toxicokinetic behavior of a chemical in different species. All that is required is

a change in the species-specific values of the mechanistic determinants of toxicity, i.e., the physicochemical, biochemical and physiological parameters. Once the model has been constructed and validated in a species, the overall behavior of the same chemical in different species can be validated and compared. In doing so, the PBTK model may allow the quantitative evaluation of interspecies uncertainty and may ultimately enhance the accuracy of health risk assessment process. This can be stated in the form of a hypothesis:

"PBTK models can be used to quantitate the interspecies toxicokinetic uncertainty factors"

Despite its important implications in risk assessment, surprisingly, there have been few attempts to test this hypothesis (Clewell and Jarnot, 1994). If valid, this approach can serve as a logical tool to determine the chemical-specific interspecies toxicokinetic uncertainty factors.

1.5. OBJECTIVES

1.5.1. General objective

To elucidate the magnitude and mechanistic basis of the animal-human toxicokinetic uncertainty factor ($UF_{AH\text{-}TK}$) for organic chemicals, using a physiological modeling approach.

1.5.2. Specific objectives

(i) To determine the magnitude of $UF_{AH\text{-}TK}$ for the carbamate pesticide aldicarb following the development and validation of rat and human physiological models.

(ii) To determine the magnitude of the $UF_{AH\text{-}TK}$ for eleven volatile organic chemicals, using previously published rat and human physiological models.

(iii) To identify the mechanistic determinants and the magnitude of $UF_{AH\text{-}TK}$ determined per preceding objectives, by developing physiologically-based algebraic expressions of the toxicokinetics of organic chemicals at steady-state in rats and humans.

1.6. APPROACH

The magnitude of the $UF_{AH\text{-}TK}$ was initially determined by developing rat and human PBTK models for the carbamate pesticide aldicarb, and then the methodology was extended to determine the magnitude of $UF_{AH\text{-}TK}$ of eleven other chemicals. Subsequently, the PBTK models for steady-state conditions were simplified to develop algebraic expressions which were then used to identify the critical determinants of $UF_{AH\text{-}TK}$. In the following sub-sections, the methodological approaches used to accomplish the above objectives are briefly outlined.

1.6.1. Determination of the toxicokinetic interspecies uncertainty factor for the carbamate pesticide aldicarb with physiological models

The first objective of the thesis is to evaluate the applicability of physiological models in the determination of interspecies uncertainty factors, using the carbamate pesticide aldicarb (ALD) as a model chemical. Initially, a physiological model that describes ALD toxicokinetics in rats and humans will be developed. The physiological parameters for the rat and human PBTK models (blood flow rates, cardiac output, and tissue volumes) will be obtained from the literature. For the determination of the tissue:blood partition coefficients of ALD a novel approach will be developed that will facilitate their calculation. This will involve the characterization of each tissue compartment as a mixture of neutral lipids, phospholipids, and water, as well as the

determination of oil and water solubility of ALD, since these physicochemical properties approximate the solubility of ALD in tissue lipids and water. This tissue composition-based model framework will provide the means for the "automatic" calculation of the tissue:blood partition coefficients of ALD (during each simulation run). The biochemical parameters (maximum rate of aldicarb oxidation and the Michaelis constant) will be determined in both species by quantitating the levels of metabolites produced during *in vitro* microsomal incubations.

The adequacy of the rat tissue composition PBTK model for ALD will be assessed by comparing the model simulations of the blood time-course concentrations of the metabolite (aldicarb sulfoxide, ALX) with those obtained from *in vivo* intravenous administration of ALD. Due to the unavailability of human tissue concentration data, and since ethical considerations prohibit experimentation in humans, the validation of the human model will be based on available data that describe profile of ALD-induced cholinesterase inhibition in humans. This will necessitate the expansion of the PBTK model to include the description of ALD-induced acetylcholinesterase inhibition. The model will be validated first in the rat by comparing the simulations of acetylcholinesterase inhibition patterns in blood with experimental data obtained from the *iv* administrations and then in humans. Once both the rat and human models have been validated, they will be run under the same exposure scenario and the respective areas under the blood and brain concentrations vs time curves

(AUC) will be estimated. The interspecies toxicokinetic uncertainty factor, i.e., the rat/human ratio of the AUCs will be calculated and compared with the default value.

1.6.2. Determination of the interspecies toxicokinetic uncertainty factor for organic chemicals with physiological models

Upon the demonstration of the applicability of the PBTK-based methodology in the evaluation of the $UF_{AH\text{-}TK}$ of aldicarb, the same approach will be applied in the estimation of $UF_{AH\text{-}TK}$ for other chemicals. Validated animal and human PBTK models will be run under the same exposure scenario to estimate the total dose received, blood and tissue concentrations of the parent compound, and concentrations of the metabolite in animals and humans. Then the ratio of the respective concentrations will reflect the magnitude of the toxicokinetic component of the interspecies uncertainty factor. At the same time the accuracy of the default interspecies toxicokinetic uncertainty factor will be assessed by comparing the respective ratios, and the degree of deviation from 3.16.

1.6.3. Mechanistic determinants of the toxicokinetic interspecies uncertainty factors

With the applicability of physiological models in the estimation of $UF_{AH\text{-}TK}$ well established, the unanswered question pertains to the nature of the factors that determine the toxicokinetic variability across species. Since

the interspecies toxicokinetic uncertainty factors used in risk assessments typically are for a chronic exposure scenario leading to steady-state condition, the steady-state concentrations of chemicals will be predicted by simplifying the PBTK model equations. Analytical expressions for predicting steady-state conditions in rats and humans will be developed by simplifying the PBTK model equations such that the predictions provided by both approaches will be identical.

These equations will permit the characterization of the magnitude and mechanistic determinants of the components of the interspecies toxicokinetic uncertainty factors. The values of the mechanistic parameters in rats and humans will be used to estimate the rat/human ratio of blood and tissue concentrations for the same exposure scenario, and the degree of deviation of these ratios from the currently used factor of 3.16 will be examined to identify situations where the current default approach should be adequate.

CHAPTER 2

Article No 1

(Published in:Toxicology and Industrial Health,

Vol. 11, No. 5, pp. 511-522, 1995)

AN APPROACH FOR INCORPORATING TISSUE COMPOSITION DATA INTO PHYSIOLOGICALLY BASED PHARMACOKINETIC MODELS

MICHAEL PELEKIS, PATRICK POULIN, AND KANNAN KRISHNAN

Département de médecine du travail et d'hygiène du milieu,

Université de Montréal, C. P. 6128, Succ. Centre-ville,

Montréal, Québec, Canada, H3C 3J7

1. Address all correspondence to: K. Krishnan, Département de médecine du travail et d'hygiène du milieu, Faculté de médecine, Université de Montréal, 2375 chemin de la Côte Ste. Catherine, Montréal, PQ, CANADA, H3T IA8. Tel.:(514) 343-6581. Fax:(514) 343-2200.

2. Abbreviations: ACSL®, Advanced Continuous Simulation Language; DNA, deoxyribonucleic acid; DCM, dichloromethane; GSH, glutathione; Cl, liver concentration of DCM; PCs, partition coefficients; PBPK, physiologically based pharmacokinetic; QSAR, quantitative structure activity relationship; Cv, venous blood concentration of DCM; VOCS, volatile organic chemicals.

3. Key Words: tissue composition, PBPK models, partition coefficients.

ABSTRACT

The objective of this study was to develop an approach for incorporating tissue composition data into physiologically based pharmacokinetic (PBPK) models in order to facilitate "built-in" calculation of tissue:air partition coefficients (PCs) of volatile organic chemicals. The approach involved characterizing tissue compartments within PBPK models as a mixture of neutral lipids, phospholipids, and water (instead of using the conventional description of them as "empty " boxes). This approach enabled automated calculation of the tissue solubility of chemicals from n-octanol and water solubility data, since these data approximate those of solubility in tissue lipids and water. Tissue solubility was divided by the saturable vapor concentration at 37^0C to estimate the tissue:air PCs within PBPK models, according to the method of Poulin and Krishnan (1995c). The highest and lowest lipid and water levels for human muscle, liver, and adipose tissues were obtained from the literature and incorporated within the tissue composition-based PBPK model to calculate the tissue:air PCs of dichloromethane (DCM) and simulate the pharmacokinetics of DCM in humans. The PC values predicted for human tissues were comparable to those estimated using rat tissues in cases where the relative levels of lipids and water were comparable in both species. These results suggest that the default assumption of using rat tissue:air PCs in human PBPK models may be acceptable for certain tissues (liver, adipose tissues), but questionable for

others (e.g., muscle). The PBPK modeling exercise indicated that the interindividual differences in tissue dose arising from variations of tissue:air PCs may not be reflected sufficiently by venous blood concentrations. Overall, the present approach of incorporating tissue composition data into PBPK models would not only enhance the biological basis of these models but also provide a means of evaluating the impact of interindividual and interspecies differences in tissue composition on the tissue dose surrogates used in PBPK-based risk assessments.

INTRODUCTION

Physiologically based pharmacokinetic (PBPK) models incorporate data on physiological parameters, biochemical rate constants, and partition coefficients (PCs) to provide simulations of tissue dose of chemicals in exposed animals. Very few studies have attempted to incorporate data on specific tissue components within PBPK models. Among those that have are D'Souza *et al.* (1988), Frederick *et al.* (1992), and Krishnan *et al.* (1992), which included tissue concentrations of glutathione (GSH), nonprotein sulfhydryls, and DNA, respectively, in PBPK models. The inclusion of this kind of tissue component data was useful for describing the reactivity of specific chemicals within PBPK models. The reactivity of chemicals in these cases (i.e., GSH conjugation, DNA binding) was described as a second order process, which required the specification of the tissue concentration of the co-reactant (i.e., GSH, DNA). The reactivity of volatile organic chemicals (VOCs) is only secondary to the normal tissue uptake process.

The tissue uptake of VOCs in PBPK models is often described as a perfusion-limited process requiring estimates of tissue blood flow rates and tissue:blood PCs. The tissue:blood PCs of VOCs are obtained by dividing tissue:air PC values by the blood:air PC provided as input to the model. It has recently been shown that tissue:air PCs of VOCs can be predicted with information on (1) the neutral lipid, phospholipid, and water contents of tissues, and (2) the solubility of chemicals in n-octanol (or vegetable oil),

water (or saline), and air (Poulin and Krishnan, 1995a,c). Therefore, tissue:air PCs may be calculated within PBPK models if they contain data on the lipid and water contents of tissues and data on chemical solubility.

The objective of the present study was to develop an approach for incorporating tissue composition data into PBPK models to facilitate a "built-in" calculation of tissue:air PCs of VOCs, using dichloromethane (DCM) as an example.

METHODS

To develop and illustrate an approach for incorporating tissue composition data into PBPK models, we chose to work with a previously published human PBPK model for DCM. This PBPK model was developed and validated by Andersen *et al.* (1987, 1991). It consists of four tissue compartments (liver, adipose tissue, slowly perfused tissues, and richly perfused tissues) interconnected by systemic circulation and a gas-exchange lung, and it describes tissue uptake of DCM as a perfusion-limited process. These authors provided the human blood:air and rat tissue:air PCs of DCM as input parameters. The human tissue:blood PCs required were calculated by dividing rat tissue:air PCs with the human blood:air PC of DCM. Whereas Andersen *et al.* (1987, 1991) estimated human blood:air PC of DCM experimentally, they assumed the tissue:air PCs of DCM to be species-invariant, and thus used the tissue:air PCs of DCM determined with rat tissues in the human model.

Instead of being provided as inputs, tissue:air and blood:air PCs could be calculated using the tissue composition- and blood composition-based algorithms (Poulin and Krishnan, 1995c,d) if the PBPK model included data on (1) levels of lipids and water in tissues and blood, and (2) n-octanol, water, and air solubility of DCM. In the present work, we only considered incorporation of tissue composition data into the PBPK model along with

information on DCM solubility in air, water, and n-octanol to predict the tissue:air PCs of DCM. To facilitate this process, the volume fraction of neutral lipids, phospholipids, and water in each tissue can be included in the PBPK model. Alternatively, the volume of tissues specified in the conventional PBPK models can be replaced by the actual volumes of neutral lipids, phospholipids, water, and other components (e.g., GSH, DNA, proteins) in each tissue. Of these, the data on lipid and water contents can be used in the tissue composition-based algorithm along with DCM solubility data to calculate tissue:air PCs (Poulin and Krishnan, 1995a,c).

Tissue Composition-Based PBPK Model

The incorporation of tissue composition data into PBPK models written in ACSL® (Advanced Continuous Simulation Language, Mitchell and Gauthier Inc., Concord, MA) was accomplished as follows:

1. The tissue:air PCs of DCM listed as input parameters in the INITIAL section of the conventional DCM PBPK model (.CSL) file written in ACSL® (Andersen *et al.* 1987, 1991; Krishnan and Andersen, 1994) were deleted.

2. The fractional volumes of neutral lipids, phospholipids, and water in each tissue were included as input parameters in the INITIAL section of the .CSL file.

3. Additionally, data on the solubility of DCM in water, n-octanol, and air (i.e., saturable vapor concentration) were included as input parameters in the INITIAL section of the .CSL file.

4. In the subsection of the INITIAL section entitled "calculated parameters," equations were included for (1) estimating DCM solubility in each tissue, (2) generating the tissue:air PC numbers by dividing DCM solubility in tissues by its saturable vapor concentration (Poulin and Krishnan, 1995c), and (3) calculating tissue:blood PCs by dividing the predicted human tissue:air PCs by the experimentally determined human blood:air PC (Andersen *et al.* 1991).

The tissue composition-based PBPK model written in ACSL®, as outlined above, is shown in the Appendix. When the PBPK model was run, the solubility of DCM in various tissues (muscle, liver, richly perfused tissues, adipose tissues) and the tissue:air PCs were estimated. The tissue:air PCs, in turn, were used as inputs for the calculation of tissue:blood PCs.

Accounting for Variability of Human Tissue Composition in PBPK Models

The available approaches for evaluating the impact of the uncertainty and variability of PBPK model parameters use distributions of physiological and biochemical parameters for the population of interest, but assume that the PCs vary within 20-40% of the mean values (e.g., Bois *et al.* 1990;

Krewski *et al.* 1995). The rationale underlying this assumption appears to be related to the presumed degree of error associated with the experimental measurement of PCs, and not necessarily to an understanding of the mechanistic factors contributing to interindividual variations in PCs. Since the mechanistic basis of the tissue partitioning process appears to depend on the relative levels of various lipids and water in tissues (Poulin and Krishnan, 1995a), we undertook a literature search to obtain data on the highest and lowest levels of water, total lipids, and phospholipids in human muscle, liver, and adipose tissues.

For human muscle, the highest and lowest levels of total lipids and phospholipids were obtained from Fletcher (1972) and Simon and Rouser (1969), while corresponding data on water content were obtained from Mitchell *et al.* (1945) and Forbes *et al.* (1953). The extreme values of total lipid and water content of human adipose tissue were obtained from Thomas (1962) and Forbes *et al.* (1953), and the data on phospholipid content of mammalian adipose tissue were obtained from Shapiro (1977). In doing so, we neglected three older reports (see Thomas, 1962) of greater (and probably unrealistic) water content of human adipose tissues (28-50%). For human liver, data on the highest and lowest levels of water, total lipids, and phospholipids were derived from the following sources: Long (1961), Simon and Rouser (1969), Rouser *et al.* (1969), and Fiserova-Bergerova (1983). The highest (and lowest) neutral lipid levels in various tissues were estimated

as the difference between the highest (or lowest) total lipid and the highest (or lowest) phospholipid levels. Of the above references, Simon and Rouser (1969) and Rouser *et al.* (1969), the sources of data on the lowest phospholipid content of tissues, reported the results as mg lipid phosphorus, without specifying the required conversion factor for calculating the actual concentration of phospholipids. Therefore, the data on mg lipid phosphorus provided by these authors were multiplied with the conversion factor (25) obtained from Nelson (1967). In collecting these data, no effort or judgement was made to differentiate experimental errors from true variability, or to classify the data according to sex, age, or disease state.

The human tissue composition data were then arranged to represent the extremes of lipid and water contents, i.e., high and low (Table 1). The "high" tissue composition data set corresponded to the highest neutral lipid levels in tissues, and the "low" tissue composition data set corresponded to the lowest neutral lipid level obtained from the literature for each human tissue. In the case of adipose tissue, the low (high) lipid levels were combined with high (low) water levels such that the total of volume fractions does not exceed 1. Using these extremities of human tissue composition data, we calculated the tissue solubility of DCM in liver (also a representative for richly perfused tissues), adipose tissues, and slowly perfused tissues (muscle). The human tissue:air and tissue:blood PCs were then estimated as detailed in the preceding section.

Model Simulations

Simulations of the venous blood (Cv) and liver (Cl) concentrations of DCM in humans exposed to 100 ppm of DCM for six hours were obtained using the "high" and "low" tissue composition-based DCM PBPK model. These were compared with the simulations obtained using the conventional DCM PBPK model as described by Andersen *et al.* (1991). All simulations were conducted using ACSL® (version 11.2.1) for IBM-PC.

RESULTS

The tissue:air PCs of DCM predicted using extreme values of human tissue composition data obtained from the literature were compared with the PC values used by Andersen *et al.* (1991) (Table 2). These authors used rat tissue:air PCs in the human PBPK model with the assumption that the tissue:air PCs are species-invariant. These tissue:air PCs, with the exception of muscle:air, were within the range of PCs predicted using data on extremities of human tissue composition. The simulations of Cv in humans exposed to 100 ppm DCM for six hours obtained with the conventional PBPK model (Andersen *et al.* 1991) are compared with those obtained using the tissue composition-based PBPK models in Figure 1. The simulations of Cl obtained with the conventional and tissue composition-based models are presented in Figure 2. For both Cv and Cl, the simulations of the conventional PBPK model for DCM (Andersen *et al.* 1991) were within, or very close to, the range predicted by the present approach.

DISCUSSION

Tissue:blood PCs, representing the relative distribution of chemicals between tissues and blood at equilibrium, constitute an important set of input parameters for PBPK models. These PCs can be estimated as a ratio of chemical solubility (in the absence of any additional active uptake or binding processes) in tissues and blood, which in turn is determined by the relative contents of neutral lipids, phospholipids, and water in these matrices (Poulin and Krishnan, 1995a). Such tissue or blood composition data have not been included routinely in the PBPK models, even though they would facilitate the estimation of tissue and blood solubility, and thus of tissue:blood PCs of chemicals. The approach presented in this article enables the consideration of the levels of critical tissue components necessary to facilitate the automated calculation of tissue:air PCs of VOCs within PBPK models.

All previous PBPK modeling efforts have assumed tissue:air PCs to be species-invariant and have conducted interspecies, particularly rat to human, extrapolations (Ramsey and Andersen, 1984; Reitz *et al.* 1988, 1990; Ward *et al.* 1988; Koizumi, 1989; Tardif *et al.* 1995). The scientific basis for such an assumption has never been presented or investigated. According to the approach used here, the tissue lipid and water contents are the principal determinants of tissue:air PCs. Consequently, if the water and

lipid contents of the various tissues in rats and humans are comparable, then the tissue:air PCs in these species would be comparable as well.

Table 3 presents a comparison of the tissue composition data used in the present study with those of the rat. These data indicate that the percentages of the various constituents in liver and adipose tissue of the rat and human are comparable. It is logical then that the human liver:air and adipose tissue:air PCs of DCM are comparable to those previously obtained using rat tissues (Andersen *et al.* 1987, 1991). The rat/human difference in muscle:air PCs may be attributed to differences in neutral lipid levels, associated with type of muscle analyzed. Even though the range of rat muscle neutral lipid levels was not considered in the present study, at least a single literature value (shown in Table 3) is outside the reported range for human muscle. In this context, it might be interesting to undertake a systematic comparison of rat and human muscle:air PCs of VOCs.

The tissue composition data used here represent the extremities of lipid and water levels found in the literature, and it is important to realize that the high and the low sets do not actually reflect any one individual. In choosing to use these extreme values, our strategy was to examine the magnitude of difference in PC values and tissue dose of DCM associated with these plausible, if not realistic, upper and lower limits of tissue lipid and water levels.

Human blood composition data also can be incorporated within PBPK models using the methodological approach presented in this article. We think more work is necessary to elucidate the role and importance of protein binding as a determinant, however, before a conclusion is reached about the mechanistic factors of human blood:air PCs (Featherstone and Schoenborn, 1964; Lam *et al.* 1990; Poulin and Krishnan, 1995a).

The PBPK model framework used here allows consideration of the impact of variability in the type and content of tissue lipids on the pharmacokinetics and target tissue dose of chemicals. The simulation exercise indicated that for DCM, the Cv is not influenced markedly by changes in tissue composition. The liver concentrations obtained using the high and low tissue composition data sets were found to differ, however, by about a factor of two. The magnitude of change in tissue:air PCs of DCM is smaller than might be anticipated for the range of tissue neutral lipid levels considered in the present study. This may be a consequence of the hydrophilicity-lipophilicity characteristics of DCM [log n-octanol:water PC=1.25 (Howard, 1990)], such that its tissue solubility may not be more sensitive to changes in lipid levels than to tissue water levels. This may not be the case with more lipophilic chemicals, however, the solubility in water of which is negligible.

In the present study, DCM solubility in n-octanol was used as a surrogate for DCM solubility in neutral lipids. The use of n-octanol, however, leads to erroneous predictions of tissue solubility, particularly for chemicals containing oxygen (e.g., alcohols, ketones, acetate esters) (Poulin and Krishnan, 1995b). These hydrophilic organics exhibit a greater affinity for n-octanol than for biotic neutral lipids, and consequently n-octanol solubility data overestimate the tissue lipid solubility of these chemicals (Poulin and Krishnan, 1995b). Therefore, in extending the present approach to organics containing one or more oxygen atoms in their molecule, it is preferable to use solubility data obtained in vegetable oils (olive or corn) instead of n-octanol, as the surrogate for biotic lipids (Poulin and Krishnan, 1995b).

The proposed approach of incorporating tissue composition data into PBPK models would change the way we describe the volume of tissue compartments to include more biologically relevant information. This model structure should allow the consideration of inter-individual differences not only in physiological and biochemical parameters, but also in tissue composition (i.e., neutral lipids, phospholipids, water). The latter aspect has not been addressed in previous attempts at uncertainty and variability analyses of PBPK models, but should be possible with the use of the tissue composition-based PBPK modeling framework. Once the critical determinants of blood solubility are elucidated, they can be incorporated within PBPK models such that tissue:blood PCs of VOCs and nonvolatile

organics, alike, can be estimated within PBPK models. Such an approach should contribute to reducing animal use in the estimation of PCs required for developing PBPK models. The obvious disadvantage of this approach, however, is the increase in the number of input parameters, even though such parameters, once determined for a particular species, should not change from a PBPK model of one chemical to another, unless a chemical is shown to affect tissue lipid levels during or following exposures. Since both water solubility and n-octanol:water PCs of organic chemicals can be estimated from their molecular structures (e.g., Hansch and Leo, 1979; Suzuki, 1991), the incorporation of tissue composition-based algorithms within PBPK models for predicting tissue:air and tissue:blood PCs provides the starting point for developing QSAR-type PBPK models.

Copies of the tissue composition-based PBPK model for DCM written in ACSL® are available by writing to the authors.

APPENDIX

TISSUE COMPOSITION-BASED PBPK MODEL

WRITTEN IN ADVANCED CONTINUOUS SIMULATION LANGUAGE®

```
INITIAL SECTION

!Constants

CONSTANT SA= 35.59          !Saturable vapour concentration of DCM at
                            !37^0C (mol/m^3)

CONSTANT SO= 4561.0         !Solubility of DCM in n-octanol (mol/m^3)

CONSTANT SW= 256.5          !Solubility of DCM in water (mol/m^3)

CONSTANT NL= 0.0853         !Neutral lipid content of human liver (as a
                            !fraction of liver volume)

CONSTANT PL= 0.0617         !Phospholipid content of human liver (as a
                            !fraction of liver volume)

CONSTANT WL= 0.790          !Water content of human liver (as a fraction
                            !of liver volume)

CONSTANT OL= 0.0630         !Other components in human liver (as
                            !fraction of liver volume), calculated as 1-
                            !(NL+PL+WL)

CONSTANT PBA =8.94          !Human blood:air PC of DCM from Andersen
                            !et al. (1991)
```

```
!Calculated parameters
SL = [SO*(NL+0.3*PL)+SW*(WL+0.7*PL)]
                                    !DCM solubility in human liver calculated
                                    !according to Poulin and Krishnan (1995c)
PLA = SL/SA                         !Liver: air PC of DCM
PLB= PLA/PBA                        !Liver:blood PC of DCM
```

REFERENCES

ANDERSEN, M.E., CLEWELL, H.J., III, GARGAS, M.L., MAc NAUGHTON, M.J., REITZ, R.H., NOLAN, R.G., and McKENNA, M. (1991). "Physiologically based pharmacokinetic modeling with dichloromethane, its metabolite carbon monoxide and blood carboxyhemoglobin in rats and humans." Toxicol. Appl. Pharmacol. 108:14-27.

ANDERSEN, M.E., CLEWELL, H.J., in, GARGAS, M.L., SMITH, F.A., and REITZ, R.H. (1987). "Physiologically based pharmacokinetics and the risk assessment process for methylene chloride." Toxicol. Appl. Pharmacol. 87:185-205.

BOIS, F.Y., ZEISE, L., and TOZER, T.N. (1990). "Precision and sensitivity of pharmacokinetic models for cancer risk assessment. Tetrachloroethylene in mice, rats and humans." Toxicol. Appl. Pharmacol. 102:300-315.

D'SOUZA, R.W., FRANCIS, W.R., and ANDERSEN, M.E. (1988). "Physiological model for tissue glutathione depletion and increased resynthesis after ethylene dichloride exposures." J. Pharmacol. Exp. Ther. 245:563-568.

FEATHERSTONE, R.M. and SCHOENBORN, B.P. (1964). "Protein and lipid binding of volatile anaesthetic agents." Br. J. Anaesthesiol. 36:50-154.

FISEROVA-BERGEROVA, V. (1983). "Gases and their solubility: A review of fundamentals." In:Modeling of Inhalation Exposure Vapors: Uptake, Distribution and Elimination, Vol. I (V. Fiserova-Bergerova, ed.). CRC Press, Boca Raton, FL. pp. 3-29.

FLETCHER, R.F. (1972). "Lipids of human myocardium." Lipids 7:728-732.

FORBES, R.M., COOPER, A.R., and MITCHELL, H.H. (1953). "The composition of the adult human body as determined by chemical analysis." J. Biol. Chem. 166:359-365.

FREDERICK, C.B., POTTER, D.W., CHANG-MATEU, M.I., and ANDERSEN, M.E. (1992). "A physiologically based pharmacokinetic and toxicodynamic model to describe the oral dosing of rats with ethyl acrylate and its implications for risk assessment." Toxicol. Appl. Pharmacol. 114:246-260.

HANSCH, C. and LEO, A. (1979). "The fragment method of calculating partition coefficients." In:Substituent Constants for Correlation Analysis in Chemistry and Biology (C. Hansch and A. Leo, eds.). Wiley & Sons, New York. pp. 18-43.

HOWARD, P. H. (1990). Handbook of Environmental Fate and Exposure Data for Organic Chemicals. Volume 2 Solvents. Lewis Publishers, Chelsea, MI.

KOIZUMI, A. (1989). "Potential of physiological pharmacokinetics to amalgamate kinetic data of trichloroethylene and tetrachloroethylene obtained in rats and man." Br. J. Ind. Med. 46:239-249.

KREWSKI, D., WANG, Y., BARTLETT, S., and KRISHNAN, K. (1995). "Uncertainty, variability, and sensitivity analyses in physiological pharmacokinetic models." J. Biopharm. Stats. In press.

KRISHNAN, K. and ANDERSEN, M.E. (1994). "Physiologically based pharmacokinetic modeling in toxicology." In: Principles and Methods of Toxicology (W.A. Hayes, ed.). 3rd ed. Raven Press Ltd., New York. pp. 149-188.

KRISHNAN, K., GARGAS, M.L., FENNELL, T.R., and ANDERSEN, M.E. (1992). "A physiologically based description of ethylene oxide dosimetry in the rat." Toxicol. Ind. Health 9:121-140.

LAM, C.W., GALLEN, T.J., BOYD, J.F., and PERSON, D.L. (1990). "Mechanism of transport and distribution of organic solvents in blood." Toxicol. Appl. Pharmacol. 104:117-129.

LONG, C. (1961). Biochemists' Handbook. E. & F. N. Spon, Ltd., London, England. p. 1192.

MITCHELL, H.H., HAMILTON, T.S., STEGGERDO, F.R., and BEAN, H.W. (1945). "The chemical composition of the adult human body and its bearing on the biochemistry of growth." J. Biol. Chem. 158:625-638.

NELSON, G.J. (1967). "The phospholipid composition of plasma in various mammalian species."Lipids 2:323-327.

POULIN, P. and KRISHNAN, K. (1995a). "A biologically based algorithm for predicting human tissue:blood partition coefficients." Human Exptl. Toxicol. 14:273-280.

POULIN, P. and KRISHNAN, K. (1995b). "An algorithm for predicting tissue:blood partition coefficients of organic chemicals from n-octanol:water partition coefficient data." J. Toxicol. Environ. Health 46:101-113.

POULIN, P. and KRISHNAN, K. (1995c). "A tissue composition based algorithm for predicting tissue:air partition coefficients of organic chemicals." Toxicol. Appl. Pharmacol. In press.

POULIN, P. and KRISHNAN, K. (1995d). "A mechanistic algorithm for predicting blood:air partition coefficients of organic chemicals with the consideration of reversible binding in hemoglobin." Toxicol. Appl. Pharmacol. In press.

RAMSEY, J.C. and ANDERSEN, M.E. (1984). "A physiologically based description of the inhalation pharmacokinetics of styrene in rats and humans." Toxicol. Appl. Pharmacol. 73:159-175.

REITZ, R.H., McCROSKEY, P.S., PARK, C.N., ANDERSEN, M.E., and GARGAS, M.L. (1990). "Development of a physiologically based pharmacokinetic model for risk assessment with 1,4-dioxane." Toxicol. Appl. Pharmacol. 105:37-54.

REITZ, R.H., McDOUGAL, J.N., HIMMELSTEIN, M.W., NOLAN, R.J., and SCHUMANN, A.M. (1988). "Physiologically based pharmacokinetic modeling with methyl chloroform: Implications for interspecies, high-low dose and dose route extrapolations." Toxicol. Appl. Pharmacol. 95:185-199.

ROUSER, G., SIMON, G., and KRITCHEVSKY, G. (1969). "Species variations in phospholipid class distribution of organs: 1. Kidney, liver and spleen." Lipids 4:599-606.

SHAPIRO, B. (1977). "Adipose tissue." In: Lipid Metabolism in Mammals, Vol. I (F. Snyder, ed.).Plenum Press, New York. pp. 287-308.

SIMON, G. and ROUSER, G. (1969). "Species variations in phospholipid class distribution of organs: 2. Heart and skeletal muscle." Lipids 4:607-615.

SUZUKI, T. (1991). "Development of an automatic estimation system for both the partition coefficient and aqueous solubility." J. Computer-Aided Design 5:149-166.

TARDIF, R., LAPARE, S., CHAREST-TARDIF, G., BRODEUR, J., and KRISHNAN, K. (1995)."Physiologically based pharmacokinetic modeling of a mixture of toluene and xylene in humans." Risk Anal. 15:335-342.

THOMAS, L.W. (1962). "The chemical composition of adipose tissue of man and mice." Q. J. Exp. Physiol. Cogn. Med. Sci. 47:179-190.

WARD, R.C., TRAVIS, C.C., HETRICK, D.M., ANDERSEN, M.E., and GARGAS, M.L. (1988)."Pharmacokinetics of tetrachloroethylene." Toxicol. Appl. Pharmacol. 93:108-117.

ACKNOWLEDGMENTS

This study represents an initiative undertaken as a part of Dr. Krishnan's research program on physiological modeling, which is supported by grants from the Canadian Network of Toxicology Centres (CNTC), Fonds de la recherche en santé du Québec (FRSQ), Fonds pour la formation de chercheurs et l'aide à la recherche (FCAR), and the Natural Sciences and Engineering Research Council of Canada (NSERC).

TABLE 1. Low and High Human Tissue Composition Data Obtained from the Literature

Tissues	Neutral lipids (fraction of tissue weight)		Phospholipids (fraction of tissue weight)		Water (fraction of tissue weight)	
	Low	High	Low	High	Low	High
Liver	0.0186	0.0853	0.0054	0.0617	0.67	0.79
Muscle	0.0271	0.0806	0.0039	0.0244	0.70	0.80
Adipose tissue	0.7100	0.8700	0.0018	0.0022	0.23	0.10

TABLE 2. Comparison of Predicted Human Tissue:Air PCs with Experimentally Determined Rat Tissue:Air PCs of DCM

PCs	Predicted range		Experimental[c]
	Low[a]	High[b]	
Liver:air	7.44	19.3	13.05
Muscle:air	8.69	17.16	7.33
Adipose tissue:air	92.73	112.31	110.86

[a]Predicted with low tissue composition data.

[b]Predicted with high tissue composition data.

[c]PC values correspond to those used by Andersen *et al.* (1991) in the human DCM PBPK model. These PC values had been obtained in a previous study using rat tissues (Andersen *et al.* 1987).

TABLE 3. Comparison of the Percent Water and Lipid Contents of Rat and Human Tissues

	% water		% phospholipids		% neutral lipids	
Tissue	Human[1]	Rat[2]	Human	Rat	Human	Rat
Liver	67-79	70	0.5-6.2	2.5	1.9-8.5	3.5
Muscle	70-80	74	0.4-2.4	1.0	2.7-8.1	0.87
Adipose tissue	10-23	12	0.18-0.22	0.2	71-87	85

[1] Presented as a range; data from this study.

[2] Data from a compilation by Poulin and Krishnan (1995b).

FIGURE LEGENDS

FIGURE 1. Simulations of Cv in humans exposed to 100 ppm for six hours obtained with the conventional (0) and tissue composition-based (High, +; Low,∇) PBPK models.

FIGURE 2. Simulations of Cl in humans exposed to 100 ppm for six hours obtained with the conventional (0) and tissue composition-based (High, +; Low, ∇) PBPK models.

Figure 1

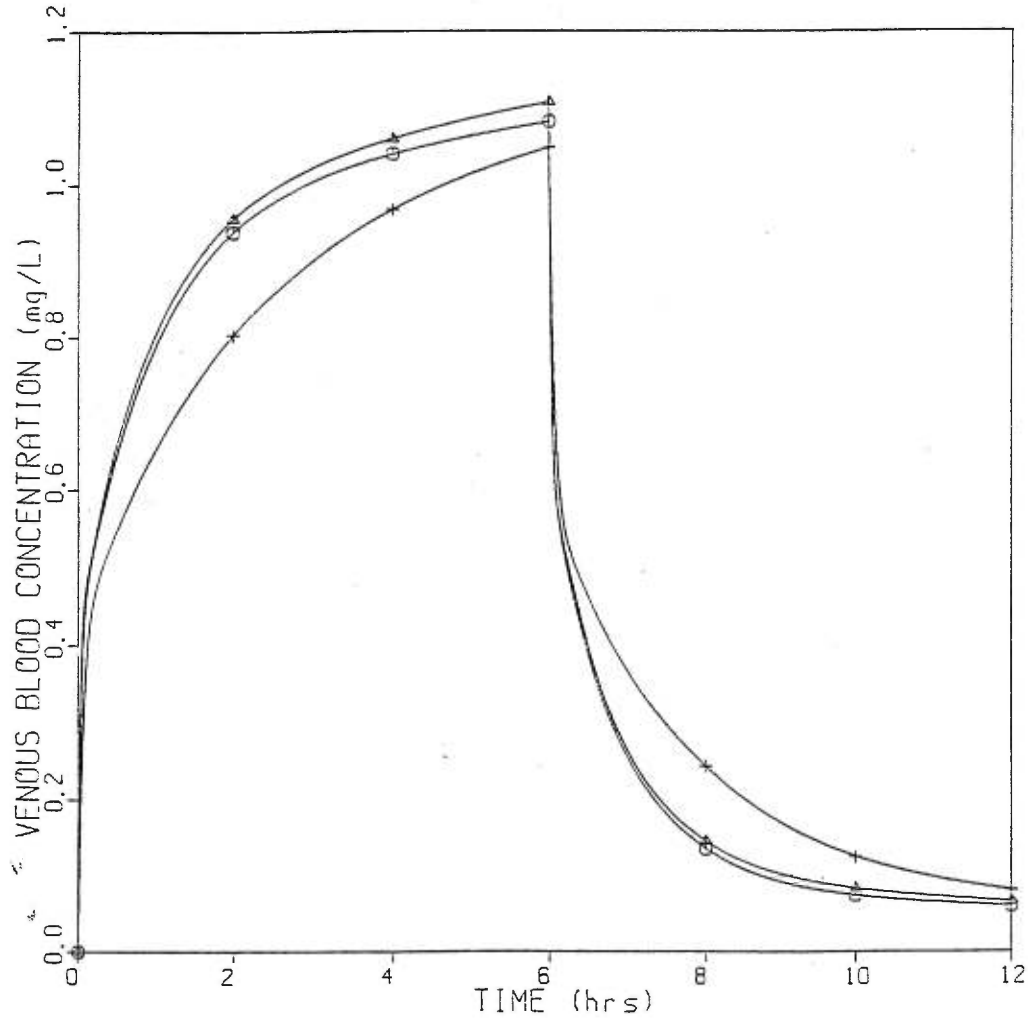
VENOUS BLOOD CONCENTRATION (mg/L)
0.0
0.2
0.4
0.6
0.8
1.0
1.2
0
2
4
6
8
10
12
TIME (hrs)

Figure 2

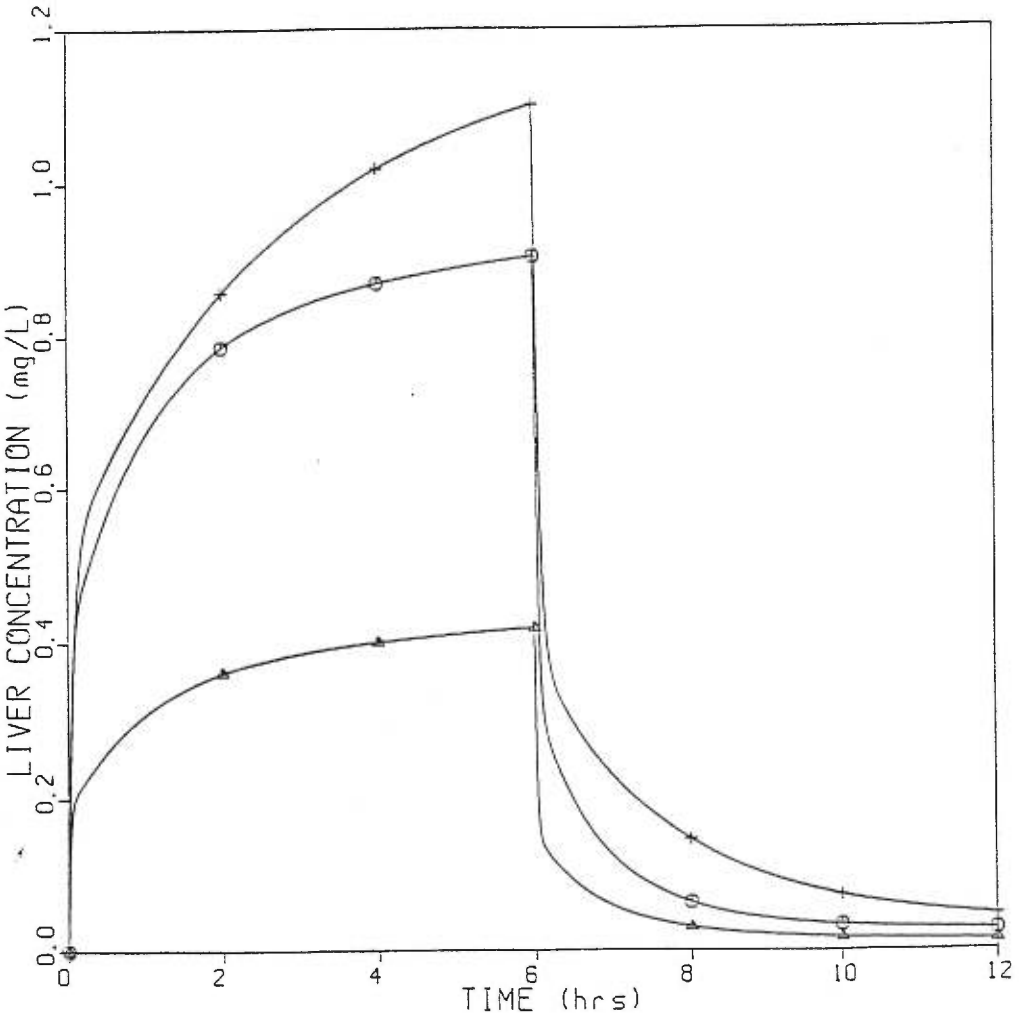
LIVER CONCENTRATION (mg/L)
0.0
0.2
0.4
0.6
0.8
1.0
1.2
0
2
4
6
8
10
12
TIME (hrs)

Article No 2

(Published in: Xenobiotica, Vol. 27(11), pp. 1113-1120, 1997)

Determination of the rate of aldicarb sulfoxidation in rat liver, kidney and lung microsomes

MICHAEL PELEKIS AND KANNAN KRISHNAN*

Département de médecine du travail et d'hygiène du milieu

Université de Montréal, C. P. 6128, Succ. Centre-ville

Montréal, QC, Canada, H3C 3J7

*Author for correspondence.

Abstract

1. The rate of sulfoxidation of aldicarb (2-methyl-2-(methylthio) propanal O-[(methylamino) carbonyl oxime], Temik®) in rat hepatic, renal and pulmonary microsomes was determined by quantitating the levels of aldicarb sulfoxide and aldicarb sulfone produced during incubations. Under *in vitro* experimental conditions used in the present study, aldicarb sulfoxide was the only metabolite produced, and further metabolism of aldicarb sulfoxide to aldicarb sulfone was negligible.

2. The average maximal velocity (μmoles/min/mg protein) for the sulfoxidation of aldicarb, based on measurements of product formation, in liver, kidney and lung microsomes was 5.41, 39.51, and 2.45, respectively. The corresponding values for the Michaelis constant (μM) were 184, 1050 and 188, respectively.

3. These results imply that under *in vivo* conditions (i) aldicarb sulfoxidation is not likely to be saturable even at lethal doses in the rat, and (ii) aldicarb clearance in rat liver and kidney will be limited by the rate of blood flow and not metabolizing enzyme levels.

Introduction

Aldicarb (2-methyl-2-(methylthio) propanal O-[(methylamino) carbonyl oxime], Temik®) is widely used to control insects, mites and nematodes (World Health Organization 1991). In mammals, it is readily absorbed and distributed to all tissues by systemic circulation (Knaak *et al.* 1966, Andrawes *et al.* 1967, Dorough *et al.* 1970, Cambon *et al.* 1979). It is initially oxidized to aldicarb sulfoxide (ALX) and subsequently to aldicarb sulfone; aldicarb and its metabolites are susceptible to hydrolysis, with the subsequent dehydration giving rise to the corresponding oximes and nitriles (Baron and Merriam 1988). Although hydrolysis destroys the insecticidal activity, both aldicarb and its oxidative metabolites, ALX and aldicarb sulfone, are potent cholinesterase inhibitors (Hastings *et al.* 1970, Cambon *et al.* 1979, Baron and Merriam 1988).

Whereas the *in vitro* and *in vivo* metabolism of aldicarb has been studied in a variety of mammalian and non-mammalian species and plants (Knaak *et al.* 1966, Metcalf *et al.* 1966, Andrawes *et al.* 1967, Bull *et al.* 1967, Dorough and Ivie 1968, Bartley *et al.* 1970, Dorough *et al.* 1970, Montesissa *et al.* 1991, 1994, 1995), the maximal velocity (Vmax) and the Michaelis affinity constant (Km) for aldicarb sulfoxidation have only been determined in fish. Schlenk and Buhler (1991) determined the Vmax and Km for aldicarb sulfoxidation in rainbow trout using liver, kidney and gill microsomes. In all three tissues, ALX was the

major metabolite, with trace amounts of ALX oxime being formed in the liver, and aldicarb oxime in kidney and liver.

The information on the quantitative nature (i.e., rate and affinity) of the metabolism of aldicarb is essential to evaluate its biopersistance and profile of elimination in other non-target species such as rodents and humans. Accordingly, the objective of the present study was to determine the Vmax and Km for aldicarb sulfoxidation in rat liver, kidney and lung microsomes.

Materials and methods

Materials

Aldicarb (ALD), aldicarb sulfoxide (ALX), aldicarb sulfone (ALU) were obtained from Chem Service (West Chester, PA) and were at least 98% pure. The purity of the carbamates was verified by HPLC analysis (EPA method 531.1) prior to all experiments. NADPH, Tris-HCl, Tris-acetate, potassium chloride, potassium phosphate, sucrose, and EDTA were obtained from Sigma Chemical Co. (St. Louis, Mo). Methanol (HPLC grade), glycerol, and sodium pyrophosphate were purchased from Fisher Chemicals (Montréal, Qué.). NaOH and *o*-phthalaldehyde (2-dimethylamino ethanediol hydrochloride, OPA) were purchased from Pickering Laboratories (Mountain View, CA).

Preparation of microsomes

Male Sprague-Dawley rats weighing 180-200 g were obtained from Charles River Canada (St. Constant, Qué) and maintained in stainless steel cages on Purina Certified Rodent Chow (Ralston-Purina Co., Ontario, Canada) and water ad libitum. Following a four to seven day acclimatization period, the rats were euthanized (following exposure to CO_2), exsanginated and the tissues (liver, kidney and lung) from individual animals were obtained. All tissues were blotted with filter paper (Whatman No. 1), weighed and washed with ice cold Tris-HCl buffer (0.1 M, pH=7.4) containing 0.1 M KCl and 1 mM EDTA. Liver and kidney tissues from several animals were pooled and homogenized in Tris-HCl buffer (0.1 M, pH=7.4, 1:4 v/v) with a Teflon® homogenizer. The tissue

homogenates were initially centrifuged at 10,000g for 20 min and the supernatant was re-centrifuged at 100,000g for 60 min. The resulting pellet was re-suspended in the above buffer and the homogenate centrifuged at 100,000g for 60 min. The final pellet was suspended in 0.1 M Tris-HCl containing 0.25 M sucrose and 5 mM EDTA at a volume equal to the weight of the tissue. The same procedure was followed for the preparation of lung microsomes, except that in the second centrifugation 0.1 M potassium pyrophosphate buffer (pH 7.4) was used, and the final pellet was suspended in 0.01 M Tris-acetate buffer containing 1 mM EDTA and 20% (v/v) glycerol (pH 7.4) (Reitz *et al.* 1996). The microsomes were stored at -70^{0}C and were used within two months of preparation. The concentration of protein in the microsomes was determined immediately after the last centrifugation with the Bio-Rad® method (Bio-Rad Laboratories, Hercules, CA). Briefly, this method involves the incubation of an aliquot of the microsomal preparation with the Bio-Rad Dye reagent (mixture of Coomasie Brilliant Blue, ethanol and phosphoric acid) and the subsequent determination of the optical density of the solution at 595 nm (Bradford 1976).

In vitro assays

The experimental approach consisted of the addition of ALD to a mixture of microsomes, 5 mM NADPH and 0.1 M potassium phosphate buffer (pH 7.4) containing 5 mM EDTA, in a total volume of 1 ml. The optimal NADPH concentration (5 mM) and pH (7.4) were chosen on the basis of preliminary studies with rat liver and/or kidney microsomes (data not shown). The rate of

ALD metabolism was assayed by measuring the production of ALX and ALU. In all assays duplicate controls were used as references. In the first one, ALD was incubated with buffer alone and was used to check for contamination and/or non-enzymatic degradation of ALD. In the second control experiment, all components, except NADPH, were added to the incubation mixture and was used to evaluate the residual metabolic activity of the microsomes. All incubations were conducted in 5-ml glass screw cap tubes at 37 ^{0}C.

Time-course assays

The linearity of incubation time was determined by incubating ALD (5.25 or 10.5 μM final concentration, in 20 μl of methanol) with 0.14-0.51 mg/ml microsomal protein for a period of up to 60 min (liver & lung: 60 min; kidney: 45 min). Microsomal protein was added to tubes already containing 5 mM NADPH, and the reaction was initiated with the addition of ALD (in 20 μl of methanol). At different time points, the reaction was terminated by adding 0.5 ml of methanol and immersion of the assay tubes in ice. All tubes were centrifuged for 15 min at 3200 g (4^{0}C) to remove the protein precipitate. The supernatant was transferred to 2 ml glass vials sealed with Teflon®-coated rubber septa and analyzed immediately for levels of ALX.

Protein-course assay

The linear range of microsomal protein concentration was determined by incubating ALD (final concentration: 5.25 or 10.5 μM) with various amounts of

protein (final concentration: 0.06-12 mg/ml) for 10 min and measuring the concentrations of ALX.

Kinetic analyses

The kinetic parameters for ALD sulfoxidation were determined by adding various quantities of ALD (dissolved in 20 μl methanol; final concentrations: 36-3700 μM) to a mixture of microsomes (corresponding to 0.18-0.32 mg protein per ml), cofactor (5 mM NADPH) and of 0.1 M potassium phosphate buffer (pH 7.4, 1 ml final volume) at 37^{0}C and determining the concentration of ALX at the end of a ten minute incubation period.

Analytical methods

For the separation and quantitation of ALD and its metabolites, the EPA method 531.1 was used (USEPA 1989). A Varian® high pressure liquid chromatography (HPLC) system equipped with an autosampler (Model 9100), and a programmable fluorescence detector (Model 9070) linked to a Varian® Star LC workstation was used. A dual post-column derivatization system (PCX-5100, Pickering Laboratories, Mountain View, CA) was connected to the HPLC system. The post-column reaction unit consisted of two reagent pumps, an HPLC column thermostat controlled at 42^{0}C, and two reaction coils. The first reaction coil was heated to 100^{0}C for NaOH hydrolysis of ALD, ALX and ALU and the second one was kept at ambient temperature for OPA derivatization of the methyl amine resulting from the hydrolysis of the carbamates.

The separation was achieved with a Pickering C18 column (250 mm x 4.6 mm ID, 5 mm packing) which was placed in the thermostat of the post-column reaction unit and maintained at 42^0C. The mobile phase employed a simple water:methanol gradient. The initial composition was 8% methanol:92% water, which was maintained for a 1-minute hold period, after which a 20-min linear gradient program to 20% methanol:80% water was begun. The mobile phase composition was then changed to 50:50 and an 8-minute gradient to 80% methanol:20% water was initiated. Subsequently, the mobile phase was set at 100% methanol for 2 min to provide column cleanup, before returning to the initial condition. The flow rate was 1 ml/min. Under these conditions, ALX elutes first (14.5 min) followed by ALU (16.5 min) and ALD (25.5 min). The separated carbamates were derivatized with OPA to improve sensitivity and selectivity, and the fluorescence of the resulting 1-methylthio-2-methylisoindole was quantified. Both NaOH solution and the OPA reagent in the post-column reaction unit were constantly pumped at a flow rate of 0.3 ml/min during the whole sequential cycle. The injection volume was 10 μl. Excitation and emission wavelengths of the fluorescence detector were set at 330 and 466 nm, respectively. Calculations of the concentrations of carbamates in samples were based on area measurement.

Data analysis

The metabolic constants (Vmax and Km) for aldicarb sulfoxidation in rat liver, kidney and lung microsomes were determined from Hanes-Woolf plots of

the data on ALX concentration obtained at the end of incubation with the corresponding initial concentrations of ALD.

Results

The initial series of studies focused to determine the linear range of incubation time and protein concentration with respect to ALD sulfoxidation in rat tissue microsomes. Figure 1 shows the time-course of ALX formation in rat liver, kidney and lung microsomal preparations for an initial ALD concentration of 5.25 μM (liver and kidney) and 10.5 μM (lung). With the choice of 10 minutes from the linear part of this curve, the influence of protein concentration on the rate of ALX formation was elucidated. The effect on ALD sulfoxidation was linear for microsomal protein concentrations of up to 1 mg/ml in liver, 0.6 mg/ml in kidney, and 0.4 mg/ml in lung microsomes respectively (Fig. 2).

The final series of experiments involved the determination of the rate of ALX formation by liver, kidney and lung microsomes following a 10-min incubation with 36-3700 μM ALD (final concentrations). From the measurement and analysis (Hanes-Woolf plot) of ALX concentrations at the end of ALD incubations during this series of experiments, the maximal velocity for metabolism (Vmax) and Michaelis affinity constant (Km) for ALD sulfoxidation in rat liver, kidney and lung microsomes were estimated (Figs 3-5). The Vmax (μmol/min/mg protein) for ALD metabolism in liver, kidney and lung microsomes were 5.41, 39.51 and 2.45 respectively, with the corresponding Km's (μM) being 184, 1050 and 188. Under the experimental condition of the present study, (i) incubation of ALD with liver, kidney and lung microsomes resulted exclusively in

the formation of ALX, and (ii) the oxidation of ALX to ALU by either liver, kidney or lung microsomes was negligible (data not shown).

Discussion

Aldicarb sulfoxidation is considered to be a bioactivation process since the primary oxidative metabolite (ALX) is more potent than the parent chemical (ALD) as an acetylcholinesterase inhibitor (World Health Organization 1991). The *in vitro* metabolism of ALD has been investigated using subcellular fractions or whole cells isolated from rats, rabbits, sheep, cattle, goat, chicken, and fish (Andrawes *et al.* 1967, Montesissa *et al.* 1991, 1994, 1995, Schlenk and Buhler 1991, Venkatesh *et al.* 1991). All of these studies except that of Schlenk and Buhler (1991), and Venkatesh *et al.* (1991), are at best semi-quantitative in nature. In general, these latter studies have shown that (1) ALX is the major product of ALD sulfoxidation, and (2) ALD sulfoxidation could be mediated both by cytochrome P450 and flavin-containing monooxygenases (FMO). The experimental designs used in these latter studies could additionally provide a qualitative characterization of the profile of metabolites found at the end of incubation, but not quantitative information (Vmax, Km) on ALD metabolism. Schlenk and Buhler (1991) and Venkatesh *et al.* (1991) on the other hand, reported the Vmax and Km for ALD sulfoxidation using microsomes from fish organs and purified renal and hepatic FMO from mouse, respectively. Since such quantitative information on ALD oxidation in rat tissues is not available in the literature, the present study estimated the affinity and maximal velocity of ALD sulfoxidation using microsomes isolated from rat liver, kidney and lungs.

The Michaelis affinity constant for ALD oxidation in rat liver and kidney microsomes are comparable to those reported by Venkatesh *et al.* (1991) using purified FMO from mouse tissues. Regardless of the preparation and species, the affinity constant for metabolism of a substrate is anticipated to be the same, as long as the same isoenzyme(s) is (are) involved. This has formed the very basis of some, current default approaches for *in vitro to in vivo* and interspecies extrapolations of xenobiotic metabolism (Krishnan and Andersen 1994). The fact that the Km values estimated in the present study are comparable to those reported by Venkatesh *et al.* (1991) [liver: 196 μM, kidney: 385 μM] adds further support to the preceding practice.

The results of the present study indicate that the Km for ALD sulfoxidation is comparable in liver and lung (184 vs 188 μM). Such a similarity in Km for the sulfoxidation of several FMO substrates has been reported previously (Venkatesh *et al.* 1991). Based on the Km values obtained in the present study, it may be suggested that ALD oxidation is not saturable even at lethal doses in the rat ($LD_{50} \approx 1$ mg/kg, World Health Organization 1991). Therefore, the rate of ALD oxidation in rat liver, kidney and lung can be described as a first order process. The intrinsic clearance values (Vmax/Km) for ALD sulfoxidation in rat liver, kidney and lung are 7.06, 1.02 and 0.051 l min^{-1} respectively. For the first order conditions, the clearance of ALD in each of these tissues can be calculated as:

$$\frac{[V_{max}\ (mg/min)/K_m\ (mg/l)] * Q_t\ (l/min)}{[V_{max}\ (mg/min)/K_m\ (mg/l)] + Q_t\ (l/min)}$$

where Q_t is the rate of blood flow to tissue t (liver=0.016 l/min, kidney=0.013 l/min, lung=0.090 l/min) (ILSI 1994). Since the numerical value of (Vmax/Km) is very large with respect to Q_t in rat liver and kidney, Q_t in the denominator of the above equation becomes negligible, making organ clearance of ALD equal to Q_t. The pulmonary clearance of ALD, however, is not limited solely by Q_t. Therefore, in the case of lungs, both intrinsic clearance parameters and Q_t are critical determinants of ALD clearance. This is principally due to the fact that Qt for lungs is very large (i.e., equal to cardiac output), and the volume of lungs is small relative to other metabolizing tissues. Given that the volume of liver is greater than that of kidney and lungs, the former is likely to be the most important tissue metabolizing ALD in the rat. The rate of enzymatic sulfoxidation of ALD in rat organs, and its dependence on blood flow rates, elucidated in the present study, have important implications for predicting the *in vivo* kinetics of ALD in the rat and subsequent extrapolation to humans for risk assessment purposes.

References

ANDRAWES, N. R., DOROUGH, H. W., and LINDQUIST, D. A., 1967, Degradation and elimination of Temik in rats. *Journal of Agricultural and Food Chemistry*, **60**, 979-987.

BARON, R. L., and MERRIAM, T. L., 1988, Toxicology of Aldicarb. *Reviews of Environmental Contamination and Toxicology*, **105**, 1-70.

BARTLEY, W. J., ANDRAWES, N. R., CHANCEY, E. L., BAGLEY, W. P., and SPURR, H. W., 1970, The metabolism of Temik aldicarb pesticide [2-methyl-2-(methylthio) propionaldehyde O-(methylcarbamoyl)oxime] in the cotton plant. *Journal of Agricultural and Food Chemistry*, **18**, 446-453.

BRADFORD, M. M., 1976, A rapid and sensitive method for the quantitation of microgram quantities of protein utilizing the principle of protein-dye binding. *Analytical Biochemistry*, **72**, 248-254.

BULL, D. L., LINDQUIST, D. A., and COPPEDGE, J. R., 1967, Metabolism of 2-methyl-2-(methylthio)propionaldehyde O-(methylcarbamoyl) oxime (Temik, UC-21149) in insects. *Journal of Agricultural and Food Chemistry*, **15**, 610-616.

CAMBON, C., DECLUME, C., and DERACHE, R., 1979, Effect of the insecticidal carbamate derivatives (carbofuran, primicarb, aldicarb) in the activity of acetylcholinesterase in tissues from pregnant rats and fetuses. *Toxicology and Applied Pharmacology*, **49**, 203-208.

DOROUGH, H. W., and IVIE, G. W., 1968, Temik-S^{35} in a lactating cow. *Journal of Agricultural and Food Chemistry*, **16**, 460-464.

DOROUGH, H. W., DAVIS, R. B., and IVIE, G. W., 1970, Fate of Temik-carbon-14 in lactating cows during a 14-day feeding period. *Journal of Agricultural and Food Chemistry*, **18**, 135-142.

ILSI, 1994, Physiological parameter values for PBPK models. *International Life Sciences Institute , Risk Science Institute*, Washington, DC.

HASTINGS, F. L., MAIN, A. R., and IVERSON, F, 1970, Carbamylation and affinity constants of some carbamate inhibitors of acetylcholinesterase and their relation to analogous substrate constants. *Journal of Agricultural and Food Chemistry*, **18**, 497-502.

KNAAK, J. B., TALLANT, M. J., and SULLIVAN, L. J., 1966, The metabolism of 2-methyl-2-(methylthio) propionaldehyde O-(methylcarbamoyl)oxime in the rat. *Journal of Agricultural and Food Chemistry*, **14**, 573-578.

KRISHNAN, K., and ANDERSEN, M. E., 1994, Physiologically based pharmacokinetic modeling in toxicology. In *Principles and Methods of Toxicology,* edited by A. W. Hayes (New York, Raven Press).

METCALF, R. L., FUKUTO, T. R., COLLINS, C., BORCK, K., BURK, J. M., REYNOLDS, H. T., and OSMAN, M. F., 1966, Metabolism of 2-methyl-2-(methylthio)-propionaldehyde O-(methylcarbamoyl) oxime in plant and insect. *Journal of Agricultural and Food Chemistry*, **14**, 579-584.

MONTESISSA, C., AMORENA, M., DE LIGUORO M. and LUCISANO A.,1991, Aldicarb sulfoxidative pathway in broilers: *in vitro* and *in vivo* evaluation. *Acta Veterinaria Scandinavica*, Suppl. **87**, 396-398.

MONTESISSA, C., HUVENEERS, M. B. M., HOOGENBOOM, L. A. P., AMORENA, M., DE LIGUORO M. and LUCISANO A., 1994, The oxidative metabolism of aldicarb in pigs: *In vivo - in vitro* comparison. *Drug Metabolism and Drug Interactions*, **11**(2): 127-138.

MONTESISSA, C., DE LIGUORO M., AMORENA, M., LUCISANO A., and CARLI, S., 1995, *In vitro* comparison of aldicarb oxidation in various food-producing animal species. *Veterinary and Human Toxicology*, **37**, 333-336.

REITZ, R. H., GARGAS, M. L., MENDRALA, A. L., and SCHUMAN, A. M., 1996, *In vivo and in vitro* studies of perchloethylene metabolism for physiologically based pharmacokinetic modeling in rats, mice and humans. *Toxicology and Applied Pharmacology*, **136**, 289-306.

SCHLENK, D., and BUHLER, D. R., 1991, Role of flavin-containing monooxygenase in the *in vitro* biotransformation of aldicarb in rainbow trout (Oncorhynchus mykiss). *Xenobiotica*, **21**, 1583-1589.

USEPA,1989, 531.1. Measurement of N-methycarbamates in water by direct aqueous injection HPLC with post column derivatazation, Environmental Monitoring Systems Laboratory, Office of Research and Development, Cincinnati, Ohio.

VENKATESH, K., LEVI, P. E., and HODGSON, E., 1991, The flavin-containing monooxygenase of mouse kidney, *Biochemical Pharmacology*, **42**, 1411-1420.

WORLD HEALTH ORGANIZATION, 1991, Aldicarb, *Environmental Health Perspectives*, **121**, 20.

Figure Legends

Figure 1. Aldicarb sulfoxide (ALX) produced by the sulfoxidation of aldicarb by rat liver (M, protein concentration: 0.5 mg/ml; ALD: 5.25 μM), kidney (▲, protein concentration: 0.47 mg/ml; ALD: 5.25 μM) and lung (■, protein concentration: 0.14 mg/ml; ALD: 10.5 μM) microsomes as a function of incubation time. The symbols represent experimental data (mean ± SE, n=3).

Figure 2. Aldicarb sulfoxide (ALX) produced by the sulfoxidation of aldicarb by rat liver (M, 5.25 μM), kidney (▲, 10.5 μM) and lung (■, 10.5 μM), microsomes as a function of the concentration of microsomal protein. The experimental data (symbols, mean ± SE, n=3) correspond to the amount of ALX measured at the end of a 10-min incubation.

Figure 3. Hanes-Woolf plot of aldicarb sulfoxidation in rat liver microsomes. v refers to the initial rate of reaction (μmol/min/mg protein) and [S] refers to the initial aldicarb concentration (μM).

Figure 4. Hanes-Woolf plot of aldicarb metabolism in rat kidney microsomes.

Figure 5. Hanes-Woolf plot of aldicarb metabolism in rat lung microsomes.

Figure 1

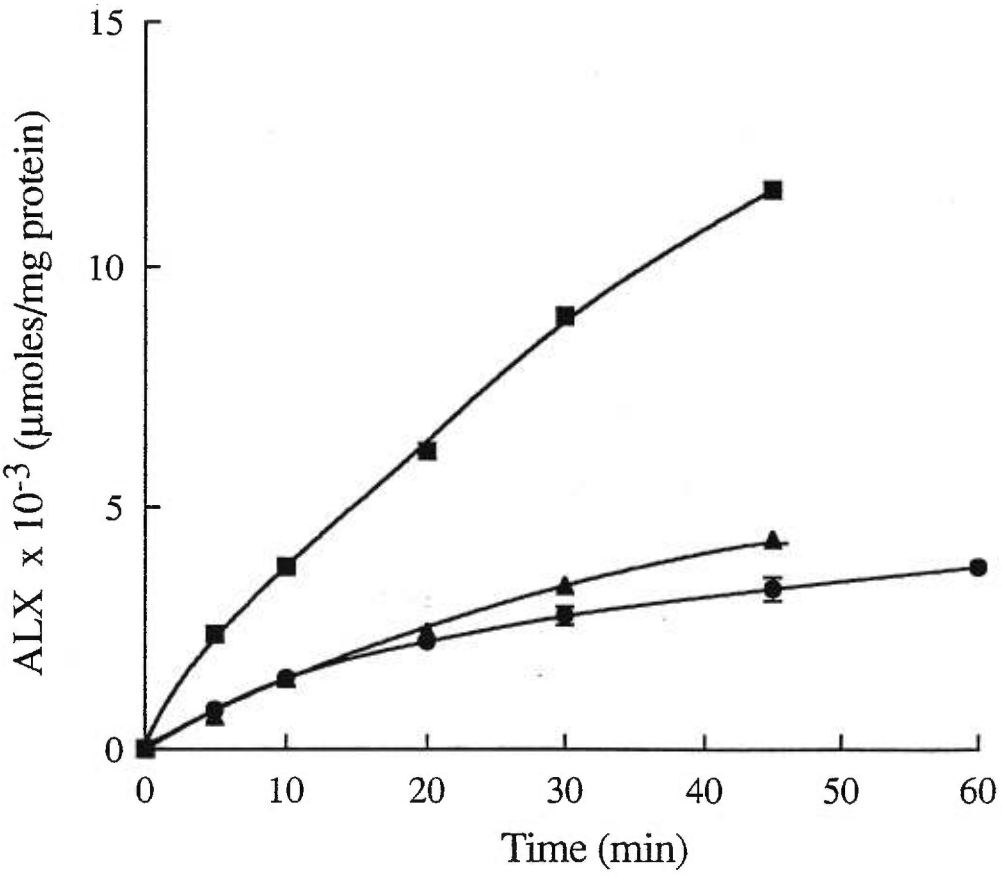

Figure 2

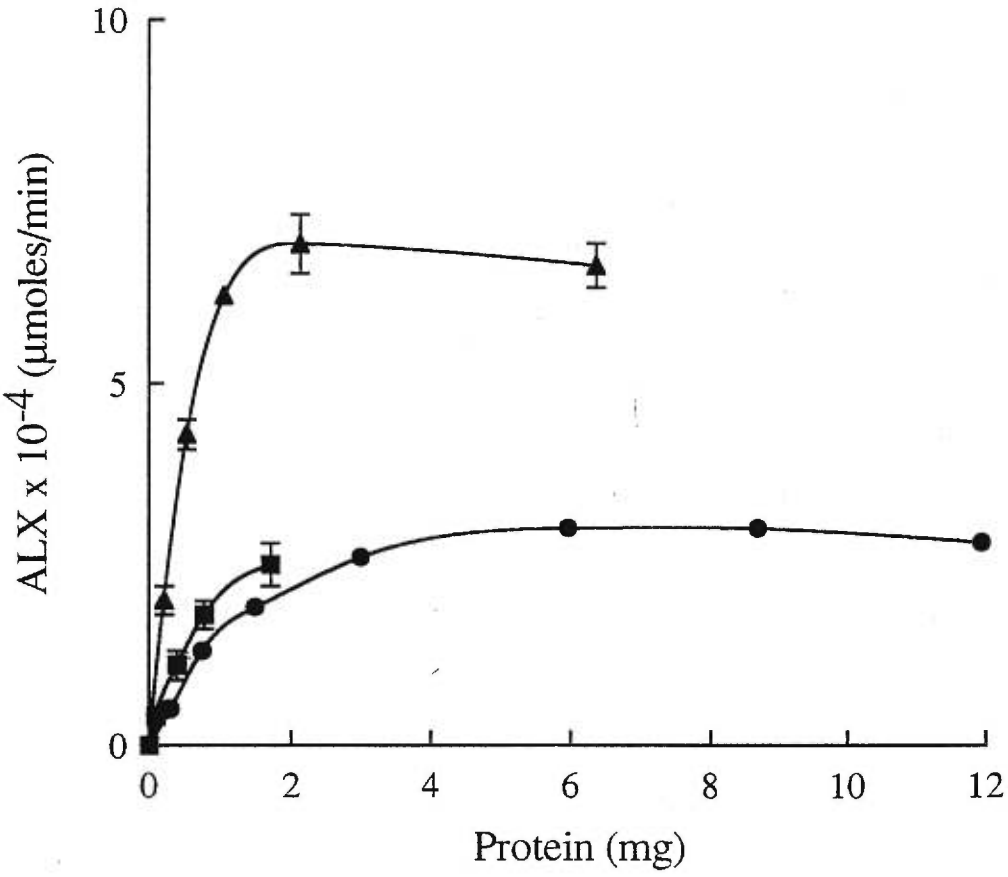

Figure 3

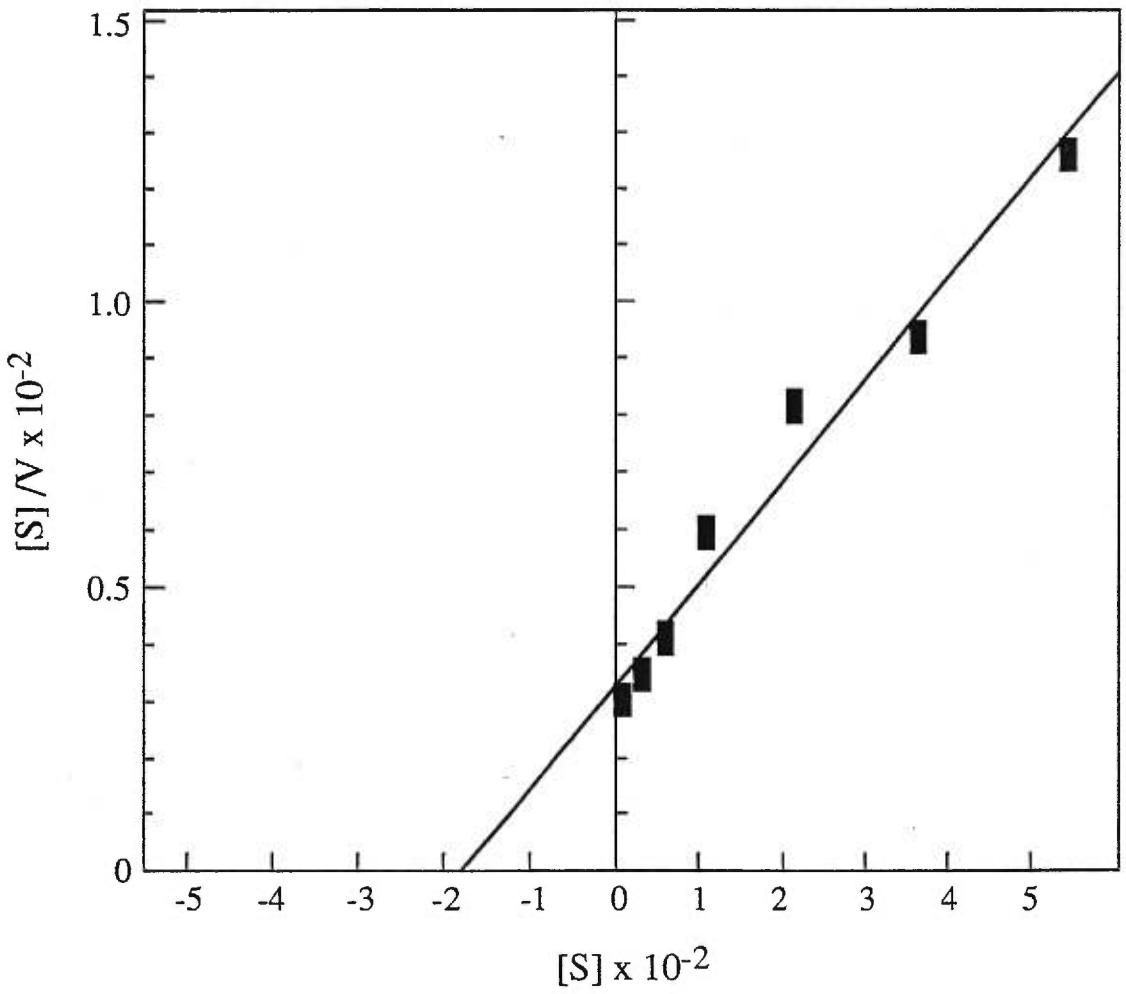

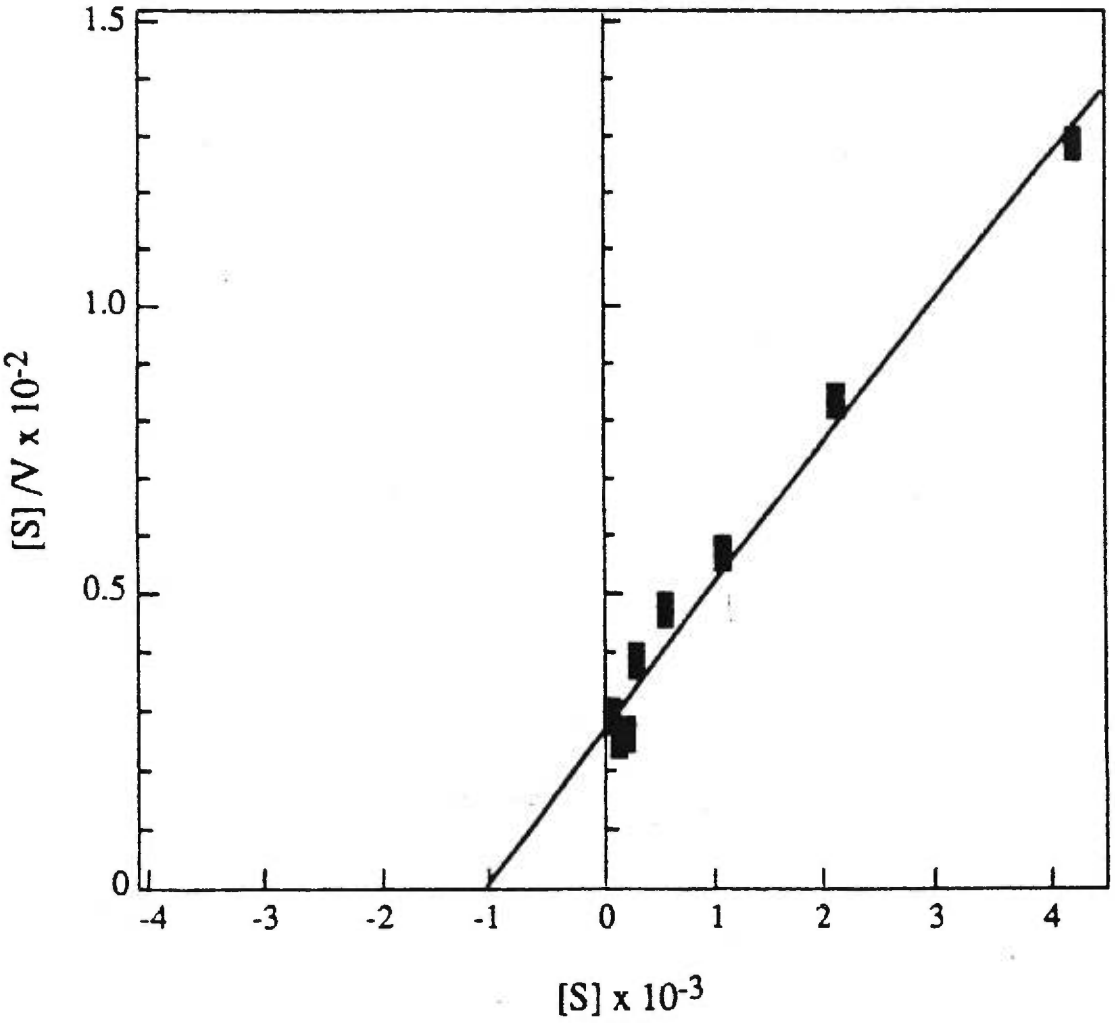
1.5
1.0
0.5
0
[S] /V x 10-2
-4
-3
-2
-1
0
1
2
3
4
[S] x 10-3

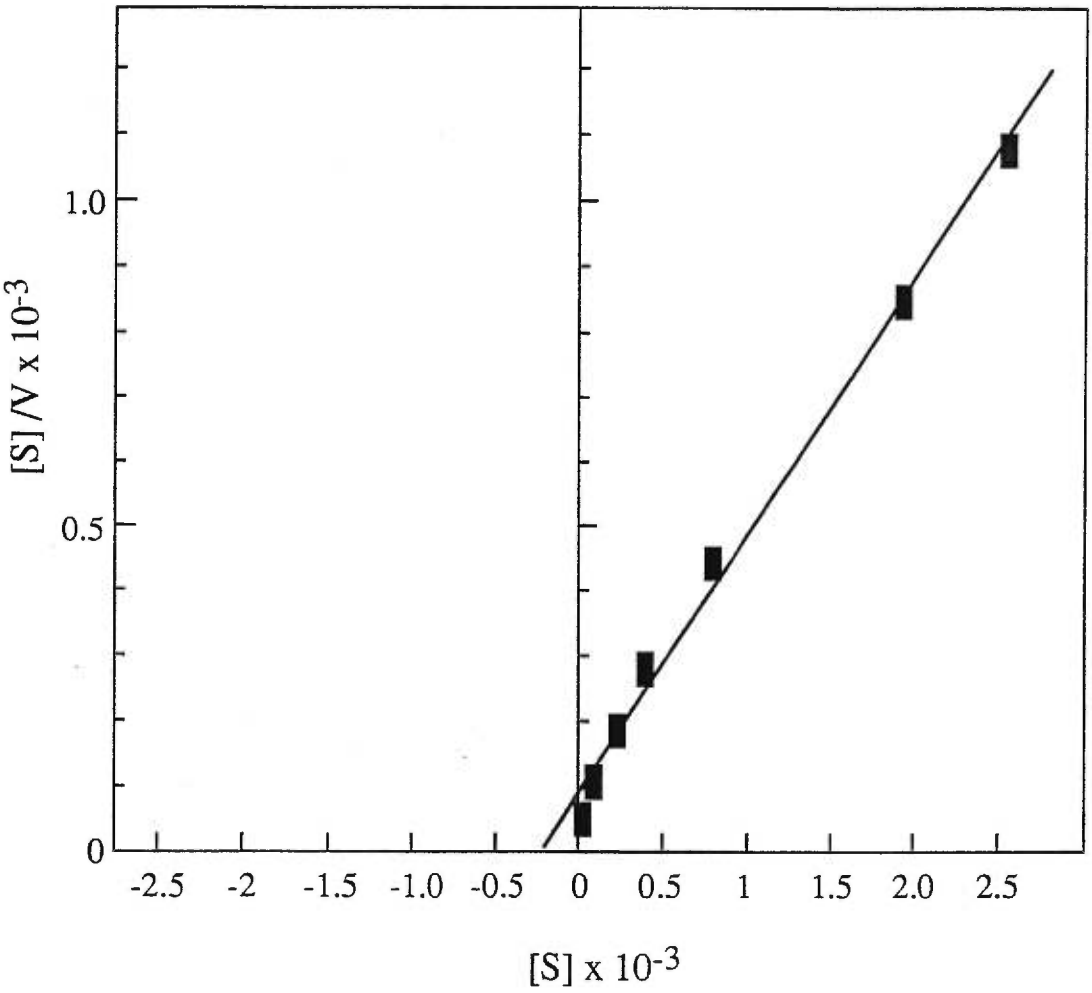
1.0
0.5
0
[S] /V x 10-3
-2.5
-2
-1.5
-1.0
-0.5
0
0.5
1
1.5
2.0
2.5
[S] x 10-3

Article No 3

(To be submitted to: Toxicology and Applied Pharmacology)

PHYSIOLOGICAL MODELING AND DERIVATION OF THE RAT TO HUMAN TOXICOKINETIC UNCERTAINTY FACTOR FOR THE CARBAMATE PESTICIDE ALDICARB

MICHAEL PELEKIS AND KANNAN KRISHNAN

[1]Département de médecine du travail et d'hygiène du milieu, Université de Montréal, C. P. 6128, Succ. Centre-ville, Montréal, QC, Canada, H3C 3J7

Address all correspondence to: Kannan Krishnan, Département de médecine du travail et hygiène du milieu, Université de Montréal, 2375 Côte Ste-Catherine, Bureau 4105, Montréal, Québec, Canada, H3T 1A8, Tel.: (514) 343-6581, Fax: (514) 343-2200

ABSTRACT

Aldicarb (ALD, 2-methyl-2-(methylthio)-propionalaldehyde O-(methyl-carbamoyl) oxime, Temik®) is widely used as an insecticide, nematocide and acaricide, and it is oxidized to aldicarb sulfoxide (ALX) and aldicarb sulfone (ALU). Neither a toxicokinetic model nor an estimate of the target tissue dose of ALD and its metabolites in exposed organisms is available. The objective of this study was: (i) to develop a physiologically-based toxicokinetic (PBTK) model for ALD in the rat and humans, and (ii) to determine the interspecies toxicokinetic uncertainty factor($UF_{AH\text{-}TK}$) of ALD. The model consists of a series of mass balance differential equations that describe the time course behavior of ALD in blood, liver, kidney, lungs, brain, fat, and rest of the body compartments. The physiological parameters of the model (blood flow rates, cardiac output, and tissue volumes) were obtained from the literature, while the maximum velocity (mg/kg/min) and the Michaelis constant (mg/L) for ALD oxidation in rats and humans were determined by *in vitro* microsomal assays. The estimation of the tissue:blood partition coefficient was accomplished within the PBTK model by representing the tissues as a composite of neutral lipids, phospholipids and water, and providing the vegetable oil:water partition coefficient as input parameter. The validity of the rat PBTK model was assessed by comparing the model simulations of ALX time-course blood concentrations and the inhibition patterns of acetylcholinesterase (AChE) in erythrocytes and plasma obtained by administering rats ALD (0.1 and 0.4 mg/kg, *iv*). The human PBTK model was

validated by comparing the simulations of AChE inhibition patterns in blood with human experimental data obtained from oral administrations of ALD. The $UF_{AH\text{-}TK}$ for ALD was determined by dividing the areas under the blood and brain concentration vs time curve (AUC_{CV}, AUC_{CBr}) for ALD and ALX in the rat and in human exposed to the same dose. The results indicate that with respect to parent chemical, equivalent applied doses in rats and humans result in a 9.5-fold difference in the AUC_{CV} and AUC_{CBR} respectively, in the two species, and 17-fold difference in the AUC_{CV} and AUC_{CBR} with respect to the metabolite. In other words, in order to have toxicokinetic equivalence in rats and humans, the former species must be exposed to a dose that is 9.5 and 17 times higher than the human with respect to the parent chemical and the metabolite respectively. Overall, the present study demonstrates the applicability of PBTK models in the quantitative evaluation of $UH_{AH\text{-}TK}$, and shows that their current default values are inaccurate, at least with respect to ALD, which has potential negative implications in the alleged protection of risk estimates derived from them.

INTRODUCTION

Aldicarb (ALD, 2-methyl-2-(methylthio)-propionalaldehyde O-(methyl-carbamoyl) oxime) is an oxime carbamate introduced by Union Carbide Corporation in 1962 under the trade name Temik®. It is currently produced by Rhone-Poulenc and is applied in the soil to protect root systems, the foliage and fruit of several crops including cotton, sugar beets, sugar cane, citrus fruits, potatoes, beans, peanuts and ornamental plants from attack by insects, mites and nematodes and a variety of other pests (Bird *et al.* 1984, Baron and Merriam 1988, WHO 1991). In 1988 the amount of aldicarb applied annually in the United States was 5.5 million pounds (USEPA, 1988).

Its high acute mammalian toxicity (LD_{50} in mice and rats is 1 mg/kg) makes it one of the most toxic of all currently registered insecticides. The LD_{50} of its oxidative metabolites aldicarb sulfoxide (ALX) and aldicarb sulfone (ALU) are 1 mg/kg and 20-25 mg/kg respectively, whereas that of the hydrolytic metabolites (oximes and nitriles) is considerably less (LD_{50}=350–8060 mg/kg) (Carpenter and Smyth 1965, Weiden *et al.* 1965, Gaines 1969, Wilkinson *et al.*1983).

Both ALD and its oxidative metabolites are potent acetylcholinesterase (AChE) inhibitors (Hastings *et al.* 1970, Cambon *et al.* 1979, Baron and Merriam 1988). They exert their neurotoxic effects by inhibiting this key enzyme in nerve

synapses and myoneural junctions. The inhibition of AChE involves the formation of an enzyme-inhibitor complex followed by reaction of the inhibitor at the active site of the enzyme to give the carbamylated enzyme. Carbamylated AChE is readily hydrolyzed to regenerate the active enzyme. Although the carbamylated enzyme is sufficiently stable to disrupt cholinergic transmission, acetylcholinesterase activity is regenerated rapidly following subacute doses. ALX is more potent inhibitor of both insect and bovine erythrocyte cholinesterases than are ALD and ALU themselves, and ALU is less potent than ALD (Baron and Merriam 1988).

The usual practice for non-cancer risk assessment uses measures of applied dose in animals to assess the potential effects of chemicals in humans. The interspecies uncertainty factor (UF_{AH}=10) is applied to account for uncertainty regarding the relationship between applied dose and effective dose across species, along with other uncertainty factors that account for variability in the human population and scenario of exposure. The default UF_{AH} has recently been subdivided into two components, $UF_{AH\text{-}TK}$ and $UF_{AH\text{-}TD}$, each equal to 3.16, to account separately for interspecies differences in toxicokinetics and toxicodynamics (Renwick 1991,1993; USEPA 1994).

Despite the extensive application of the UF_{AH}, conclusive experimental or theoretical justification to support or refute its magnitude has never been provided, and its use has been hypothesized to result in safe-sided exposure

limits. A more scientific approach would be to use the known principles of toxicokinetics to relate exposure concentration to tissue dose to estimate $UF_{AH\text{-}TK}$. Physiologically-based toxicokinetic models (PBTK) are of potential use in this context. Their mechanistic and biological foundation makes the estimation of tissue doses across species possible and accurate. The same model can be used to describe the toxicokinetics of a chemical across and within species. All that is required is a change in the species-specific values of the mechanistic determinants of toxicokinetics, i.e., the physicochemical, biochemical and physiological parameters. Once the model has been constructed and validated in a species, the toxicokinetic behavior of the same chemical in different species can be validated and compared.

Thus, the toxicokinetic equivalence of the same chemical in different species can be evaluated in a quantitative manner and the magnitude of the default interspecies toxicokinetic uncertainty factor $UF_{AH\text{-}TK}$ can be assessed with the use of PBTK models. For this reason a PBTK model for ALD in the rat and humans was developed to perform the rat to human extrapolation and to determine the rat/human toxicokinetic uncertainty factor.

METHODS

I. EXPERIMENTAL

a) Chemicals

ALD, ALX, and ALU were obtained from Chem-Service (West Chester, PA) and were at least 98% pure. Potassium phosphate, sodium phosphate, sodium chloride and acetylcholine iodide were obtained from Sigma Chemical Co. (St. Louis, Mo). Methanol, dichloromethane, ethyl acetate (HPLC grade) and Triton X-100 were purchased from Fischer Chemicals (Montréal, Québec, Canada). NaOH, O-phthalaldehyde (OPA) and thiofluor (N, N-Dimethyl-2-mercaptoethylamine hydrochloride) were purchased from Pickering Laboratories (Mountain View, CA).[^{3}H] acetylcholine iodide, POPOP [1,4-Bis (5-phenyl-2-oxazolyl benzene)], and PPO (5-phenyl-2-oxazolyl benzene), were obtained from New England Nuclear Co., (Dupont, Boston, MA).

b) Animals

Male Sprague-Dawley rats weighing 180-200 g were obtained from Charles River Canada (St. Constant, Qué). Upon receipt, rats were placed in groups of three in stainless steel wired-mesh cages and quarantined for 1-week period. All rats were provided with Purina Certified Rodent Chow (Ralston-Purina Co., Ontario, Canada) and water *ad libitum*. Following the *in vivo* experiments rats were euthanized by CO_2 inhalation and exsanguination. All

animal procedures were done according to the guidelines of the Canadian Animal Care Committee.

c) Human microsomes

Pooled human liver microsomes were obtained from Human Biologics (Phoenix, AR). Liver samples were obtained from seven males deceased in various accidents. Their age ranged between 19 and 68, all were disease free, and none was taking any medication at the time of death. After preparation, microsome quality was checked by measuring the activity of nine different P-450 enzymes, as well as the content of P-450 (two different methods), cytochrome b5 and NADPH-cytochrome c reductase (Table 1).

d) Analytical method for the quantification of ALD and ALX

For the separation and quantitation of ALD and its metabolites, the EPA method 531.1 was used (USEPA 1989). A Varian® high pressure liquid chromatography (HPLC) system equipped with an autosampler (Model 9100), and a programmable fluorescence detector (Model 9070) linked to a Varian® Star LC workstation was used. A dual post-column derivatization system (PCX-5100, Pickering Laboratories, Mountain View, CA) was connected to the HPLC system. The post-column reaction unit consisted of a pulse-free reagent pumping system (two reagent pumps), a mixer to combine the flows of the reagent and eluate, and a pressurized continuous-flow reactor, two reagent pumps, an HPLC column thermostat controlled at 42^0C, and two reaction coils.

The first reaction coil was heated to 100^{0}C for NaOH hydrolysis of carbamates and the second one was kept at ambient temperature for OPA derivatization of the methyl amine resulting from the hydrolysis of the carbamates.

The separation was achieved with a Pickering C18 column (250 mm x 4.6 mm ID, 5 mm packing) which was placed in the thermostat of the post-column reaction unit and maintained at 42^{0}C. The mobile phase employed a simple water:methanol gradient. The initial composition was 8% methanol:92% water, which was maintained for a 1-minute hold period, after which a 20-min gradient program to 20% methanol:80% water was begun. The mobile phase composition was then changed to 50:50 and an 8-minute gradient to 80% methanol:20% water was initiated. Subsequently, the mobile phase was set at 100% methanol for 2 min to provide column cleanup, before returning to the initial condition. The flow rate was 1 ml/min. Under these conditions, ALX elutes first (14.5 min) followed by ALU (16.5 min) and ALD (25.5 min).

The separated carbamates were first hydrolyzed by sodium hydroxide (NaOH) at 100^{0}C to release the alcohol (R-OH), carbonate and methyl amine. In the second post-column reaction, methylamine reacts with o-phthalaldehyde (OPA) and the nucleophilic Thiofluor® to form a highly fluorescent 1-alkyl-2-methylisoindole derivative. Both NaOH solution and the OPA reagent in the post-column reaction unit were constantly pumped at a flow rate of 0.3 ml/min during the whole sequential cycle. The injection volume was 10 μl. Excitation and emission wavelengths of the fluorescence detector were set at 330 and

466 nm, respectively. Calculations of the concentrations of carbamates in samples were based on area measurement.

e) *In vitro* studies

i) Measurement of the oil:buffer partition coefficients of ALD and ALX

Partitioning of ALD and ALX between vegetable oil and phosphate buffer was determined as follows: 2 ml of potassium phosphate buffer (pH=7.4), 2 ml of corn oil (Mazola® brand) and 20 μL of ALD or ALX solution were added in screw-capped glass test tubes. Two sets of 15 test tubes (5 tubes per time point for ALD and ALX) were prepared and placed in a water bath at 37^0C. The tubes were shaken by means of a mechanical shaker for 30, 60 and 120 min respectively. Following 15 min equilibration period, the aqueous phase was pipetted into HPLC vials for quantitation of the carbamates (see analytical method below). The carbamate concentration in the oil phase was calculated as [total amount added to the test tubes-amount measured in aqueous phase]/volume of oil. The oil:buffer partition coefficient was estimated from the ratio of the respective carbamate concentration in the two phases.

ii) Measurement of the rate of sulfoxidation of ALD

The metabolic rate constants for aldicarb sulfoxidation in rats were previously determined *in vitro* by incubating ALD with rat liver, kidney and lung microsomal preparations as described previously (Pelekis and Krishnan 1997). The same methodology was used for the determination of the metabolic

parameters using human liver microsomes. Briefly, the experimental approach consisted of the addition of ALD to a mixture of microsomes, 5 mM NADPH and 0.1 M potassium phosphate buffer (pH 7.4) containing 5 mM EDTA, in a total volume of 1 ml. The rate of ALD metabolism was assayed by measuring the production of ALX and ALU.

Following the characterization of the linearity of ALD oxidation as a function of microsomal protein concentration and incubation time, the kinetic parameters for ALD sulfoxidation were determined by adding various quantities of ALD to a mixture of microsomes (corresponding to 0.5 mg protein per ml), cofactor (5 mM NADPH) and of 0.1 M potassium phosphate buffer (pH 7.4, 1 ml final volume) at 37^0C and determining the concentration of ALX at the end of a ten minute incubation period. The metabolic constants (Vmax and Km) for aldicarb sulfoxidation were determined from a Hanes-Woolf plot of the data on ALX concentration obtained at the end of incubation with the corresponding initial concentrations of ALD (56-1051 :M).

f) *In vivo* studies

i) Intravenous administration of ALD and ALX in rats

Twenty-four male Sprague-Dawley rats (260-280 g) were grouped in lots of 3 in plastic cages containing dustless woodchips. ALD (0.4 and 0.1 mg/kg in saline) was administered via the tail vein, and the rats were returned to their cages until sacrifice. In a separate series of experiments, 21 rats in groups of 3

were administered ALX (0.3 and 0.1 mg/kg in saline). At selected intervals following the *iv* administration, rats were anaesthetized by exposing them to CO_2, and whole blood was collected from the *vena cava* using a 10-ml heparinized syringe. A portion of blood (approximately 3 ml) was separated, processed (see section iii, below) and frozen at -70^{0}C to be used for subsequent measurements of cholinesterase inhibition. The rest of the blood was used immediately for the extraction and quantitation of carbamates. The procedures used in the extraction of carbamates and measurement of cholinesterase inhibition are described below.

ii) Extraction of carbamates

A portion of rat blood (5 ml) was transferred to screw-capped glass tube and an aliquot of 5-ml of dichloromethane was added. The contents of the tubes were shaken vigorously for 15 min to extract the carbamates from blood. The organic layer was separated by centrifugation (1500g, 10 min) on a bench centrifuge and was transferred to a 15-ml glass tube. The extraction process was repeated once more with dichloromethane and a third time with ethyl acetate to ensure complete recovery of ALD and ALX. The combined solvent phases were evaporated under a stream of dry nitrogen and the residue was dissolved in 1 ml of methanol. The tubes were vortexed for 10 sec and the contents of the tubes were transferred to HPLC vials for analysis.

(iii) Measurement of AChE inhibition in the rat

1. Tissue collection and preparation

Whole blood was transferred to heparinized tubes and centrifuged at 2,000g at 5^{0}C to separate the plasma from erythrocytes. The undiluted plasma was frozen at -70^{0}C. The erythrocytes were diluted (1:1 v/v) in 0.1 M sodium phosphate buffer (pH 8) containing 1% Triton X-100, and were stored at -70^{0}C until analysis time.

2. Determination of AChE inhibition

The radiometric assay of Johnson and Russell (1975) as modified by Norstrandt *et al.* (1993) was used to determine the AChE activity in red blood cells (RBC) and plasma. This approach was employed because it has been shown to be more appropriate for carbamate-treated tissues (Nostrandt *et al.* 1993). In the modified assay tissues are not subjected to extensive dilution or long incubation times, thus avoiding the potential problem of reactivation (decarbamylation) of cholinesterase activity of carbamate-inhibited samples.

Following the determination of optimum substrate concentrations and linearity of the reaction with respect to protein concentration, the AChE activity was determined at 25±1^{0}C. The selection of the temperature was based on previous studies that have shown that the reactivation rate is temperature dependent (Reiner and Aldridge, 1967) and that cholinesterase reactivation in carbaryl-treated rats is approximately twofold faster at 37^{0}C

than at 25^{0}C (Padilla and Hooper, 1992). In the assay the total reaction volume was 100 μl, of which up to 40-80 μl was tissue homogenate (1:1 homogenate) and 20-60 μl was substrate (0.6 mM acetylcholine iodide and 0.1 μCi of [^{3}H] acetylcholine iodide (90 mCi/mmol) per 20 (or 60) μl; final substrate concentration was 1.2 mM). After a 10-min incubation time, the reaction was stopped by adding 0.1 ml of a mixture of 1 M chloroacetic acid, 0.5 M NaOH and 2 M NaCl, followed by 4.0 ml of scintillation liquid mixture (0.5% PPO, 0.03% POPOP in toluene and 10% isoamyl alcohol). The vials were placed in a Wallac 1410 liquid scintillation counter and the tritium activity in the samples was counted within 24 hr. The counting efficiency as determined by external quench standards was approximately 45%. AChE activity was calculated from the slope of the standard curve as follows:

AChE activity (μmoles acetylcholine hydrolyzed/min) =

$$= \text{slope (in cpm/min)} \times \frac{\text{acetylcholine concentration (μmoles/ml)}}{\text{cpm after total hydrolysis}}$$

II. Modeling

a) Description of the rat and human models

Fig. 1 depicts the conceptual representation of the rat and human PBTK models for ALD. It consists of seven tissue compartments inter-connected by systemic circulation. The tissue compartments correspond to: the metabolizing tissues (liver, kidney and lung), the main excretory tissue (kidney), adipose tissue (fat), the target tissues (blood and brain) and the rest of the body. Two

routes of administration are considered in the model: oral intake for simulation of exposure via drinking water and food, and intravenous administration for simulation of experimental dosing. The dose of ALD ingested is made available for absorption in the GI tract, and the process is described using first-order kinetics. The distribution of ALD to the tissues depends on their blood perfusion and the affinity of the tissues for ALD, and is described as a perfusion-limited process. The ALX model is similar to that of ALD, but the ALX input to the model is either through the venous blood exiting the ALD-metabolizing tissue compartments or through the exposure routes mentioned above.

Each tissue compartment was described as a composite of water, neutral lipids and phospholipids (Pelekis *et al.* 1995). This tissue composition-based model framework allowed the calculation of the tissue:blood partition coefficients (during each simulation run) from the oil:buffer PC provided as input parameter. The only additional input parameters required for simulations were the physiological parameters and metabolic rate constants. While the oxidation of ALD to ALX is described as a saturable process characterized by Vmax (maximal velocity) and Km (Michaelis constant), the hydrolysis of both ALD and ALX was described as a first order process. The oxidation of ALX to ALU was not described in either model since the formation of the latter did not occur in either rat or human microsomal preparations, and only traces were observed in the *in vivo* rat experiments.

Because of the lack of human toxicokinetic data, the human PBTK model was validated by comparing the simulations of AChE inhibition patterns in whole blood with human experimental data. This necessitated the addition of the necessary code in the blood compartment to model the ALD and ALX-induced AChE inhibition, which was described as a second order process, using the output of the toxicokinetic component of the model, i.e., the concentration of ALD and ALX in the blood and the respective bimolecular rate constants.

b) Model parameterization

i) Physiological parameters

The physiological parameters were obtained from the literature and were expressed as a function of body weight or cardiac output (Table 2) (ILSI, 1994). The concentration of AChE in tissues was obtained from Maxwell *et al.* (1987) and Venkataraman and Naga Rani (1994), (Table 3).

ii) Physicochemical parameters

1. Partition coefficients

The tissue:blood partition coefficients (PCs) of ALD and ALX can be estimated by dividing their respective solubilities in tissues and blood (Poulin and Krishnan 1995 a, b, 1996). Alternatively, the tissue:blood PCs can be predicted by dividing tissue:water PCs with the blood:water PC. The tissue:water and blood:water PCs can, in turn, be estimated from oil:water

partition coefficient (Poulin and Krishnan 1995b). Tissue:water and blood:water PCs ($P_{T:W}$) for ALD and ALX were predicted as follows:

$$P_{T:W} = (KOW*FNL_T) + (1*FW_T) + (KOW*0.3*FPL_T) + (1*0.7*FPL_T)$$

where:

KOW = vegetable oil:buffer partition coefficient

FNL_T = fraction of neutral lipid in the tissue

FW_T = fraction of water in the tissue, and

FPL_T = fraction of phospholipid in the tissue

The tissue:blood PCs ($P_{T:B}$) of ALD and ALX were calculated as:

$$P_{T:B} = \frac{\text{Solubility of carbamate in tissue}}{\text{Solubility of carbamate in blood}} = \frac{\text{Tissue:water PC}}{\text{Blood:water PC}} =$$

$$= \frac{(KOW*FNL_T) + (1*FW_T) + (KOW*0.3*FPL_T) + (1*0.7*FPL_T)}{(KOW*FNL_B) + (1*FW_B) + (KOW*0.3*FPL_B) + (1*0.7*FPL_B)}$$

The partitioning of each carbamate into tissues was expressed as the sum partitioning in neutral lipids (i.e., triglycerides, diglycerides, monoglycerides, cholesterol and other non-polar lipids), phospholipids (i.e., phosphatidyl choline, phosphatidyl ethanolamine, phosphatidyl serine, sphingomyelin, and other lipids that contain phosphoric acid esterified at one position of the glycerol molecule) and water fractions comprising each tissue.

The partitioning in blood was modeled as the sum of the partitioning into plasma (63%) and partitioning into erythrocytes (37%). The solubility of the carbamates in neutral lipids, water and phospholipids was assumed to correspond to their solubilities in vegetable oil, buffer or an additive function of the solubility in buffer (70%) and vegetable oil (30%) respectively. The rationale and justification of this method of estimation of partition coefficients, and the use of vegetable oil as a surrogate of neutral lipids are discussed elsewhere (Poulin and Krishnan 1995a, b, 1996).

The calculation of the $P_{T:B}$ of ALD and ALX in the PBTK model was accomplished by:

(a) describing each tissue compartment in terms of their fractional volumes of neutral lipids, phospholipids and water (Altman and Dittmer 1961, Long 1961, Martin *et al.* 1982, Poulin and Krishnan 1995a, b, 1996, Table 4)

(b) providing the vegetable oil:water partition coefficients as input parameters, and

(c) writing the equations that calculate the tissue:water PC of each tissue as well as the ratio of tissue:water and blood:water PCs to provide tissue:blood PCs (Pelekis *et al.* 1995).

2. Oral absorption constant

Previous studies have shown that gastrointestinal absorption of carbamates occurs by passive transport and independent of pH, which is

evident by the lack of ionizable groups in ALD and that its oral absorption constants can be predicted from its n-octanol:water partition coefficient (Houston *et al.* 1975). The oral absorption constant of ALD was determined from the following equation:

$$\log K_O = 0.146*\log P - 0.193$$

where:

K_O =oral absorption constant, and

P =n-octanol:water partition coefficient

iii) Biochemical parameters

1. Metabolic rate constants

The Km for ALD oxidation used in the rat and human models corresponded to that determined during *in vitro* rat and human studies. The Vmax for metabolism of ALD was calculated from the corresponding *in vitro* values, on the basis of the mass recovery of the microsomal fraction using the formula:

$$Vmax_{(in\ vivo)} = Vmax_{(in\ vitro)} * C_p * F_t,$$

where:

$Vmax_{(in\ vivo)}$ is expressed in mg/min/animal

$Vmax_{(in\ vitro)}$ is expressed in mg/min/mg protein

C_p is the concentration of protein in the microsomal sample (expressed in mg protein/g tissue)

F_t is the volume fraction of the tissue (g tissue/body weight of the animal in which microsomes were prepared), and

* denotes multiplication.

2. Urinary excretion constants for ALX and ALD

The rate constant for the urinary excretion of ALX was derived by adjusting its magnitude so that approximately 20% of the administered dose was excreted unchanged after 24 hr. Previous *in vivo* rat studies have shown following the administration of 0.1 mg/kg ALX (p.o.) a fifth of the dose is excreted unchanged in the urine (Andrawes *et al.* 1967). Model simulations show that when the urinary rate constant is set equal to 0.217/(min*kg) the amount of ALX excreted in the urine is 19.8% of the administered dose. The rate constant for the urinary excretion of ALD was assumed to be the same as that of ALX, based on the very close structural and physicochemical properties of the two carbamates and agreement of model predictions on the combined amount of ALX and ALD excreted following administration of ALD (p.o.). (Andrawes *et al.* 1967). The urinary excretion rate constants for ALX and ALD in humans were obtained by allometric extrapolation ($BW^{-0.26}$) of the corresponding rat parameters.

3. Hydrolysis rate constants for ALX and ALD

With the metabolism and urinary excretion rate constants in place in the model, the first order rate constant of ALX hydrolysis in the rat was calculated

by fitting model simulations to experimental data on venous blood concentration (CV) of ALX obtained following *iv* administration of 0.1 and 0.3 mg/kg. The ALX constants for the rate of hydrolysis and urinary excretion were also applied in the ALD model to simulate the toxicokinetic behavior of the parent compound in the rat. Sensitivity analysis of the ALD model (data not shown) indicated that the ALD hydrolysis and urinary excretion rates have little effect on the model predictions (i.e., they are both among the least sensitive parameters). This is not unexpected since ALD does not remain in the body for any considerable length of time. Furthermore, with these constants the overall simulated rate of hydrolysis as well as the amount found in urine (i.e., ALD and ALX combined) are the same with those observed in the experimental studies (Knaak 1966; Andrawes 1967).

The hydrolysis rate constants for ALX and ALD in humans were obtained by allometric extrapolation ($BW^{-0.26}$) of the corresponding rat parameters. The use of the same hydrolysis constant is supported by recent studies that showed considerable similarities in carboxylesterase (the main hydrolytic enzyme) activity, physical and immunological properties in rats and humans (Satoh and Hosokawa 1995).

iv) Toxicodynamic parameters

The critical effect for the evaluation of safe exposure to carbamate pesticides traditionally has been RBC, plasma and brain AChE inhibition

(Aldridge and Magos 1978; Kaloyanova and El Batawi 1991). The mechanism of carbamate inhibition of cholinesterases involves the formation of an intermediate enzyme-carbamate complex, followed by the dissociation of the leaving group and the subsequent formation of the carbamylated enzyme complex which is then hydrolyzed to form the free enzyme and the methyl amine moiety of the carbamate.

The rate of AChE inhibition is a function of the affinity constant K_a, the carbamylation constant, K_2 and the reactivation (or decarbamylation) rate constant K_3, as well as the respective concentrations of the carbamate in the target tissue. The ratio of K_2/K_a is the bimolecular inhibition constant, K_I, and is the main determinant of the overall inhibitory power of the carbamates. The inhibitory action of ALD and ALX were considered to be additive, since the mechanism of action is identical for both carbamates.

The same sequence of events is involved in the normal physiological interaction between the cholinesterases and the normal substrates, the difference being in the reaction rates. By way of comparison, acetylcholine, the normal substrate of AChE has a K_a, a K_I and a K_3 of $2x10^{-5}$ mM, $1.5x10^{9}$ $mM^{-1}min^{-1}$ and $3x10^{5}$ min^{-1} respectively, while the corresponding values for ALD are 10 mM, 16 mM^{-1} min^{-1} and 0.018 min^{-1} (Reiner and Aldridge 1967, O'Brien *et al.*1966).

The K_a, K_2 and K_3 constants for AChE inhibition by ALD determined previously with bovine erythrocytes (Hastings *et al.* 1970; Kuhr and Dorough 1976; Table 5) were used to model the AChE inhibition in RBC and plasma in rats and humans in the present study. This working strategy was supported by previous studies that have shown blood AChE from different species at the same pH and temperature to have the same reaction constants for individual methyl- and dimethyl-carbamates (Iverson and Main 1969, Hastings *et al.* 1970). Further, all N-methylcarbamates produce identical carbamylated enzyme complexes (methylcarbamyl acetylcholinesterase) thus the value of K_3 is the same for all N-methylcarbamates (Kuhr and Dorough 1976). The bimolecular inhibition constant for ALX was estimated from the corresponding constant for ALD and the reported difference in potency between the two carbamates. Inhibition kinetics studies with bovine RBCs (Bull *et al.* 1967) have shown that ALX is 23 times more potent than ALD. Since AChE inhibited by ALD and ALX will have identical decarbamylation rates, it follows that bimolecular inhibition constant K_i of ALX is 23 times higher than that of ALD.

c) Model Simulation

The physiological, physicochemical and biochemical parameters were incorporated with algebraic and mass balance differential equations to describe the rate of change in the amount of ALD and ALX in each tissue. The complete

description of the model is given in the Appendix. A typical mass balance equation has the form:

$VT*dCT_{ALD}/dt = QT*(CA_{ALD}-CVT_{ALD})$!amount of ALD in tissue T

$- (K_H* CVT_{ALD}*VT)$!amount of ALD hydrolyzed by !esterases

where:

VT	= volume of tissue, (L)
dCT_{ALD}/dt	= rate of change in the concentration of ALD in the tissue T, (mg/L/min)
QT	= blood flow rate to the tissue T, (L/min)
CA_{ALD}	= concentration of ALD in the arterial blood entering the tissue, (mg/L)
CVT_{ALD}	= concentration of ALD in the venous blood exiting the tissue, (mg/L)
K_H	= first order hydrolysis rate constant for ALD, (min^{-1}), and
*	denotes multiplication

The first order hydrolysis rate constant is a composite constant describing the hydrolytic activity of all esterases and was applied in all tissue compartments except fat, and the rate of inhibition of AChE was described in the target tissues as a second order process using bimolecular rate constants. Although AChE contributes to the hydrolysis of the carbamates and the

bimolecular constant can be considered as a component of the first order hydrolysis rate constant, within the model these constants operate independent of each other. In other words, the first order rate constant accounts for the reduction in the concentration of the carbamates in the tissues due to hydrolysis mediated by all types of esterases including AChE, whereas the bimolecular rate constant describes the extent of interaction of the carbamates with the AChE to produce the inhibited enzyme. This conceptual approach is supported by the very small concentration of AChE, 0.049 % of the concentration of all esterases in the body (Table 3) (Maxwell *et al.* 1987).

Since the inhibition constants were reported in terms of $(\mu mol/L)^{-1}\ min^{-1}$, for the description of the AChE inhibition, the concentration of the carbamates in blood was converted from mg/L to μmol/L by dividing by the respective MW. The differential equation describing the inhibition of AChE by ALD and ALX in tissue compartment was of the following form:

$$dAChE_T/dt = -(K_{AChEALD}*CT_{ALD}*CA_{ChET}*VT) \quad \text{!inhibition of AChE by ALD}$$
$$-(K_{AChEALX}*CT_{ALX}*CA_{ChET}*VT) \quad \text{!inhibition of AChE by ALX}$$
$$+(K_{RACh}*CA_{ChEI}*VT) \quad \text{!regeneration of AChE}$$

where:

$dAChE_T/dt$ = the rate of change of free AChE in the tissue, (μmol/min)

$K_{AChEALD}$ = bimolecular rate constant for ALD reaction with AChE, $(\mu mol/L)^{-1}\ min^{-1}$

CT_{ALD} = concentration of aldicarb in the tissue, (μmol/L)

$K_{AChEALX}$ = bimolecular rate constant for ALX reaction with AChE, $(\mu mol/L)^{-1} min^{-1}$

CT_{ALX} = concentration of aldicarb sulfoxide in the tissue, (μmol)

CA_{ChET} = concentration of free AChE in the tissue, (μmol/L)

VT = volume of tissue, (L)

K_{RACh} = reactivation constant of inhibited AChE, (min^{-1})

CA_{ChEI} = concentration of inhibited AChE, (μmol/L)

Due to the transient nature of ALD- and ALX-induced AChE inhibition no attempt was made to model the rate of synthesis and degradation of the enzyme (Maxwell *et al.* 1987). The equations, describing the toxicokinetics and toxicodynamics of ALD, were incorporated in the model, which upon running generated systematically AChE inhibition time-course patterns for different exposure scenarios. Every time the model was run, the model generated both the concentrations in the tissue and blood compartments of ALD and ALX capable of inhibiting the AChE and the extent of inhibition. The algebraic and differential equations representing the ALD model were written as a program and solved with a commercially-available software, namely ACSL® (Advanced Continuous Simulation Language, Concord, MA, Version 11.4.1).

d) Model Validation

The validity of the rat PBTK model was assessed by comparing the model simulations of ALX time-course blood concentrations and the inhibition patterns of AChE in RBC and plasma obtained by administering rats ALD (0.1 and 0.4 mg/kg, *iv*). The human PBTK model was validated by comparing the simulations of AChE inhibition patterns in whole blood with human experimental data obtained from oral administrations of ALD (Haines 1971). Twelve adult volunteers with no known exposure to ALD or other cholinesterase inhibitors, were divided into three test groups and adminstered aqueous ALD in single doses of 0.025, 0.05 and 0.10 mg/kg. Whole blood AChE activity was measured radiometrically, at 18 hours and 1 hour prior to exposure and at 1, 2, 4 and 6 hours following exposure (Table 11, Haines 1971). For the calculation of % inhibition the average activity of all 12 subjects measured 18 and 1 hr prior to administration, was taken as the control activity, and the average % inhibition at 1, 2, 4, and 6 hours was calculated.

III. Determination of the interspecies uncertainty factors

This involved running the rat and human PBTK models for 24 hr under the same exposure dose (mg/kg, p.o.) and calculating the areas under the venous blood and brain concentrations vs time curves (AUC) in both species, as well as the respective ratios.

RESULTS

Partition coefficients

The tissue:blood PCs calculated by using the oil:water partition coefficients for ALD and ALX are shown in Table 6. Their magnitude along with the high oral absorption constant help explain the observations of several studies that have shown ALD to be absorbed and distributed rapidly in all tissues of the body (Knaak *et al.* 1966, Andrawes *et al.* 1967).

Biochemical parameters for the rate of sulfoxidation of aldicarb in rats and humans

The metabolic rate constants for ALD sulfoxidation in rat liver, kidney and lungs are summarized in Table 7. For the measurement of the human rate constants, the initial series of studies focused to determine the linear range of incubation time and protein concentration with respect to ALD sulfoxidation in human liver microsomes. Figure 2 shows the time-course of ALX formation in human liver microsomal preparations (protein concentration: 0.4 mg/ml) for an initial ALD concentration of 10.5 µM. With the choice of 10 minutes from the linear part of this curve, the influence of protein concentration on the rate of ALX formation was elucidated. The effect on ALD sulfoxidation was linear for microsomal protein concentrations of up to 1 mg/ml (Fig. 3). The final series of experiments involved the determination of the rate of ALX formation by liver microsomes following a 10-min incubation with 56-1051 µM ALD (final concentrations). From the measurement and analysis (Hanes-Woolf plot) of

ALX concentrations at the end of ALD incubations during this series of experiments, the maximal velocity for metabolism (Vmax) and Michaelis affinity constant (Km) for ALD sulfoxidation in human liver microsomes were estimated (Fig 4). The Vmax (μmol/min/mg protein) and Km (μM) for ALD metabolism in liver microsomes was 8.62 and 1670 respectively. Under the experimental condition of the present study, (i) incubation of ALD with human liver microsomes resulted exclusively in the formation of ALX, and (ii) the oxidation of ALX to ALU did not occur (data not shown).

These results, along with the high acute toxicity of ALD (LD_{50}=1 mg/kg, World Health Organization 1991) which prohibits the build up of high concentrations in the body, indicate that saturable kinetics is impossible to be reached. Thus, the sulfoxidation of ALD in humans can be described as a first order process because of the large value of the Michaelis constant in liver (Pelekis and Krishnan 1997). For highly metabolized chemicals, clearance, CL (L/min), is approximately equal to the rate of blood flow, Q_T (L/min). Because clearance, CL (L/min), is equal to Q_T*E and the extraction ratio $E=CL_{int}/CL_{int}+Q_T$, where CL_{int}=Vmax/Km, the clearance of ALD can be calculated as:

$$\frac{[\text{Vmax (mg/min)/Km (mg/L)}] * Q_T \text{ (L/min)}}{[\text{Vmax (mg/min)/Km (mg/L]} + Q_T \text{ (L/min)}}$$

Since the numerical value of CL_{int} is very large (7.06 and 1.02 for liver and kidney respectively in the rat; the corresponding values in humans are 255 and 68 respectively) with respect to Q_T (0.016 and 0.013 for liver and kidney respectively in the rat; the corresponding values in humans are 1.23 and 0.95 respectively), Q_T in the denominator of the above equation becomes negligible, making organ clearance of ALD equal to Q_T in both tissues. Thus, metabolic clearance in these tissue can be simply described by multiplying the concentration of ALD in the arterial blood entering the tissue with the rate of blood flow to the tissue (Poulin and Krishnan 1998).

$$\frac{dA_{met}}{dt} = \frac{Vmax * C_{vl}}{Km + C_{vl}} = QT*CA$$

Modeling ALX toxicokinetics in the rat

With the oil:water PCs and the urinary excretion rate constant for ALX provided as input, the ALX portion of the ALD PBTK model was used to simulate ALX kinetics in rats. The estimation of the urinary excretion rate of ALX was based on data from a previous study. For both ALX doses, when the constant is set equal to 0.217min*kg, 19.8% of the dose is found in the urine after 24 hr, which is the same as the percentage observed in the *in vivo* study (Andrawes *et al.* 1967).

Previous studies have demonstrated the importance hydrolytic esterases play in the detoxification of ALD (Gupta and Dettbarn 1993). Since esterases are widely distributed in the body (Maxwell *et al.* 1987), in the model, hydrolysis was described in all tissue compartments except fat. The first order rate constant for hydrolysis was derived by fitting ALX model simulations to data on venous blood concentration (CV) of ALX obtained following *iv* administration of 0.1 and 0.3 mg/kg. This was achieved by first incorporating the urinary rate constant (0.217/min*kg) to the model and then adjusting the first order hydrolysis rate constant, so that the predicted CV_{ALX} were the same as that observed in experimental studies. The best fit was obtained when the hydrolysis rate constant was set equal to 0.00724 $kg*min^{-1}$ (Fig. 5) and the model predicted that about 80% of the dose will be hydrolyzed within 24 hr. These results are in agreement with those from a previous *in vivo* study in which about 40% of carbonyl-^{14}C ALX was liberated as CO_2, (an end-product of hydrolysis) (Andrawes *et al.* 1967). The discrepancy between the experimental and simulated hydrolysis rates can be explained by the fact that not all hydrolyzed ALX is emitted as CO_2 (Knaak *et al.* 1966).

Modeling ALD toxicokinetics in the rat

Using the measured metabolic rate constants for ALD sulfoxidation, the ALD model was set to simulate the venous blood concentrations of ALD and ALX following administration of 0.4 or 0.1 mg/kg ALD (*iv*). Fig. 6 shows the simulated time course of the blood ALD concentration following the *iv*

administration of a single dose of 0.1 and 0.4 mg/kg. A dominant characteristic of ALD toxicokinetics, well illustrated in this study, is its rapid clearance from blood. The experimental studies failed to detect any ALD in blood as early as 10 min after both *iv* administrations. This behavior was anticipated because of the high metabolic rate constants of ALD oxidation, and the relatively small (but very toxic) doses administered. The ALX formed from the oxidation of ALD is eliminated at a much slower rate, and only hydrolytic and urinary processes are involved in its excretion and these observations are consistent with previous studies (Knaak *et al.* 1966, Andrawes *et al.* 1967). Fig. 7 presents a comparison of the predicted and experimental venous blood concentration of ALX (CV_{ALX}) in rats administered 0.4 or 0.1 mg/kg ALD (*iv*).

The rate of enzymatic sulfoxidation of ALD in tissue compartments, and their dependence on blood flow rates, was investigated as it has important implications in the prediction of the *in vivo* kinetics of ALD in the rat and other species where metabolic rate constants may not be known. Figures 7-9 compare the concentrations of ALX in the venous blood (CV_{ALX}) of the rat calculated with:

(a) the usual saturable kinetic equations,

(b) with the flow limited metabolism equation in the liver and kidney compartments (metabolism in the lung compartment was described as a saturable process), and

(c) with flow limited metabolism in all three metabolizing tissues, respectively.

Since all three approaches give the same results with respect to (CV_{ALX}), as well as for all the other tissue concentrations (data not shown), it is evident that to model the toxicokinetic behavior of ALD in humans and other species, one does not have to obtain independent measurements of the metabolic rate constants by either *in vivo* or *in vitro* experiments. In other words, due to the high metabolic rates, the sulfoxidation of ALD can be described as a blood flow limited process, without compromising the predictive power of the model. The accuracy of the model is not compromised even if metabolism is described in just one of the three tissue compartments. Furthermore, a comparison of the relative contribution of the three metabolizing tissues with respect to the amount of ALX produced, shows that modeling metabolic clearance as a saturable or blood flow-limited process, results in no appreciable difference in the overall amount of ALX produced (Table 8).

Modeling ALX toxicodynamics in the rat

Tables 9 & 10 summarize the experimental data on the inhibition of AChE in RBC and plasma respectively, in the rat following *iv* administration of 0.3 and 0.1 mg/kg ALX. Cholinergic symptoms were observed in all treated rats and included weakness in the hind limbs, lacrimation, and tremors and decreased AChE activity. Signs of poisoning were noticed within 5 minutes of administration and lasted for 2-3 hr.

Having reliable and continuous estimates of the concentrations of ALX in all tissues over time, the model then simulated the inhibition profile of AChE in RBC and plasma by incorporating the inhibition rate constants for ALX. The simulated and measured time course of AChE inhibition in erythrocytes following intravenous ALX administration are shown in Figs 10 & 11. The experimental data and simulations suggest that the maximum inhibition was between 88 and 96% and was reached within 10 and 25 min for the low and high doses, respectively. The AChE activity decreased very rapidly, was dose-dependent and returned to normal levels within 10 hr of administration.

Modeling ALD toxicodynamics in the rat

Similar inhibition patterns were observed in rats treated with 0.4 and 0.1 mg/kg ALD. The simulated and measured time course of the AChE inhibition in erythrocytes and plasma following *iv* administration of ALD is shown in Figs 12-15. The maximum inhibition was more than 80% and it was reached within the first hour after administration. The AChE activity decreased very rapidly in all three tissues, was dose dependent and returned to normal levels 10-13 hours after administration. The substantial and the rapid inhibition patterns are in agreement with previously published studies on ALD-induced AChE inhibition (DePass *et al.* 1985) and can be explained by the very fast distribution of ALX in the body as well as the high carbamylation rate constants.

Modeling ALD toxicokinetics and toxicodynamics in humans

Model simulations show that following the administration of 0.1 mg/kg (p.o.), all of the ALD will be eliminated within 1 hr (Fig 16). This is in agreement with the observations of Haines (1971) and Cope and Romine (1973), who could only recover minimal amounts of the carbamate in urine following oral administration.

Further evidence that the metabolism of ALD can be described as a flow limited process is provided in Figs 17-20, where the simulated profile of (CV_{ALX}) in humans has been calculated by:

(a) allometric extrapolation of the rat liver, kidney and lung metabolic parameters,

(b) using the measured human liver parameters (the kidney and lung parameters were obtained by allometric extrapolation of the rat values),

(c) with the blood flow limited equations in all three metabolizing tissues, and

(d) with metabolism occurring only in the liver (as a flow limited process),

Therefore, as in the case of rat, the sulfoxidation of ALD in the human model can be described as occurring only in the liver or as a blood flow-limited process with no loss of predictive power by the model.

Due to the lack of toxicokinetic data in humans direct validation of the human PBTK model was not possible, and the accuracy of the integrated model was based on the inhibition patterns of AChE observed in humans

exposed to ALD. Figs. 21-23 show the predicted and simulated inhibition patterns of AChE in human whole blood. The pattern of AChE inhibition in human RBCs is similar to that seen in the rat and the simulation data are in agreement with the observations in all human studies that indicate peak effects within 1 hr of administration and rapid recovery (Haines 1971; Cope and Romina 1973; Rhone-Poulenc 1992).

Determination of the interspecies toxicokinetic uncertainty factor ($UF_{AH\text{-}TK}$)

The $UF_{AH\text{-}TK}$ was determined using the validated rat and human PBTK models. This was achieved by dividing the area under the venous blood and brain concentration vs time curves (AUC_{CV} and AUC_{CBR}) for ALD and ALX in the rat and human exposed to the same dose (0.1 mg/kg, p.o.). AUC is the time integral of systemic exposure to the chemical, and the $UF_{AH\text{-}TK}$ based on AUC integrates interspecies differences in the efficiency of absorption as well as metabolism and elimination. It represents not only the amount of the chemical that is present in the blood or tissue, but also the duration of its presence, and thus provides a measure of the opportunity a chemical has to interact with the targets of toxicity (Clewell and Jarnot 1994). Doses are considered kinetically equivalent in terms of integrated exposure, i.e., the area under the blood or tissue concentration curve (mass/unit volume)(time).

Table 12 shows the rat/human ratios for the AUC_{CV} of ALD and ALX in an average 70 kg human and a 0.25 kg rat exposed to the same applied dose (mg/kg, p.o.). These ratios represent the interspecies toxicokinetic uncertainty factor, $UF_{AH\text{-}TK}$, and describe the toxicokinetic difference between rats and humans with respect to the parent compound and the metabolite. The results indicate that with respect to parent chemical, equivalent applied doses in rats and humans result in a 9.5-fold difference in the AUC_{CV} and AUC_{CBR} respectively, in the two species, and about 17-fold difference in the AUC_{CV} and AUC_{CBR} with respect to the metabolite. In other words, in order to have toxicokinetic equivalence in terms of AUC_{CV} and AUC_{CBR} of ALD and ALX in rats and humans, the former species must be exposed to a dose that is approximately 9.5 and 17 times larger than the human with respect to the parent chemical and the metabolite respectively.

DISCUSSION

The use of the NOAEL or LOAEL/uncertainty factor procedure yields an estimate of an exposure that is thought to "have a reasonable certainty of no harm". Adverse effects however, develop at the target tissues from the interaction of the toxic moiety with cellular components or receptors. Because tissue dose is not always proportional to exposure concentration, a more appropriate method of deriving risk estimates should involve the quantitative relationship between exposure levels and target tissue dose, and further the relationship between tissue dose and observed response in animals and humans (Andersen, 1992). Through the years the procedure has been in use, there have been calls for improving its accuracy, by incorporating available mechanistic information that translates exposure dose to tissue dose and by providing a numerical estimate of the uncertainty that is involved, i.e., provide justification for the magnitude of the uncertainty factors.

The expression of toxicity can depend on the magnitude, duration and frequency of exposure and the mechanistic determinants of the disposition (adsorption, distribution, metabolism and elimination) of a chemical include both time- and concentration-dependent processes. Physiologically-based toxicokinetic (PBTK) modeling techniques have been used to characterize the disposition of chemicals in tissues for the past 20 years (Bischoff and Brown 1966). PBTK models are appealing in that a comprehensive mass

balance approach is used to represent the processes of chemical disposition and are useful in describing the relationship between exposure and target tissue dose.

The PBTK approach was used in the present study to estimate the concentration of ALD and its metabolite ALX in the blood and brain, which were subsequently used to determine the interspecies toxicokinetic uncertainty factor. Initially, quantitative estimates of relevant mechanistic parameters were obtained and a PBTK model that describes the toxicokinetic behavior of ALD and ALX in rats was developed and validated. Then, the mechanistic parameters in humans were determined in humans and a human PBTK model was constructed. Because of the unavailability of human toxicokinetic data the human model was expanded to simulate the ALD- and ALX-induced AChE inhibition in blood and was validated with available AChE inhibition data. The adequacy of the expanded model was also tested successfully in the rat.

Since blood and brain are the target tissues, the rat and human PBTK models were run to simulate the concentration of the carbamates in these tissues under a realistic exposure scenario (0.1 mg/kg ALD, p.o.). Then the corresponding AUCs were calculated the ratio of which is equal to the $UF_{AH\text{-}TK}$. The results of the present study indicate that the use of the default $UF_{AH\text{-}TK}$ (=3.16) with respect to the parent compound and the metabolite

would not be enough to correct for interspecies differences. Considering that the parent compound remains in the body for a fraction of the time that the metabolite does comparing the $UF_{AH\text{-}TK}$ for the metabolite is more appropriate. Although the default approach utilizes $UF_{AH\text{-}TK}$ to correct applied doses of the parent compound, this is not improper because most of the observed response to ALD exposure is due to the action of ALX. The results of the present study indicate that the use of the default interspecies toxicokinetic factor would underestimate toxicokinetic equivalence by a factor of 5.4 (=17.3/3.16).

The $UF_{AH\text{-}TK}$ is used in the default approach to correct toxicokinetic differences over lifetime exposures. In the case of ALD however, this is not relevant because both ALD and ALX are eliminated from the body within one day. This point has been taken into consideration by the EPA in the recent RfD determination of ALD, where the uncertainty factor that corrects for subchronic to chronic extrapolation is not used (IRIS, 1996).

Of the mechanistic determinants of ALD disposition, metabolic parameters play a dominant role since almost all of the applied dose is converted very fast to ALX. Due to its very fast oral absorption rate, the results of the present study would be applicable to other routes of administration.

The toxicokinetic approach used in the present study to determine the $UF_{AH\text{-}TK}$, provides an alternative to the traditional applied dose methodology. The advantage of the toxicokinetic approach is that using an internal measure of effective tissue exposure should provide a more meaningful basis for estimating risk than using applied dose, and that the incorporation of toxicokinetic information should increase the accuracy of the dose, route and species extrapolations required in the risk assessment process.

Overall, the present study has demonstrated the applicability of PBTK models in the quantitative evaluation of interspecies toxicokinetic uncertainty factor, and shown that the current default values are inaccurate, at least with respect to ALD, which has potential negative implications in the alleged protection of risk estimates derived from them. However, the degree of accuracy cannot be evaluated based on the results of just one chemical. In order to evaluate this aspect, the methodology described in this study will have to be applied in the determination of the $UH_{AH\text{-}TK}$ for other chemicals.

ACKNOWLEDGEMENTS

The authors would like to thank Dr. Stephanie Padilla of the Neurotoxicology Division (MD-74B), National Health and Environmental Effects Research Laboratory, USEPA, for the AChE inhibition studies, and Mrs Pierrette Gagnon and Diane Talbot for their technical assistance. Financial support from the Natural Sciences and Engineering Research Council of Canada (NSERC) and the Canadian Network of Toxicology Centres (CNTC) is gratefully appreciated.

APPENDIX

```
PROGRAM: ALDICARB.CSL
!Created by Michael  Pelekis
!Program to simulate the toxicokinetics ALD in rats and humans following oral and/or intravenous administration.
!The parameters listed below are for rats; the human parameters are given in Tables 2-7.
INITIAL                                          !section of program
!Physiological parameters
!Volumes of tissue compartments
CONSTANT  BW    =0.275                           !Body weight (kg)
CONSTANT  KVF   =0.07                            !Fraction fat tissue (% of BW, L)
CONSTANT  KVL   =0.034                           !Fraction liver tissue (% of BW, L)
CONSTANT  KVU   =0.005                           !Fraction lung tissue(% of BW, L)
CONSTANT  KVK   =0.007                           !Fraction kidney tissue (% of BW, L)
CONSTANT  KVBR =0.006                            !Fraction brain tissue (% of BW, L)
CONSTANT  KVTBL=0.074                            !Fraction of total blood tissue (arterial and venous) (% of BW, L)
CONSTANT  KVVBL=0.048                            !Fraction of venus blood tissue (% of BW, L)
CONSTANT  KVABL=0.026                            !Fraction of arterial blood tissue (% of BW, L)
CONSTANT  KVBO =0.09                             !Fraction of the rest of the body (% of BW, L)
          VF    =KVF*BW                          !Volume of fat tissue (L)
          VL    =KVL*BW                          !Volume of liver tissue (L)
          VU    =KVU*BW                          !Volume of lung tissue (L)
          VK    =KVK*BW                          !Volume of kidney tissue (L)
          VBR   =KVBR*BW                         !Volume of brain tissue (L)
          VTBL  =KVTBL*BW                        !Volume of total blood tissue (L)
          VVBL  =KVVBL*BW                        !Volume of venous blood (L)
          VABL  =KVABL*BW                        !Volume of arterial blood (L)
          VBO   =KVBO*BW                         !Volume body tissue (L),
!Blood flow to tissue compartments
CONSTANT  KQCR=0.233                             !Cardiac output rate (L/min/kg)
```

```
CONSTANT  KQFR =0.07          !Fraction of cardiac output to fat (% of QC)
CONSTANT  KQLR =0.183         !Fraction of cardiac output to liver (% of QC)
CONSTANT  KQKR =0.144         !Fraction of cardiac output to kidney (% of QC)
CONSTANT  KQBR =0.02          !Fraction of cardiac output to brain (% of QC)
CONSTANT  KQBO =0.583         !Fraction of cardiac output to body (% of QC)
          QC   =KQCR*BW**0.74 !Cardiac output (L/min)
          QF   =KQFR*QC       !Blood flow to fat (L/min)
          QL   =KQLR*QC       !Blood flow to liver (L/min)
          QK   =KQKR*QC       !Blood flow to kidney (L/min)
          QBR  =KQBR*QC       !Blood flow to brain (L/min)
          QBO  =KQBO*QC       !Blood flow to body (L/min)
!Calculation of Partition Coefficients
CONSTANT  KOW  =1.83          !ALD oil/water partition coefficient
CONSTANT  KOWX=0              !ALD oil/buffer partition coefficient
CONSTANT  FWL  =0.70          !fraction of water in liver
CONSTANT  FLL  =0.06          !fraction of lipid in liver
CONSTANT  FNLL =0.58          !fraction of neutral lipid in liver lipid
CONSTANT  FPLL =0.42          !fraction of phospholipid in liver lipid
CONSTANT  FWF  =0.12          !fraction of water in fat
CONSTANT  FLF  =0.855         !fraction of lipid in fat
CONSTANT  FNLF =0.9975        !fraction of neutral lipid in fat lipid
CONSTANT  FPLF =0.0025        !fraction of phospholipid in fat lipid
CONSTANT  FWK  =0.78          !fraction of water in kidney
CONSTANT  FLK  =0.06          !fraction of lipid in kidney
CONSTANT  FNLK =0.975         !fraction of neutral lipid in kidney lipid
CONSTANT  FPLK =0.025         !fraction of phospholipid in kidney lipid
CONSTANT FWBR =0.700*VBR      !fraction of water in brain
CONSTANT  FLBR =0.060*VBR     !fraction of lipid in brain
CONSTANT  FNLBR=0.420*FLBR    !fraction of neutral lipid in brain
```

```
CONSTANT  FPLBR=0.580*FLBR      !fraction of phospholipid in brain
CONSTANT FWB   =0.743*VBO       !fraction of water in body
CONSTANT  FLB   =0.019*VBO      !fraction of lipid in body
CONSTANT  FNLB =0.459*FLB       !fraction of neutral lipid in body
CONSTANT  FPLB =0.541*FLB       !fraction of phospholipid in body
CONSTANT FWE   =0.63            !fraction of water in erythrocytes
CONSTANT  FLE   =0.00506        !fraction of lipid in erythrocytes
CONSTANT  FNLE =0.23            !fraction of neutral lipid in erythrocytes
CONSTANT  FPLE =0.77            !fraction of phospholipid in erythrocytes
CONSTANT  FWPL =0.96            !fraction of water in plasma
CONSTANT FLPL   =0.0023         !fraction of lipid in plasma
CONSTANT  FNLPL=0.639           !fraction of neutral lipid in plasma
CONSTANT  FPLPL=0.361           !fraction of phospholipid in plasma
          SLA   =((KOW*FNLL)+(1*FWL)+(KOW*0.3*FPLL)+(1*0.7*FPLL))/VL                  !solubility of ALD in liver
          SFA   =((KOW*FNLF)+(1*FWF)+(KOW*0.3*FPLF)+(1*0.7*FPLF))/VF                  !solubility of ALD in fat
          SBRA =((KOW*FNLBR)+(1*FWBR)+(KOW*0.3*FPLBR)+(1*0.7*FPLBR))/VBR              !solubility of ALD in brain
          SBA   =((KOW*FNLB)+(1*FWB)+(KOW*0.3*FPLB)+(1*0.7*FPLB))/VBO                 !solubility of ALD in R.O.B.
          SKA   =((KOW*FNLK)+(1*FWK)+(KOW*0.3*FPLK)+(1*0.7*FPLK))/VK                  !solubility of ALD in kidney
          SEA   =((KOW*FNLE)+(1*FWE)+(KOW*0.3*FPLE)+(1*0.7*FPLE))/(VTBL*0.37)         !solubility of ALD in RBC
          SPLA =((KOW*FNLPL)+(1*FWPL)+(KOW*0.3*FPLPL)+(1*0.7*FPLPL))/(VTBL*0.63)
                                                                                      !solubility of ALD in plasma
          PLBA =SLA/((0.37*SEA)+(0.63*SPLA))                                          !ALD liver/blood PC
          PFBA =SFA/((0.37*SEA)+(0.63*SPLA))                                          !ALD fat/blood PC
          PKBA =SKA/((0.37*SEA)+(0.63*SPLA))                                          !ALD kidney/blood PC
          PBBA = SBA/((0.37*SEA)+(0.63*SPLA))                                         !ALD R.O.B./blood PC
          PUBA =PLBA                                                                  !ALD lung/blood PC
          PBBRA= SBRA/((0.37*SEA)+(0.63*SPLA))                                        !ALD brain/blood PC
          SLX   =((KOWX*FNLL)+(1*FWL)+(KOW*0.3*FPLL)+(1*0.7*FPLL))/VL                 !solubility of ALX in liver
          SFX   =((KOWX*FNLF)+(1*FWF)+(KOW*0.3*FPLF)+(1*0.7*FPLF))/VF                 !solubility of ALX in fat
```

```
SBRX =((KOWX*FNLBR)+(1*FWBR)+(KOW*0.3*FPLBR)+(1*0.7*FPLBR))/VBR  !solubility of ALX in brain
SBX  =((KOWX*FNLP)+(1*FWP)+(KOW*0.3*FPLP)+(1*0.7*FPLP))/VBO      !solubility of ALX in R.O.B.
SKX  =((KOWX*FNLK)+(1*FWK)+(KOW*0.3*FPLK)+(1*0.7*FPLK))/VK       !solubility of ALX in kidney
SEX  =((KOWX*FNLE)+(1*FWE)+(KOW*0.3*FPLE)+(1*0.7*FPLE))/(VTBL*0.37) !solubility of ALX in RBC
SPLX =((KOWX*FNLPL)+(1*FWPL)+(KOW*0.3*FPLPL)+(1*0.7*FPLPL))/(VTBL*0.63)
                                                                 !solubility of ALX in plasma

PLBX =SLX/((0.37*SEA)+(0.63*SPLA))                               !ALX liver/blood PC
PFBX =SFX/((0.37*SEA)+(0.63*SPLA))                               !ALX fat/blood PC
PKBX =SKX/((0.37*SEA)+(0.63*SPLA))                               !ALX kidney/blood PC
PBBX = SBX/((0.37*SEA)+(0.63*SPLA))                              !ALX R.O.B./blood PC
PUBX =PLBX                                                       !ALX lung/blood PC
PBBRX= SBRX/((0.37*SEA)+(0.63*SPLA))                             !ALX brain/blood PC
!Metabolic parameters for ALD metabolism
CONSTANT VMAXALC  =0          !Rate constant for ALD metabolism in liver (mg/kg/min)
CONSTANT VMAXAKC  =0          !Rate constant for ALD metabolism in kidney(mg/kg/min)
CONSTANT VMAXAUC  =0          !Rate constant for ALD metabolism in lung (mg/kg/min)
         VMLA =VMAXALC*BW**0.74  !Rate of metabolism of ALD in liver  (mg/min)
         VMKA =VMAXAKC*BW**0.74  !Rate of metabolism of ALD in kidney (mg/min)
         VMUA =VMAXAUC*BW**0.74  !Rate of metabolism of ALD in lung (mg/min)
CONSTANT KMAL     =1          !Michaelis-Menten constant for ALD metabolism in liver (mg/L)
CONSTANT KMAK     =1          !Michaelis-Menten constant for ALD metabolism in kidney(mg/L)
CONSTANT KMAU     =1          !Michaelis-Menten constant for ALD metabolism in lung  (mg/L)
CONSTANT KELHAC   =1          !1st order hydrolysis rate constant for ALD (min-1/kg)
         KELHA    =KELHAC/(BW**0.25)  !1st order hydrolysis rate for ALD  (min-1)
CONSTANT KELHXC   =1          !1st order hydrolysis rate constant for ALX  (min-1/kg)
         KELHX    =KELHXC/(BW**0.25)  !1st order hydrolysis rate for ALX  (min-1)
CONSTANT KELUAC   =1          !Urinary excretion rate constant for ALD (min-1/kg)
         KELUA    =KELUAC*(BW**0.75)  !Urinary excretion rate for ALD (min-1)
CONSTANT KELUXC   =1          !Urinary excretion rate constant for ALX (min-1/kg)
```

```
            KELUX       =KELUXC*(BW**0.75)      !Urinary excretion rate for ALD (min-1)
!Definition of Chemical Exposure
CONSTANT    DOSEIVA     =1                      !Dose of ALD administered intravenously (mg/kg)
            AIVA        =BW*DOSEIVA             !Amount of ALD administered intravenously (mg)
CONSTANT    DOSEORA     =1                      !Dose of ALD administered orally (mg/kg)
            AORA        =BW*DOSEORA             !Amount of ALD administered intravenously (mg)
CONSTANT    OACA        =1.132                  !Oral absorption constant for ALD (min-1)
CONSTANT    DOSEIVX     =1                      !Dose of ALX administered intravenously (mg/kg)
            AIVX        =BW*DOSEIVX             !Amount of ALX administered intravenously (mg)
CONSTANT    DOSEORX     =1                      !Dose of ALX administered orally (mg/kg)
            AORX        =BW*DOSEORX             ! Amount of ALX administered intravenously (mg)
CONSTANT    OACX        =1                      !Oral absorption constant for ALX (min-1)
END                                             !of INITIAL section of program

DYNAMIC                                         !section of program
ALGORITHM       IALG    =2                      !Gear's integration algorithm
NSTEPS          NSTP    =1000                   !Number of integration steps
MAXTERVAL       MAXT    =1.0E+33                !Maximum integration step
MINTERVAL       MINT    =1.0E-33                !Minimum integration step
CINTERVAL       CINT    =0.1                    !Communication interval
DERIVATIVE                                      !section of program
!Aldicarb in venous blood compartment
            RAVBA       =((QF*CVFA)+(QL*CVLA)+(QBO*CVBOA)+(QK*CVKA)+(QBR*CVBRA))-(QC*CVBA)-RAHVB
            AVBA        =INTEG(RAVBA,0.0)+AIVA
            CVBA        =AVBA/VVBL
            AUCCVBA     =INTEG(CVBA,0.0)
!Amount of aldicarb eliminated via hydrolysis in venous blood compartment
            RAHVB       =KELHA*CVBA*VVBL
            AAHVB       =INTEG(RAHVB,0.0)
```

```
!Aldicarb in arterial blood compartment
        RAABA     =QC*(CVUA-CABA)-RAHAB
        AABA      =INTEG(RAABA, 0.0)
        CABA      =AABA/VABL
!Amount of aldicarb eliminated via hydrolysis in arterial blood compartment
        RAHAB     =KELHA*CABA*VABL
        AAHAB     =INTEG(RAHAB,0.0)
!Aldicarb in lung compartment
        RAUA      =QC*(CVBA-CVUA)-RMETUA-RAHU
        AUA       =INTEG(RAUA,0.)
        CUA       =AUA/VU
        CVUA      =CUA/PUBA
!Amount of aldicarb oxidized by FMO in lung compartment
        RMETUA    =(VMUA*CVUA)/(KMAU+CVUA)
        AALXU     =INTEG(RMETUA,0.)
        CALXU     =AALXU/VU
!Amount of aldicarb eliminated via hydrolysis in lung compartment
        RAHU      =KELHA*CVUA*VU
        AAHU      =INTEG(RAHU,0.0)
!Aldicarb in kidney compartment
        RAKA      =QK*(CABA-CVKA)-RMETKA-RAHK-RAELUR
        AKA       =INTEG(RAKA,0.)
        CKA       =AKA/VK
        CVKA      =CKA/PKBA
!Amount of aldicarb oxidized by FMO in kidney compartment
        RMETKA    =((VMKA*CVKA)/(KMAK+CVKA))
        AALXK     =INTEG(RMETKA,0.0)
        CALXK     =AALXK/VK
!Amount of aldicarb eliminated via hydrolysis in kidney compartment
```

```
            RAHK        =KELHA*CVKA*VK
            AAHK        =INTEG(RAHK,0.0)
!Amount of aldicarb eliminated via urine
            RAELUR      =KELUA*CABA*VK
            AEUA        =INTEG(RAELUR,0.0)
!Aldicarb in brain compartment
            RABRA       =QBR*(CABRA-CVBRA)-RAHBR
            ABRA        =INTEG(RABRA,0.0)
            CBRA        =ABRA/VBR
            CVBRA       =CBRA/PBBRA
!Amount of aldicarb eliminated via hydrolysis in body compartment
            RAHBR       =(KELHA*CVBRA*VBR)
            AAHBR       =INTEG(RAHBR,0.0)
!Aldicarb in body compartment
            RABOA       =QBO*(CABA-CVBOA)-RAHBO
            ABOA        =INTEG(RABOA,0.0)
            CBOA        =ABOA/VBO
            CVBOA       =CBOA/PBOBA
!Amount of aldicarb eliminated via hydrolysis in body compartment
            RAHBO       =(KELHA*CVBOA*VBO)
            AAHBO       =INTEG(RAHBO,0.0)
!Aldicarb in fat compartment
            RAFA        =QF*(CABA-CVFA)
            AFA         =INTEG(RAFA,0.)
            CFA         =AFA/VF
            CVFA        =CFA/PFBA
!ARSTX = Amount of ALD remaining in the stomach
            RASTA       =-OACA*ARSTA
            ARSTA       =INTEG(RASTA,AORA)
```

```
!AST = Aldicarb input from stomach
            AISTA       =OACA*ARSTA
!Aldicarb in liver compartment
            RALA        =QL*(CABA-CVLA)-RMETLA-RAHL+AISTA
            ALA         =INTEG(RALA,0.)
            CLA         =ALA/VL
            CVLA        =CLA/PLBA
!Amount of aldicarb oxidized by FMO in liver
            RMETLA      =(VMLA*CVLA)/(KMAL+CVLA)
            AALXL       =INTEG(RMETLA,0.)
            CALXL       =AALXL/VL
!Amount of aldicarb eliminated via hydrolysis in liver compartment
            RAHL        =KELHA*CVLA*VL
            AAHL        =INTEG(RAHL,0.0)
!Total amount of ALD oxidized to ALX
            TALX        =AALXU + AALXK + AALXL
!Total mass (amount) of ALD found in rat
            TMASSA      =AVBA+AABA+AUA+AKA+ABRA+ABOA+AFA+ALA+TALX+TAAH+AEUA
!TDOSEA = Total amount of ALD administered
            TDOSEA      = AIVA+AORA
!ALX in venous blood
            RAVBX       =((QF*CVFX)+(QL*CVLX)+(QBO*CVBOX)+(QK*CVKX)+(QBR*CVBRX))-(QC*CVBX)-RAHVB
            AVBX        =INTEG(RAVBX,0)+AIVX
            CVBX        =AVBX/VVBL
            AUCCVBX     =INTEG(CVBX,0.0)
!ALX eliminated from venous blood via hydrolysis
            RHVBX       =(KELHX*CVBX*VVBL)
            AHVB        =INTEG(RHVBX,0.0)
!ALX in arterial blood
```

```
            RAABX       =QC*(CVUX-CABX)-RHABX
            AABX        =INTEG(RAABX, 0.0)
            CABX        =AABX/VABL
!ALX eliminated from arterial blood via hydrolysis
            RHABX       =KELHX*CABX*VABL
            AHAB        =INTEG(RHABX,0.0)
!ALX in lung
            RAUX        =QC*(CVBX-CVUX)-RHU
            AUX         =INTEG(RAUX,0)+AALXU
            CUX         =AUX/VU
            CVUX        =CUX/PUBX
!ALX eliminated from lungs via hydrolysis
            RHUX        =KELHX*CVUX*VU
            AHU         =INTEG(RHUX,0.0)
!ALX in fat compartment
            RAFX        =QF*(CABX-CVFX)
            AFX         =INTEG(RAFX,0.)
            CFX         =AFX/VF
            CVFX        =CFX/PFBX
!ALX in kidney compartment
            RAKX        =QK*(CABX-CVKX)-RELU-RHKX
            AKX         =INTEG(RAKX,0) + AALXK
            CKX         =AKX/VK
            CVKX        =CKX/PKBX
!ALX eliminated from kidney via urine
            RELU        =KELUX*CVKX*VK
            AEUX        =INTEG(RELU,0.0)
!ALX eliminated from kidney via hydrolysis
            RHKX        =KELHX*CVKX*VK
```

```
      AHK       =INTEG(RHKX,0.0)
!ALX in the rest of brain compartment
      RABRX     =QBR*(CABX-CVBRX)+AISTX-RHBRX
      ABRX      =INTEG(RABRX,0.)
      CBRX      =ABRX/VBR
      CVBRX     =CBRX/PBRX
!Amount of ALX eliminated via hydrolysis in brain
      RHBRX     =KELHX*CVBRX*VBR
      AHBR      =INTEG(RHBRX,0.0)
!ALX in liver compartment
      RALX      =QL*(CABX-CVLX)-RHLX
      ALX       =INTEG(RALX,0) + AALXL
      CLX       =ALX/VL
      CVLX      =CLX/PLBX
!ALX eliminated from liver via hydrolysis
      RHLX      =KELHX*CVLX*VL
      AHL       =INTEG(RHLX,0.0)
!ARSTX = Amount of ALX remaining in the stomach
      RASTX     =-OACX*ARSTX
      ARSTX     =INTEG(RASTX,AORX)
!AST = ALX input from stomach
      AISTX     =OACX*ARSTX
!ALX in the rest of body compartment
      RABOX     =QBO*(CABX-CVBOX)+AISTX-RHBOX
      ABOX      =INTEG(RABOX,0.)
      CBOX      =ABOX/VBO
      CVBOX     =CBOX/PBOX
!Amount of ALX eliminated via hydrolysis in rest of the body
      RHBOX     =KELHX*CVBOX*VBO
```

```
            AHBO        =INTEG(RHBOX,0.0)
!Total mass (amount) of ALX found in rat
            TMASSX      =AVBX+AABX+AUX+AFX+ALX+ABRX +ABOX+TAXH+AKX+AEUX
            TDOSEX      =AIVX+TALX
!MODELING OF AChE INHIBITION.
CONSTANT    KAA         =10.3          !Equilibrium assotiation constant for ALD (mM)
CONSTANT    K2A         =146           !Carbamoylation constant for ALD (min-1)
            KIA         =K2A/KAA       !Bimolecular inhibition constant for ALD (mM-1*min-1)
CONSTANT    FACTOR      =23            !Potency factor for ALX
            KIX         =FACTOR*KIA    !Bimolecular inhibition constant for ALX (mM-1*min-1)
CONSTANT    K3A         =0.018         !Re-activation constant for ALD and ALX (min-1)
CONSTANT    MWA         =190.3         !Molecular weight of aldicarb (g/mol)
CONSTANT    MWX         =206.3         !Molecular weight of aldicarb sulfoxide (g/mol)

!AChE INHIBITION IN BRAIN
CONSTANT    AACHEBR     =0.11E-06      !Amount of AChE in the brain (mmoles)
            CACHEBR     =AACHEBR/VBR   !Concentration of AChE in the brain (mM)
            CVBRA2      =CVBRA/MWA     !Converts CVBRA in mM
            CVBRX2      =CVBRX/MWX     !Converts CVBRX in mM
            RFACHEBR=(((-KIA*CFACHEBR*CVBRA2)+(-KIX*CFACHEBR*CVBRX2))+(K3A*CIACHEBR))*VBR
            AFACHEBR=INTEG(RFACHEBR,AACHEBR)  !amount of free AChE in brain (mmol)
            CFACHEBR    =AFACHEBR/VBR  !Concentration of free AChE in RBC's  (mM)
            CIACHEBR=CACHEBR-CFACHEBR  !concentration of inhibited AChE in brain (mM)
            PFACHEBR=(CFACHEBR/CACHEBR)*100      !percent of free AChE in brain!
AChE INHIBITION IN RBC
CONSTANT    AACHER      =1.21E-04      !Amount of AChE in the RBC's (mmoles)
CONSTANT    HC          =0.37          !Hematocrit
            VRBC        =VTBL*PRBC     !Volume of RBC
            CACHER      =AACHER/VRBC   !Concentration of AChE in RBC's (mM)
```

```
            CVBA2       =((0.65*CVBA)+(0.35*CABA))/MWA
            CVBX2       =((0.65*CVBX)+(0.35*CABX))/MWX
            RFACHER     =(((-KIA*CFACHER*CVBA2)+(-KIX*CFACHER*CVBX2))+(K3A*CIACHER))*VRBC
            AFACHER     =INTEG(RFACHER,AACHER)    !Amount of free AChE in RBC's (mmol)
            CFACHER     =AFACHER/VRBC             !Concentration of free AChE in RBC's  (mM)
            CIACHER     =CACHER-CFACHER           !Concentration of inhibited AChE in RBC's (mM)
            PFACHER     =(CFACHER/CACHER)*100     !Percent of free AChE in RBC's
!AChE INHIBITION IN PLASMA
CONSTANT    AACHEP      =1.01-06                  !Amount of AChE in plasma (mmoles)
            VPLA        =VTBL*(1-HC)              !Volume of plasma
            CACHEP      =AACHEP/VPLA              !Concentration of AChE in plasma (mM)
            CVPLA2      =((0.65*CVBA)+(0.35*CABA))/MWA
            CVPLX2      =((0.65*CVBX)+(0.35*CABX))/MWX
            RFACHEP     =(((-KIA*CFACHEP*CVPLA2)+(-KIX*CFACHEP*CVPLX2))+(K3A*CIACHEP))*VPLA
            AFACHEP     =INTEG(RFACHEP,AACHEP)    !Amount of free AChE in RBC's (mmol)
            CFACHEP     =CACHEP-CFACHEP           !Concentration of inhibited AChE in plasma (mM)
            PFACHEP     =(CFACHEP/CACHEP)*100     !Percent of free AChE in plasma
CONSTANT    TSTOP       =1440                     !Lenght of experiment (min)
TERMT(T.GE.TSTOP)                                 !Stop simulation when T>TSTOP
END                                               !of derivative section of program
END                                               !of dynamic section of program
END                                               ! of program section of program
```

REFERENCES

Aldridge, W.H., and Magos, L. (1978). Carbamates, thiocarbamates and thiocarbamtes, Commission of the European Communities, Luxembourg.

Altman, P.L., and Dittmer, D.S. (1962). Growth including reproduction and morphological development. Fed. Proc. 337-366.

Andersen, M.E. (1992). Mechanistic toxicology research and biologically-based modeling: partners for improving quantitative risk assessments. CITT Activities, **12**,1-8.

Andrawes, N. R., Dorough, H. W., and Lindqiust, D. A. (1967). Degradation and elimination of Temik in rats. J. Agric. Food Chem. **60**, 979-987.

Baron, R. L., and Merriam, T. L., 1988, Toxicology of Aldicarb. Rev. Environ. Contam. Toxicol. **105**, 1-70.

Bird, A.P, G.W., Leavitt, R.A., Rose, L.M. (1984). Dynamics of aldicarb soil residues associated with Pratylenchus penetrans control in dry bean production, Plant Disease, **68** (10), 873-874.

Biscoff, K.B. and Brown, R.G. (1966). Drug distribution in mammals. Chem. Engin. Prog. Symp. **62**, 33-45.

Bull, D. L., Lindquist, D. A., and Coppedge, J. R.(1967). Metabolism of 2-methyl-2-(methylthio)propionaldehyde O-(methylcarbamoyl) oxime (Temik, UC-21149) in insects. J. Agric. Food Chem. **15**, 610-616.

Cambon, C., Declume, C., and Derache, R. (1979). Effect of the insecticide carbamate derivatives (carbofuran, primicarb, aldicarb) in the activity of acetylcholinesterase in tissues from pregnant rats and foetuses. Toxicol. App. Pharmac. **49**, 203-208.

Carpenter, C.P. and Smyth, H.F.(1965). Recapitulation of Toxicodynamics and acute toxicity studies on Temic, Mellon Institute Report No. 28-78, EPA Pesticide petition No. 9F0798

Clewell, H.J. III, and Jarnot, B.M. (1994). Incorporation of pharmacokinetics in noncancer risk assessment: Example with chloropentafluorobenzene, Risk Analysis, **14**(3), 265-276.

Cope, O.E. and Romine, R.R. (1973). Temic Aldicarb pesticide. Results of aldicarb ingestion and exposure studies with humans and results of monitoring human exposure in working environments, Unpublished study, File No. 18269, Union Carbide Agricultural Co. Project No. 111A13, 116A16, File No. 18269.

DePass, L.R., Weaver, E.V. and Mirro, E.J. (1985). Aldicarb sulfoxide/ aldicarb sulfone mixture in drinking water of rats: effects on growth and acetylcholinesterase activity. J. of Toxicol. Environ. Health, **16**, 163-172.

Gaines, T.B. (1969). Acute toxicity of pesticides, Toxicol. Appl. Pharmacol **14**, 515-534.

Gupta. R., and Dettbarn, W.D.(1993). Role of carboxylesterases in the prevention and potentiation of N-methylcarbamate toxicity, Chem.-Biol. Inter. **87**, 295-303.

Haines, R.G. (1971). Ingestion of aldicarb by human volunteers: a controlled study of the effects of aldicarb on man, Unpublished study, Union Carbide Agricultural Co., Terryton, N.Y.

Hastings, F. L., Main, A. R., and Iverson, F. (1970). Carbamylation and affinity constants of some carbamate inhibitors of acetylcholinesterase and their relation to analogous substrate constants. J. Agric. Food Chem. **18**, 497-502.

Houston, J.B., Upshall, D.G., and Bridges, J.W.(1975). Further studies using carbamate esters as model compounds to investigate the role of lipophilicity in the gastrointestinal absorption of foreign compounds, J. of Pharmac. Exper. Therap. **195**, 67-72.

ILSI, (1994). Physiological parameter values for PBTK models. International Life Sciences Institute, Risk Science Institute, Washington, DC.

IRIS, (1996). Integrated Risk Information System, Aldicarb, USEPA.

Iverson, F., and Main, A.R. (1969). Effect of charge on the carbamylation and binding constants of eel acetylcholinesterase in reaction with neostigmine and related carbamates, Biochemistry, **8**, 1889-1904.

Johnson, C.D. and Russell, R.L.(1975). A rapid radiometric assay for cholinesterase suitable for multiple determinations, Anal. Biochem. **64**, 229-238.

Kaloyanova, F.P. and El Batawi, M.A. (1991). Human Toxicology of Pesticides, CRC Press, Boca Raton

Knaak, J. B., Tallant, M. J., and Sullivan, L. J.(1966). The metabolism of 2-methyl-2-(methylthio) propionaldehyde O-(methylcarbamoyl)oxime in the rat. J. Agric. Food Chem. **14**, 573-578.

Kuhr, R.J. and Dorough, H.W. (1976). Carbamate Insecticides: Chemistry, Biochemistry, and Toxicology, CRC Press, Boca Raton, Fla.

Long, C. (1961). Biochemists' Handbook, Van Nostrand Reinhold Co., N.Y.

Martin, H. and Worthing, C.R.(1977). Pesticide Manual, British Crop Protection Council, Worcestershire, England.

Maxwell, D. M, Len, D.E., Groff, W.A, Kaminski, A., and Froehlich, H.L. (1987). The effects of blood flow and detoxification on in vivo cholinesterase inhibition by soman in the rats. Toxicol. Appl. Pharmacol. **88**, 66-76.

Norstrandt, A.C., Duncan, J.A., and Padilla, S. (1993). A modified spectrophotometric method appropriate for measuring cholinesterase activity in tissue from carbaryl-treated animals. Fund. Appl. Pharmacol. **21**, 196-203.

O'Brien, R.D., Hilton, B.D., and Gilmour, L. (1966). The reaction of carbamates with cholinesterase, Mol. Pharmacol. **2**, 593.

Padilla, S. and Hooper, M.J. (1992). Cholinesterase measurements in tissues from-carbamate-treated animals: Cautions and recommendations. Proceedings of the U.S. EPA Workshop on Cholinesterase Methodologies, pp. 63-81. Office of Pesticides Programs, U.S. Environmental Protection Agency, Washington, DC.

Pelekis, M., Poulin, P., and Krishnan, K. (1995), An approach for incorporating tissue composition data into physiologically based pharmacokinetic models, Toxicol. Ind. Health, **11**(5), 511-522.

Pelekis, M., and Krishnan, K. (1997). Determination of the rate of aldicarb sulphoxidation in rat liver, kidney and lung microsomes. Xenobiotica, **27**(11), 1113-1120.

Poulin, P., and Krishnan, K. (1995a). A biologically-based algorithm for predicting human tissue:blood partition coefficients of organic chemicals, Hum. Exper. Toxicol. **14**, 273-280.

Poulin, P., and Krishnan, K. (1995b). An algorithm for predicting tissue:blood partition coefficients of organic chemicals, J. Toxicol. Environ. Health **46**,117-129.

Poulin, P., and Krishnan, K. (1996). A tissue composition-based algorithm for predicting tissue:air partition coefficients of organic chemicals. Toxicol. Appl. Pharmacol. **136**, 126-130.

Poulin, P., and Krishnan, K. (1998). Molecular structure-based prediction of the toxicokinetics of inhaled vapors in humans, Int. J. Toxicol. (Submitted)

Reiner, E., and Aldridge, W.N. (1967). Effects of pH on inhibitionn and spontaneous reactivation of acetylcholinesterase treated with esters of phosphorus acids and of carbamic acids, Biochem. J. 105: 171.

Renwick, A.G. (1991). Safety factors and establishment of acceptable daily intakes, Food Addit. Contamin. **8**, 135-150.

Renwick, A.G. (1993). Data-derived safety factors for the evaluation of food additives and environmental contaminants, Food Addit. Contamin. **10**, 275-305.

Rhone-Poulenc. (1992). A safety and tolerability study of aldicarb at various dose levels in healthy male and female volunteers. Inveresk Clinical Research Report No. 7786.

Satoh, T., and Hosokawa, M. (1995). Molecular aspects of carboxylesterase isoforms in comparison within other esterases, Toxicol. Lett., **82/83**, 439-445.

US Environmental Protection Agency, (1988). Aldicarb Special Review Technical Support Document. Washington, DC: Office of Pesticides and Toxic Substances; June.

US Environmental Protection Agency, (1989). Method 531.1. Measurement of N-methycarbamates in water by direct aqueous injection HPLC with post column derivatazation, Environmental Monitoring Systems Laboratory, Office of Research and Development, Cincinnati, Ohio.

US Environmental Protection Agency, (1994). Methods for derivation of reference concentrations and application of inhalation dosimetry. Research Triangle ParK, NC:Office of Health and Environmental Assessment, Envirnmental Criteria and Assessment Office, EPA/600/8-90/066F.

Venkataraman, B.V., and Naga Rani, M.A. (1994). Species variation in the specificity of cholinesterases in human and rat blood samples. Indian J. Physiol. Pharmacol. **38,** 211-213.

Weiden, M.H.J., Moorfield, H.H. and Payne, L.K (1965). O-(methyl-carbomyl)-oximes: A class of carbamate insecticides-Acarides. J. Econ. Entomol. **58,** 154-155.

Wilkinson, C.F., Babish, J.G., Lemley, A.T., and Doderlund, D.M. (1983). A toxicological evaluation of aldicarb and its metabolites in relation to the potential human health impact of aldicarb resudues in Long Island ground water, New York, Cornell University, Committee from the Institute for Comparative and Environmental Toxicology (Unpublished report).

World Health Organization, (1991). Aldicarb, Environmental Health Perspectives, 121, 20

Table 1. P450 Enzyme Content and Activities for Pooled Human Microsomes[1]

Content	
Cytochrome P450 (Omura & Sato)	0.48 nmol/mg
Cytochrome P450 (Matsubara)	0.55 nmol/mg
Cytochrome b5	0.51 nmol/mg
NADPH- cytochrome c reductase	271nmol/mg/min

Activity (pmol/mg microsomal protein/min)		
CYP1A2	7-Ethoxyresorufin O-dealkylation	48.4±1.4
CYP1A2	Caffeine N3-demethylation	83.5±2.2
CYP2A6	Coumarin 7-hydroxylation	1400±170
CYP2C9	Tolbutamide methyl-hydroxylation	210±1
CYP2C19	S-Mephenytoin 4'-hydroxylation	143±1
CYP2D6	Dextromethorphan O-demethylation	303±3
CYP2E1	Chlorzoxazone 6-hydroxylation	1300±60
CYP3A4/5	Testosterone 6∃-hydroxylation	4960±400
CYP4A9/11	Lauric acid 12-hydroxylation	1290±70

[1] Data provided by Human Biologics (Phoenix, AR)

Table 2: Physiological parameters used in the ALD PBTK models[1]

Tissue volumes (% of body weight)		
	Rat	**Human**
Liver	3.4	2.6
Lung	0.5	0.8
Kidney	0.7	0.4
Brain	0.6	2.0
Fat	7.0	21.4
Blood	7.4	7.9
Rest of body	71.4	55.9
Flow rates (L/min)		
Cardiac output	0.09	5.41
Flow distribution (% Cardiac output)		
Liver	18.3	22.7
Kidney	14.4	17.5
Brain	2.0	11.4
Fat	7.0	7.0
Rest of body	58.3	41.4

[1] Data from ILSI 1994

TABLE 3: Concentration of esterases in rats[1]

Tissue	AChE[2]	BuChE & CaChE[3]
Brain	37.8	564
Liver	0.89	45500
Lung	1.94	12900
Kidney	0.48	16500
Plasma	1.12	4220
RBC	0.92	--
Rest of body	5.08	11000

[1] Data from Maxwell *et al.* (1987), and Venkataraman and Naga Rani (1994); expressed in nmoles/kg tissue

[2] AChE: Acetylcholinesterase

[3] BuChE: Butyrylcholinesterase, CaChE: Carboxylcholisterase

Table 4: Water and lipid composition of rat and human tissues[1]

Tissue Compartment	Water (Fraction of tissue weight)		Total lipids (Fraction of tissue weight)		Phospholipids (Fraction of tissue weight)		Neutral lipids (Fraction of tissue weight)	
	Rat	Human	Rat	Human	Rat	Human	Rat	Human
Liver	0.700	0.720	0.060	0.0670	0.42	0.42	0.58	0.58
Kidney	0.780	0.770	0.060	0.0520	0.025	0.35	0.975	0.65
Rest of the body[2]	0.743	0.750	0.019	0.045	0.541	0.23	0.459	0.77
Lung	0.700	0.75	0.060	0.012	0.42	0.75	0.58	0.25
Fat	0.120	0.150	0.855	0.800	0.0025	0.0025	0.9975	0.9975
Brain	0.700	0.790	0.060	0.110	0.42	0.58	0.58	0.42
Erythrocytes	0.630	0.743	0.0051	0.065	0.77	0.32	0.23	0.68
Plasma	0.960	0.960	0.0023	0.023	0.361	0.361	0.639	0.639

[1] Data from Altman and Dittmer 1961, Long 1961, Martin *et al.* 1982, Poulin and Krishnan 1995a, b, 1996.

[2] Average of slowly perfused tissues

Table 5: Reaction constants for carbamates and AChE

	K_a	K_2	K_I	K_3
	(mM)	(min^{-1})	($mM^{-1}min^{-1}$)	(min^{-1})
ALD	10.3	146	14.2	0.018
ALX	--	--	326[2]	0.018

[1] Data from Hastings *et al.* (1970) and Kuhr and Dorough (1976).

[2] Estimated from the corresponding constant for ALD and the difference in potency between the two carbamates.

Table 6: Partition coefficients used in the ALD PBTK models

	Rat	Human
Liver:Blood	0.94	0.93
Lung:Blood	0.94	0.93
Kidney:Blood	1.05	1.01
Brain:Blood	0.94	0.93
Fat:Blood	2.0	1.81
Rest of body:Blood	0.91	0.91

Table 7: Biochemical parameters used in the ALD PBTK models

	Rat		Human	
	Vmax (mg/kg/min)	Km (mg/L)	Vmax (mg/kg/min)	Km (mg/L)
Liver	718	35	3497	317.8
Kidney	587	199.6	587	199.6
Lung	5.26	35.8	5.26	35.8

Table 8. Comparison of the contribution of metabolising tissues when metabolism is described as a saturable and a blood flow-limited process in the rat[1]

	Amount of ALX produced (% of total)	
	Saturable Metabolism[1]	Blood flow-limited Metabolism
Liver	19.8	13.7
Kidney	14.7	10.8
Lung	65.5	75.4

[1] The total amount of ALX produced when metabolism is described as saturable and flow limited process was 0.1064 mg and 0.1074 mg, respectively. The dose in both cases is 0.4 mg/kg (and the amount 0.11mg)

Table 9. Inhibition of AChE in rat RBC following the *iv* administration of 0.3 mg/kg and 0.1 mg/kg ALX (average±SEM)

0.3 mg/kg		0.1 mg/kg	
Time (min)	AChE (% of control)	Time (min)	AChE (% of control)
Control	100±4.3	Control	100±4.3
15	2.94±0.18	10	5.17±0.49
30	4.46±0.68	20	6.28±1.74
45	5.06±0.09	30	8.86±2.12
60	3.82±0.19	45	10.93±0.41
90	5.47±0.56	60	15.2±1.57
120	9.97±1.27	90	35.9±10.5
360	33.4±6.92	120	32.5±12.2

Table 10. Inhibition of AChE in rat RBC and plasma following the *iv* administration of 0.4 and 0.1 mg/kg ALD (average±SEM)

0.4 mg/kg			0.1 mg/kg		
	AChE (% of control)			AChE (% of control)	
Time (min)	RBC	Plasma	Time (min)	RBC	Plasma
Control	100±7.4	100±5.0	Control	100±2.4	100±7.0
30	5.80±0.4	7.80±0.5	15	4.58±0.04	13.2±0.73
60	2.80±0.2	7.05±0.4	30	9.40±2.4	13.7±1.6
120	5.70±0.9	11.3±1.8	45	6.99±2.0	15.0±1.09
180	13.1±2.2	21.8±0.5	60	10.6±1.4	23.3±2.16
240	45.7±17.5	67.5±21.8	90	26.3±3.4	27.2±3.9
360	71.0±7.97	105±11.5	120	43.5±16.7	52.3±16
480	79.2±9.9	107±3.53		--	--

Table 11: Inhibition of AChE in human blood following oral administration of ALD (average±SEM)

	AChE (% of control)		
Time (min)	0.1 mg/kg	0.05 mg/kg	0.025 mg/kg
Control	100±7.0	100±7.0	100±7.0
60	35.7±1.9	43.5±6.3	55.5±6.3
120	29.1±4.1	49.7±4.7	62.1±5.8
240	58.8±5.4	85.6±4.7	88.7±4.7
360	76.3±4.2	91.0±4.7	93.4±9.7

Table 12: Interspecies toxicokinetic uncertainty factors (UF_{AH-TK}) for ALD and ALX obtained with the PBTK models

	UF_{AH-TK}	
Metric	ALD	ALX
AUC_{CV}[1]	0.105	0.058
AUC_{CBR}[1]	0.106	0.058

[1] Both rat and human were exposed to 0.1 mg/kg (p.o.)

Figure Legends

Figure 1: Schematic representation of the physiologically-based toxicokinetic model for aldicarb.

Figure 2: Aldicarb sulfoxide (ALX) produced by the sulfoxidation of aldicarb by human liver (protein concentration: 0.5 mg/ml; ALD: 5.25 μM), microsomes as a function of incubation time. The symbols represent experimental data (mean ± SE, n=3).

Figure 3. Aldicarb sulfoxide (ALX) produced by the sulfoxidation of aldicarb by human liver (5.25 μM), as a function of the concentration of microsomal protein. The experimental data (symbols, mean ± SE, n=3) correspond to the amount of ALX measured at the end of a ten minute incubation.

Figure 4. Hanes-Woolf plot of aldicarb sulfoxidation in human liver microsomes. v refers to the initial rate of reaction (μmol/min/mg protein) and [S] refers to the initial aldicarb concentration (μM).

Figure 5: Time course for the venous blood concentration of ALX in rats after an *iv* dose of 0.3 mg/kg (o----o) and 0.1 mg/kg (∇---∇) ALX. The symbols represent experimental data whereas the solid line is PBTK model simulation.

Figure 6: Time course simulation for the venous blood concentration of ALD in rats after an *iv* dose of 0.4 mg/kg (- - - -) and 0.1 mg/kg (——) ALD. Due to its very fast metabolism no ALD was detected in the experimental studies.

Figure 7: Time course for the venous blood concentration of ALX in rats after an *iv* dose of 0.4 mg/kg (o----o) and 0.1 mg/kg (∇---∇) ALD. The symbols represent experimental data whereas the solid line is PBTK model simulation.

Figure 8: Time course for the venous blood concentration of ALX in rats after an *iv* dose of 0.4 mg/kg (o----o) and 0.1 mg/kg (∇---∇) ALD. The symbols represent experimental data whereas the solid line is PBTK model simulation obtained with the metabolism being described as a flow-limited process in the liver and kidney compartments. Metabolism in the lungs was described as a saturable process.

Figure 9: Time course for the venous blood concentration of ALX in rats after an *iv* dose of 0.4 mg/kg (o----o) and 0.1 mg/kg (∇---∇) ALD. The symbols represent experimental data whereas the solid line is PBTK model simulation obtained with the metabolism being described as a flow-limited process in the liver, kidney and lung compartments.

Figure 10: Time course inhibition pattern of RBC AChE activity in rats after an *iv* dose of 0.3 mg/kg ALX. The symbols represent experimental data whereas the solid line is PBTK model simulation.

Figure 11: Time course inhibition pattern of RBC AChE activity in rats after an *iv* dose of 0.1 mg/kg ALX. The symbols represent experimental data whereas the solid line is PBTK model simulation.

Figure 12: Time course inhibition pattern of RBC AChE activity in rats after an *iv* dose of 0.4 mg/kg ALD. The symbols represent experimental data whereas the solid line is PBTK model simulation.

Figure 13: Time course inhibition pattern of RBC AChE activity in rats after an *iv* dose of 0.1 mg/kg ALD. The symbols represent experimental data whereas the solid line is PBTK model simulation.

Figure 14: Time course inhibition pattern of plasma AChE activity in rats after an *iv* dose of 0.4 mg/kg ALD. The symbols represent experimental data whereas the solid line is PBTK model simulation.

Figure 15: Time course inhibition pattern of plasma AChE activity in rats after an *iv* dose of 0.1 mg/kg ALD. The symbols represent experimental data whereas the solid line is PBTK model simulation.

Figure 16: Simulated time course for the venous blood concentration of ALD in humans after an oral dose of 0.1 mg/kg ALD.

Figure 17: Time course for the venous blood concentration of ALX in humans after an oral dose of 0.1 mg/kg ALD. The PBTK model simulation was obtained with the metabolism being described as a saturable process in the liver, kidney and lung compartments using the corresponding rat parameters

Figure 18: Time course for the venous blood concentration of ALX in humans after an oral dose of 0.1 mg/kg ALD. The PBTK model simulation was obtained with the metabolism being described as a saturable process in the liver, kidney and lung compartments using the human parameters for the liver and the rat parameters for the kidney and lung compartments

Figure 19: Time course for the venous blood concentration of ALD in humans after an oral dose of 0.1 mg/kg ALD. The symbols represent experimental data whereas the solid line is PBTK model simulation obtained with the metabolism being described as a flow-limited process in the liver, kidney and lung compartments.

Figure 20: Time course for the venous blood concentration of ALD in humans after an oral dose of 0.1 mg/kg ALD. The symbols represent experimental data whereas the solid line is PBTK model simulation obtained with the metabolism being described as a flow-limited process only in the liver compartment.

Figure 21: Time course of blood AChE activity in humans after oral administration of 0.1 mg/kg ALD. The symbols represent experimental data whereas the solid line is PBTK model simulation.

Figure 22: Time course of blood AChE activity in humans after oral administration of 0.05 mg/kg ALD. The symbols represent experimental data whereas the solid line is PBTK model simulation.

Figure 23: Time course of blood AChE activity in humans after oral administration of 0.025 mg/kg ALD. The symbols represent experimental data whereas the solid line is PBTK model simulation.

Figure 1

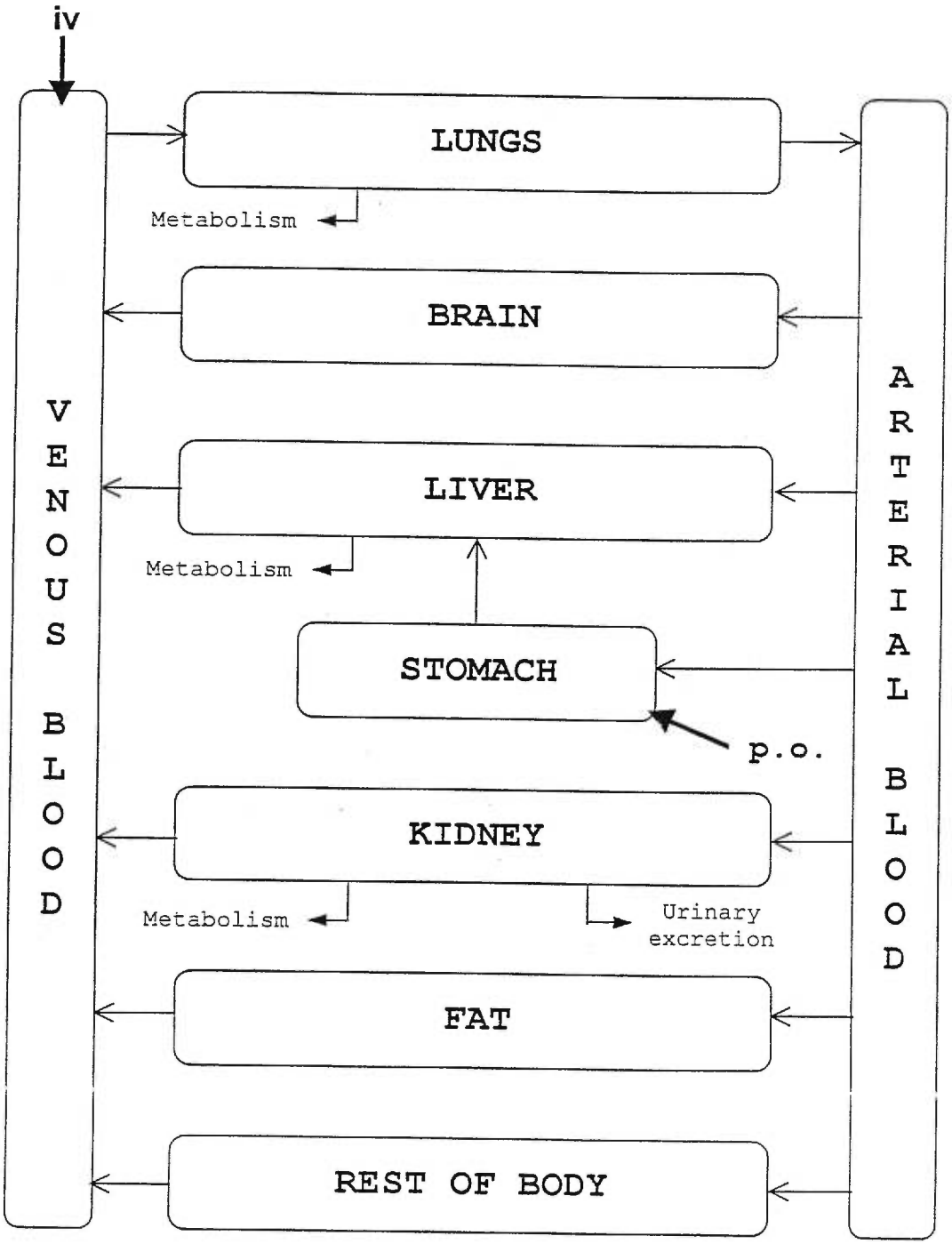
iv
VENOUS BLOOD
LUNGS
Metabolism
BRAIN
LIVER
Metabolism
STOMACH
p.o.
KIDNEY
Metabolism
Urinary excretion
FAT
REST OF BODY
ARTERIAL BLOOD

Figure 2

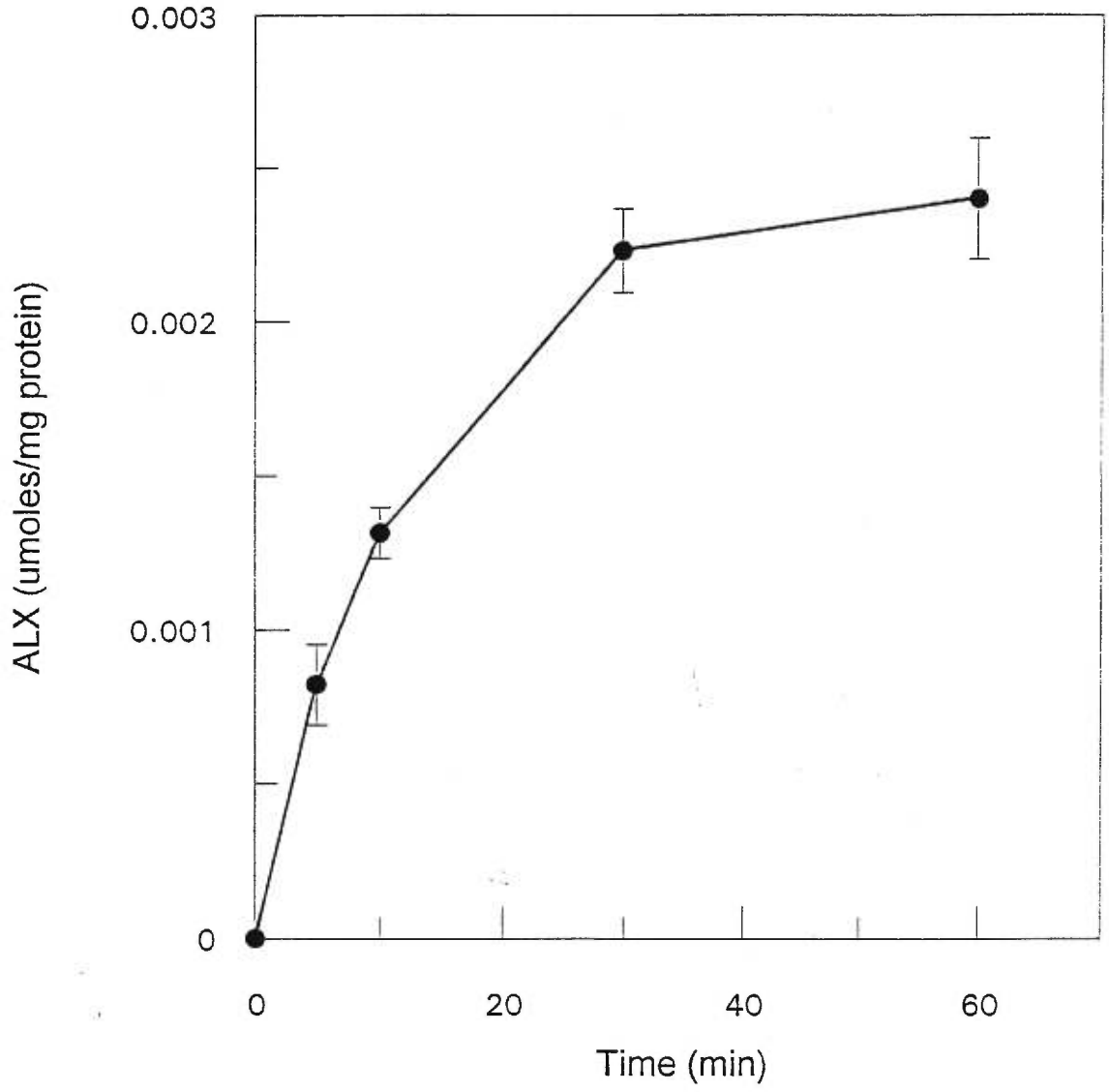

Figure 3

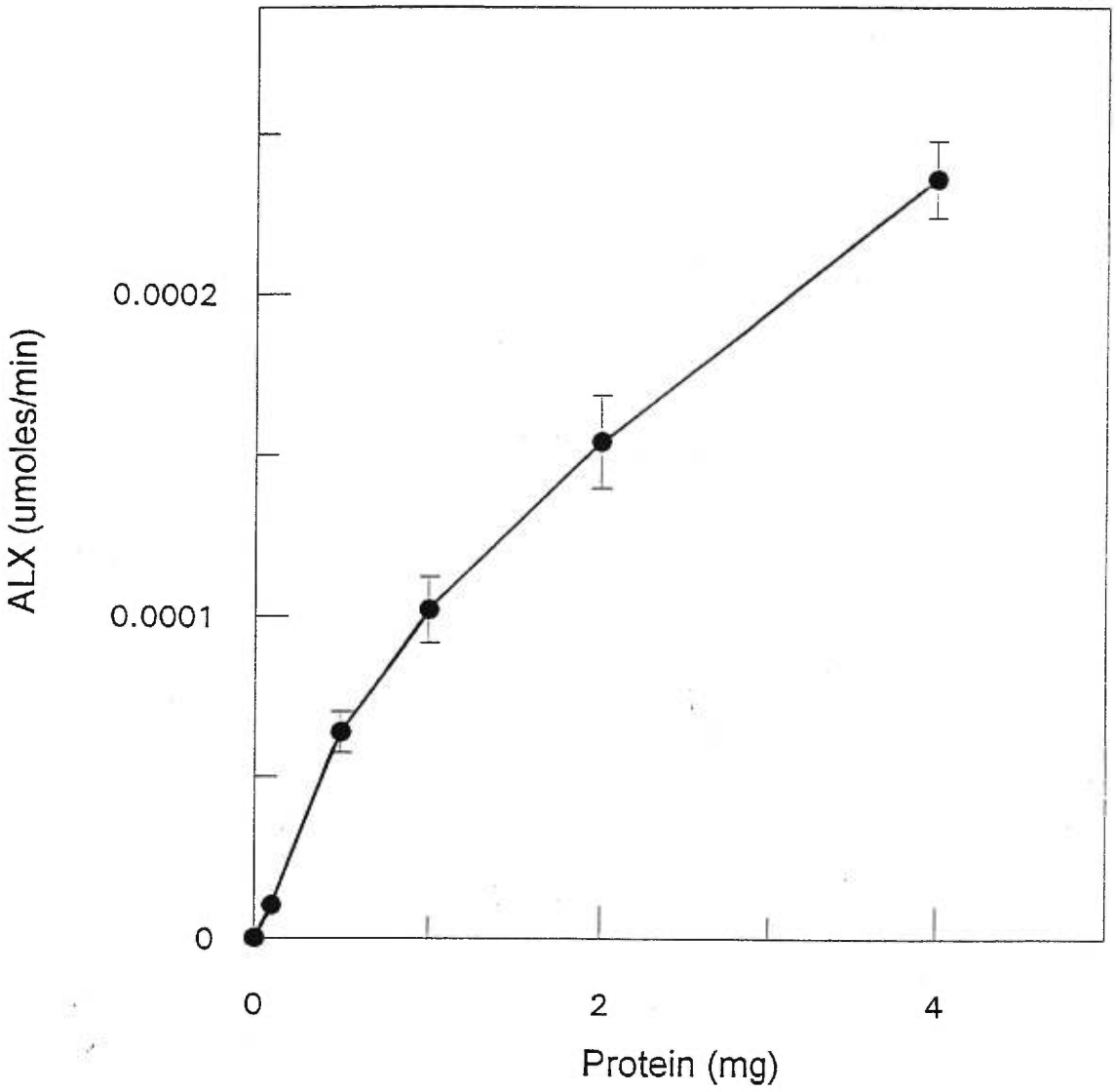

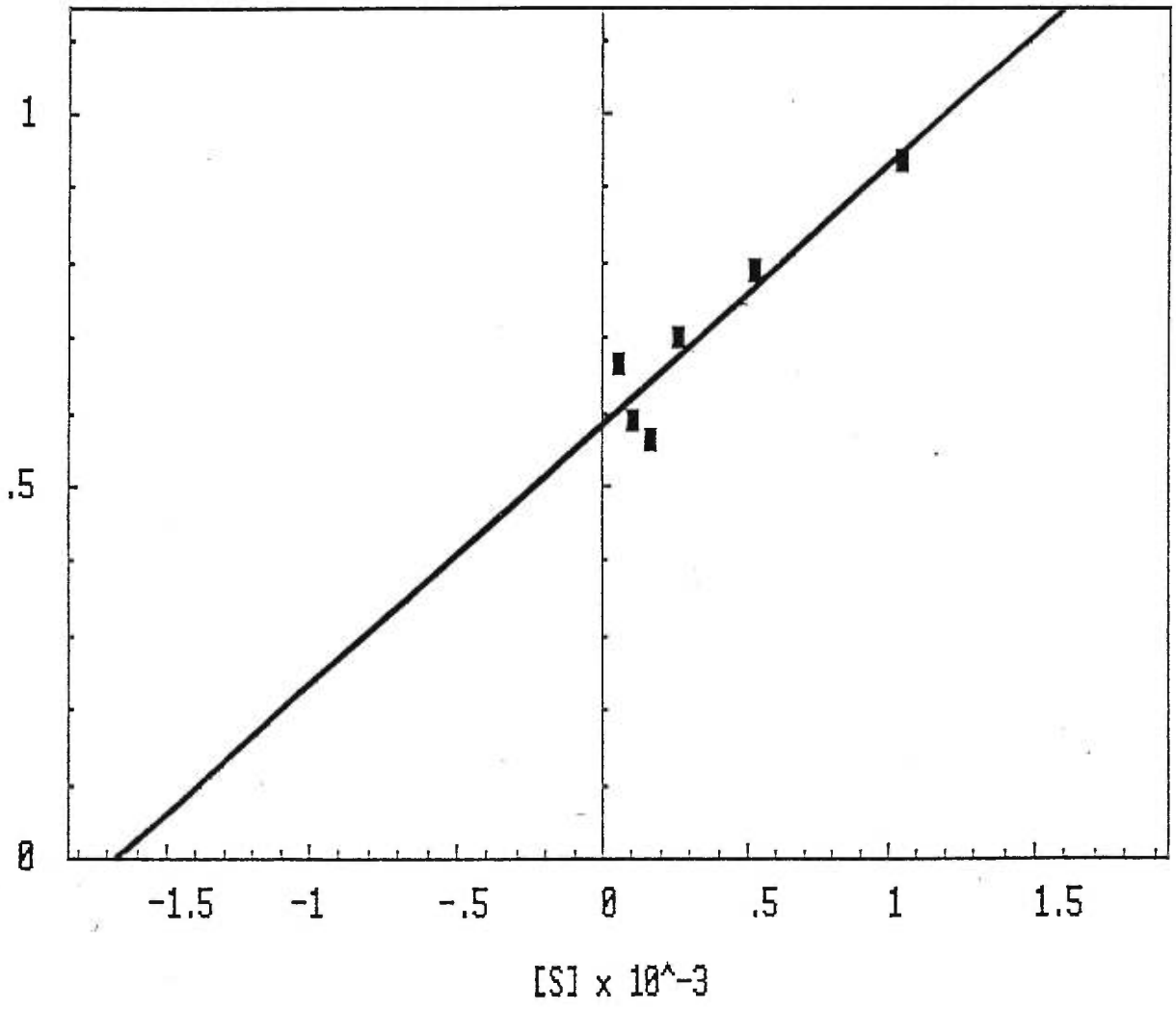
1
.5
0
-1.5
-1
-.5
0
.5
1
1.5
[S] x 10^-3

Figure 5

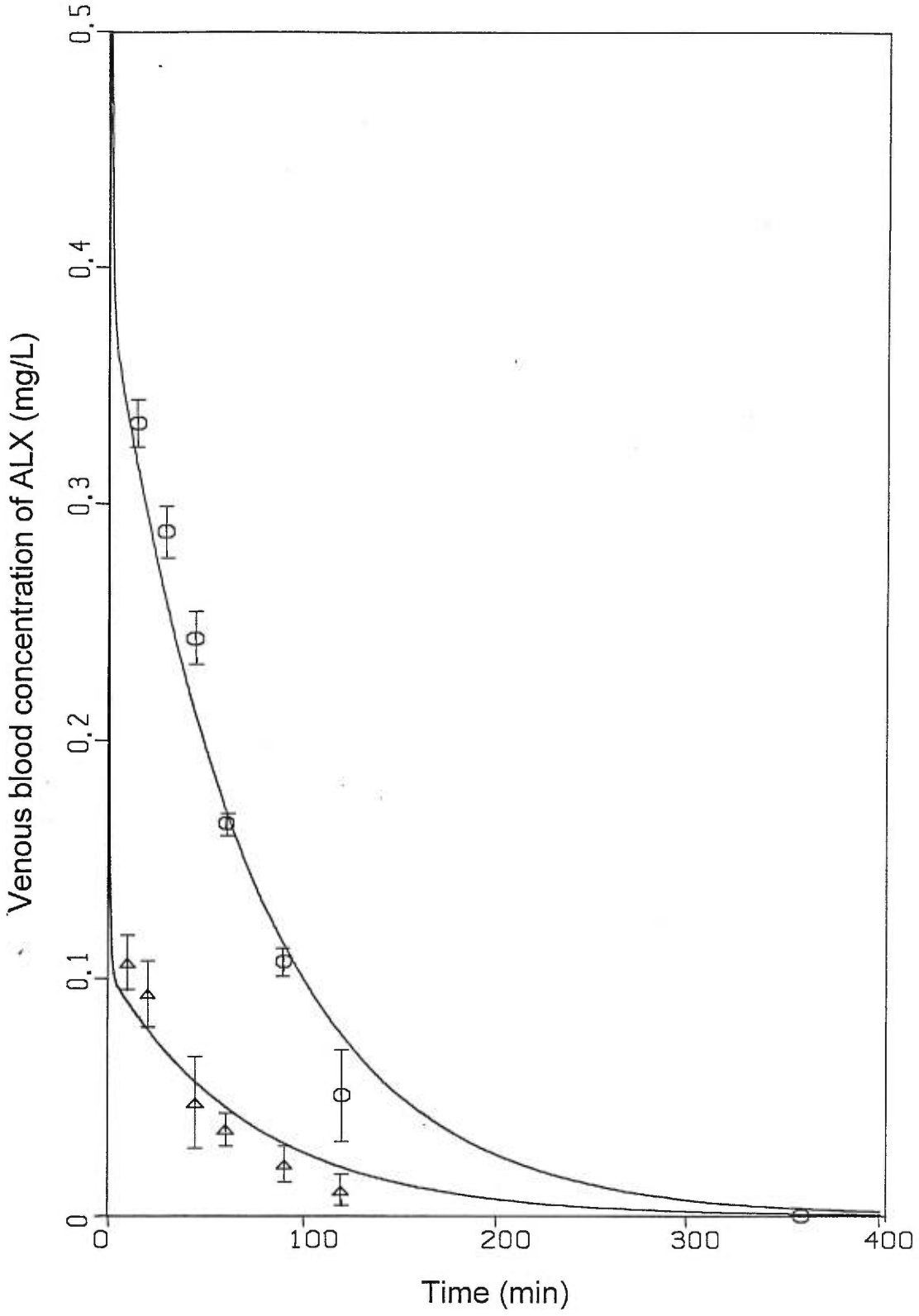
Venous blood concentration of ALX (mg/L)
0
0,1
0,2
0,3
0,4
0,5
0
100
200
300
400
Time (min)

Figure 6

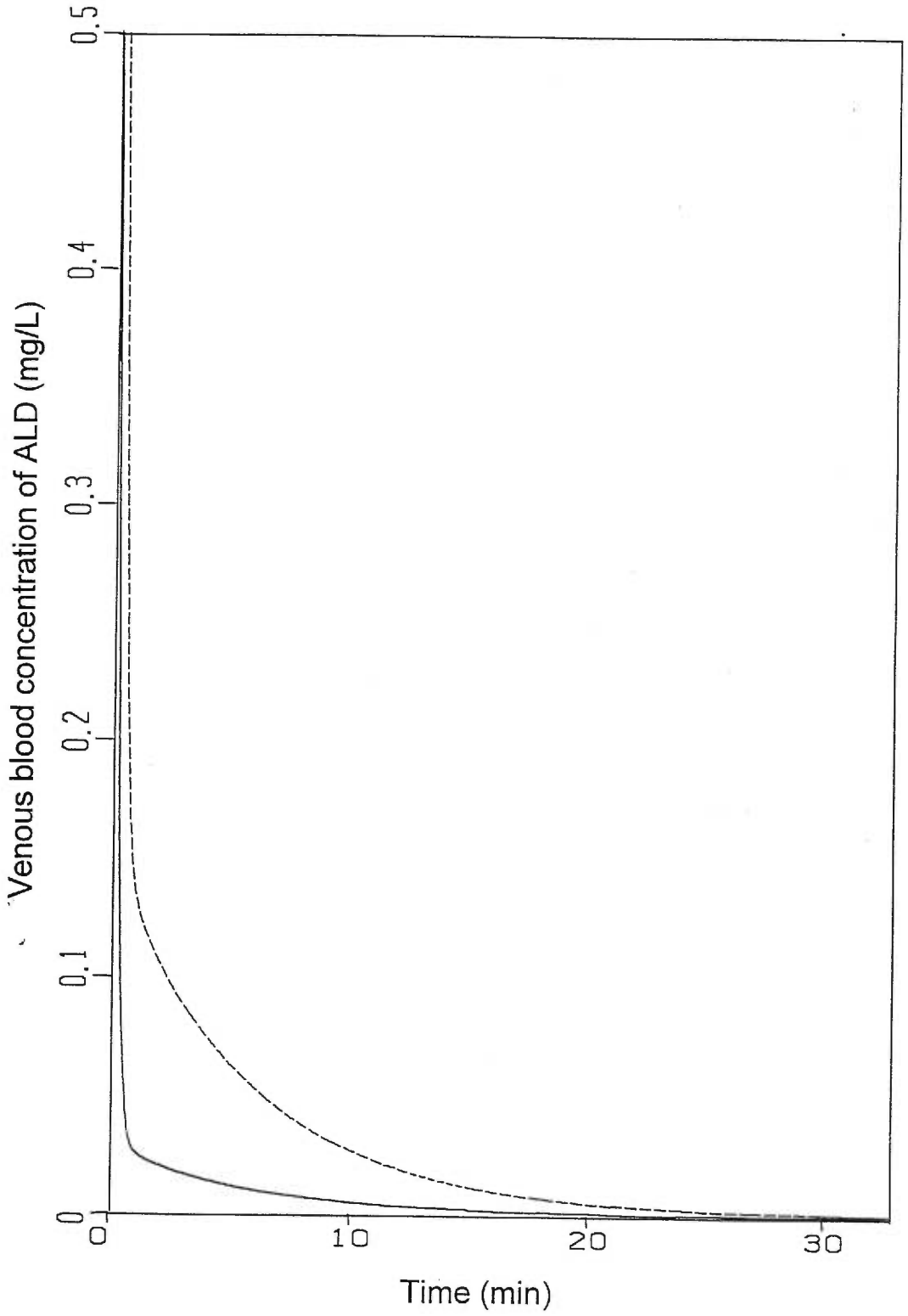
Venous blood concentration of ALD (mg/L)
0.5
0.4
0.3
0.2
0.1
0
0
10
20
30
Time (min)

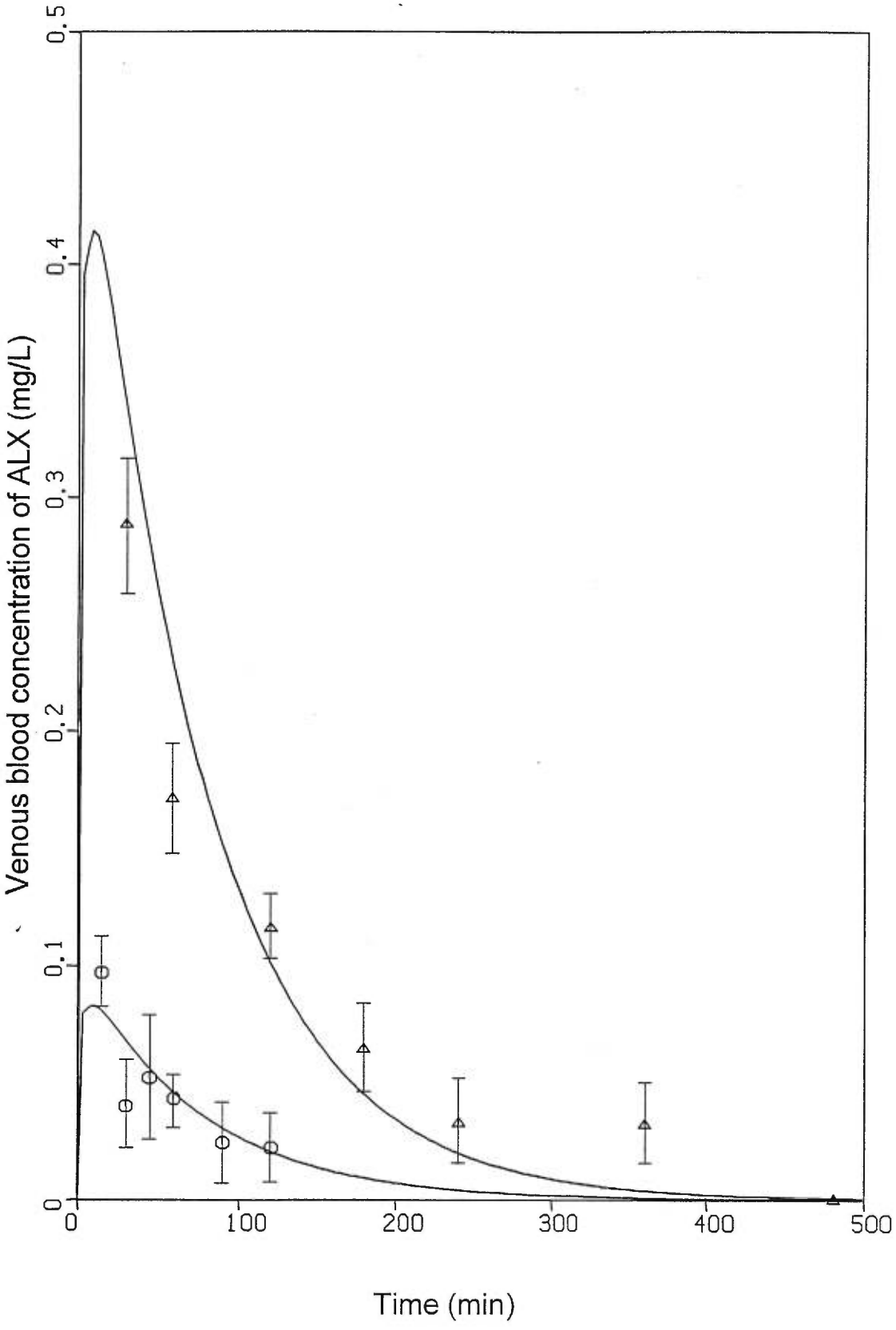
Venous blood concentration of ALX (mg/L)
0
0.1
0.2
0.3
0.4
0.5
0
100
200
300
400
500
Time (min)

Figure 8

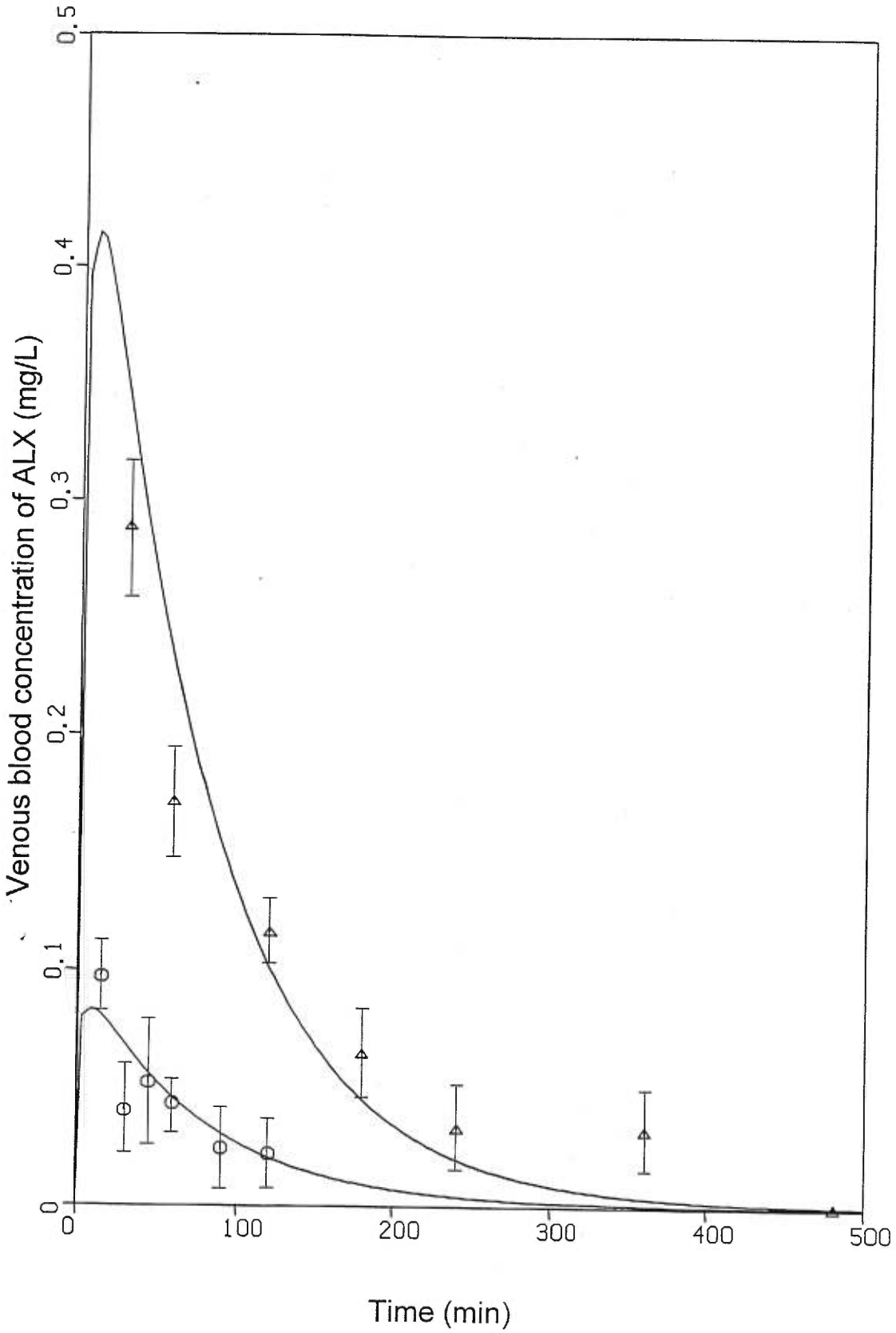
Venous blood concentration of ALX (mg/L)
0
0.1
0.2
0.3
0.4
0.5
0
100
200
300
400
500
Time (min)

Figure 9

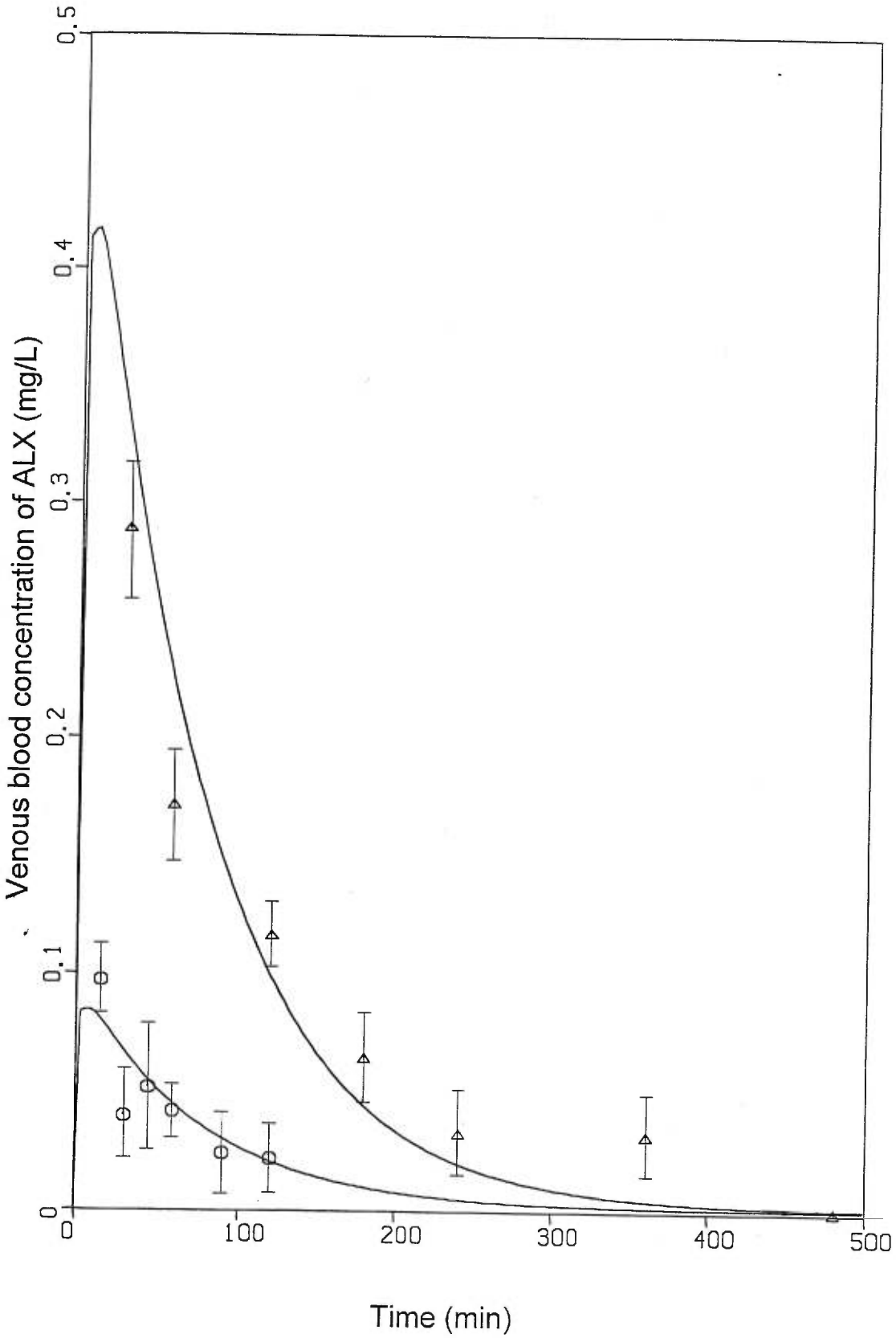
Venous blood concentration of ALX (mg/L)
0
0.1
0.2
0.3
0.4
0.5
0
100
200
300
400
500
Time (min)

Figure 10

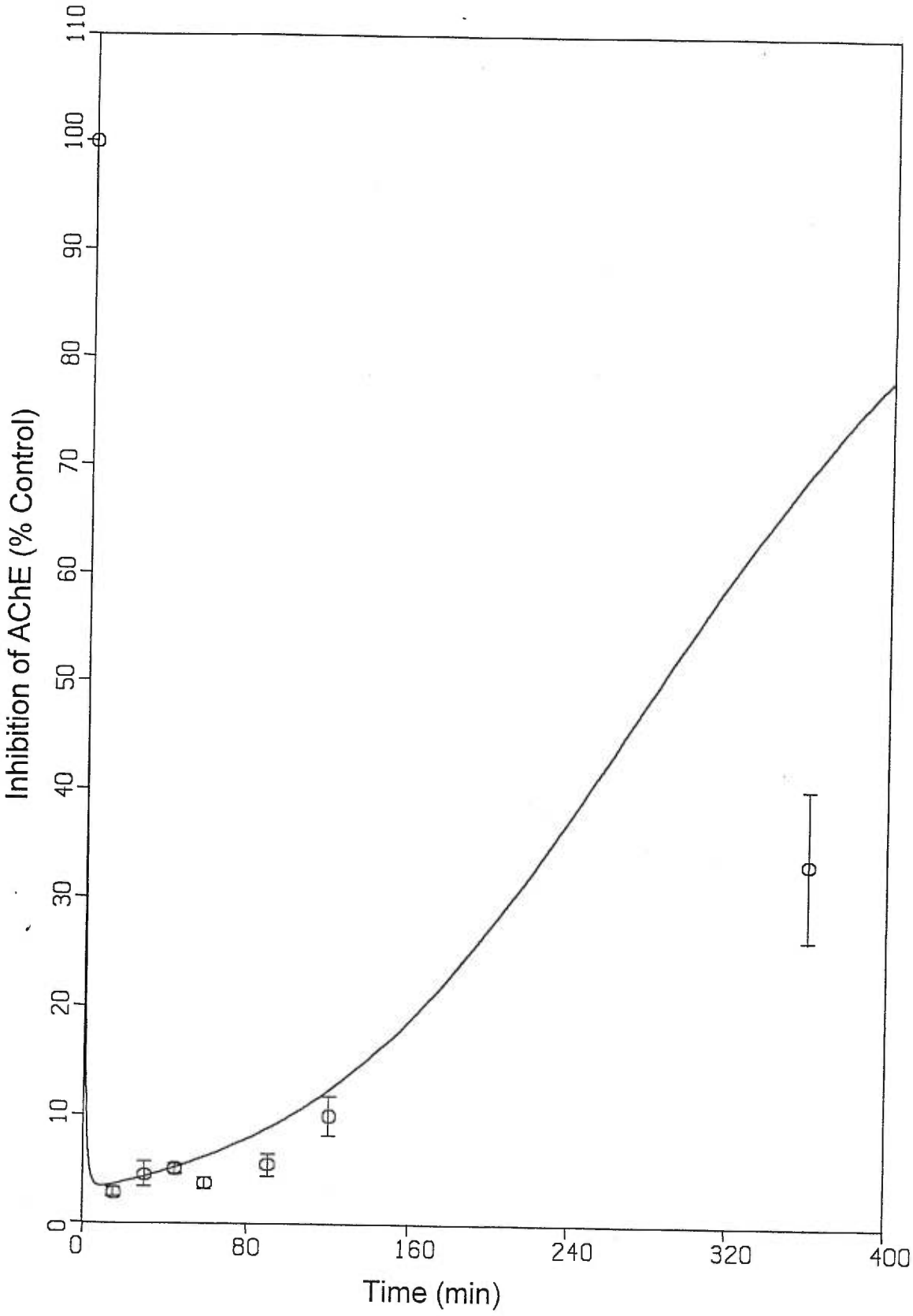
Inhibition of AChE (% Control)
0
10
20
30
40
50
60
70
80
90
100
110
0
80
160
240
320
400
Time (min)

Figure 11

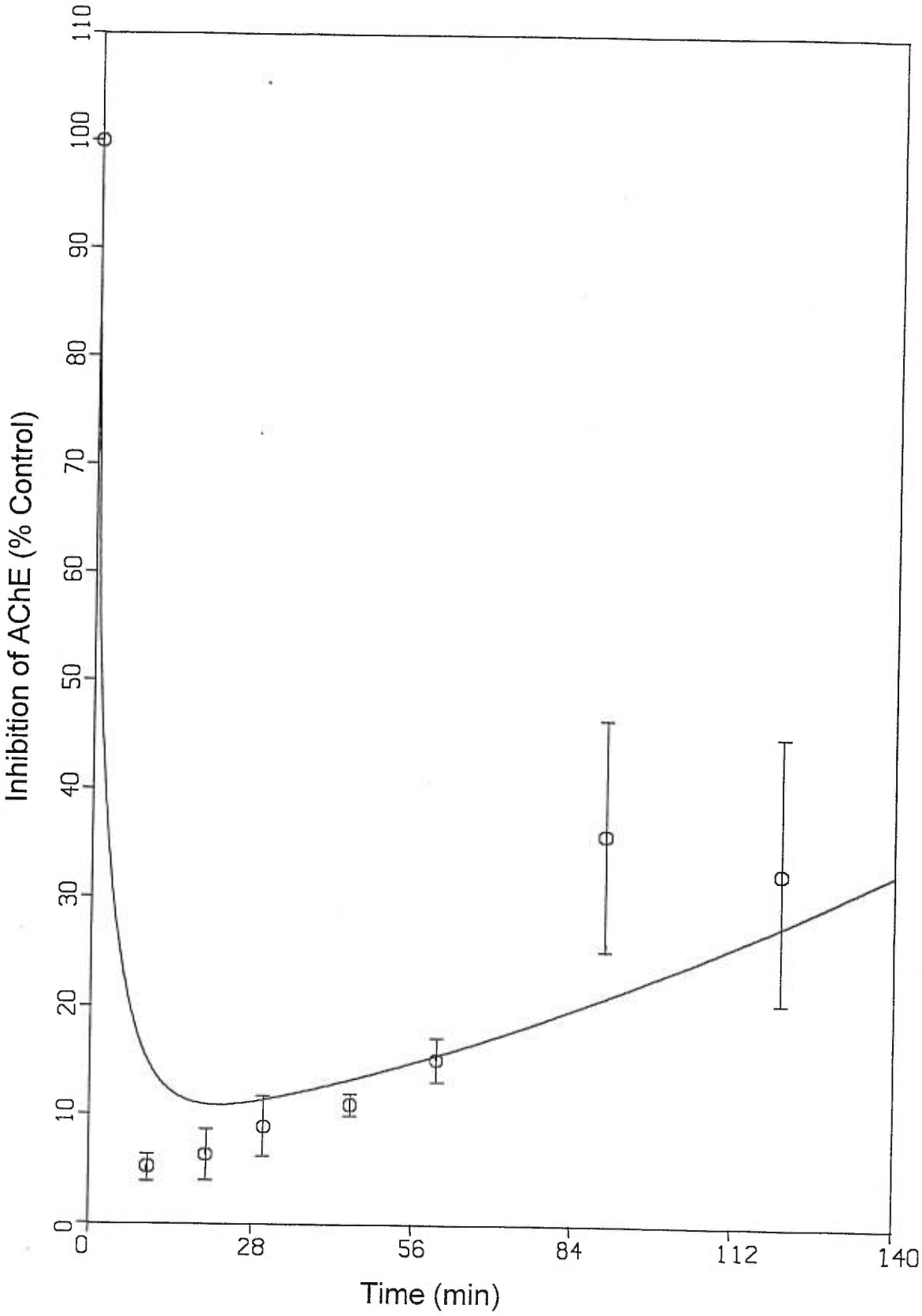
Inhibition of AChE (% Control)
110
100
90
80
70
60
50
40
30
20
10
0
0
28
56
84
112
140
Time (min)

Figure 12

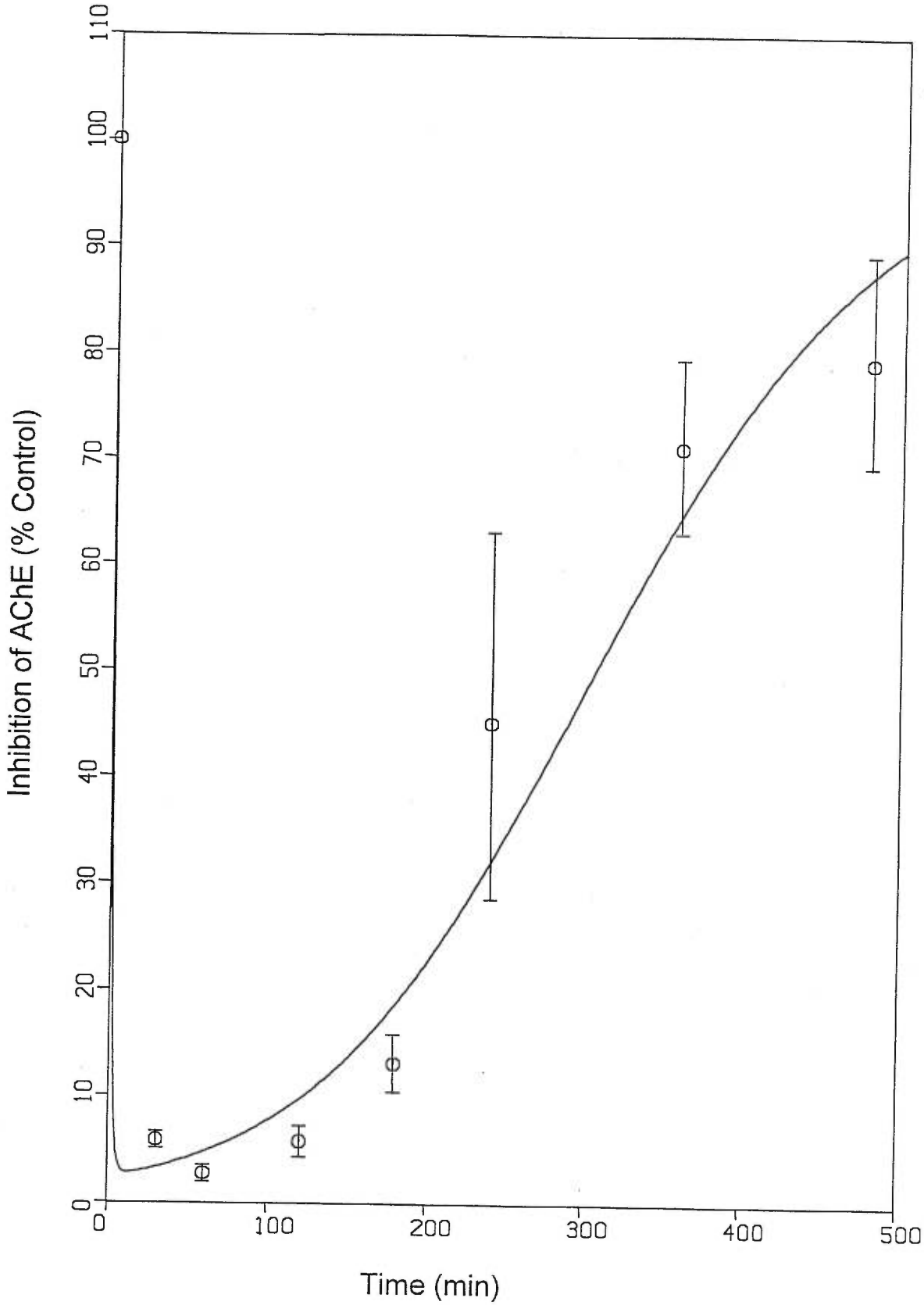
Inhibition of AChE (% Control)
Time (min)
0
10
20
30
40
50
60
70
80
90
100
110
0
100
200
300
400
500

Figure 13

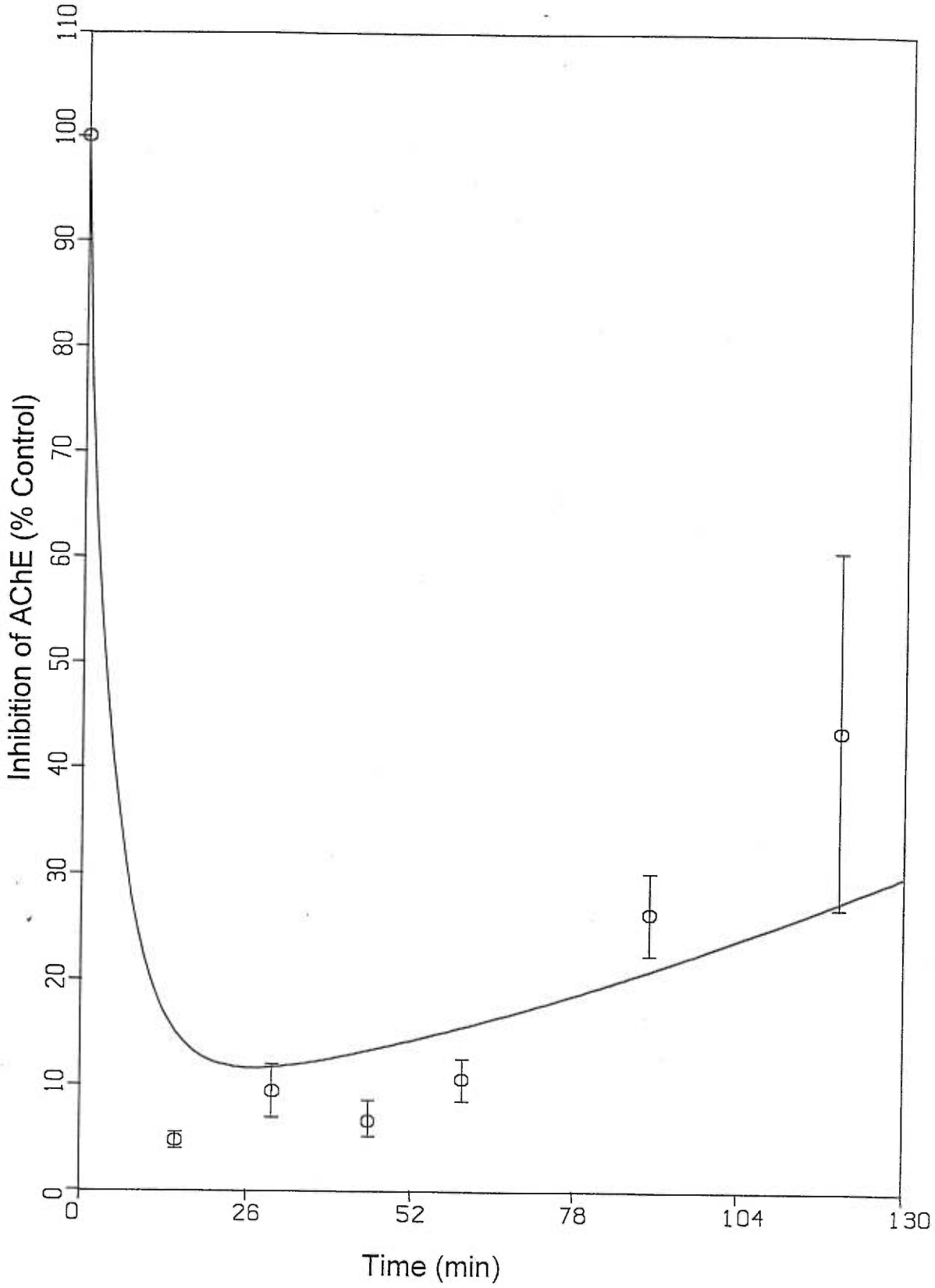
Inhibition of AChE (% Control)
0
10
20
30
40
50
60
70
80
90
100
110
0
26
52
78
104
130
Time (min)

Figure 14

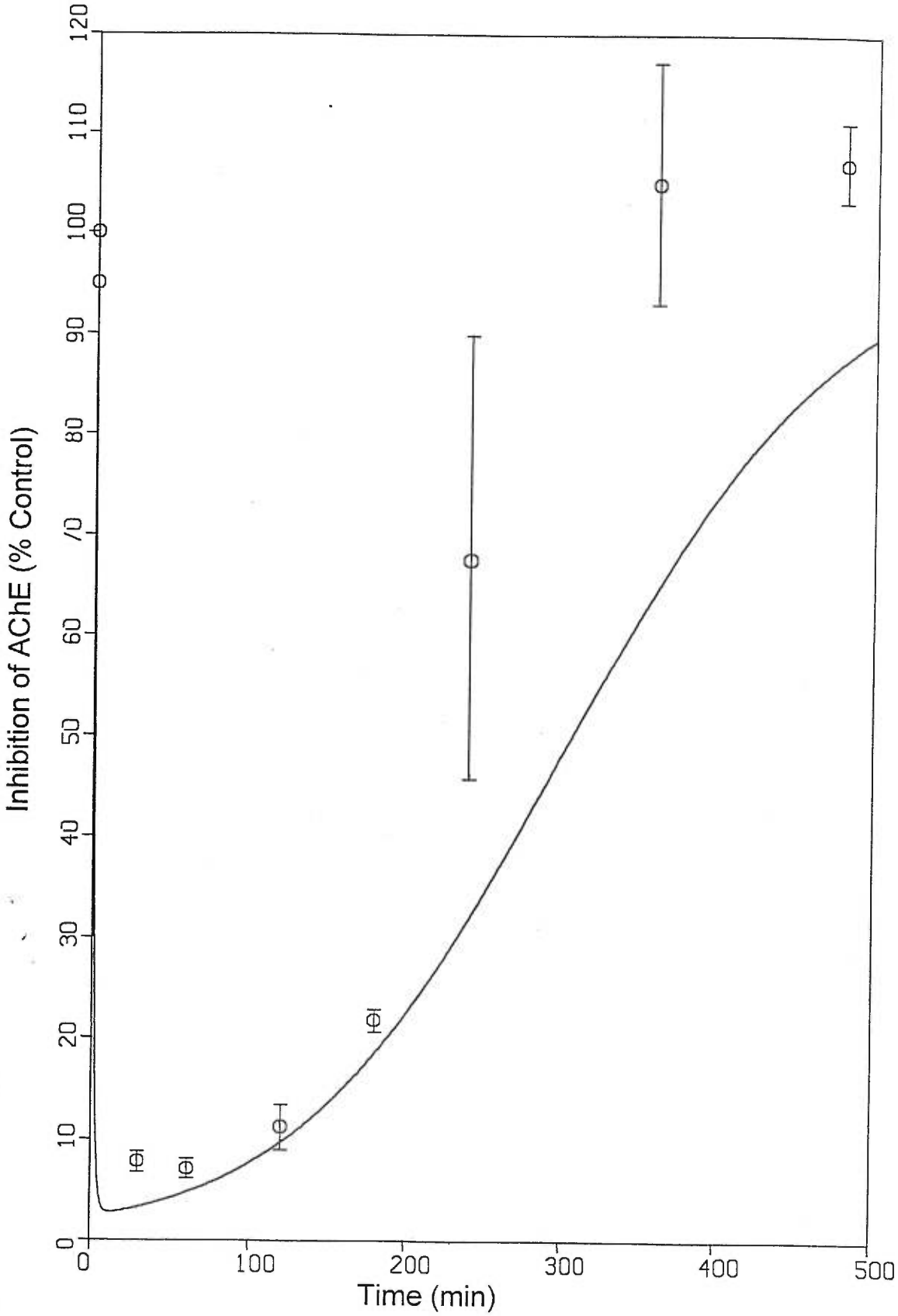
Inhibition of AChE (% Control)
0
10
20
30
40
50
60
70
80
90
100
110
120
0
100
200
300
400
500
Time (min)

Figure 15

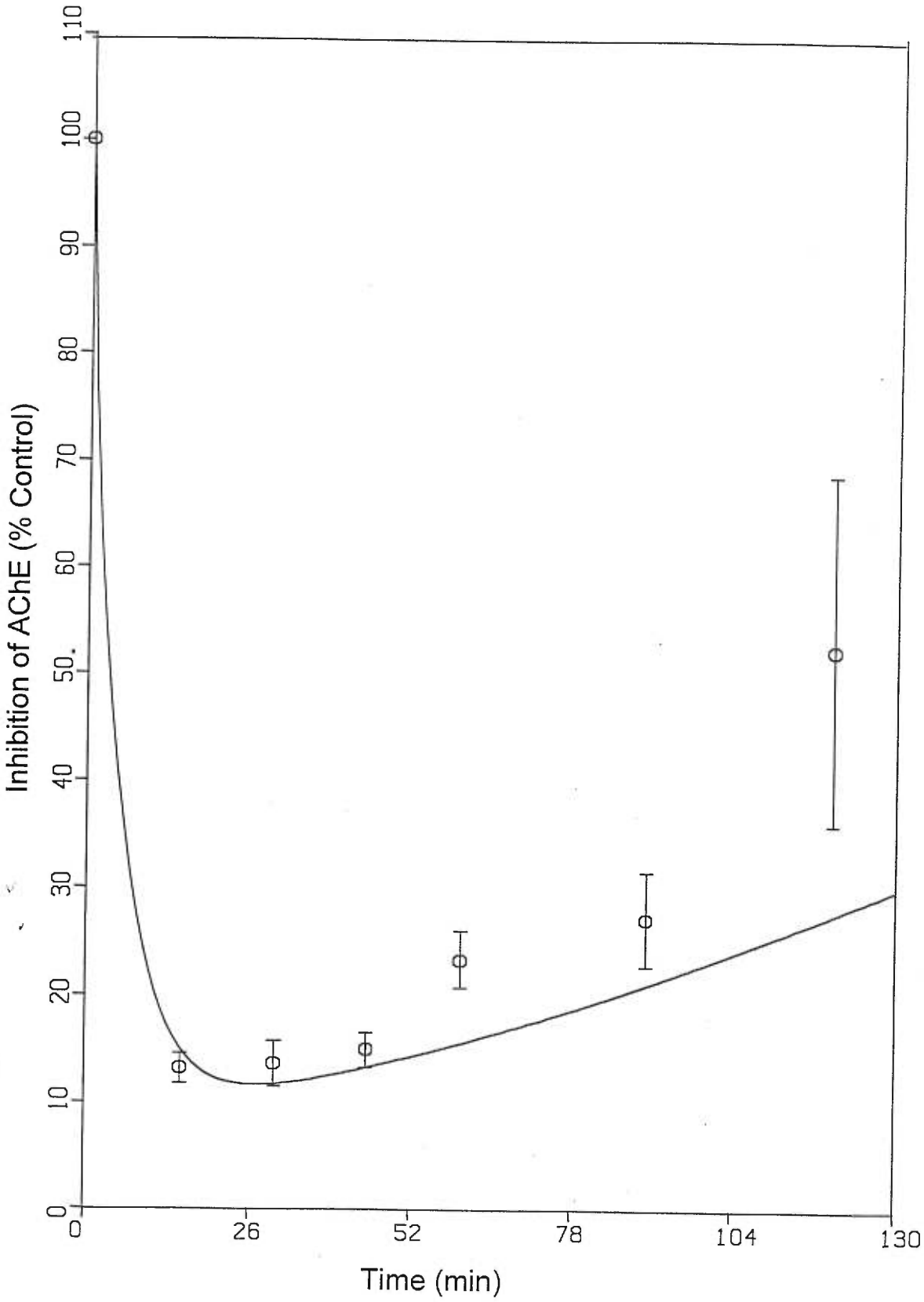
Inhibition of AChE (% Control)
0
10
20
30
40
50
60
70
80
90
100
110
0
26
52
78
104
130
Time (min)

Figure 16

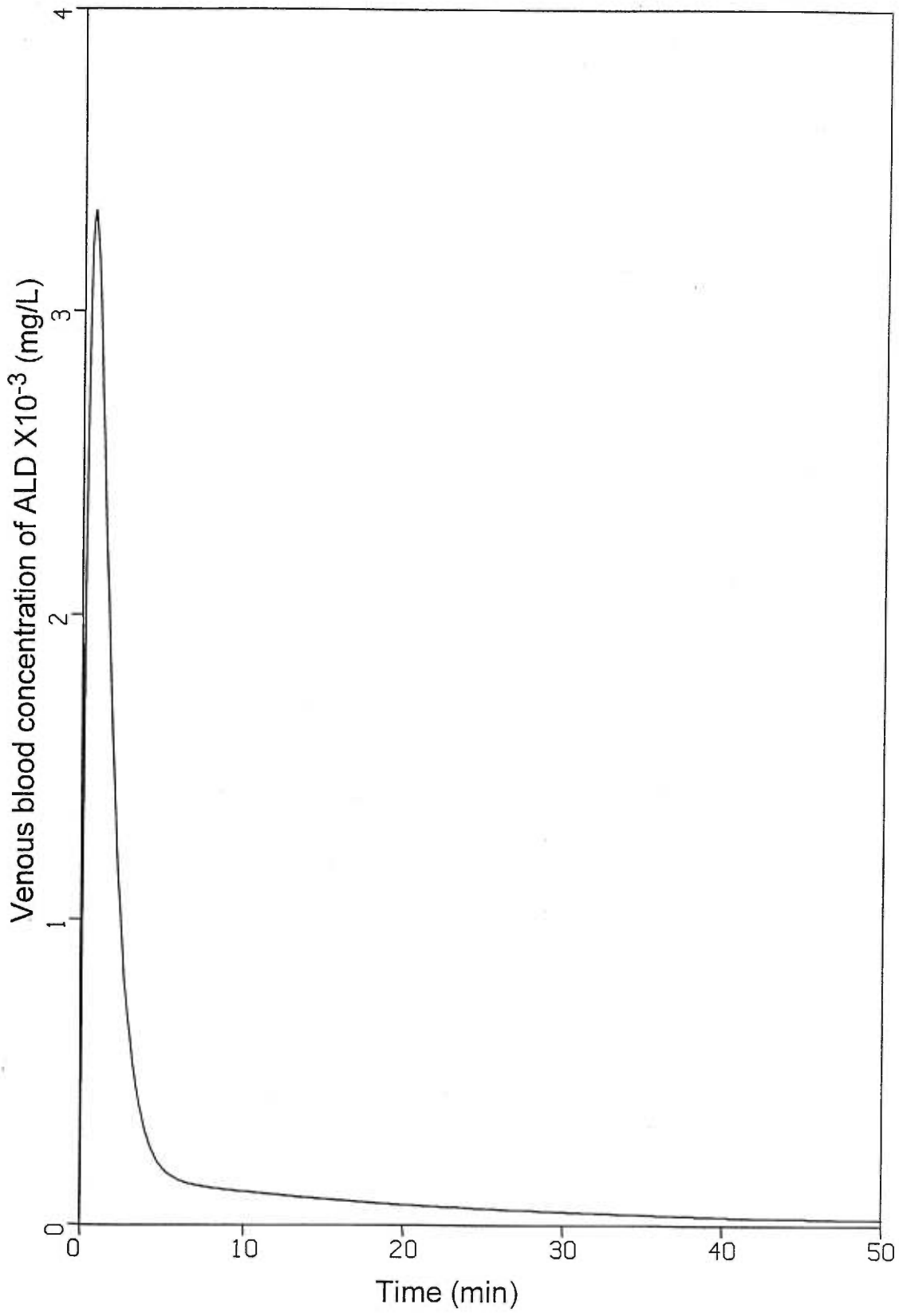
Venous blood concentration of ALD X10-3 (mg/L)
0
1
2
3
4
0
10
20
30
40
50
Time (min)

Figure 17

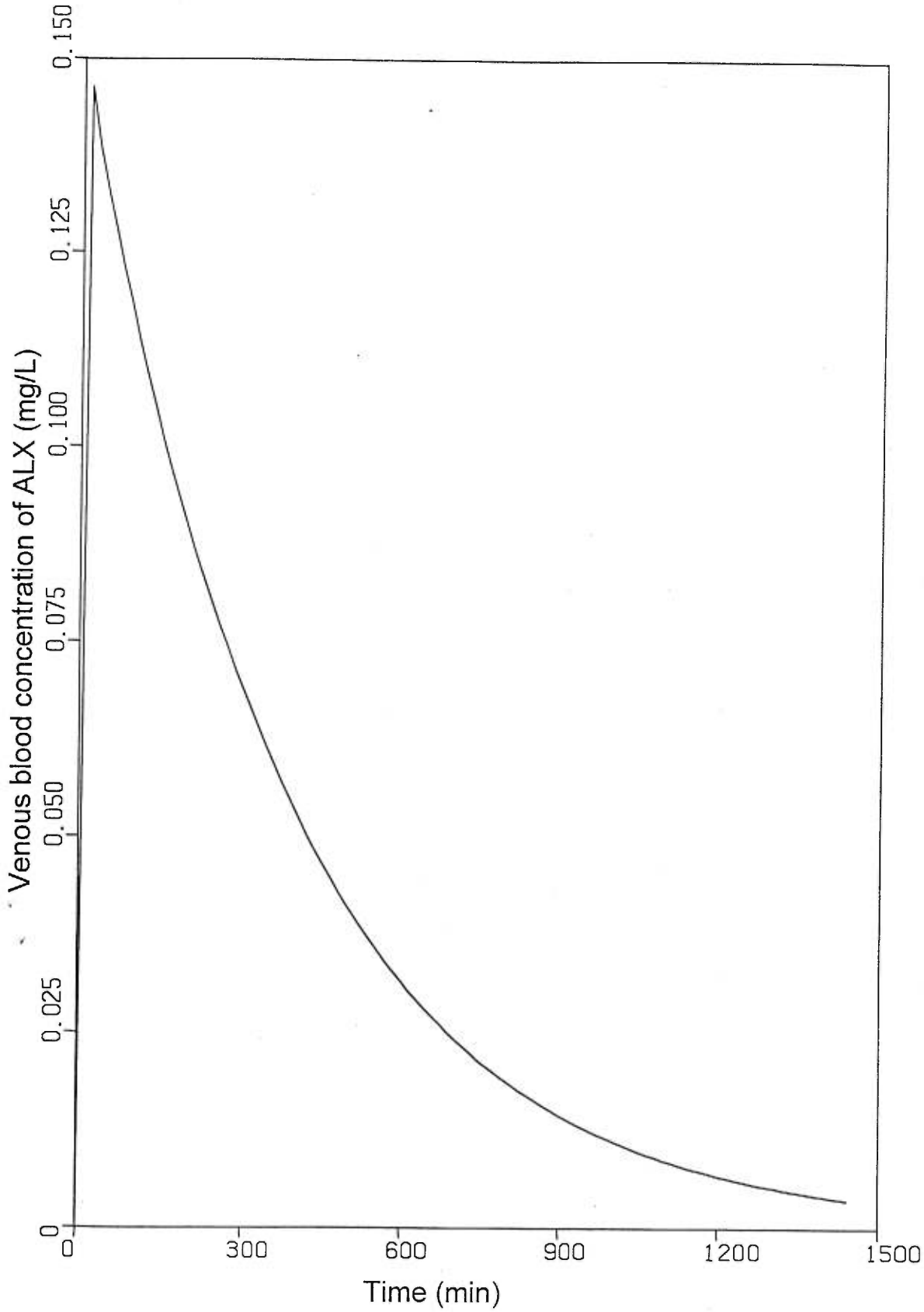
Venous blood concentration of ALX (mg/L)
0.150
0.125
0.100
0.075
0.050
0.025
0
0
300
600
900
1200
1500
Time (min)

Figure 18

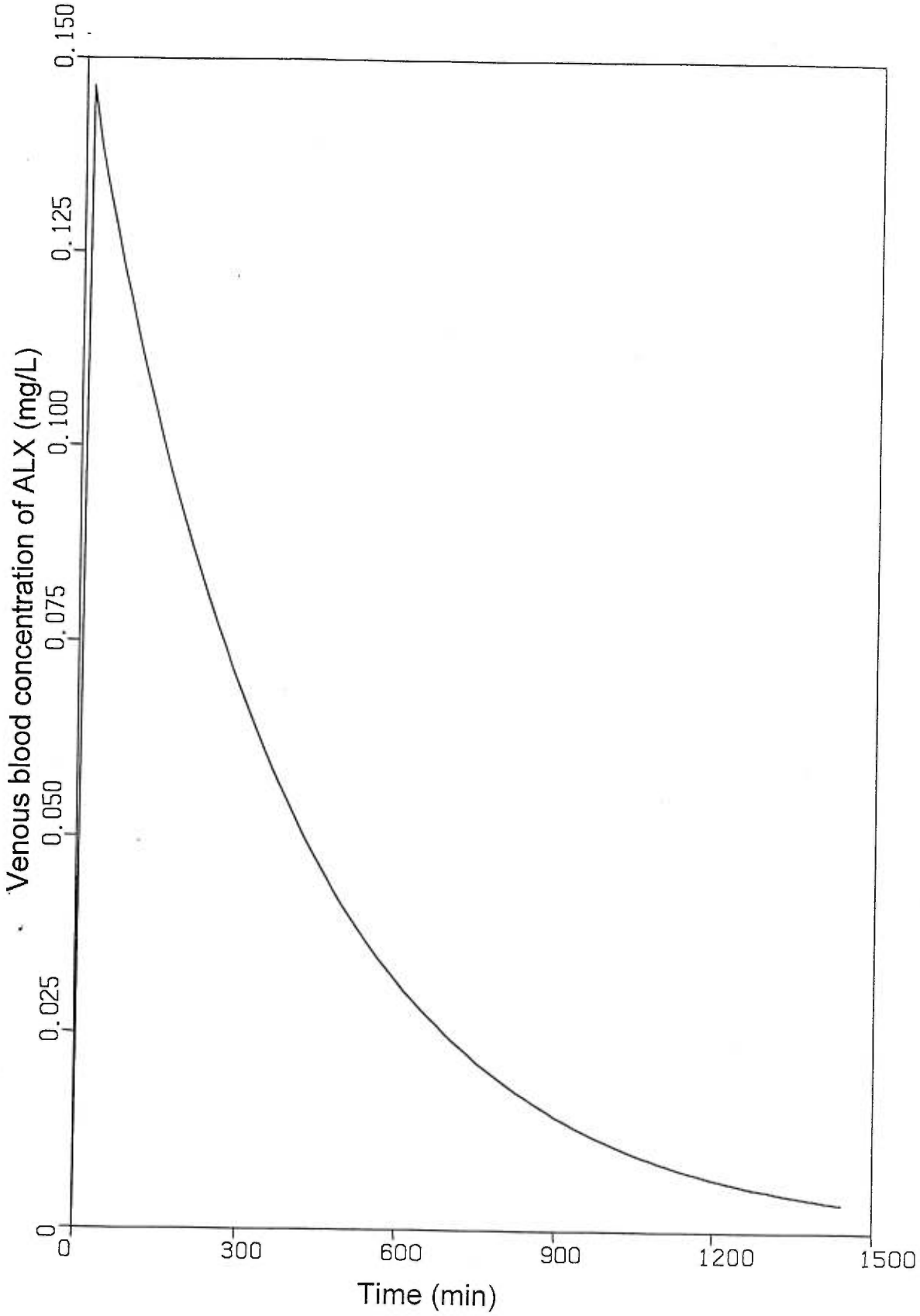
Venous blood concentration of ALX (mg/L)
0.150
0.125
0.100
0.075
0.050
0.025
0
0
300
600
900
1200
1500
Time (min)

Figure 19

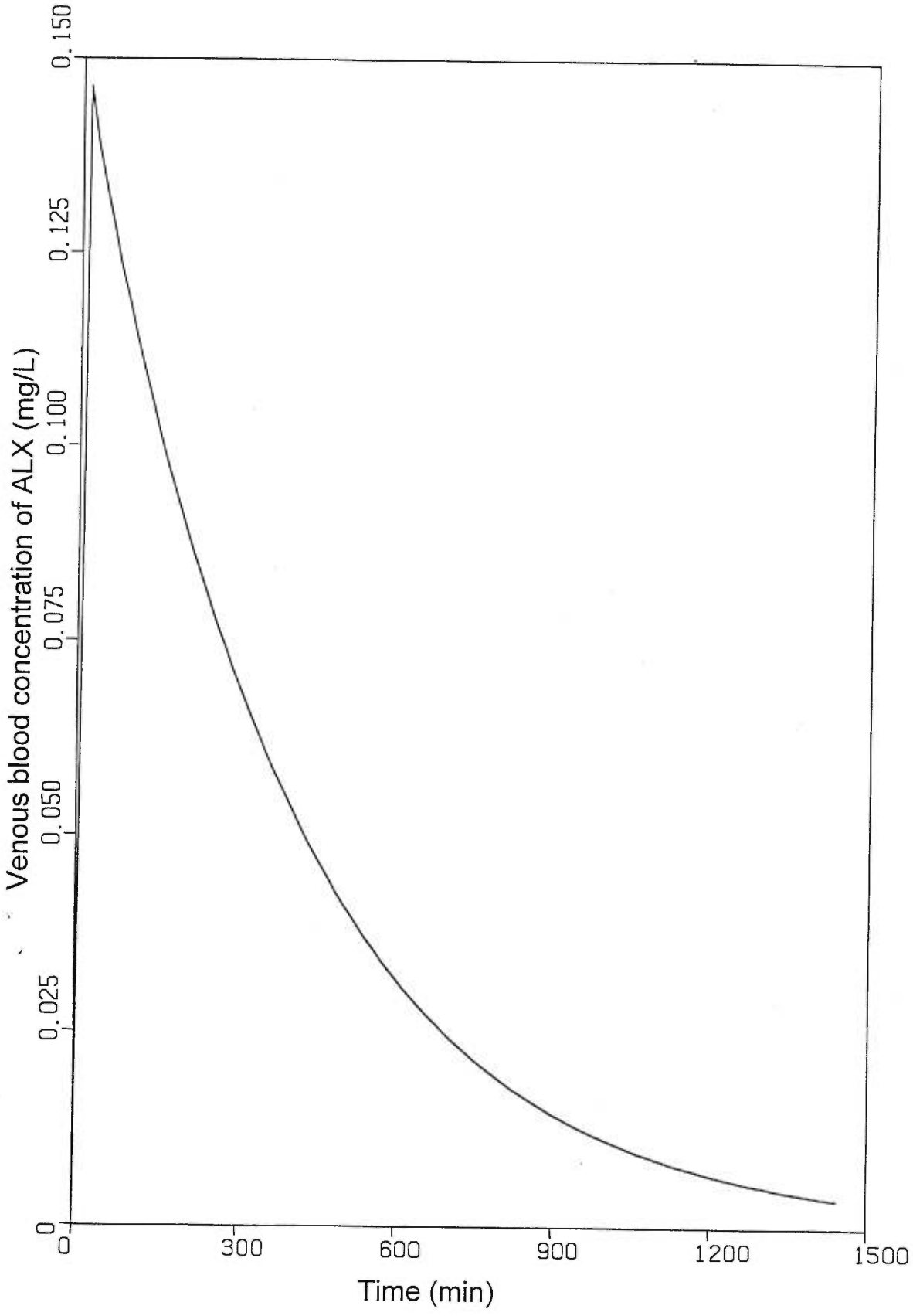
Venous blood concentration of ALX (mg/L)
0.150
0.125
0.100
0.075
0.050
0.025
0
0
300
600
900
1200
1500
Time (min)

Figure 20

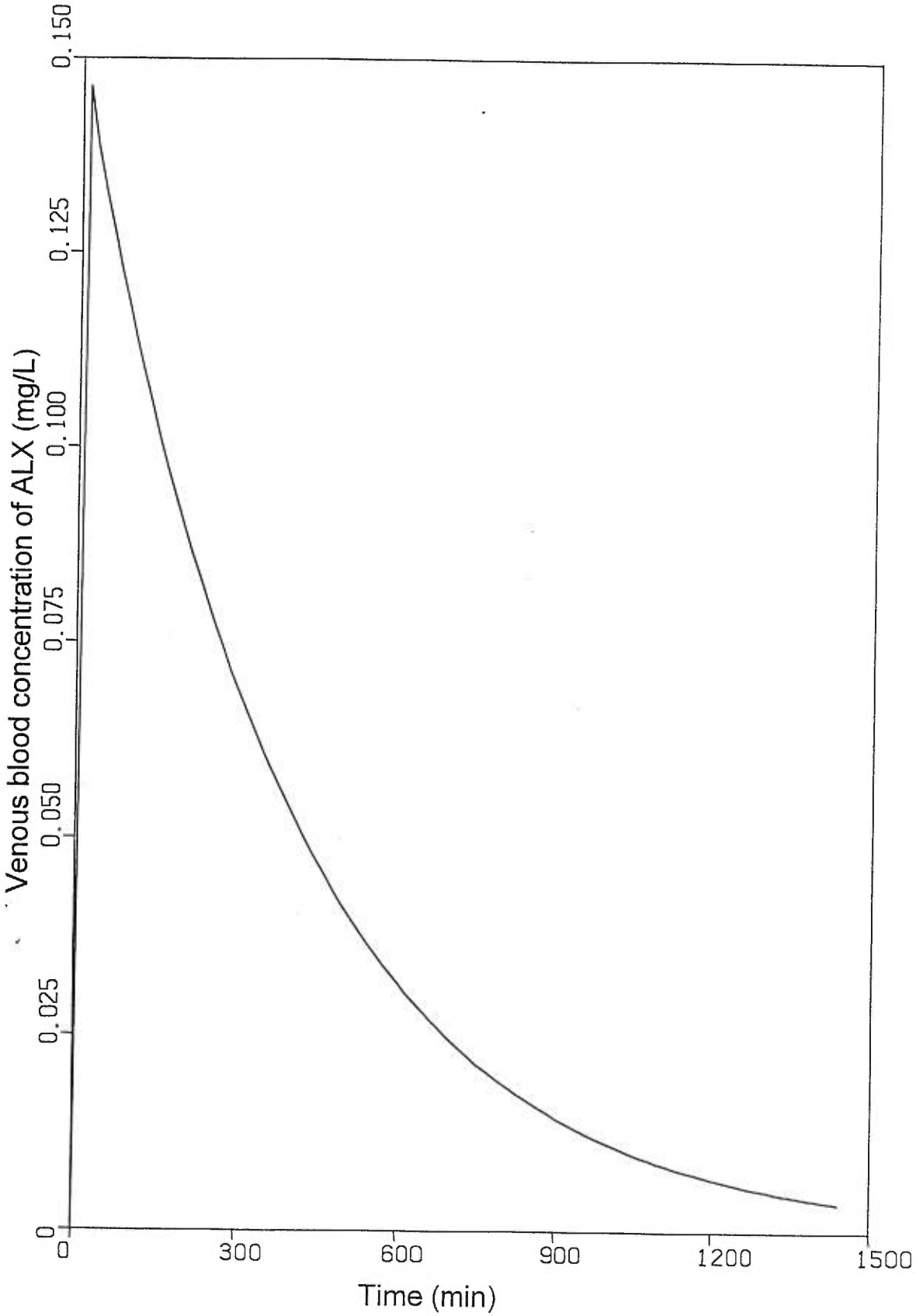
Venous blood concentration of ALX (mg/L)
0.150
0.125
0.100
0.075
0.050
0.025
0
0
300
600
900
1200
1500
Time (min)

Figure 21

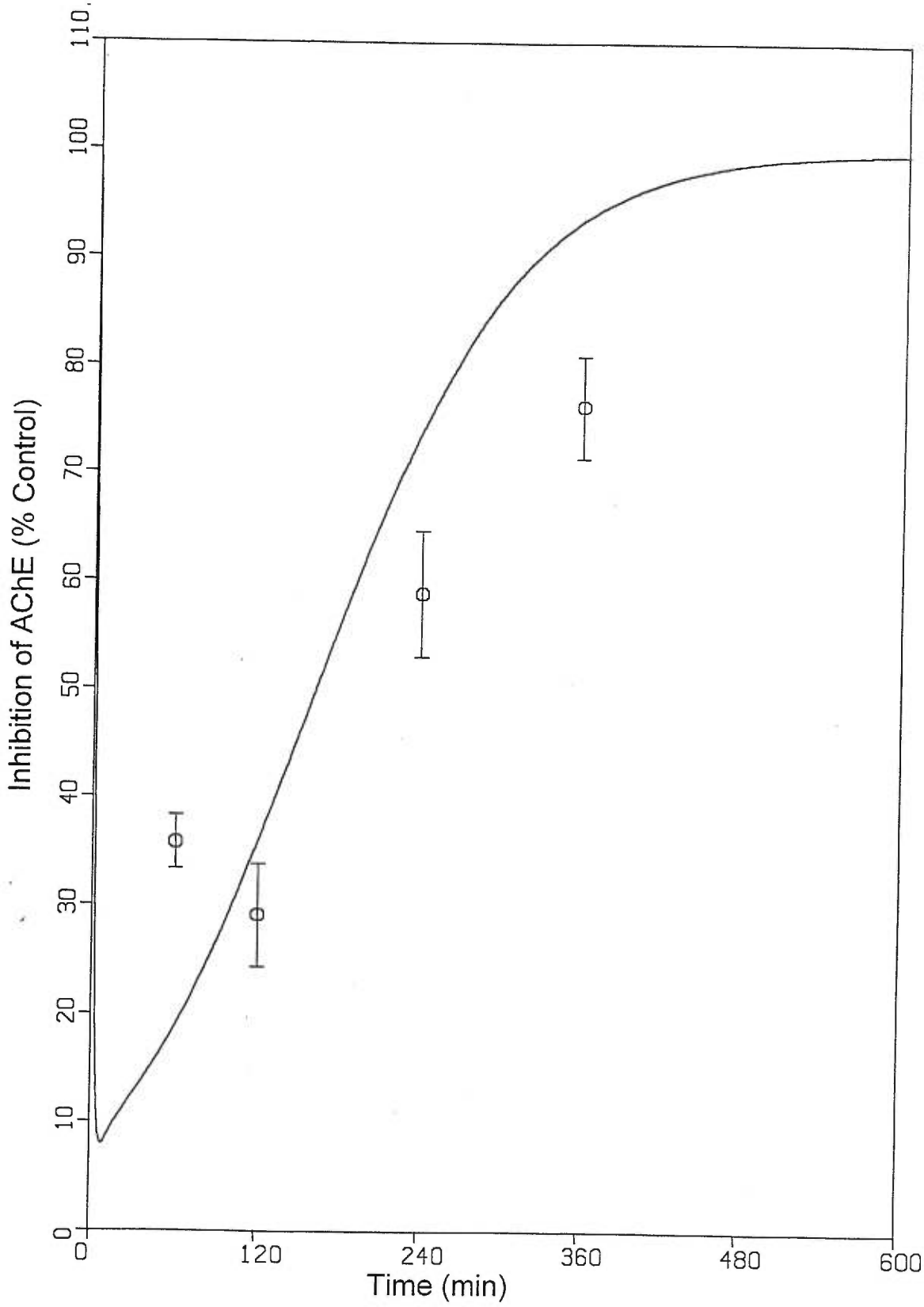
Inhibition of AChE (% Control)
0
10
20
30
40
50
60
70
80
90
100
110
0
120
240
360
480
600
Time (min)

Figure 22

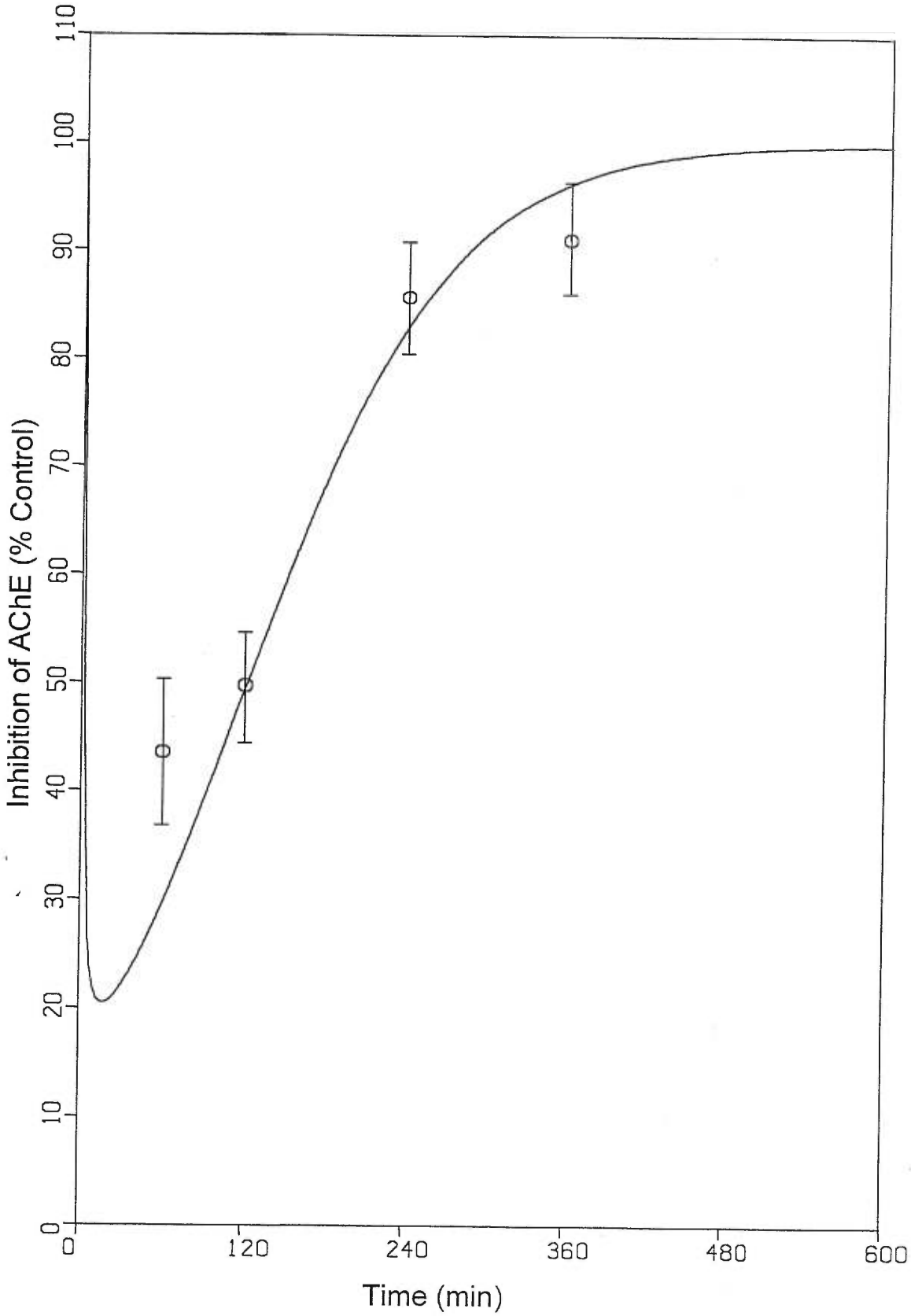
Inhibition of AChE (% Control)
0
10
20
30
40
50
60
70
80
90
100
110
0
120
240
360
480
600
Time (min)

Figure 23

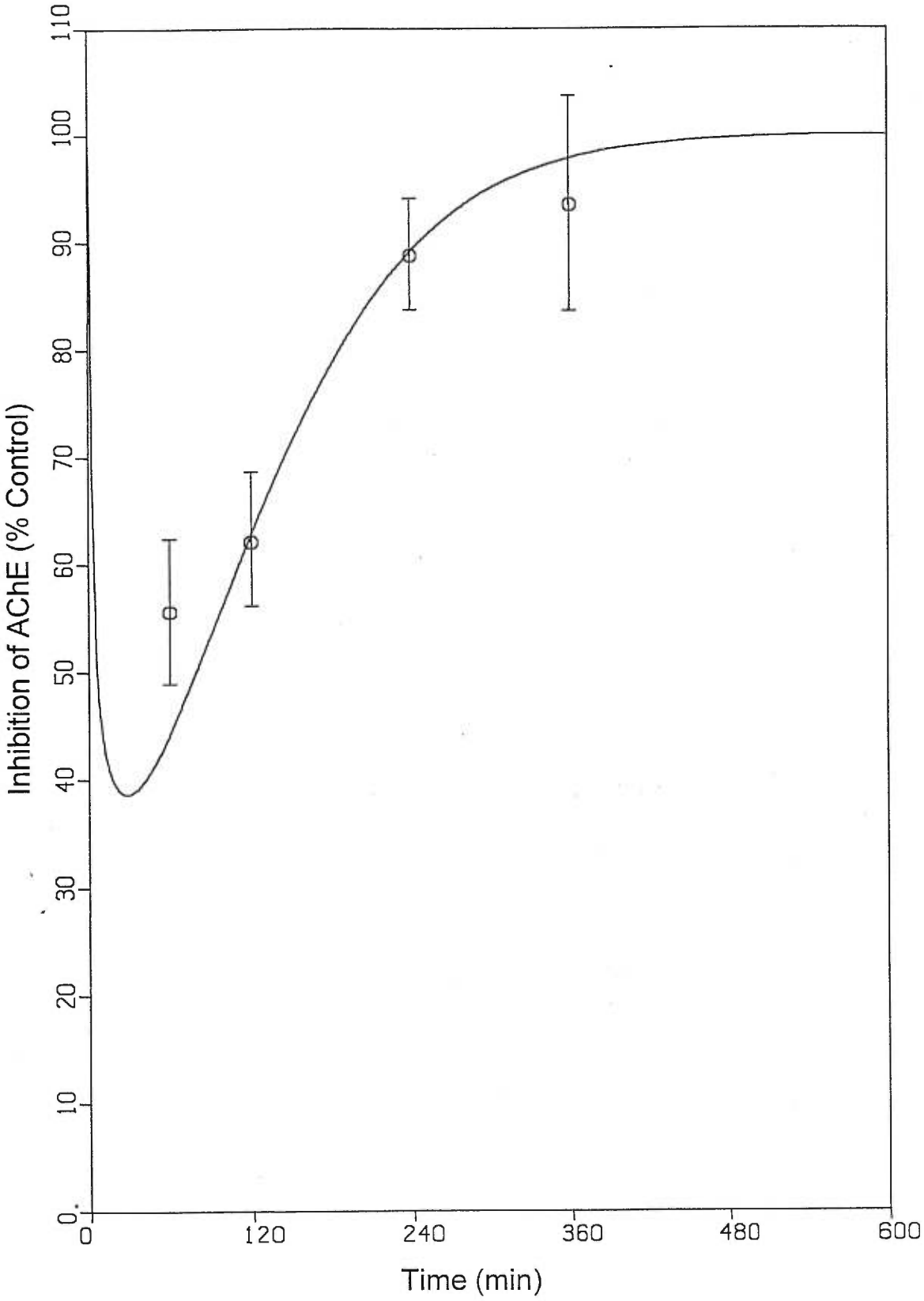
Inhibition of AChE (% Control)
0
10
20
30
40
50
60
70
80
90
100
110
0
120
240
360
480
600
Time (min)

CHAPTER 3

Article No 4

(To be submitted to: Regulatory Toxicology and Pharmacology)

PHYSIOLOGICAL MODEL-BASED DERIVATION OF INTERSPECIES UNCERTAINTY FACTORS FOR NONCANCER RISK ASSESSMENTS

MICHAEL PELEKIS AND KANNAN KRISHNAN[1]

Département de médecine du travail et d'hygiène du milieu,

Université de Montréal, C. P. 6128, Succ. Centre-ville,

Montréal, Québec, Canada, H3C 3J7

[1]To whom correspondence and reprint requests should be addressed at Département de médecine du travail et d'hygiène du milieu, Université de Montréal, 2375 Côte Ste Catherine, Bureau 4105, Montréal, Québec, Canada, H3T 1A8, Tel.: (514) 343-6581, Fax: (514) 343-2200

ABSTRACT

Health risk assessments for non-carcinogenic chemicals are conducted using animal data, whenever the no-observable adverse effect level (NOAEL) cannot be confidently established with available human data. The use of animal data to estimate safe levels for humans introduces several uncertainties, which are addressed with the use of uncertainty (safety) factors. The animal NOAEL is divided by a series of multiplicative factors of 10, each of which accounts for the uncertainty associated with interspecies, intraspecies and exposure scenario extrapolations, to estimate the reference dose (RfD). In practice, the interspecies uncertainty factor, UF_{AH}, of 10 reflects the magnitude of correction that is required to derive human-equivalent doses. Recently, the default UF_{AH} was subdivided into two components to account separately for interspecies differences in toxicokinetics and toxicodynamics ($UF_{AH\text{-}TK}$=3.16, $UF_{AH\text{-}TD}$=3.16). Even though the UF_{AH} in its composite or dissociated form is widely used, there is no basis to support or refute the magnitude of these factors for specific chemicals. The objective of the present study was to derive interspecies toxicokinetic uncertainty factors ($UF_{AH\text{-}TK}$) for several chemicals using validated physiological models. The approach involved the estimation of blood and tissue concentrations of the parent compound and the liver concentration of metabolites with validated rat and human physiologically-based toxicokinetic models for continuous exposure to dichloromethane (DCM), tetrachloroethylene (TETRA), 1,4-dioxane, (DIOX), toluene (TOL), m-

xylene (XYL), styrene (STY), carbon tetrachloride (CATE), ethyl benzene (ETBE), chloroform (CHLO), trichloroethylene (TRI) and vinyl chloride (VICH). The respective rat/human concentration ratios provided an estimate of the $UF_{AH\text{-}TK}$ and the results suggest that exposing rats and humans to the same ambient concentration yields 5.24±1.78 times greater dose (mg/kg) in the rat than in humans. However, in order to have equivalent blood and tissue concentrations in both rats and humans, the former must be exposed to a dose (mg/kg) that is on average 6.32 times higher than humans, if the parent compound is the moiety of concern, and 1.15 times higher when the toxic effects are caused by the metabolite. Since the dose received and clearance are greater in the rat (by a factor of 5.24 and 6.32 respectively) than in humans, the overall rat-human $UF_{AH\text{-}TK}$ for VOCs is 1.0. The $UF_{AH\text{-}TK}$ derived in the present study using a physiological modeling approach provides a scientific basis for its magnitude and suggests that the currently used $UF_{AH\text{-}TK}$ of 3.16 may result in incorrect risk estimates.

INTRODUCTION

The reference dose or reference concentration (RfD, RfC) is defined as "an estimate of a daily exposure to the human population that is likely to be without an appreciable risk of deleterious effects during lifetime" (USEPA, 1997). They are generally expressed in mg/kg BW/day or mg/m^3/day, and are estimated from the following equation:

$$RfD = \frac{\text{NOAEL or LOAEL}}{\text{UF(s) * MF}}$$

where:

NOAEL (no observable adverse effect level) = the highest exposure level at which there are no statistically or biologically significant increases in the frequency of occurrence of adverse effects in the exposed population compared to its appropriate control,

LOAEL (lowest observable adverse effect level) = lowest exposure level at which there is statistically significant increase in the frequency of occurrence of adverse effects in the exposed population compared to its appropriate control,

UF(s) = uncertainty or safety factor(s), and

MF = modifying factor that addresses the adequacy of the toxicological database

The uncertainty factor is "a number that reflects the degree or amount of uncertainty that must be considered when experimental data are extrapolated to humans exposed under particular scenarios (e.g., environmental, occupational)" (NAS, 1977). The UF typically accounts for toxicokinetic and toxicodynamic heterogeneity between animals (A) and humans(H), (UF_{AH}=10X) and within human population (UF_{HH}=10X), and the duration of the studies. Recently, the default UF_{AH} was differentiated into two components, $UF_{AH\text{-}TK}$ and $UF_{AH\text{-}TD}$, and the UF_{AH} of 10 was subdivided into two multiplicative factors of 3.16 each (USEPA, 1989, Renwick, 1991,1993). Eventhough the UF_{AH} in its composite or dissociated form is widely used in non-cancer risk assessments, regardless of the identity of chemicals and the nature of the endpoint, there is no conclusive experimental or theoretical justification to support or refute this practice and the magnitude of the UF_{AH}.

In the past, there was no quantitative tool that would permit either the estimation of the overall UF_{AH} or its components, and risk assessors were forced to use the default values. The advent of physiologically-based toxicokinetic (PBTK) modeling techniques has provided a tool that could be used to quantitate the UF_{AH}. The mechanistic and biological foundation of PBTK models makes the estimation of tissue doses across species possible. In most cases, all that is required is a change in the species-specific values of the mechanistic determinants of toxicokinetics, i.e., the physicochemical, biochemical and physiological parameters. Once the PBTK model has been

constructed and validated in a species, the toxicokinetic behavior of the same chemical in different species can be simulated and compared. Thus, the toxicokinetic equivalence of same chemical in different species can be evaluated in a quantitative manner and the magnitude of the $UF_{AH\text{-}TK}$ can be assessed.

The objective of the present study was to estimate the magnitude of the rat-to-human toxicokinetic uncertainty factor using validated PBTK models for the following volatile organic chemicals (VOCs): dichloromethane (DCM), tetrachloroethylene (TETRA), 1,4-dioxane, (DIOX), toluene (TOL), m-xylene (XYL), styrene (STY), carbon tetrachloride (CATE), ethyl benzene (ETBE), chloroform (CHLO), trichloroethylene (TRI), and vinyl chloride (VICH).

APPROACH

The approach involved: (i) simulating the kinetics of DCM, TETRA, DIOX, TOL, XYL, STY, CATE, ETBE, CHLO, TRI and VICH, using validated rat and human PBTK models under three different exposure scenarios (8-hr, 24-hr and 30 day continuous exposure), (ii) calculating the blood and tissue concentrations of parent chemicals, dose received, and hepatic concentration of the metabolites at the end of exposures in rats and humans, and (iii) using the results of step (ii) to calculate the numerical values of $UF_{AH\text{-}TK}$. The chemicals chosen for the present study represent those for which PBTK models have previously been developed and validated in both rats and humans. Since the primary objective of the present study relates to the quantification of the $UF_{AH\text{-}TK}$, the proposed methodology is independent of whether the chemical is carcinogen or not. All simulations were conducted using a four compartmental PBTK model framework depicted in Figure 1. Briefly, input to the system occurs via inhalation, and the chemical in the alveolar air is assumed to equilibrate in the lung with capillary blood so that the chemical concentration in arterial blood and alveolar air is at a constant ratio specified by the blood:air partition coefficient. Arterial blood leaving the lungs at a flow rate equal to the cardiac output is distributed to four principal tissue groups: the fat tissue, representing the total body adipose tissue; the slowly perfused tissues, representing muscle and skin; the richly perfused tissues, representing visceral organs (excluding the liver) and brain; and the liver tissue, representing the organ with the major metabolic capacity. The

chemical in the arterial blood is distributed rapidly throughout the tissue volume, and the chemical concentration in the venous blood exiting each group is determined by the tissue:blood partition coefficient. Venous blood from each tissue group is combined simultaneously to yield the mixed venous blood returning to the lungs (Ramsey and Andersen, 1984).

In these PBTK models, the rate of change in the amount of chemical in each tissue compartment (dAT/dt) was described with mass balance differential equations (MBDEs) of the following type:

dAT/dt= QT*(CA-CVT)-RAM

where:

QT =blood flow rate to the tissue (L/hr)

C =concentration of chemical

A =arterial blood

VT =venous blood leaving tissue, and

RAM =rate of the amount of chemical metabolized (mg/hr)

Metabolism was described to occur only in the liver. The set of MBDEs constituting the PBTK models was solved by numerical integration with the aid of Fortran-based software package (Advanced Continuous Simulation Language®, Version 11.4.1, Mitchell & Gauthier Associates, Concord, MA). The numerical values of all parameters for the rat and human PBTK models

for DCM, TETRA, DIOX, TOL, XYL, STY, CATE, ETBE, CHLO, TRI and VICH were obtained from Andersen *et al.* (1991), Ward *et al.* (1988), Reitz *et al.* (1990a), Tardif *et al.* (1993, 1995), Ramsey and Andersen (1984), Paustenbach *et al.* (1988), Tardif *et al.* (1997), Reitz *et al.* (1990b), Allen *et al.* (1993) and Fisher *et al.* (1990), and Reitz *et al.* (1996), respectively (Tables 1-3).

The initial set of exercises involved providing the same exposure concentration (1 ppm) as input to rat and human PBTK models to simulate the concentration in arterial and venous blood (CA, CV), the tissue concentrations (CT) [liver (L), fat (F), slowly perfused tissues (S) and richly perfused tissues (R)], and the concentration of the metabolite in the liver (CM) after 8-hr, 24-hr and 720-hr (30 days) of continuous exposure. The next set of simulation exercises focused to determine the dose received (mg/kg) by rats and humans during an identical exposure scenario (1, 24 or 720 h; 1 ppm). In the last set of simulations the CA, CV, CT, and CM were determined when both species received equivalent doses.

The simulation results (i.e., CA, CV, CL, CF, CR, CS, CM, dose received) obtained in rats were divided by those obtained with the human PBTK models. The resulting rat-to-human ratios generated during the three simulation exercises correspond to the overall $UF_{AH\text{-}TK}$ or its components, namely $UF_{AH\text{-}uptake}$ and $UF_{AH\text{-}clearance}$.

RESULTS

Table 4 shows the rat/human ratios of blood and tissue concentrations of parent chemicals and the liver concentration of metabolites, when both species are exposed to 1 ppm of each VOC for 8, 24 or 720 hr. These ratios represent the rat-to-human toxicokinetic uncertainty factors, $UF_{AH\text{-}TK}$, as a function of the dose measure to be used in risk assessments. If for DCM, for example, CL is the dose surrogate of choice, then the rat exposure concentration should be divided by 0.4 to get the human equivalent exposure concentration (HEC). On the other hand, if equivalent venous blood concentration (CV_{DCM}) is desired then the rat exposure concentration should be divided by 1.47 to get HEC (for lifetime, continuous exposure scenario). The average value of $UF_{AH\text{-}TK}$ for all dose surrogates based on parent chemical concentration (i.e., CA, CV, CR, CS, CF and CL) is close to unity (0.81±0.21). These results then suggest that continuous exposure to the same ambient concentration will result in just about the same tissue and blood concentrations of parent chemicals in rats and humans. However, the liver concentration of metabolites is likely to be greater in rats on average by a factor of 5.17±3.38 (during continuous exposures) for the VOCs investigated in the present study. This is a likely consequence of enhanced metabolic clearance in rats compared to humans.

Table 5 presents the rat-to-human ratios of the dose received (mg/kg) during 8, 24 or 720 hr exposure to 1 ppm of each of the VOCs. When rats and

humans are exposed to the same ambient concentration for an identical length of time, the rat receives, on an average, between 4.48 and 5.24 times the dose received by humans. The magnitude of the difference in uptake, i.e., dose received (Table 5) is comparable to the magnitude of the rat-to-human difference in CM (Table 4). The fact that the overall $UF_{AH\text{-}TK}$ based on parent chemical concentrations is close to unity (Table 4) can then be explained by greater uptake and clearance of these chemicals in rats than in humans, by about the same factor.

For all chemicals, there is a small difference in the $UF_{AH\text{-}TK}$ for the different exposure durations (Tables 4 & 5). This is due to the fact that while the rat tissues reach steady-state fairly quickly, the time required for human tissues to attain steady-state is considerably longer (e.g., 300-hr, Pelekis and Krishnan 1997). Thus, as the human tissues attain steady-state, the concentration in human tissues (i.e., the denominator) increases and the ratio decreases. Since uncertainty factors apply to continuous exposure scenarios, i.e., conditions in which steady-state has been reached, all subsequent exercises were conducted for 720-hr exposures.

To investigate differences in metabolic clearance when equivalent doses are administered in both species, the ambient exposure concentration specified in the rat PBTK models was adjusted so that the total dose received was equivalent to that of a human exposed to 1 ppm. The results in

specified in the rat PBTK models was adjusted so that the total dose received was equivalent to that of a human exposed to 1 ppm. The results in Table 6 suggest that the average blood and tissue concentrations of parent chemicals in the rat are lower on average by a factor of 0.17±0.03 (0.12-0.21) than in humans, and the average concentration of metabolites is also lower in the rat by a factor of 0.87±0.32. In other words, in order to have equivalent blood and tissue concentrations in both rats and humans, the former must be exposed to a dose (mg/kg) that is on average 5.88 times higher than in humans if the parent compound is the moiety of concern and 1.15 times when the metabolite is the dose surrogate of choice. Since the dose received and clearance are greater in the rat (by a factor of 5.24 and 6.32 respectively) than in humans, the overall rat-human $UF_{AH\text{-}TK}$ for VOCs is 1.0. The $UF_{AH\text{-}TK}$ derived in the present study using a physiological modeling approach then, provides a scientific basis for its magnitude and suggests that the currently used $UF_{AH\text{-}TK}$ of 3.16 may result in inaccurate risk estimates.

DISCUSSION

Current risk assessment approaches estimate risk by correlating the incidence of response for various exposure levels in animals and humans with exposure or administered (applied) dose. Adverse effects, however, develop at the target tissues from the interaction of the toxic moiety with cellular components or receptors and the currently used approaches fail to account for the fundamental toxicokinetic processes in a quantitative manner. Although this limitation had been recognized and acknowledged for a long time, analytical methods could not provide estimates of target tissue dose, and risk assessors were restricted to investigating exposure concentration or at best blood concentrations of toxicants with responses.

The advent of analytical methodologies and physiological modeling techniques have permitted the investigation of the exposure-tissue concentration across and within species in a realistic and accurate way. In the present study, the toxicokinetic equivalence of VOCs in rats and humans was examined quantitatively with the aid of validated PBTK models and the toxicokinetic interspecies uncertainty factors of eleven VOCs were determined.

The results of this study indicate that the magnitude of $UF_{AH\text{-}TK}$ varies among chemicals and depends on the dose surrogate used, and whether the

metabolite or the parent compound is the toxic moiety. For example, in the case of styrene, if dose received was used as a metric the UF_{AH-TK} would be 4.29, while the UF_{AH-TK} based on blood concentrations would be approximately 1. Comparison of these values with the default values of UF_{AH-TK}, clearly shows that if one of the tissues were the target organ, the default uncertainty factor would overestimate the risk, while extrapolation based on dose received would not result in any appreciable difference. The results also show that for the chemicals used in the present study the UF_{AH-TK} varies between 0.06 and 1.45, thus indicating that the use of the default UF_{AH-TK} (3.16) would overestimate the derived exposure limits, by a factor as large as 3. Additionally, the results refute the unidirectionality of the UF_{AH-TK}, which is based on the assumption that physiological clearance in humans is less than in laboratory animals.

With respect to dose received, the default extrapolation is performed on the basis of body surface ($BW^{0.67}$). Thus, to extrapolate a dose from a 0.25 kg rat to a 70 kg human the factor would be $(70/0.25)^{0.67}= 6.5$. The results of the present study indicate that the default method will produce erroneous results and the dose received could be overestimated or underestimated by as much as a factor of 3 (in the case of DIOX).

The approach described in the present study provides an alternative to the default methodology, and is advantageous in that an internal measure

of effective dose-rather than applied dose- is used in evaluating risk. The incorporation of mechanistic toxicokinetic information increases the accuracy of interspecies extrapolation and addresses the request of the regulatory agencies to consider such information when it is available and incorporate in the evaluation of risk.

REFERENCES

Allen, B.C., and Fisher, J.W. (1993). Pharmacokinetic modeling of trichloroethylene and trichloroacetic acid in humans. *Risk Anal.* **13,** 71-86.

Andersen, M.E., Clewell, H.J., Gargas, M.L., MacNaughton, M.G., Reitz, R.H., Nolan, R.J., McKenna, M.J. (1991). Physiologically based toxicokinetic modeling with dichloromethane, its metabolite carbon monoxide, and blood carboxyhemoglobin in rats and humans. *Toxicol. Appl. Toxicol.* **108,** 14-27.

Fisher, J.W., Whittaker, T.A., Taylor, D.H., Clewell, H.J., III, and Andersen, M.E. (1990). Physiologically based toxicokinetic modeling of the lactating rat and nursing pup: a multiroute exposure model for trichloroethylene and its metabolite trichloroacetic acid. *Toxicol. Appl. Pharmacol.* **102,** 497-513.

National Academy of Sciences (1977). Drinking Water and Health, Vol. 1. National Academy of Sciences, Washington, DC.

Pastenbach, D.J., Clewell, H.J., III, Gargas, M.L., Andersen, M.E. (1988). A physiologically based toxicokinetic model for inhaled carbon tetrachloride, *Toxicol. Appl. Pharmacol.* **96,** 191-211.

Ramsey, J.C., and Andersen, M.E. (1984). A physiologically-based description of the inhalation pharmacokinetics of styrene in rats and humans, *Toxicol. Appl. Pharmacol.* **73,** 159-175.

Reitz, R.H., McCroskley, P.S., Park, C.N., Andersen, M.E., Gargas, M.L. (1990a). Development of a physiologically based toxicokinetic model for risk assessment with 1,4-dioxane. *Toxicol. Appl. Pharmacol.* **105,** 37-54.

Reitz, R.H., Mandrela, A.L., Corley, et al. (1990b). Estimating the risk of liver cancer associated with human exposures to chloroform using physiologically-based pharmacokinetic modeling. *Toxicol. Appl. Pharmacol.* **105,** 443-459.

Reitz, R.H., Gargas, M.L., Andersen, M.L., Provan, W.M. and Green, T.L. (1996). Predicting cancer risk from vinyl chloride exposure with a physiologically based toxicokinetic model. *Toxicol. Appl. Pharmacol.* **137,** 253-267.

Renwick, A.G. (1991). Safety factors and establishment of acceptable daily intakes, *Food Addit. Contamin.* **8,** 135-150.

Renwick, A.G. (1993). Data-derived safety factors for the evaluation of food additives and environmental contaminants. *Food Addit. Contamin.* **10,** 275-305.

Tardif, R., Lapare, S., Krishnan, K., Brodeur, J. (1993). Physiologically based modeling of the toxicokinetic interaction between toluene and m-xylene in the rat, *Toxicol. Appl. Pharmacol.* **120,** 266-273.

Tardif, R., Lapare, S., Brodeur, J., Krishnan, K. (1995). Physiologically-based modeling of a mixture of toluene and xylene in humans, *Risk Anal.* **15,** 335-342.

Tardif, R., Charest-Tardif, G., Brodeur, Krishnan, K. (1997). Physiologically-based toxicokinetic modeling of a ternary mixture of alkyl benzenes in rats and humans. *Toxicol. Appl. Pharmcol.* **144,** 120-134.

USEPA (1989). *Interim methods for development of inhalation doses*, EPA/ 600/888/066F.

USEPA (1997), *Integrated risk information system (IRIS), Background document,* National Center for Environmental Assessment, Cincinnati, OH.

Ward, R.C., Travis, C.C., Hetric, D.M., Andersen, M.E., and Gargas, M.L. (1988), Toxicokinetics of tetrachloroethylene. *Toxicol. Appl. Pharmacol.* **93,**108-117.

Table 1: Physiological parameters used in the rat and human PBTK models for the estimation of UF_{AH-TK}

CHEM.	BW[1]		VFC[2]		VSC		VLC		VRC		QPC[3]		QCC[4]		QFC[4]		QSC		QLC		QRC	
	Rat	Human	Rat	Human	Rat	Human	Rat	Human	Rat	Human	Rat	Human	Rat	Human	Rat	Human	Rat	Human	Rat	Human	Rat	Human
DCM	0.22	83	7	23	75	62	4	3.14	5	3.71	15	15	12.6	16	9	5	15	19	20	24	56	52
TETRA	0.25	70	7	20	75	62	4	4	5	5	22.2	15	14.4	16	9	5	15	19	25	25	51	51
DIOX	0.40	70	7	23.1	70	56.1	4	3.1	5	3.71	15	30	15	30	5	5	18	18	25	25	52	52
TOL	0.25	70	9	19	72	62	4.9	2.6	5	5	15	18	15	18	9	5	15	26	25	26	51	44
XYL	0.25	70	9	19	72	62	4.9	2.6	5	5	15	18	15	18	9	5	15	25	26	26	51	44
STY	0.30	83	9	9	73	73	4	4	5	5	10.5	10.5	13.1	13.1	9	9	12	12	37	37	42	42
CATE	0.42	70	8	10	74	62	4	4	5	5	15	11	15.5	11	4	6	20	18	25	25	51	51
ETBE	0.25	70	9	19	72	62	4.9	2.6	5	5	15	18	15	18	9	5	15	25	25	26	51	44
CHLO	0.236	70	7	23.1	76.5	59.8	2.53	3.14	5	5	15	15	15	15	5	5	19	19	25	25	51	51
TRICH	0.236	70	6	19	76	72	4	2.6	5	5	14	12.9	14	15	9	5	15	25	25	26	51	44
VICH	0.25	70	7	23.1	76.5	62.1	2.53	3.14	5	3.71	18	15	18	15	5	5	19	19	24	24	52	52

[1] Body weight (kg)

[2] Tissue volumes (VTC) expressed as % of body weight (F:fat, S:slowly perfused tissues, L:liver, R:richly perfused tissues)

[3] Pulmonary ventilation rate (L/hr/kg)

[4] Cardiac output (L/hr/kg)

[5] Tissue flows (QTC) expressed as % of cardiac output (F:fat, S:slowly perfused tissues, L:liver, R:richly perfused tissues)

Table 2: Physicochemical parameters used in the rat and human PBTK models for the estimation of $UF_{AH\text{-}TK}$

CHEMICAL	PB[1]		PF[2]		PS		PL		PR	
	Rat	Human	Rat	Human	Rat	Human	Rat	Human	Rat	Human
DCM	19.4	8.94	6.19	12.4	0.408	0.82	0.732	1.46	0.82	0.732
TETRA	18.9	10.3	121.7	159.03	1.06	7.77	3.72	6.83	3.72	6.83
DIOX	1850	3650	0.46	0.23	0.84	0.43	0.84	0.43	0.84	0.43
TOL	18	15.6	56.7	65.8	1.54	1.37	4.64	2.98	4.64	2.66
XYL	46	26.4	40.4	77.8	0.91	3.00	1.97	3.02	1.97	4.42
STY	40	52	50	50	1.0	1.0	2.7	2.7	5.7	5.7
CATE	4.52	2.64	79.4	136	1.02	1.74	3.14	5.38	3.14	5.38
ETBE	42.7	28.0	36.6	55.6	0.61	0.94	1.96	2.99	1.41	2.15
CHLO	20.8	7.43	9.76	37.7	0.67	1.62	1.01	2.29	1.01	2.29
TRICH	21.9	9.2	25.3	73.3	0.46	2.3	1.20	6.8	1.20	6.80
VICH	1.68	1.16	11.90	17.24	1.25	1.81	0.95	1.38	0.95	1.38

[1] Blood:air partition coefficient
[2] Tissue blood (PT) partition coefficient (F:fat, S:slowly perfused tissues, L:liver, R:richly perfused tissues)

Table 3: Biochemical parameters used in the rat and human PBTK models for the estimation of UF_{AH-TK}

CHEMICAL	VmaxC[1]		KM[2]		KFC[3]	
	Rat	Human	Rat	Human	Rat	Human
DCM	4.00	6.25	0.40	0.75	2.0	2.0
TETRA	0.19	0.151	0.30	0.30	1.8	0.0
DIOX	27.0	0.274	29.4	3.00	0.0	0.0
TOL	4.80	4.80	0.55	0.55	0.0	0.0
XYL	8.40	8.40	0.20	0.20	0.0	0.0
STY	8.36	8.36	0.36	0.36	0.0	0.0
CATE	0.665	0.548	0.25	0.25	0.0	0.0
ETBE	7.30	7.30	1.39	1.39	0.0	0.0
CHLO	10.4	14.9	0.25	1.50	0.0	0.0
TRICH	6.77	15.7	0.543	0.445	0.0	0.0
VICH	7.30	7.30	1.39	1.39	0.0	0.0

[1] Maximal velocity for metabolism (mg/kg/hr)

[2] Michaelis Menten constant (mg/L)

[3] First order metabolic rate constant (kg/hr)

Table 4: Interspecies toxicokinetic uncertainty factors (UF_{AH-TK}) obtained with the PBTK models[1].

CHEMICAL	CA[2]			CV			CR			CS			CF			CL			CM[3]		
	8 h	24 h	720 h	8 h	24 h	720 h	8 h	24 h	720 h	8 h	24 h	720 h	8 h	24 h	720 h	8 h	24 h	720 h	8 h	24 h	720 h
DCM	1.68	1.53	1.47	1.63	1.52	1.48	1.63	1.48	1.48	0.82	0.74	0.74	1.71	0.89	0.74	0.44	0.40	0.40	5.21	4.87	4.48
TETRA	2.73	2.37	1.54	2.53	2.27	1.57	1.38	0.83	0.85	0.49	0.21	0.21	27.7	11.4	1.21	1.30	0.76	0.80	17.9	16.1	11.5
DIOX	0.11	0.05	0.03	0.11	0.05	0.04	0.21	0.11	0.07	0.21	0.11	0.07	0.21	0.11	0.08	0.17	0.09	0.06	5.89	3.24	1.77
TOL	1.11	1.09	1.07	1.09	1.07	0.93	1.91	1.66	1.66	1.23	1.07	1.07	5.36	2.24	0.82	1.25	1.09	1.09	2.26	2.31	2.05
XYL	1.31	1.24	1.06	1.24	1.19	1.06	0.55	0.47	0.47	0.38	0.32	0.32	4.75	1.71	0.55	0.54	0.46	0.46	2.50	2.38	2.07
STY	1.15	1.01	0.93	1.09	1.00	0.95	1.09	0.95	0.95	1.12	0.95	0.95	2.23	1.20	0.91	0.91	0.79	0.79	5.07	4.80	4.29
CATE	1.64	1.65	1.46	1.56	1.58	1.47	0.91	0.85	0.86	0.95	0.86	0.86	4.97	2.80	0.86	0.90	0.83	0.84	9.07	8.09	8.90
ETBE	1.17	1.10	0.91	1.15	1.10	0.93	0.76	0.61	0.61	0.75	0.61	0.61	3.94	1.55	0.61	0.59	0.48	0.48	2.54	2.53	2.13
CHLO	1.80	1.69	1.52	1.64	1.58	1.47	0.73	0.65	0.65	0.68	0.61	0.61	2.24	0.86	0.38	1.43	1.28	1.28	8.30	7.91	7.12
TRICH	1.32	1.24	1.05	1.33	1.27	1.13	0.24	0.20	0.20	0.27	0.22	0.23	3.97	1.34	0.39	0.05	0.05	0.05	5.21	4.75	4.03
VICH	1.54	1.37	1.26	1.42	1.34	1.29	0.97	0.91	0.89	0.95	0.92	0.90	2.47	1.21	0.91	5.22	1.25	1.35	8.88	8.68	8.48
Average	1.41 ±0.63	1.28 ±0.56	1.12 ±0.43	1.34 ±0.58	1.27 ±0.54	1.12 ±0.43	0.94 ±0.54	0.79 ±0.47	0.79 ±0.48	0.71 ±0.34	0.60 ±0.34	0.60 ±0.34	5.41 ±7.56	2.30 ±3.10	0.68 ±0.32	1.16 ±1.42	0.68 ±0.42	0.68 ±0.43	6.62 ±4.48	5.97 ±4.10	5.17 ±3.38

[1] Both rat and human were exposed to 1 ppm of chemical.

[2] CA, CV, CR, CS, CF, CL, are the concentrations of the parent compound in arterial blood, venous blood, richly perfused tissues, slowly perfused tissues and fat compartments, respectively.

[3] CM refers to the concentration of the metabolite in the liver

Table 5: Rat/human dose ratios obtained with PBTK models[1].

CHEMICAL	8-h	24-h	720-h
DCM	5.16	5.37	5.67
TETRA	5.03	4.76	7.77
DIOX	1.95	2.02	2.21
TOL	3.63	3.62	3.79
XYL	3.71	3.75	3.83
STY	4.24	4.25	4.27
CATE	5.59	5.97	7.68
ETBE	3.73	3.75	3.93
CHLO	5.19	5.34	5.67
TRICH	5.39	5.60	6.05
VICH	5.70	6.12	6.77
Average	4.48 ±1.1	4.60 ±1.2	5.24 ±1.7

[1] Both rat and human were exposed to 1 ppm.

Table 6: Interspecies toxicokinetic uncertainty factors (UF_{AH-TK}) when both rats and humans receive equivalent doses.

CHEMICAL	CA[1]	CV	CR	CS	CF	CL	CM[2]
	720-h	720-h	720-h	720-h	720-h	720-h	720-h
DCM	0.26	0.26	0.26	0.13	0.13	0.07	0.79
TETRA	0.17	0.17	0.10	0.02	0.14	0.09	1.32
DIOX	0.02	0.02	0.03	0.03	0.03	0.03	0.80
TOL	0.25	0.24	0.44	0.28	0.22	0.29	0.54
XYL	0.28	0.28	0.12	0.08	0.14	0.12	0.54
STY	0.22	0.22	0.22	0.22	0.21	0.18	1.00
CATE	0.19	0.19	0.11	0.11	0.11	0.11	1.05
ETBE	0.24	0.23	0.16	0.15	0.16	0.12	0.54
CHLO	0.26	0.27	0.11	0.11	0.07	0.22	1.25
TRICH	0.19	0.17	0.03	0.04	0.06	0.01	0.67
VICH	0.20	0.20	0.14	0.14	0.14	0.18	1.25
Average	0.21±0.07	0.20±0.07	0.16±0.12	0.12±0.08	0.13±0.06	0.13±0.08	0.87±0.32

[1] CA, CV, CR, CS, CF, CL, are the concentrations of the parent compound in arterial blood, venous blood, richly perfused tissues, slowly perfused tissues and fat compartments, respectively.

[2] CM refers to the concentration of the metabolite in the liver

Figure legend

Figure 1: Conceptual representation of the physiologically-based toxicokinetic model used in the derivation of the toxicokinetic interspecies uncertainty factors

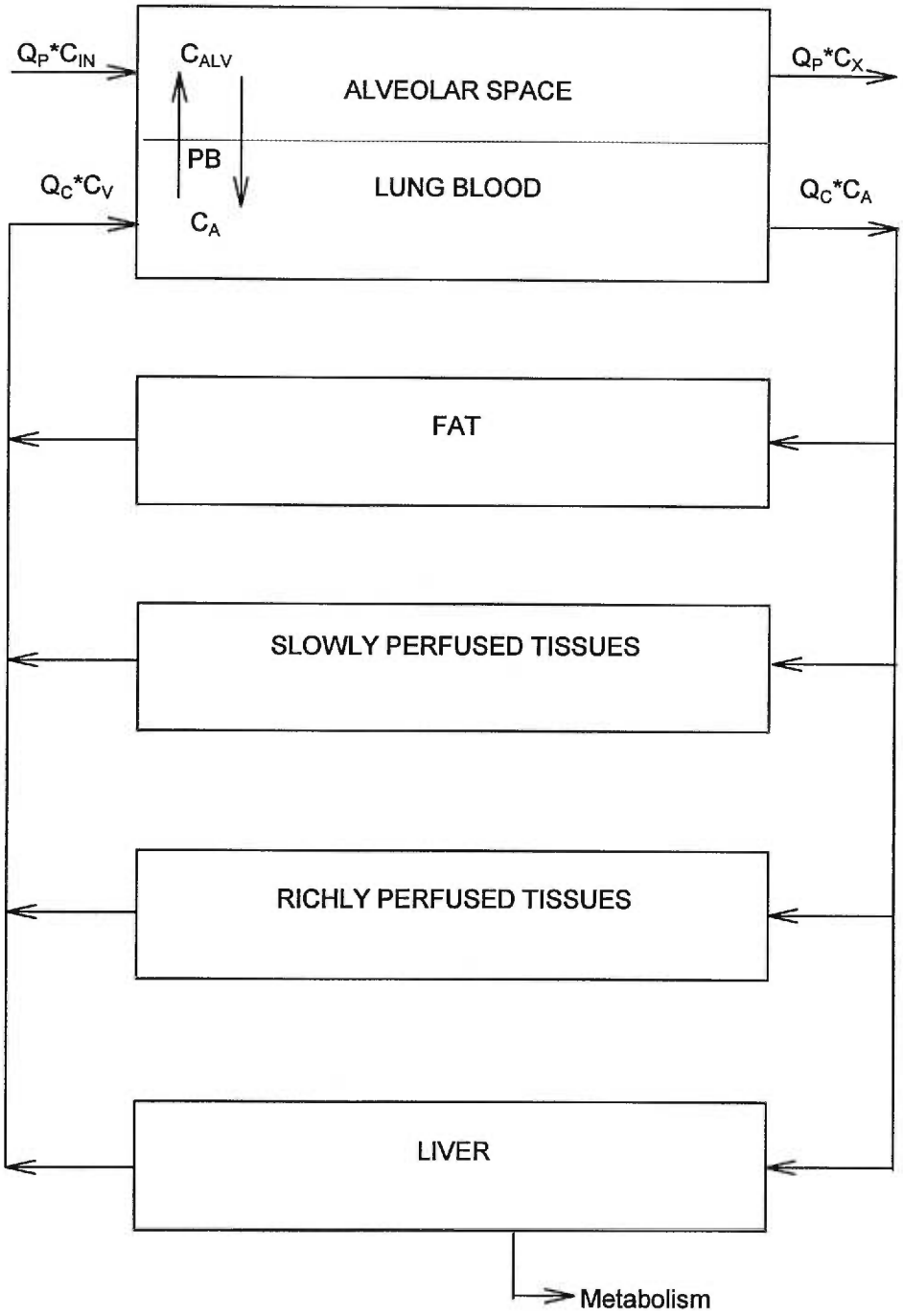
Q_P*C_{IN}
C_{ALV}
ALVEOLAR SPACE
Q_P*C_X
PB
Q_C*C_V
LUNG BLOOD
Q_C*C_A
C_A
FAT
SLOWLY PERFUSED TISSUES
RICHLY PERFUSED TISSUES
LIVER
Metabolism

Article No 5

(Published in Toxicology Methods, 7:207-228, 1997)

PHYSIOLOGICALLY-BASED ALGEBRAIC EXPRESSIONS FOR PREDICTING STEADY-STATE TOXICOKINETICS OF INHALED VAPORS

MICHAEL PELEKIS[1], DANIEL KREWSKI[2] AND KANNAN KRISHNAN[1]

[1]Département de médecine du travail et hygiène du milieu, Université de Montréal, C.P. 6128, Succ. Centre-ville, Montréal, Québec, Canada, H3C 3J7

[2]Health Protection Branch, Health Canada, Ottawa, Ontario, Canada, K1A 0L2

Keywords PBPK models, pharmacokinetic modeling, steady state, toxicokinetics, VOCs, toluene, m-xylene

Address all correspondence to: Kannan Krishnan, Département de médecine du travail et hygiène du milieu, Université de Montréal, 2375 Côte Ste. Catherine, Bureau 4105, Montréal, Québec, Canada, H3T 1A8, Tel.: (514) 343-6581, Fax: (514) 343-2200

SUMMARY

Algebraic expressions are developed for predicting steady-state toxicokinetics of volatile organic chemicals (VOCs) by simplifying the mathematical descriptions used in physiologically-based toxicokinetic (PBTK) models. The equations developed in the present study use 5 or less input parameters (instead of the 17 used in conventional PBTK models) to predict steady-state tissue or blood concentrations of VOCs at low exposure concentrations. The adequacy of the steady-state equations was assessed by comparing blood and tissue concentrations obtained using these equations with those generated by validated rat and human PBTK models for toluene and m-xylene. The results of the present study show that for ≤ 1 ppm exposures of rats and humans to toluene or m-xylene, the difference in the steady-state blood and tissue concentrations calculated using the algebraic expressions and full-fledged PBTK models is less than 1%. The algebraic expressions developed in the present study represent a simpler and faster method of describing the steady-state toxicokinetics of VOCs, that lead to essentially the same predictions as the conventional PBTK models at low exposure concentrations.

INTRODUCTION

Physiologically-based toxicokinetic (PBTK) models utilize mathematical descriptions of the uptake, distribution, metabolism and elimination of chemicals to provide estimates of blood and tissue concentrations from ambient exposure concentrations. The PBTK model framework used for non-reactive, volatile organic chemicals (VOCs) typically consists of four tissue compartments [liver (L), slowly perfused tissues (S), richly perfused tissues (R), and fat (F)], interconnected by systemic circulation and a gas exchange lung compartment [1]. The rate of change in chemical concentration in the tissue compartments is described by means of a series of mass balance differential equations (MBDEs) which are based on the proven or hypothetical interrelations among certain physiological, physicochemical and biochemical parameters.

In the PBTK models for VOCs metabolized primarily in liver, the input parameters include: (1) volumes (V) of tissue compartments (VL, VS, VR and VF), (2) rate of blood flow (Q) to tissues (QL, QS, QR and QF), (3) rate constants representing hepatic metabolism (Vmax, maximal velocity of metabolism; Km, Michaelis affinity constant), (4) partition coefficients [blood:air (PB), liver:blood (PL), slowly perfused tissues:blood (PS), richly perfused tissues:blood (PR), fat:blood (PF], (5) cardiac output (QC), and (6) alveolar ventilation rate (QP).

Regardless of whether or not steady-state is reached, the PBTK model will require the estimates of all 17 of these parameters, as well as an assessment of the impact of the sensitivity, uncertainty and variability associated with each of these input parameters [2,3]. Since steady-state concentrations are not determined or influenced by flows and volumes, it may not be necessary to use the conventional PBTK model with all the above input parameters to predict steady-state concentrations. In principle, it should be possible to predict steady-state tissue and blood concentrations with fewer input parameters, primarily partition coefficients and metabolic rate constants.

Operationally, steady-state represents a situation in which the input-output difference in chemical concentration is constant over time, i.e., the rate of change in chemical concentration in the various tissue compartments is equal to zero. At steady-state, the amount of chemical metabolized equals the difference between the amount inhaled and the amount exhaled. In other words, the arterio-venous concentration difference at steady-state is attributed to the amount of chemical removed by metabolism. During chronic human exposure to low ambient concentrations of environmental pollutants, steady-state is likely to be reached. In such cases, it is possible that the blood and target tissue concentrations of chemicals can be predicted using fewer input parameters than in a full-fledged PBTK model. A previous effort on steady-state analysis of inhaled vapors focused to develop algebraic expressions for predicting the steady-state blood:air partition coefficients and

rate of uptake of inhaled vapors [4]. The applicability and subsequent validation of this approach for predicting the arterial blood, venous blood and tissue concentrations of VOCs at steady-state have not been demonstrated. The objective of the present study is to develop and validate simple, closed-form algebraic expressions for predicting steady-state toxicokinetics of VOCs.

METHODS

The methodology involved (1) development of algebraic expressions to predict steady-state concentrations of VOCs in tissues and blood, by simplifying mechanistically-based mathematical descriptions used in PBTK models, and (2) comparison of the steady-state concentrations for m-xylene and toluene calculated using results of step (1) with those obtained using previously validated PBTK models [5,6].

Development of algebraic expressions to predict steady-state concentrations of VOCs

The concentrations (C) of interest are CA, CV and CT, where A = arterial blood, V = venous blood, and T = tissue. In order to calculate CT, the numerical values of the chemical concentration in venous blood exiting the tissue (CVT) and the tissue:blood partition coefficient (PT) should be known. For non-metabolizing tissues, at steady-state (ss), $CVT_{SS} = CA_{SS}$. Therefore, if CA_{SS} is known, CT_{SS} can be computed as CA_{SS} times PT. CA_{SS} can be calculated as follows [1]:

$$CA_{SS} = \frac{QP*CI + QC*CV_{SS}}{QC + (QP/PB)} \qquad (1)$$

where CI is the chemical concentration in inhaled air (mg/L), and * denotes multiplication.

Since QP = QC, Eqn. 1 is reduced to:

$$CA_{SS} = \frac{CI + CV_{SS}}{1 + (1/PB)} \qquad (2)$$

For situations where QP ≠ QC, an Eqn. of the above type can still be generated except that it will have numerical values representing the ratio of QP/QC which may deviate from 1. Eqn. 2 describes the steady-state concentration of VOC in arterial blood exiting pulmonary gas-exchange compartment, and has CV_{SS} as the sole unknown (since PB and CI are considered as known, input parameters).

The CV in PBTK models for VOCs is calculated from the venous blood concentrations exiting each tissue compartment as follows [1]:

$$CV = \frac{(QF*CVF) + (QR*CVR) + (QS*CVS) + (QL*CVL)}{QC} \qquad (3)$$

Since at steady-state, the concentration of chemical in arterial blood (CA_{SS}, entering a tissue compartment) and venous blood (CVT_{SS}, exiting the tissue)

will be equal for all non-metabolizing tissue compartments, CV_{SS} can be calculated as follows:

$$CV_{SS} = \frac{(QF*CA_{SS}) + (QR*CA_{SS}) + (QS*CA_{SS}) + (QL*CVL_{SS})}{QC} \quad (4)$$

Regrouping the Q's for non-metabolizing tissues, Eqn. 4 becomes:

$$CV_{SS} = \frac{[CA_{SS}*(QF + QR + QS)] + (QL*CVL_{SS})}{QC} \quad (5)$$

Since QF + QR + QS = (QC - QL), Eqn. 5 can be re-written as follows:

$$CV_{SS} = \frac{[CA_{SS}*(QC - QL)] + (QL*CVL_{SS})}{QC} \quad (6)$$

For metabolizing tissues, the concentration of chemical in the venous blood exiting the tissue can be estimated by accounting for the extraction ratio (E) as follows [7]:

$$CVL_{SS} = CA_{SS}*(1-E) \quad (7)$$

Inserting Eqn. 7 into Eqn. 6 gives

$$CV_{SS} = \frac{[CA_{SS}*(QC - QL)] + [QL*CA_{SS}*(1-E)]}{QC} \quad (8)$$

Expanding the numerator, Eqn. 8 becomes,

$$CV_{SS} = \frac{CA_{SS}*QC - CA_{SS}*QL + CA_{SS}*QL - CA_{SS}*QL*E}{QC} \quad (9)$$

Simplification of Eqn. 9 gives

$$CV_{SS} = \frac{CA_{SS}*(QC - QL*E)}{QC} \quad (10)$$

Since QL/QC is a species-specific constant (QLC), Eqn. 10 can be re-written as:

$$CV_{SS} = CA_{SS}*(1 - QLC*E) \quad (11)$$

Eqn. 11 then provides the steady-state concentration of a VOC in the mixed venous blood pool. Inserting Eqn. 11 into Eqn. 2, gives

$$CA_{SS} = \frac{CI + [CA_{SS}*(1 - QLC*E)]}{1 + (1/PB)} \quad (12)$$

Re-grouping CA_{SS}, Eqn. 12 can be re-written as:

$$CA_{SS} = \frac{CI}{(1/PB) + (QLC*E)} \quad (13)$$

Eqn. 13 gives the concentration of a VOC in arterial blood exiting the gas-exchange compartment, at steady-state. CA_{SS}, obtained with Eqn. 13 is multiplied by the corresponding tissue:blood partition coefficients to obtain CT_{SS}. Alternatively, $[CA_{SS}*(1 - E)]$ is used for calculating chemical concentrations in metabolizing tissues. Table 1 compares the algebraic expressions developed in the present study with the more complex equations currently used in the PBTK models for VOCs.

Assessment of the adequacy of the proposed steady-state solutions

The adequacy of the proposed steady-state equations was assessed by comparing CA_{SS}, CV_{SS} and CT_{SS} obtained with those generated by previously validated rat and human PBTK models for toluene (TOL), and m-xylene (XYL) [5,6]. To predict CA_{SS}, CV_{SS} and CT_{SS} of TOL and XYL according to the algebraic equations shown in Table 1, only the partition coefficients (PT, PB), extraction ratio (E), and QL are required as input. The numerical values of PT, PB (for TOL and XYL, in rats and humans) and QL were obtained from Tardif *et al.* [3,4]. Since (i) $CL_H = QL*E$, and (ii) $CL_H = (QL*Vmax/Km)/(QL + Vmax/Km)$, E can be calculated as $(Vmax/Km)/(QL +$

Vmax/Km) [8]. The only additional input parameters required for calculating E then were Vmax and Km. The values of these parameters for rats and humans were also obtained from Tardif *et al.* [5,6]. Calculation of steady-state tissue and blood concentrations using the Eqns listed in Table 1 was done for 1 ppm and 10 ppm of TOL or XYL in inhaled air.

CA_{SS}, CV_{SS} and CT_{SS} during continuous exposures to 1 ppm and 10 ppm of TOL and XYL were also obtained using previously validated rat and human PBTK models. The structure of the PBTK models for TOL and XYL used in the present study (Figure 1) and their parameters (Table 2) were obtained from Tardif *et al.* [5,6]. In these models, input to the system occurs via inhalation, as defined by the alveolar ventilation rate (QP) and inspired concentration (CONC) which was set equal to 1 ppm or 10 ppm. The models were parametrized to simulate continuous exposure until steady-state condition was reached. The time to steady-state was postulated to correspond to seven times the largest tissue time constant in the respective models (Table 3): 13 hr and 19 hr for the rat XYL and TOL PBTK models, respectively. The calculated time to steady-state, however, was 347 hr and 293 hr respectively for the human XYL and TOL PBTK models. Solutions to the MBDEs constituting these PBTK models were obtained by numerical integration with the aid of a Fortran-based software package (Advanced Continuous Simulation Language®, Version 11.3.3, Mitchell & Gauthier Associates, Concord, MA).

The percent discrepancy between the steady-state solution (S_{SS}) and PBTK model simulations (S_{PBTK}) was calculated as $100*(|S_{PBTK} - S_{SS}|/S_{PBTK})$.

RESULTS

Tables 4 and 5 summarize the steady-state blood and tissue concentrations of XYL and TOL in rats and humans obtained with the conventional PBTK models, and with the simpler algebraic expressions derived in the present study. The manner in which the steady-state concentrations were predicted with the algebraic expressions is shown in the Appendix.

The predicted C_{SS} are compared with the PBTK model-simulated C_{SS}, which were obtained at 13 hr, 19 hr, 347 hr and 293 hr using the rat XYL, rat TOL, human XYL, and human TOL models, respectively. The above times to steady-state calculated with the knowledge of tissue time constants (Table 3) corresponded well with the model-simulated steady-state kinetic profile in all cases (Figs 2-3).

Following exposure of rats to 1 ppm XYL or TOL, the steady-state blood and tissue concentrations obtained with the two methods differed by less than 1% (Table 4). Specifically, the largest percent difference (0.47 and 0.59% respectively for XYL and TOL) was associated with CL_{SS}. When XYL exposure concentration is increased to 10 ppm, the steady-state liver concentrations obtained with both methods differ by 6.71%. In the case of TOL, the largest percent difference (7.63%) at 10 ppm exposure was also observed in the liver compartment (Table 4).

The percent difference between the calculated and model-simulated steady-state blood and tissue concentrations in humans followed the same trend as in rats. Accordingly, the steady-state concentrations of XYL and TOL for 1 ppm exposures obtained with the two methods differed by $\leq 0.88\%$ and $\leq 0.99\%$, respectively (Table 5). The percent difference, however, was greater at high exposure concentrations (10 ppm). In this case, the largest percent difference for XYL and TOL (~10%) was observed for CL_{SS} (Table 5).

DISCUSSION

The conventional PBTK modeling approach involves solving the MBDEs with the use of commercially-available simulation software or spreadsheet programs (reviewed in ref. 9). With either methodology, the solution to the MBDEs is obtained using numerical integration methods, the order and type of which may depend on the stiffness (i.e., the magnitude of difference between the largest and smallest time constants in the model) associated with the model compartments. Regardless of the stiffness, the interrelationships between concentrations in various model compartments, once the system is at steady-state, would be anticipated to be stable, and determined primarily by the partition coefficients and hepatic extraction ratio. Simple algebraic expressions accounting only for these parameters, based on mechanistic understanding as provided by PBTK models, would then be sufficient to provide predictions of steady-state kinetics of chemicals. The present study has shown that the steady-state concentrations of XYL and TOL calculated using the algebraic expressions are essentially the same as those obtained using full-fledged PBTK models at very low exposure concentrations ($\leq$ 1 ppm).

The conventional PBTK modeling approach involves the use of at least 17 input parameters for simulating the kinetics (regardless of whether steady-state is reached) of lipophilic VOCs such as TOL and XYL. The analysis conducted in the present study suggests that fewer parameters

determine the steady-state behavior of such VOCs within PBTK models. Conceptually, our understanding of (1) the system being modeled and (2) the impact of uncertainty associated with input parameters will be clearer if such simplifications of system behavior at steady-state are generated. Accordingly, the present effort indicates that E, PB and QLC are the sole determinants of CA_{SS} and CV_{SS}, whereas PTs are additional determinants of CT_{SS}. This simplification for VOCs has then permitted the identification of those parameters (i.e., Vmax, Km, QLC, PB, PT) that are critical to the prediction of steady-state kinetics. Specifically, tissue volumes (VL, VF, VS, VR, BW) and flows (QC, QP, QR, QS, QF) do not influence steady-state predictions, and as such complicated sensitivity/uncertainty/variability analyses of PBTK models for VOCs involving all the above parameters are not required, particularly if C_{SS} is the dose surrogate of interest.

Given the fact that human exposure to environmental contaminants is frequently characterized by very low level repeated exposures, the steady-state solutions proposed in this study should be relevant and useful. The PBTK models can as well be used to simulate C_{SS}, as has been done to-date, except that such an effort will require the use of simulation software or numerical integration algorithm. Further, the impact of the various model parameters on uncertainty and variability in tissue concentrations will remain unknown. As shown in the Appendix, the calculation of steady-state concentrations of VOCs is very simple, requiring only the numerical values of (i) E which varies from 0 to 1, (ii) QLC which has been reported to be 0.25 in

most literature sources, and (iii) partition coefficients which are mainly determined by the relative content of lipids and water in tissues and blood [10,11]. This set of defined parameters would appear to be particularly relevant for further analysis/refinement of PBTK models developed to predict C_{SS} in people exposed chronically to constant, very low atmospheric concentrations of VOCs.

Even though tissue volumes and flow rates do not have a direct influence on the steady-state concentrations of VOCs, these parameters are important in determining the time constant of model compartments. The tissue time-constant, which is equal to V*P/Q for non-metabolizing tissues, and V*P/(Q + Vmax/Km) for metabolizing tissues, indicates the time required to attain 50% of the steady-state concentration. Accordingly, following a period of exposure equivalent to one time-constant, the tissue compartment would have accumulated 50% of the C_{SS}. Based on this projection, the system would be anticipated to attain steady-state at the end of a period equaling 7 time-constants or so. This is the reason why in the present study, the calculated values of C_{SS} were compared to the PBTK model-simulated values obtained at the end of a 7 time-constant period. To be precise, the concentrations simulated immediately following the lapse of 7 time-constants would be anticipated to be equal to 99.21875% of the C_{SS}. Therefore, the fact that the difference between the C_{SS} values obtained with both approaches is within 1%, particularly for 1 ppm exposures, is to be expected.

The percent difference, however, will continue to increase particularly in the liver compartment with increasing exposure concentrations. This is principally because the E [=$CL_{int}/(CL_{int}$ + QL), where CL_{int} = Vmax/(Km + CVL_{SS})] is calculated under first order conditions during which CVL_{SS} is negligible compared to Km. For example, no significant loss in predictive value occurs for 1 ppm exposure when CVL_{SS} is neglected in calculating the CL_{int}, and therefore E. In this particular case, the CVL_{SS} values for XYL and TOL were 0.0013 mg/L and 0.0047 mg/L in the rat compared to their Km values (0.2 and 0.55 mg/L, respectively). The preceding CVL_{SS} values are very small compared to the respective Km values. Therefore, the fact that CVL_{SS} is neglected in calculating CL_{int} does not make any difference in the resulting E value. This is the reason why, despite the negligence of CVL_{SS} in CL_{int} and E calculations, the present approach provides predictions that are almost identical to those generated by PBTK models, for 1 ppm TOL or XYL exposures. However, when the CVL_{SS} values increase by a factor of 10 (≅ values anticipated at 10 ppm exposures) or greater, the CVL_{SS} will no longer be negligible with respect to Km. Accordingly, the 7-10% difference between both methods observed for 10 ppm exposures is accounted for almost entirely by the quantitative difference between Km and (CVL_{SS} + Km) (Table 6). The greater the value of Km, the lower will the difference be, for a given exposure concentration.

In general, the percent difference between the proposed method and PBTK models will be much lower, for the very low ambient concentrations

($\leq$ 1 ppm) of VOCs to which humans are exposed. The algebraic expressions developed in the present study would represent a simpler, faster and more economical way to facilitate tissue dose-based risk assessments for such situations, than conventional, full-fledged PBTK model.

APPENDIX: A sample calculation of blood and tissue concentrations at steady-state in rats exposed to 1 ppm (= 0.00434 mg/L air) of m-xylene using the algebraic expressions developed in the present study. Abbreviations found in the following equations are defined in the footnote of Table 1, and the numerical values of the parameters used in these calculations are listed in Table 2.

Step 1: Calculation of extraction efficiency

$$E = [(Vmax/Km)]/[QL + (Vmax/Km)] = [(3.183/0.20)]/[1.344 + (3.183/0.20) = 0.922$$

Step 2: Calculation of CA_{SS}

$$CA_{SS} = \frac{CI\ (mg/L)}{(1/PB) + (QLC*E)} = \frac{0.00434}{(1/46) + (0.25*0.922)} = 0.0172\ mg/L$$

Step 3: Calculation of CV_{SS}

$$CV_{SS} = CA_{SS}*(1 - QLC*E) = 0.0172*[1 - (0.25*0.922)] = 0.0132\ mg/L$$

Step 4: Calculation of CT_{SS}

$$CF_{SS} = CA_{SS}*PF = 0.0172*40.4 = 0.6954\ mg/L$$

$$CR_{SS} = CA_{SS}*PR = 0.0172*1.97 = 0.0339\ mg/L$$

$CS_{SS} = CA_{SS}*PS = 0.0172*0.91 = 0.0156$ mg/L

$CL_{SS} = CA_{SS}*(1 - E)*PL = 0.0172*1.97* (1 - 0.922) = 0.0026$ mg/L

ACKNOWLEDGEMENTS

This work represents an initiative undertaken as a part of Dr. Krishnan's research program on physiological modeling and risk assessment supported by grants from the Canadian Network of Toxicology Centres (CNTC), Natural Sciences and Engineering Research Council of Canada (NSERC), Fonds de la recherche en santé du Québec (FRSQ) and Fonds pour la formation de chercheurs et l'aide à la recherche (FCAR). The authors would like to thank Dr. Melvin Andersen of ICF Kaiser Inc., Morrisville, NC for reviewing sections of an earlier version of this manuscript.

REFERENCES

1. Ramsey JC, Andersen ME. A physiologically based description of the inhalation pharmacokinetics of styrene in rats and humans. *Toxicol Appl Pharmacol* 1984; 73: 159-175.

2. Krewski D, Wang Y, Bartlett S, Krishnan K. Uncertainty, variability and sensitivity analysis in physiologic pharmacokinetic models. *J Biopharm Stats* 1995; 5: 245-271.

3. Krewski D, Withey JR, Ku LF, Andersen ME. Application of physiological pharmacokinetic modeling in carcinogenic risk assessment. *Environ Health Perspect* 1994; 102 (Suppl. 11): 37-50.

4. Andersen ME. A physiologically-based toxicokinetic description of the metabolism of inhaled gases and vapors: analysis at steady-state. *Toxicol Appl Pharmacol* 1981; 60: 509-526.

5. Tardif R, Laparé S, Krishnan K, Brodeur J. Physiologically based modeling of the toxicokinetic interaction between toluene and m-xylene in the rat. *Toxicol Appl Pharmacol* 1993; 120: 266-273.

6. Tardif R, Laparé S, Charest-Tardif G, Brodeur J, Krishnan K. Physiologically based modeling of a mixture of toluene and xylene in humans. *Risk Anal* 1995; 15: 335-342.

7. Chen HSG, Gross JF. Estimation of tissue to plasma partition coefficients used in the physiological pharmacokinetic models. *J Pharmacokinet Biopharm* 1979; 7: 117-125.

8. Wilkinson GR, Shand DG. A physiological approach to hepatic drug clearance. *Clin Pharmacol Ther* 1975; 18: 377-390.

9. Haddad S, Pelekis M, Krishnan K. A methodology for solving physiologically based pharmacokinetic models without the use of simulation softwares. *Toxicol Lett* 1996; 85: 113-126.

10. Poulin P, Krishnan K. A tissue composition-based algorithm for predicting tissue:air partition coefficients of organic chemicals. *Toxicol Appl Pharmacol* 1996; 136: 126-130.

11. Poulin P, Krishnan K. A mechanistic algorithm for predicting blood:air partition coefficients of organic chemicals with the consideration of reversible binding in hemoglobin. *Toxicol Appl Pharmacol* 1996; 136: 131-137.

Table 1: Comparison of the forms of equations and input parameters used in the PBTK models and the algebraic expressions developed in the present study.

	Parameters	PBTK model	Algebraic expressions
1. Equations	Concentration in arterial blood	$CA = \frac{QP*CI + QC*CV}{QC + (QP/PB)}$	$CA_{ss} = \frac{CI}{(1/PB) + QLC*E}$
	Concentration in venous blood	$CV = \frac{\Sigma(QT*CVT)}{QC}$	$CV_{ss} = CA_{ss}* (1-QLC*E)$
	Concentration in non-metabolizing tissues (T=slowly perfused tissues, richly perfused tissues, and fat.	$CT = \frac{QT}{VT} * \int (CA-CVT)$	$CT_{ss} = CA_{ss} * PT$
	Concentration in metabolizing tissues (e.g. liver)	$CT = \frac{QL}{VL} * \int (CA-CVL) - \int RAM$	$CL_{ss} = CA_{ss} * PL*(1-E)$
2. Input parameters	Physiological	QP, QC, QF, QS, QR, QL, VF, VS, VR, VL	QL[a]
	Physico-chemical	PB, PF, PS, PR, PL	PB, PF, PS, PR, PL
	Biochemical	Vmax, Km	E[b]

Note: C, Q, V, and P terms refer to concentrations, blood flow rates, volumes and tissue:blood partition coefficients for liver (L), slowly perfused tissues (S), richly perfused tissues (R), and fat (F) compartments. QC, QP, CI, PB, Vmax, and Km refer to cardiac output, alveolar ventilation rate, inhaled concentration, blood:air partition coefficient, maximal velocity and Michaelis affinity constant for metabolism. CVT and CVL refer to chemical concentration in venous blood leaving all tissues and liver respectively. The subscript ss denotes that the values calculated are for steady-state condition. RAM=VMAX*CVL/(KM+CVL)

[a] The numerical values of QL as L/hr, and as fraction of cardiac output (QLC) are required.

[b] E=[(Vmax/Km)/(QL+Vmax/Km)]. Therefore, both Vmax and Km in addition to QL, are required as input parameters for solving this equation.

Table 2: Parameters used in PBTK models for m-xylene and toluene

PARAMETERS	m-Xylene		Toluene	
	Rat[1]	Human[2]	Rat[1]	Human[2]
Physiological				
Weights				
Body weight (BW,kg)	0.25	70.0	0.25	70.0
Tissue volumes (% of BW)				
Liver (VL)	0.049	0.026	0.025	0.019
Rapidly perfused (VR)	0.050	0.050	0.050	0.050
Slowly perfused (VS)	0.720	0.620	0.720	0.620
Fat (VF)	0.090	0.190	0.090	0.190
Flow rates (L/hr/kg)				
Alveolar ventilation (QPC)[3]	15	18	15	18
Cardiac output (QCC)[4]	15	18	15	18
Flow distribution (% cardiac output)				
Liver (QLC)	0.25	0.26	0.25	0.26
Rapidly perfused (QRC)	0.51	0.44	0.51	0.44
Slowly perfused (QSC)	0.15	0.25	0.15	0.25
Fat (QFC)	0.09	0.05	0.09	0.05
Partition coefficients				
Blood:air (PB)	46.0	26.4	18.0	15.6
Liver:blood (PL)	1.97	3.02	4.64	2.98
Rapidly perfused:blood (PR)	1.97	4.42	4.64	2.66
Slowly perfused:blood (PS)	0.91	3.00	1.54	1.37
Fat:blood (PF)	40.4	77.8	56.7	65.8
Biochemical constants				
Vmaxc (mg/kg/hr)[5]	8.40	8.40	4.80	4.80
Km (mg/L)	0.20	0.20	0.55	0.55

[1]Obtained from Tardif *et al.*, [5]

[2]Obtained from Tardif *et al.*, [6]

[3]The alveolar ventilation for an individual organism specified in the PBTK models (QP) has been calculated as QPC*BW $^{0.74}$

[4]The cardiac output for an individual organism specified in the PBTK models (QC) has been calculated as QCC*BW $^{0.74}$

[5]Vmax for an individual organism specified in the PBTK model has been calculated as Vmaxc*BW $^{0.70}$

Table 3: Time constants for the different tissue compartments of the m-xylene and toluene PBTK models.

	m-Xylene		Toluene	
TISSUE	Rat	Human	Rat	Human
	TC	TC	TC	TC
Fat	1.8783	49.5697	2.6361	41.9240
Liver[2]	0.0014	0.0059	0.0122	0.01942
Richly perfused. tissues	0.0090	0.0842	0.0211	0.0507
Slowly perfused. tissues	0.2031	1.2475	0.3437	0.5697

Note: Time constant for non-metabolizing tissues (hr)=[(VT)*(PT)]/QT; Time constant for metabolizing tissues (e.g., liver, hr)=[(VL)*(PL)]/[QL+(VMAX/KM)]

Table 4: Comparison of steady-state blood and tissue concentrations in rats obtained using conventional PBTK models with the analytical expressions derived in the present study.

	1 PPM				10 PPM			
	m-Xylene		Toluene		m-Xylene		Toluene	
Parameters	S_{PBTK}[a]	S_{SS}-Eqn[b]	S_{PBTK}	S_{SS}-Eqn	S_{PBTK}	S_{SS}-Eqn	S_{PBTK}^2	S_{SS}-Eqn[3]
CA	0.0172	0.0172	0.0162	0.0162	0.1728	0.1721	0.1644	0.1615
CV	0.0132	0.0132	0.0133	0.0133	0.1331	0.1325	0.1359	0.1328
CS	0.0156	0.0156	0.0249	0.0249	0.1572	0.1566	0.2531	0.2487
CF	0.6925	0.6954	0.9114	0.9158	6.9865	6.9542	9.2769	9.1578
CR	0.0339	0.0339	0.0749	0.0749	0.3404	0.3391	0.7629	0.7494
CL	0.0026	0.0026	0.0218	0.0217	0.0283	0.0264	0.2345	0.2166

Note: All abbreviations are defined in the footnote of Table 1. The CA, CV, CS, CF, CR and CL values were obtained at 14 hr for XYL and at 19 hr for TOL. These time periods correspond to the anticipated length of time to attain steady-state (calculated as 7X the largest time constant, shown in Table 3).

[a] Obtained by running a previously validated PBTK model [5].

[b] Obtained using the algebraic expressions derived in this article. A sample calculation is presented in the Appendix.

Table 5: Comparison of steady-state blood and tissue concentrations in humans obtained using conventional PBTK models with the analytical expressions derived in the present study.

	1 PPM				10 PPM			
	m-Xylene		Toluene		m-Xylene		Toluene	
Parameters	S_{PBTK}[a]	S_{SS}-Eqn[b]	S_{PBTK}	S_{SS}-Eqn	S_{PBTK}	S_{SS}-Eqn	S_{PBTK}	S_{SS}-Eqn
CA	0.0162	0.0162	0.0169	0.0169	0.1639	0.1623	0.1749	0.1689
CV	0.0125	0.0125	0.0143	0.0142	0.1267	0.1250	0.1485	0.1421
CS	0.0487	0.0487	0.0232	0.0231	0.4917	0.4869	0.2397	0.2314
CF	1.2603	1.2627	1.1119	1.1115	12.7216	12.6271	11.4767	11.1151
CR	0.0718	0.0717	0.0451	0.0449	0.7245	0.7174	0.4653	0.4493
CL	0.0058	0.0057	0.0198	0.0196	0.0630	0.0572	0.2183	0.1956

Note: All abbreviations are defined in the footnote of Table 1. The CA, CV, CS, CF, CR and CL were obtained at 347 for XYL and at 293 hr for TOL. These time periods correspond to the anticipated length of time to attain steady-state (calculated as 7X the largest time constant, shown in Table 3).

[a] Obtained by running a previously validated PBTK model [6].

[b] Obtained using the algebraic expressions derived in this article. A sample calculation is presented in the Appendix.

Table 6: Comparison of the percent difference between Km (Michaelis constant for hepatic metabolism) and Km + CVL_{ss} (sum of the steady-state venous blood concentration leaving liver and the affinity constant) at 1 ppm and 10 ppm of m-xylene (XYL) and toluene (TOL) in rats and humans.

Species & Chemicals	Km (mg/L)	Km + CVL_{ss}[1] (mg/L)	$\frac{\lvert(Km + CVL_{ss}) - Km\rvert}{Km} \times 100$
1 ppm Exposure			
Rat			
XYL	0.20	0.2013	0.65
TOL	0.55	0.5547	0.85
Human			
XYL	0.20	0.2019	0.95
TOL	0.55	0.5566	1.20
10 ppm Exposure			
Rat			
XYL	0.20	0.2134	6.70
TOL	0.55	0.6156	11.93
Human			
XYL	0.20	0.2189	9.45
TOL	0.55	0.6164	12.07

Note: The numerical values of rat and human CVL_{ss} for 1 ppm and 10 ppm XYL or TOL exposures were obtained by dividing CL_{ss} (from Tables 4 and 5) with PL (from Table 2).

FIGURE LEGENDS

Figure 1. Schematic of the physiologically-based toxicokinetic model for m-xylene (XYL) and toluene (TOL).

Figure 2A. PBTK model simulations of the time course of the fraction of steady-state tissue concentrations (liver 0----0; slowly perfused tissues Δ----Δ; fat+----+) attained during continuous exposure of rats to 1 ppm XYL.

Figure 2B. PBTK model simulations of the time course of the fraction of steady-state tissue concentrations (liver 0----0; slowly perfused tissues Δ----Δ; fat+----+) attained during continuous exposure of rats to 1 ppm TOL.

Figure 3A. PBTK model simulations of the time course of the fraction of steady-state tissue concentrations (liver 0----0; slowly perfused tissues Δ----Δ; fat+----+) attained during continuous exposure of humans to 1 ppm XYL.

Figure 3B. PBTK model simulations of the time course of the fraction of steady-state tissue concentrations (liver 0----0; slowly perfused tissues Δ----Δ; fat+----+) attained during continuous exposure of humans to 1 ppm TOL.

Figure 1

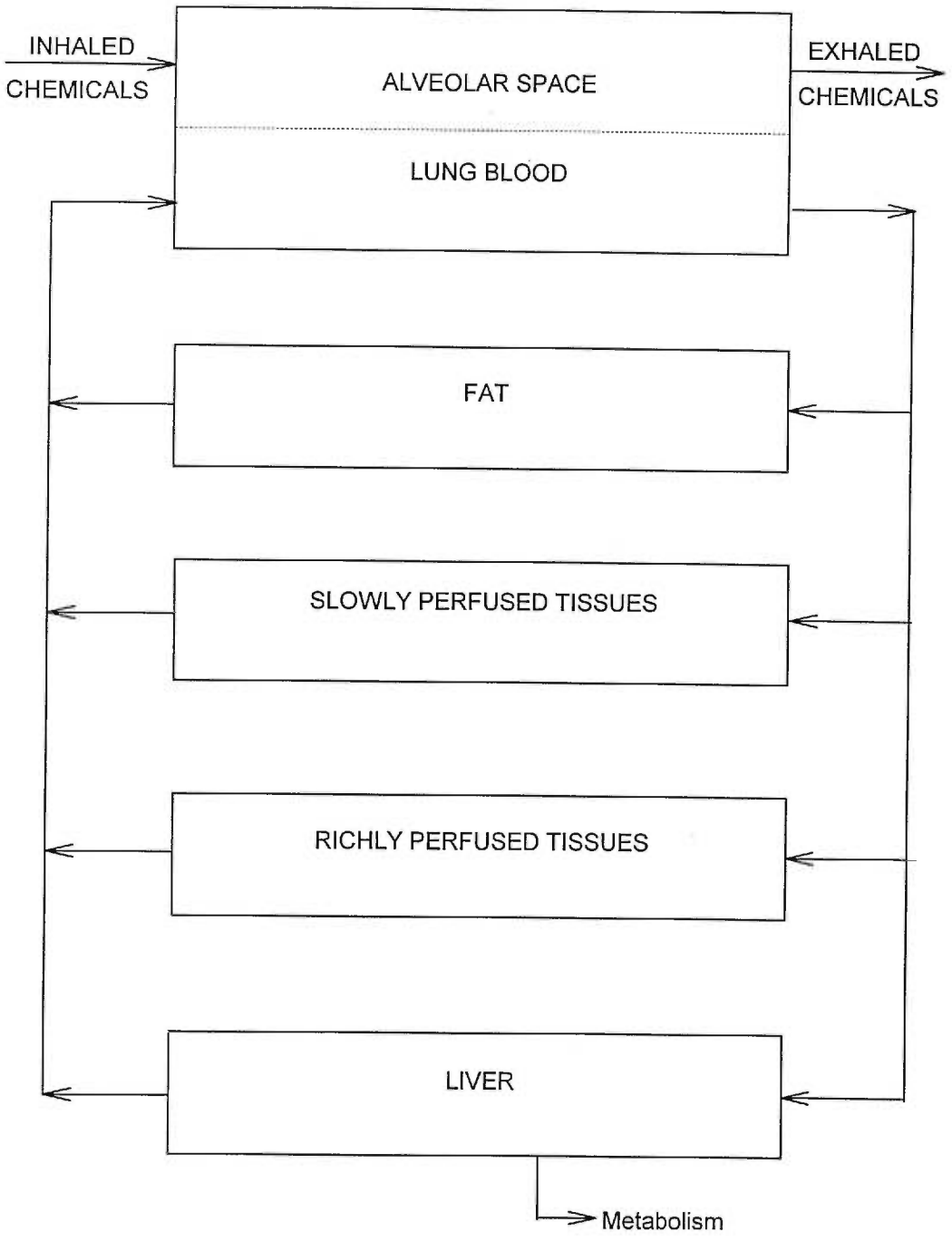
INHALED
CHEMICALS
ALVEOLAR SPACE
EXHALED
CHEMICALS
LUNG BLOOD
FAT
SLOWLY PERFUSED TISSUES
RICHLY PERFUSED TISSUES
LIVER
Metabolism

Figure 2A

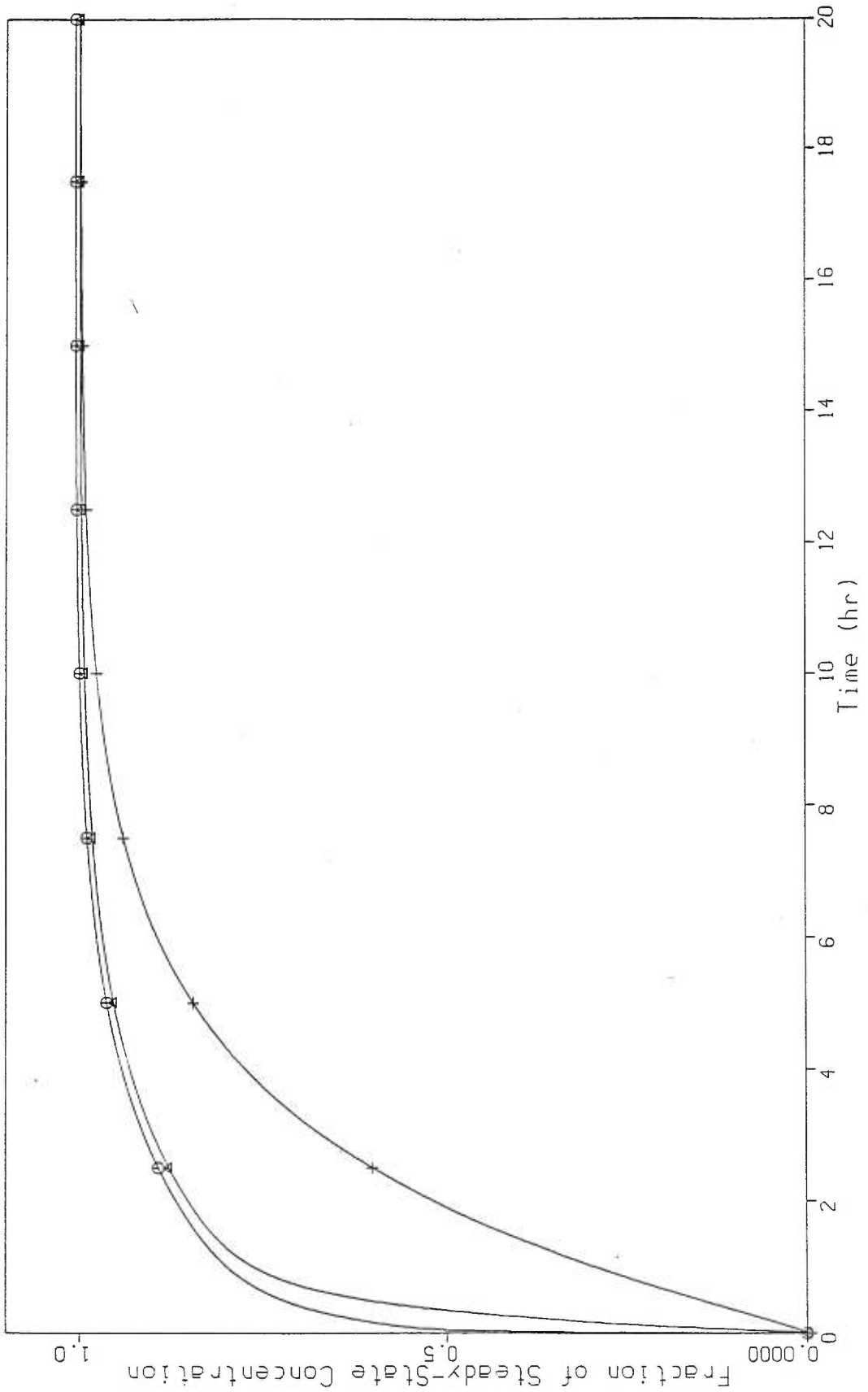
Fraction of Steady-State Concentration
0.0000
0.5
1.0
0
2
4
6
8
10
12
14
16
18
20
Time (hr)

Figure 2B

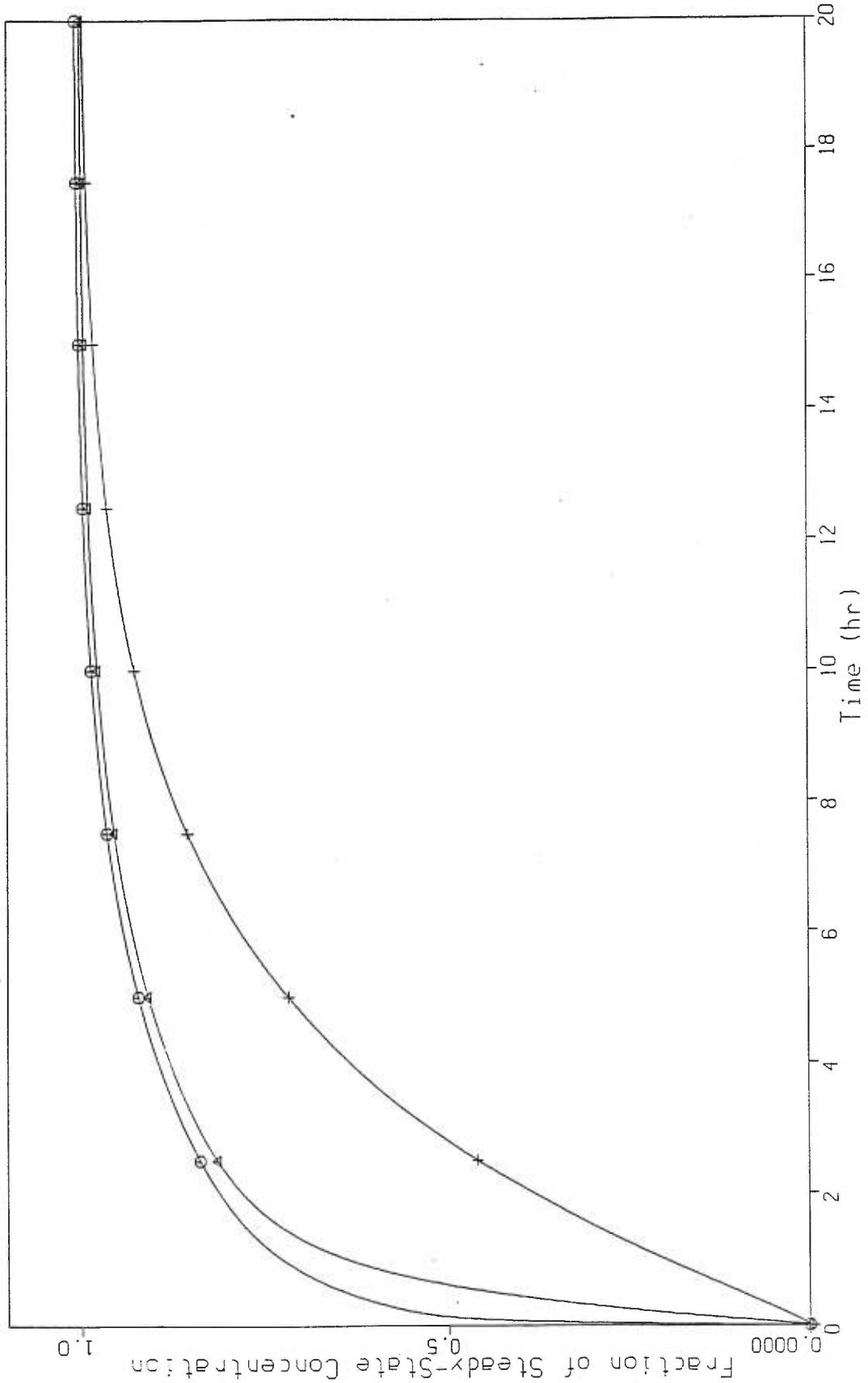
Fraction of Steady-State Concentration
0.0000
0.5
1.0
0
2
4
6
8
10
12
14
16
18
20
Time (hr)

Figure 3A

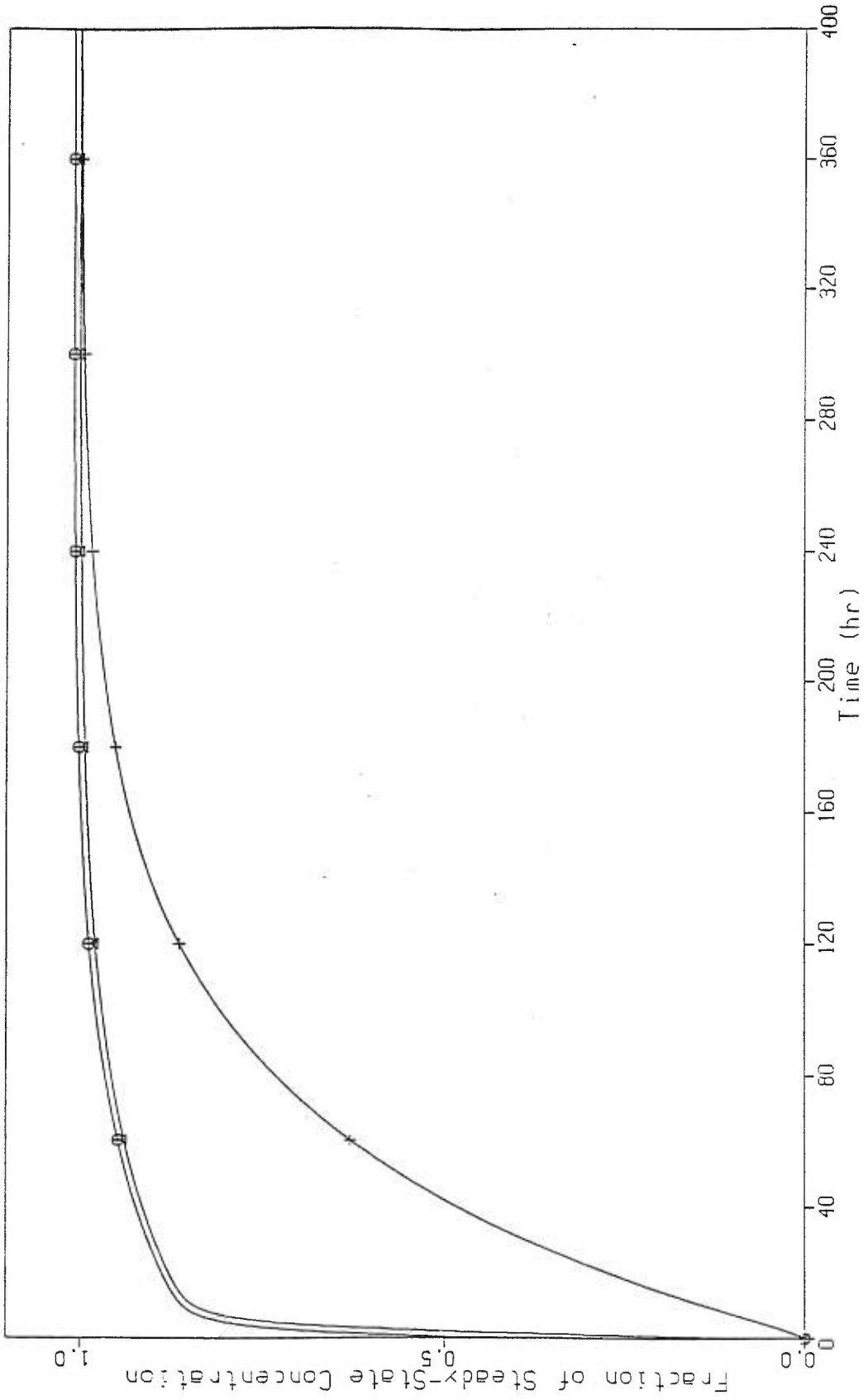
Fraction of Steady-State Concentration
0.0
0.5
1.0
0
40
80
120
160
200
240
280
320
360
400
Time (hr)

Figure 3B

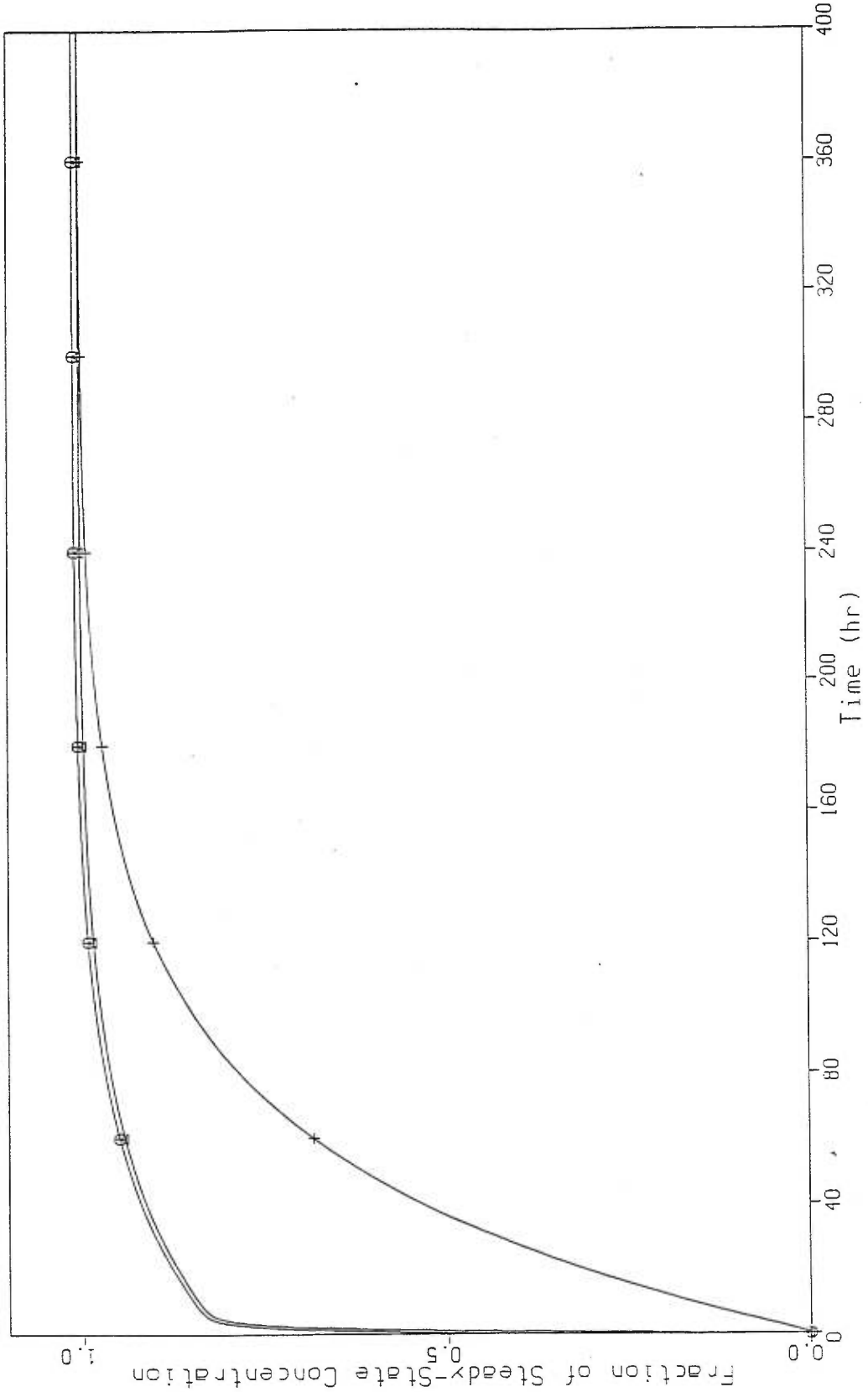
Fraction of Steady-State Concentration
0.0
0.5
1.0
0
40
80
120
160
200
240
280
320
360
400
Time (hr)

Article No 6

(To be Submitted to: Human and Ecological Risk Assessment)

MAGNITUDE AND MECHANISTIC DETERMINANTS OF THE INTERSPECIES TOXICOKINETIC UNCERTAINTY FACTOR FOR ORGANIC CHEMICALS

MICHAEL PELEKIS AND KANNAN KRISHNAN

Département de médecine du travail et d'hygiène du milieu,

Université de Montréal, C. P. 6128, Succ. Centre-ville,

Montréal, Québec, Canada, H3C 3J7

Keywords: Interspecies toxicokinetic uncertainty factors, steady-state, VOCs.

Running title: Mechanistic determinants of the interspecies toxicokinetic uncertainty factor.

Address for correspondence: Kannan Krishnan, Département de médecine du travail et hygiène du milieu, Université de Montréal, 2375 Côte Ste. Catherine, Bureau 4105, Montréal, Québec, Canada, H3T 1A8, Tel.: (514) 343-6581, Fax: (514) 343-2200

ABSTRACT

The interspecies uncertainty factor, UF_{AH}, is used to derive human equivalent doses from animal data, and was recently subdivided into two components to account separately for interspecies differences in toxicokinetics and toxicodynamics ($UF_{AH\text{-}TK}$=3.16, $UF_{AH\text{-}TD}$=3.16). Even though the UF_{AH} in its composite or dissociated form is widely used, there is no convincing scientific basis to justify the magnitude for all chemicals. In this study we use equations that describe the toxicokinetics of chemicals at steady-state to: (i) identify the mechanistic determinants of the $UF_{AH\text{-}TK}$, (ii) to determine its magnitude for several volatile organic chemicals (VOCs), and (iii) determine the magnitude of the components of $UF_{AH\text{-}TK}$, namely the $UF_{AH\text{-}TK\text{-}ABS}$ (accounting for interspecies differences in dose received or absorbed during identical inhalation exposure conditions), $UF_{AH\text{-}TK\text{-}MET}$ (referring to the factor by which the blood concentration of unchanged parent chemical differs from one species to another, due to metabolic clearance, when both species receive identical doses) and $UF_{AH\text{-}TK\text{-}DIS}$ (reflecting the magnitude of difference in chemical concentrations distributed in target tissues of two species when the arterial blood concentration in both species is identical). The results show that the body weight, the rate of ventilation, the fraction of cardiac output flowing to the liver, the blood:air partition coefficient and the extraction ratio are the only parameters that play a critical role in the extrapolation of tissue and blood doses across species, and the magnitude of

the $UF_{AH\text{-}TK}$ obtained in this study is the same with that obtained in previous studies with physiologically-based toxicokinetic models.

INTRODUCTION

The interspecies uncertainty factor (UF_{AH}) has been defined by the National Academy of Sciences as "a number that reflects the degree or amount of uncertainty that must be considered when experimental data in animals are extrapolated to man" (NAS 1977). The magnitude of UF_{AH} (i.e., 10) appears to have originated from the interspecies differences in body surfaces and basal metabolic rates (Bigwood 1973, Dourson and Stara 1983), but there is no convincing scientific basis to justify the use of 10 for all chemicals. There is an urgent need to identify the specific mechanistic determinants responsible for the interspecies differences in toxicokinetics such that the chemical-specific UF_{AH} can be calculated.

Mechanistic toxicokinetic modeling approaches are potentially of use, in this context. The physiologically-based toxicokinetic (PBTK) models have previously been used to quantify the magnitude of UF_{AH} for few chemicals (Clewell and Manor, 1994; Lawrence *et al.,* 1997; Pelekis and Krishnan, 1998). The interspecies toxicokinetic uncertainty factors ($UF_{AH\text{-}TK}$) derived in these studies are appropriate only when steady state conditions or lifetime exposures have been simulated. The dose-response assessments for both carcinogens and non-carcinogens are frequently done for continuous, lifetime exposure scenarios. Further, it's unclear from these modeling studies as to which of the parameters contribute to the magnitude of $UF_{AH\text{-}TK}$.

During repeated exposures, chemicals will attain steady-state, and the steady-state kinetics can be described with fewer parameters than the 17 normally used in PBTK models (Pelekis *et al.*, 1997). In this article, we use the equations that describe the steady-state kinetics (Table 1) to:

(i) identify the mechanistic determinants of the interspecies toxicokinetic uncertainty factor, $UF_{AH\text{-}TK}$, and

(ii) determine the magnitude of $UF_{AH\text{-}TK}$ for several volatile organic chemicals (VOCs): dichloromethane (DCM), tetrachloroethylene (TETRA), 1,4-dioxane, (DIOX), toluene (TOL), m-xylene (XYL), styrene (STY), carbon tetrachloride (CATE), ethyl benzene (ETBE), chloroform (CHLO), trichloroethylene (TRI) and vinyl chloride (VICH).

Initially, the magnitude and mechanistic determinants of $UF_{AH\text{-}TK}$ representing interspecies differences in tissue concentration for a given ambient concentration were identified. This $UF_{AH\text{-}TK}$ is referred to as $UF_{AH\text{-}TK\text{-}TOT}$. Then, the magnitude and mechanistic basis of the factors that account for interspecies differences in each of the components of the overall toxicokinetic process were characterized (Figure 1). These $UF_{AH\text{-}TK}$ are referred to as $UF_{AH\text{-}TK\text{-}ABS}$ (accounting for interspecies differences in dose received or absorbed during identical inhalation exposure conditions), $UF_{AH\text{-}TK\text{-}MET}$ (referring to the factor by which the blood concentration of unchanged parent chemical differs from one species to another, when both

species receive identical doses) and $UF_{AH\text{-}TK\text{-}DIS}$ (reflecting the magnitude of difference in chemical concentrations distributed in target tissues of two species when the arterial blood concentration in both species is identical).

In the present article, all exercises have been conducted for rat-to-human extrapolation. The conceptual approach discussed here should be applicable for other kinds of interspecies extrapolations if the required information is available or can be generated. Furthermore, the magnitude and mechanistic basis of $UF_{AH\text{-}TK}$ have been investigated using the parent chemical as the potential toxic moiety, for two reasons: (i) the validated parameter estimates to verify the present approach are only available for parent chemicals, and (ii) regardless of the "actual" toxic moiety, the parent chemical concentration in the blood/tissue still represents the point of origin.

APPROACH

MAGNITUDE AND MECHANISTIC BASIS OF $UF_{AH\text{-}TK\text{-}TOT}$

The $UF_{AH\text{-}TK\text{-}TOT}$ refers to the number with which the animal exposure concentration (ppm or mg/m^3) should be divided, to get the toxicokineticaly-equivalent exposure concentration in humans. The toxicokinetic equivalence in this context refers to identical tissue concentrations of parent chemicals in both species. The tissue concentration of parent chemicals at steady-state (CT_{SS}) can be derived as follows (Pelekis *et al.*, 1997):

$$CT_{SS} = \frac{CI*(1-E)*PT}{(1/PB)+R*QLC*E} \qquad (1)$$

where:

CI =Ambient exposure concentration

E =Hepatic extraction ratio

PT =Tissue:blood partition coefficient

PB =Blood:air partition coefficient

QLC =Blood flow to the liver (expressed as fraction of cardiac output, L/hr/kg), and

R =pulmonary ventilation/cardiac output ratio (QP/QC).

Using the above Eqn to calculate CT_{SS} in both rats and humans for identical CI, the $UF_{AH\text{-}TK\text{-}TOT}$ becomes:

$$UF_{AH\text{-}TK\text{-}TOT} = \frac{PT_R*(1-E_R)/\,[(1/PB_R) + R_R*QLC_R*E_R]}{PT_H*(1-E_H)/\,[(1/PB_H) + R_H*QLC_H*E_H]} \quad (2)$$

Whereas for metabolizing tissues this equation can be used as such, the term (1-E) can be deleted for non-metabolizing tissues (e.g., richly perfused tissues, slowly perfused tissues, and adipose tissue).

According to Eqn 2 the mechanistic factors that determine the magnitude of chemical-specific $UF_{AH\text{-}TK\text{-}TOT}$ are:

(i) Tissue:blood partition coefficient (PT)

(ii) Blood:air partition coefficient (PB)

(iii) Hepatic extraction ratio (E), and

(iv) Fraction of cardiac output reaching liver (QLC).

If and when the numerical values of these determinants are identical in two species, the $UF_{AH\text{-}TK\text{-}TOT}$ will be unity. As shown in Tables 2-4, the numerical values of QLC and E are fairly comparable between rats and humans, and thus would not be expected to contribute a great deal to toxicokinetic differences. The same however, is not true for the other two parameters. Also, the interspecies difference in PT, but not PB, would be expected to cause a proportional influence on the magnitude of the $UF_{AH\text{-}TK\text{-}TOT}$.

To test these hypotheses, Eqn 2 was used to calculate the $UF_{AH\text{-}TK\text{-}TOT}$ for eleven VOCs based on equivalent steady-state concentration in tissues (richly perfused tissues, slowly perfused tissues, liver and adipose tissue). The values of $UF_{AH\text{-}TK\text{-}TOT}$ for eleven VOCs provided in Table 5 range from 0.79 ± 0.48 (0.07-1.48), 0.60 ± 0.34 (0.07-1.07), 0.69 ± 0.45 (0.06-1.35), and 0.67 ± 0.32 (0.08-1.21) for richly perfused tissues, slowly perfused tissues, liver and fat compartments, respectively, and are identical to the $UF_{AH\text{-}TK\text{-}TOT}$ calculated with the PBTK models (Pelekis and Krishnan 1998).

Since the ventilation rate, the main determinant of chemical uptake, and the metabolic rate constant which accounts for chemical clearance, are both scaled to $BW^{0.74}$ (Guyton, 1971; Vocci and Forber 1988), one would expect the magnitude of the default $UF_{AH\text{-}TK}$ to be approximately 1. However, Eqn 2 accounts for other specific mechanistic factors that modify the magnitude of the default $UF_{AH\text{-}TK}$. The default factor ($UF_{AH\text{-}TK\text{-}TOT}$=1) for VOCs will only hold good if the numerical values of all four mechanistic determinants (i.e., E, PB, PT, QLC) are identical in both species.

The numerical value of $UF_{AH\text{-}TK\text{-}TOT}$ is a result of the interspecies differences in absorption, clearance and distribution processes. To figure out the relative contribution of interspecies differences in each of these processes to the magnitude of $UF_{AH\text{-}TK\text{-}TOT}$, it is essential to understand the mechanistic basis and magnitude of $UF_{AH\text{-}TK\text{-}ABS}$, $UF_{AH\text{-}TK\text{-}MET}$ and $UF_{AH\text{-}TK\text{-}DIS}$.

MAGNITUDE AND MECHANISTIC BASIS OF $UF_{AH\text{-}TK\text{-}ABS}$

The initial step in the continuum of toxicokinetic processes relates to the translation of the ambient exposure concentration into dose received by the animal (Fig. 1). The dose received per unit time during inhalation exposures can be calculated as:

$$\text{Dose rate (mg/kg/hr)} = \frac{QP*(CI - C_{ALV})}{BW} \quad (3)$$

where QP =Alveolar ventilation rate (L/hr)

CI =Ambient exposure concentration (mg/L)

C_{ALV} =Concentration of chemical in alveolar space (mg/L), and

BW =Body weight (kg)

Since C_{ALV}=CA/PB and CA=[CI/((1/PB)+R*QLC*E)] (Pelekis *et al.,* 1997), the dose received during a defined period of time can be calculated as follows:

$$\text{Dose (mg/kg)} = \int_0^t \frac{QP*(CI - \{CI*[PB/(1+R*QLC*E*PB)]/PB\})}{BW} \quad (4)$$

Since $QP=QPC*BW^{0.74}$, the above Eqn can be re-written as:

$$\text{Dose (mg/kg)} = \int_0^t QPC*(BW^{0.74}/BW^{1.0})*(CI - \{CI*[PB/(1+R*QLC*E*PB)]/PB\}) \quad (5)$$

Upon simplifying, Eqn 5 becomes:

$$\text{Dose (mg/kg)} = \int_0^t QPC * BW^{-0.26} * (CI * \{1-[1/(1+R*QLC*E*PB)]\}) \quad (6)$$

Eqn 6 can be applied to calculate the dose received by rats and humans. For the same exposure scenario then, the $UF_{AH\text{-}TK\text{-}ABS}$ can be calculated as:

$$UF_{AH\text{-}TK\text{-}ABS} = \frac{\int_0^t QPC_R * BW_R^{-0.26} * (CI * \{1-[1/(1+R_R*QLC_R*E_R*PB_R)]\})}{\int_0^t QPC_H * BW_H^{-0.26} * (CI * \{1-[1/(1+R_H*QLC_H*E_H*PB_H)]\})} \quad (7)$$

Since identical exposure scenario is considered, the exposure duration and concentration for rats and humans are the same. Therefore, the equation for calculating $UF_{AH\text{-}TK\text{-}ABS}$ becomes:

$$UF_{AH\text{-}TK\text{-}ABS} = (QPC_R/QPC_H) * (BW_R/BW_H)^{-0.26} * \\ * \{(1-(1/(1+R_R*QLC_R*E_R*PB_R)))/(1-(1/(1+ R_H*QLC_H*E_H*PB_H)))\} \quad (8)$$

The magnitude of $UF_{AH\text{-}TK\text{-}ABS}$ calculated using the Eqn 8 for eleven VOCs are provided in Table 6, and these values are the same with those obtained with the use of PBTK models (Pelekis and Krishnan 1998).

Therefore, steady-state analysis permits the identification of the critical, mechanistic determinants that are responsible for the interspecies

differences in dose received during identical inhalation exposure scenarios. The specific mechanistic determinants of $UF_{AH\text{-}TK\text{-}ABS}$ are as follows:

(i) Body weight (BW)

(ii) Body weight-normalized alveolar ventilation rate (QPC)

(iii) Fraction of cardiac output reaching liver (QLC)

(iv) Hepatic extraction ratio (E), and

(v) Blood:air partition coefficient (PB)

If the numerical values of all these determinants are identical in two species, then the dose received by these species, during a particular exposure scenario, is expected to be identical. However, in the case of rat-human extrapolation, the body weight difference will always be there, regardless of the magnitude of difference in the other parameters. If the interspecies difference in QPC, QLC and PB is negligible, then Eqn 8 simplifies to:

$$UF_{AH\text{-}TK\text{-}ABS}=(BW_R/BW_H)^{-0.26} \quad (9)$$

For reference body weights of 0.25 and 70 kg, in rats and humans, used in risk assessment calculations the magnitude of $UF_{AH\text{-}TK\text{-}ABS}$ will be 4.33. In other words, the rat exposure concentration should be divided by a factor of 4.33 to get the human exposure concentration that will yield the same dose received as in the rat. This default factor of 4.33 will be modified if there are

interspecies differences in QPC, QLC, E, PB. The numerical value of QPC is known to be fairly constant across mammalian species (Guyton 1971), even though there are few reports of species-specific QPC (Ward *et al.,* 1988). Considering the overwhelming evidence for the species-invariance of QPCs at resting conditions, the rat-to-human extrapolation of the first segment in the toxicokinetic continuum (Figure 1) can be conducted as follows:

$$\text{Human Exposure Concentration} = \frac{\text{Rat Exposure Concentration}}{[(1-F_R)/(1-F_H)]} \qquad (10)$$

where:

F is the modifying factor calculated as [(1/(1+R*QLC*E*PB)].

Since QLC and E are often, but not always, similar between mammalian species, the PB is likely to be the sole modifying determinant of the default $UF_{AH\text{-}TK\text{-}ABS}$ of 4.33. The magnitude of this default factor will vary if the BW of the experimental animal and the reference human do not correspond to 0.25 and 70 kg respectively. In such cases, the default $UF_{AH\text{-}TK\text{-}ABS}$ can be calculated anew as $(BW_R/BW_H)^{-0.26}$. Even though this $UF_{AH\text{-}TK\text{-}ABS}$ can provide equivalent dose received in rats and animals, this dose not mean that equal blood concentrations will result in both species for identical delivered doses.

MAGNITUDE AND MECHANISTIC BASIS OF $UF_{AH\text{-}TK\text{-}MET}$

Two species receiving the same dose per unit time may have different blood concentrations, if there is an interspecies difference in the metabolic clearance processes. During repeated exposure scenarios (i.e., steady-state conditions), the dose received per unit time is equal to the amount cleared by metabolism. Since the rate of amount metabolized equals hepatic clearance (i.e., CL_h, L/hr) times steady-state arterial concentration (CA_{SS}, mg/L) (Ings 1990), the dose rate (mg/hr) can be calculated as:

$$AMT_{MET}\ (mg/hr) = \text{Dose rate (mg/hr)} = CL_h * CA_{SS} \qquad (11)$$

Normalizing both the dose rate and CL_h on the basis of body weight, Eqn 11 becomes

$$\text{Dose rate (mg/hr/kg)} = (CL_h/BW) * CA_{SS} \qquad (12)$$

Since CL_h=QL*E, and QL=QLC*$BW^{0.74}$, Eqn 12 can be re-written as:

$$\text{Dose rate (mg/hr/kg)} = \frac{QLC * BW^{0.74} * E * CA_{SS}}{BW^{1.0}}$$

In other terms,

$$CA_{SS} = \frac{\text{Dose rate (mg/hr/kg)}}{QLC * BW^{-0.26} * E} \qquad (13)$$

For a defined dose rate, Eqn 13 can be used to calculate the corresponding CA_{SS}. If the same dose rate is given to rats and humans, then $CA_R * CL_{h,R} = CA_H * CL_{h,H}$. The calculation of CA_H/CA_R then gives $CL_{h,R}/CL_{h,H}$, or rat-to-human ratio of metabolic clearance. This clearance ratio equals the $UF_{AH\text{-}TK\text{-}MET}$, and was calculated as follows:

$$UF_{AH\text{-}TK\text{-}MET} = \frac{CA_{SS\text{-}H}}{CA_{SS\text{-}R}} = \frac{QLC_R * BW_R^{-0.26} * E_R}{QLC_H * BW_H^{-0.26} * E_H} \quad (14)$$

or

$$UF_{AH\text{-}TK\text{-}MET} = (QLC_R/QLC_H) * (BW_R/BW_H)^{-0.26} * (E_R/E_H) \quad (15)$$

From the above Eqn the specific mechanistic factors that determine the magnitude of $UF_{AH\text{-}TK\text{-}MET}$ are:

(i) Fraction of cardiac output flowing through the liver (QLC)

(ii) Body weight (BW), and

(iii) Hepatic extraction ratio (E).

If the numerical values for these three parameters are identical in two species, then $UF_{AH\text{-}TK\text{-}MET} = 1$. Since BW is different between rats and humans, $UF_{AH\text{-}TK\text{-}MET}$ will always deviate from 1. The extent of deviation is further influenced by the interspecies difference in the numerical values of QLC and E. Using the species-specific values of BW, QLC and E, the $UF_{AH\text{-}TK\text{-}MET}$ for eleven VOCs was calculated using Eqn (15) (Table 7). These

numbers (average 4.93±1.14) correspond to the chemical-specific $UF_{AH\text{-}TK\text{-}MET}$ that should be used to divide the rat dose to get the equivalent human dose which will provide the same blood concentration as in the rat during continued exposures. However, the dose level that gives an equivalent steady-state arterial concentration may not provide similar tissue doses. This aspect of interspecies differences can be addressed with the development of $UF_{AH\text{-}TK\text{-}DIS}$.

MAGNITUDE AND MECHANISTIC BASIS OF $UF_{AH\text{-}TK\text{-}DIS}$

The next logical step to consider in the exposure-tissue dose continuum is the translation of blood concentration to a tissue concentration. The tissue concentration at steady-state can be determined as follows:

$$CT_{SS} = CA_{SS} * PT * (1\text{-}E) \qquad (16)$$

The rat-to-human extrapolation factor representing the difference in tissue dose for the same arterial blood concentration can be calculated as:

$$UF_{AH\text{-}TK\text{-}DIS} = \frac{PT_R * (1\text{-}E_R)}{PT_H * (1\text{-}E_H)} \qquad (17)$$

The numerical values of $UF_{AH\text{-}TK\text{-}DIS}$ for eleven VOCs are provided in Table 8. For liver, the metabolizing tissue, the magnitude of $UF_{AH\text{-}TK\text{-}DIS}$ values are determined by two factors, namely, E and PT. However, the interspecies

difference in PT alone determines the magnitude of the $UF_{AH\text{-}TK\text{-}DIS}$ for non-metabolizing tissues such as slowly perfused tissues.

DISCUSSION

The use of interspecies toxicokinetic uncertainty factor is mandated by risk assessment guidelines, in order to account for toxicokinetic variability across species (USEPA 1985). While PBTK models are capable of estimating blood and tissue concentrations across species accurately, the current work shows that one can obtain the same results using the simplified algebraic equations developed in this paper. The magnitude of the toxicokinetic component of the $UF_{AH\text{-}TK}$ determined in the present study is identical with those derived with the PBTK models (Pelekis and Krishnan, 1998). This is because the expressions used in this paper, describe accurately the blood and tissue concentrations of chemicals at steady-state. Since the $UF_{AH\text{-}TK}$ applies to steady-state conditions, its magnitude for the various surrogate doses calculated in the present study is as accurate as that estimated with the PBTK models.

The results of the present study show that exposing rats and humans to the same ambient concentration results in a 5-fold difference in the dose received (the rat receives 5 times more chemical than the human) and about two-thirds the tissue concentration (0.69±0.07, the rat has lower tissue concentrations). Because rats metabolize chemicals at a rate that is 5 times faster than that of humans, when both rats and humans receive the same dose rate (mg/kg/hr) the blood concentration is 5 times higher in the rat. Equivalent blood concentration in rats and humans result in almost the same

tissue concentrations in both species, because the tissue: blood partition coefficients for a given chemical are almost the same in both species.

Of the approximately 20 mechanistic parameters that are needed to predict the toxicokinetic behavior of a typical VOC only a few play a critical role in determining the magnitude of the $UF_{AH\text{-}TK}$ Thus, to predict the $UF_{AH\text{-}TK}$ only the tissue:blood, blood:air partition coefficients (PTs & PBs), the extraction ratios (E), and cardiac output flowing to the liver (QLC) and the body weight-normalized alveolar ventilation rate (QPC) are required. The effect of the other parameters is restricted in determining the time constants of the various tissue compartments, which in turn determine the time required for the system to reach steady-state. Once this is achieved, they have no influence on the kinetics of the chemical and thus they are not taken into consideration in the estimation of $UF_{AH\text{-}TK}$ (Pelekis *et al.*, 1997). The equations developed in this article make possible the calculation of all relevant toxicokinetic variables that normally would require a validated PBTK model, or extensive experimental work and one can freely and accurately estimate all variables encompassed by the exposure dose–tissue concentration continuum.

Of the mechanistic determinants that play a crucial role in the magnitude of $UF_{AH\text{-}TK}$, the extraction ratio, E, is the most problematic for two reasons. First, while QLC and the partition coefficients may either be

obtained from the literature or estimated from available algorithms (Poulin and Krishnan, 1995), E must be measured either from *in vitro* or *in vivo* experiments. Alternatively, when the extraction ratio (i.e., Vmax and Km) of a specific chemical is not known one could get a pretty good idea about the range of the magnitude of $UF_{AH\text{-}TK}$, by setting E equal to 0 and 1 respectively. Since E can assume any value between 0 and 1, when the metabolic parameters are not known one could use the upper or lower limit of E, to calculate the range of $UF_{AH\text{-}TK}$. Second, all equations derived in the present work apply to all volatile chemicals at steady state, provided the exposure concentration does not contradict the first order rate metabolism assumption that was invoked in the derivation of the steady-state equations (Pelekis *et al.,* 1997). At high ambient exposure concentration, this assumption will not be true and the equations could not be used principally because the E [$=CL_{int}/(CL_{int} + QL)$, where $CL_{int} = Vmax/(Km + CVL_{SS})$] is calculated under first order conditions during which CVL_{SS} is negligible compared to Km.

Although the present study considered only rat to human extrapolation, the equations derived here are applicable to any other interspecies extrapolation (mouse to rat, mouse to human, etc.,) provided numerical values for the appropriate mechanistic determinants are available. In cases where in addition to liver, other tissues are involved in metabolic clearance, these tissues will have to be treated as metabolising tissues and the appropriate equation must be used. Additionally, the equations derived in the

present study can also be applied to derive the $UF_{AH\text{-}TK}$ for other routes of administration (e.g., oral). In such cases, the $UF_{AH\text{-}TK\text{-}ABS}$ does not have to be calculated, since it is a known parameter, while the equations for $UF_{AH\text{-}TK\text{-}MET}$ and $UF_{AH\text{-}TK\text{-}DIS}$ developed in this paper can be used directly.

REFERENCES

Bigwood, E. J. 1973. The acceptable daily intake of food additives, *CRC Crit. Rev. Toxicol.* June, 41-93.

Clewell H.J., III and Jarnot, B. M. 1994. Incorporation of pharmacokinetics in noncancer risk assessment: example with chloropentafluorobenzene. *Risk Anal.* **14**, 265-276.

Dourson, M.L., and Stara, J. F. 1983. Regulatory history and experimental support of uncertainty (safety) factors. *Reg. Toxicol. Pharmacol.* **3**, 224-238.

Guyton, A.C. 1971, *Textbook of Medical Physiology*, 4th ed., W.B. Saunders, Philadelphia.

Ings, R.M.J. (1990). Interspecies scaling and comparisons in drug development and toxicokinetics. *Xenobiotica*, **20,** 1201-1231.

Lawrence, G.S., and Gobas, F.A.P.C. 1997. A pharmacokinetic analysis of interspecies extrapolation in dioxin assessment. Chemosphere **35**, 427-452.

National Academy of Sciences 1977. *Drinking Water and Health*, Vol. 1. National Academy of Sciences, Washington, DC.

Vocci, F., and Farber, T. 1988. Extrapolation of animal toxicity data to man, *Regul. Toxicol. Pharmacol.* **8**, 389-398.

Pelekis, M., and Krishnan, K. 1998. Physiological model-based derivation of interspecies uncertainty factors for noncancer risk assessments, *Regul. and Appl. Pharmacol.* (Submitted).

Pelekis, M., Krewski, D., and Krishnan, K. 1997. Physiologically-based algebraic expressions for predicting steady-state toxicokinetics of inhaled vapors, *Toxicology Methods*, **7**, 207-228.

Poulin, P., and Krishnan, K. 1995. A biologically-based algorithm for predicting human tissue:blood partition coefficients of organic chemicals, *Hum. Exper. Toxicol.* **14**, 273-280.

USEPA, 1985, *Principles of risk assessment: a nontechnical review*. Environ Corporation, Wash., D.C.

Table 1: Equations used to calculate $UF_{AH\text{-}TK}$[A]

PARAMETERS	EQUATIONS[B]
Concentration in arterial blood	$CA_{SS} = \frac{CI}{(1/PB) + R^{c}*QLC*E^{d}}$
Concentration in venous blood	$CV_{SS} = CA_{SS}*(1-QLC*E)$
Concentration in metabolizing tissues (=T;slowly perfused tissues, richly perfused tissues, and fat)	$CL_{SS} = CA_{SS}*(1-E)*PL$
Concentration in non-metabolizing tissues (e.g., liver)	$CT_{SS} = CA_{SS}*PT$

[A] Obtained from Pelekis *et al.* 1997.

[B] CI, QLC and P terms refer to ambient exposure concentration, liver blood flow rate constant and tissue:air (blood) partition coefficients for liver (L), slowly perfused tissues (S), richly perfused tissues (R), and fat (F) compartments. The subscript ss denotes that the values calculated are for steady-state condition.

[C] R=QP/QC.

[D] E=[(Vmax/Km)/(QL+Vmax/Km)].

Table 2: Physiological parameters used in the estimation of UF_{AH-TK}[A]

CHEM.	QPC[B]		QCC[C]		QLC[D]	
	Rat	Human	Rat	Human	Rat	Human
DCM	15	15	12.6	16	20	24
TETRA	22.2	15	14.4	16	25	25
DIOX	15	30	15	30	25	25
TOL	15	18	15	18	25	26
XYL	15	18	15	18	26	26
STY	10.5	10.5	13.1	13.1	37	37
CATE	15	11	15.5	11	25	25
ETBE	15	18	15	18	25	26
CHLO	15	15	15	15	25	25
TRICH	14	12.9	14	15	25	26
VICH	18	15	18	15	24	24

[A] The numerical values of parameters were obtained from obtained from Andersen *et al.,* 1991, Ward *et al.,* 1988, Reitz *et al.,* 1990, Tardif *et al.,* 1993, 1995, Ramsey and Andersen, 1984, Paustenbach *et al.,* 1988 , Tardif *et al.,* 1997, Reitz *et al.,* 1996, Allen *et al.,* 1993 and Fischer *et al.,* 1991, and Reitz *et al.,* 1996.

[B] Pulmonary ventilation rate (L/hr/kg)

[C] Cardiac output (L/hr/kg)

[D] Blood flow to the liver (expressed as fraction of cardiac output)

Table 3: Physicochemical parameters used in the estimation of $UF_{AH\text{-}TK}$[A]

	PB[B]		PF[C]		PS		PL		PR	
CHEMICAL	Rat	Human	Rat	Human	Rat	Human	Rat	Human	Rat	Human
DCM	19.4	8.94	6.19	12.4	0.408	0.82	0.732	1.46	0.82	0.732
TETRA	18.9	10.3	121.7	159.03	1.06	7.77	3.72	6.83	3.72	6.83
DIOX	1850	3650	0.46	0.23	0.84	0.43	0.84	0.43	0.84	0.43
TOL	18	15.6	56.7	65.8	1.54	1.37	4.64	2.98	4.64	2.66
XYL	46	26.4	40.4	77.8	0.91	3.00	1.97	3.02	1.97	4.42
STY	40	52	50	50	1.0	1.0	2.7	2.7	5.7	5.7
CATE	4.52	2.64	79.4	136	1.02	1.74	3.14	5.38	3.14	5.38
ETBE	42.7	28.0	36.6	55.6	0.61	0.94	1.96	2.99	1.41	2.15
CHLO	20.8	7.43	9.76	37.7	0.67	1.62	1.01	2.29	1.01	2.29
TRICH	21.9	9.2	25.3	73.3	0.46	2.3	1.20	6.8	1.20	6.80
VICH	1.68	1.16	11.90	17.24	1.25	1.81	0.95	1.38	0.95	1.38

[A] The numerical values of parameters were obtained from obtained from Andersen *et al.,* 1991, Ward *et al.,* 1988, Reitz *et al.,* 1990, Tardif *et al.,* 1993, 1995, Ramsey and Andersen, 1984, Paustenbach *et al.,* 1988 , Tardif *et al.,* 1997, Reitz *et al.,* 1996, Allen *et al.,* 1993 and Fischer *et al.,* 1991, and Reitz *et al.,* 1996.

[B] Blood:air partition coefficient

[C] Tissue blood partition coefficient (F:fat, S:slowly perfused tissues, L:liver, R:richly perfused tissues)

Table 4: Biochemical parameters used in the estimation of $UF_{AH\text{-}TK}$[A]

CHEMICAL	VMAXC[B]		KM[C]		KFC[D]		EL[E]		CL[F]	
	Rat	Human	Rat	Human	Rat	Human	Rat	Human	Rat	Human
DCM	4.00	6.25	0.40	0.75	2.0	2.0	0.81	0.65	0.66	65.4
TETRA	0.19	0.15	0.30	0.30	1.8	0.0	0.17	0.01	0.22	8.90
DIOX	27.0	0.27	29.4	3.00	0.0	0.0	0.20	0.01	0.39	1.77
TOL	4.80	4.80	0.55	0.55	0.0	0.0	0.71	0.61	0.95	66.4
XYL	8.40	8.40	0.20	0.20	0.0	0.0	0.92	0.88	1.24	95.9
STY	8.36	8.36	0.36	0.36	0.0	0.0	0.83	0.80	1.66	102.1
CATE	0.67	0.55	0.25	0.25	0.0	0.0	0.42	0.40	085	25.26
ETBE	7.30	7.30	1.39	1.39	0.0	0.0	0.60	0.49	0.80	52.8
CHLO	10.4	14.9	0.25	1.50	0.0	0.0	0.78	0.89	098	7.43
TRICH	6.77	15.7	0.54	0.45	0.0	0.0	0.93	0.68	1.11	61.08
VICH	7.30	7.30	1.39	1.39	0.0	0.0	0.94	0.96	1.46	80.06

[A] The numerical values of parameters were obtained from obtained from Andersen *et al.,* 1991, Ward *et al.,* 1988, Reitz *et al.,* 1990, Tardif *et al.,* 1993, 1995, Ramsey and Andersen, 1984, Paustenbach *et al.,* 1988 , Tardif *et al.,* 1997, Reitz *et al.,* 1996, Allen *et al.,* 1993 and Fischer *et al.,* 1991, and Reitz *et al.,* 1996.

[B] Maximal metabolic rate constant (mg/kg/hr)

[C] Michaelis Menten constant (mg/L)

[D] First order metabolic rate constant (kg/hr)

[E] E=[(Vmax/KM)/(QL+ Vmax/KM)]

[F] CL=QL*EL

Table 5: Overall toxicokinetic interspecies uncertainty factors ($UF_{AH\text{-}TK\text{-}TOT}$)

CHEMICAL	CR[A]	CS	CL	CF
DCM	1.48	0.74	0.40	0.74
TETRA	0.85	0.21	0.80	1.21
DIOX	0.07	0.07	0.06	0.08
TOL	1.66	1.07	1.09	0.82
XYL	0.47	0.32	0.46	0.55
STY	0.95	0.95	0.79	0.91
CATE	0.85	0.85	0.83	0.85
ETBE	0.61	0.61	0.48	0.61
CHLO	0.65	0.61	1.28	0.38
TRICH	0.20	0.23	0.05	0.39
VICH	0.89	0.92	1.35	0.91
Average	0.79±0.48	0.60±0.34	0.68±0.43	0.68±0.32

[A] R:richly perfused tissues, S:slowly perfused tissues, L:liver and F:fat.

Table 6: Dose received interspecies uncertainty factors ($UF_{AH\text{-}TK\text{-}ABS}$)[A]

CHEMICAL	$UF_{AH\text{-}TK\text{-}ABS}$
DCM	5.68
TETRA	7.80
DIOX	2.10
TOL	3.80
XYL	3.84
STY	4.27
CATE	7.85
ETBE	3.94
CHLO	5.69
TRICH	6.10
VICH	6.79
Average	5.26±1.83

[A] Dose is expressed as mg/kg body weight

Table 7: Metabolic clearance interspecies uncertainty factors ($UF_{AH\text{-}TK\text{-}MET}$)[A].

CHEMICAL[B]	$UF_{AH\text{-}TK\text{-}MET}$
DCM	4.88
TETRA	7.74
DIOX	76.3
TOL	4.86
XYL	4.34
STY	4.49
CATE	3.91
ETBE	5.14
CHLO	3.88
TRICH	5.79
VICH	4.26
Average[B]	4.93±1.14

[A] Both rat and human were exposed to the same dose rate (mg/kg/hr).

[B] The unusual and great differences in the metabolic parameters for DIOX in rats and humans resulted in its very high $UF_{AH\text{-}TK\text{-}MET}$ factor which was not included in the calculation of the average value.

Table 8: Tissue concentration interspecies toxicokinetic uncertainty factors ($UF_{AH\text{-}TK\text{-}DIS}$)[A]

CHEMICAL	CR[A]	CS	CL	CF
DCM	1.12	0.50	0.27	0.50
TETRA	0.54	0.14	0.50	0.77
DIOX	1.95	1.95	1.57	2.00
TOL	1.74	1.12	1.15	0.86
XYL	0.45	0.30	0.44	0.52
STY	1.00	1.00	0.83	1.00
CATE	0.58	0.57	0.57	0.58
ETBE	0.66	0.65	0.51	0.66
CHLO	0.44	0.41	0.87	0.26
TRICH	0.18	0.20	0.04	0.35
VICH	0.69	0.69	0.94	0.69
Average	0.85±0.56	0.68±0.52	0.70±0.43	0.74±0.47

[A] R:richly perfused tissues, S:slowly perfused tissues, L:liver and F:fat.

Figure Legend

Figure 1. Components of the interspecies toxicokinetic uncertainty factor

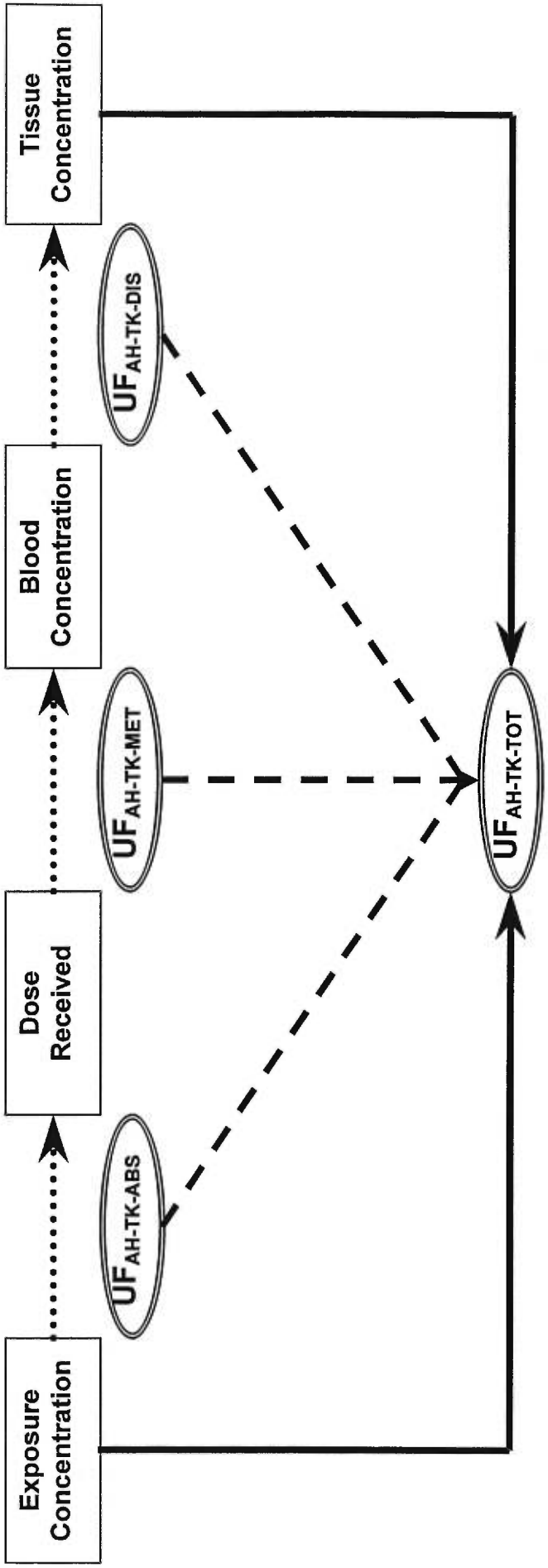
Tissue Concentration
Blood Concentration
Dose Received
Exposure Concentration
UF AH-TK-DIS
UF AH-TK-MET
UF AH-TK-ABS
UF AH-TK-TOT

CHAPTER 4

GENERAL DISCUSSION

One of the fundamental problems in risk assessment is the extrapolation of observed experimental results between animals and humans. The use of animals in toxicological studies has been based on the assumption that the extrapolation of toxicological data from animals to humans is valid, and that equivalent doses of a chemical in different species are equitoxic. The goal of the interspecies extrapolation methodologies is to estimate the equivalence of administered daily doses to animals and humans that result in equal adverse effects, i.e., doses that are toxicologically equivalent. Lacking detailed information on interspecies differences, it is frequently assumed that experimental results can be extrapolated between species when dose is standardized in terms of body weight (mg/kg/day) or surface area ($mg/m^2/day$). In the quantitative dose-response assessment of systemic toxicants the equivalence of dose has been managed arbitrarily with the use of the interspecies uncertainty factor which is used to estimate the dose to which humans can be exposed with no adverse effects.

All three approaches are based on empirical observations and have largely ignored the mechanisms involved in the expression of toxicity in animals and humans. Additionally, they develop risk estimates by correlating the incidence of response with exposure or administered (applied) dose. Because adverse effects develop at the target tissues from the interaction of

the toxic moiety with cellular components or receptors, another limitation of these approaches is their failure to account for the fundamental pharmacokinetic processes which cause the relationship between exposure dose and target tissue dose to be complex and non-linear across dose levels, dose routes and species. A more appropriate method of deriving risk estimates should involve the quantitative relationship between exposure levels and target tissue dose, and further the relationship between tissue dose and observed response in animals and humans.

In the last few years, there has been a considerable interest in applying the principles of toxicokinetics to the interspecies extrapolation of toxicological data. This dissertation has applied toxicokinetic theory in the making of reliable and convincing inferences about extrapolation of toxicological doses from studies on experimental animals to humans using the physiologically-based toxicokinetic modeling approach. The hypothesis tested was that with PBTK models, the relationship between exposure concentration and tissue dose can be established quantitatively and thus the interspecies toxicokinetic uncertainty factors can be determined from well defined principles. PBTK models that describe the toxicokinetic behavior of the carbamate pesticide aldicarb were developed and used to show how toxicokinetic information can be analyzed to derive chemical-specific values to replace the default $UF_{AH\text{-}TK}$. The same approach was also used to derive the interspecies toxicokinetic factors for eleven volatile organic chemicals.

The results demonstrated that the magnitude of $UF_{AH\text{-}TK}$ depends on the chemical and the target tissue and that 100% of the model-derived $UF_{AH\text{-}TK}$ were lower than the default values. When rats and humans are exposed to the same ambient concentration for an identical length of time, the average tissue and blood concentration of parent chemicals in rats and humans is approximately the same ($UF_{AH\text{-}TK}$=1), despite the fact that the rat receives about 5 times the dose received by humans. This is consequence of the enhanced metabolic clearance in rats compared to humans, and was confirmed by simulation of rat and human exposure to equivalent doses. When the ambient exposure concentration was adjusted so that the total dose received was equivalent to that of a human, the average clearance was greater in rats than in humans. In other words, the blood and tissue concentrations are equivalent in both rats and humans, because although the former receives on average a dose (mg/kg) that is about 5 times higher than humans it clears the parent chemical on average 5 times faster than the human, and thus the $UF_{AH\text{-}TK}$ is approximately 1.0.

While the physiological approach is far more elaborate, time-consuming, data-intensive and costly than the empirical approaches, its advantages far outweigh its costs. Its mechanistic foundation allowed for the translation of applied dose to effective dose to be done on sound scientific principles and avoided the "black box" approach of toxicokinetics used in the empirical methods of extrapolation. Furthermore, it allowed for the

identification of the parameters that contribute to the magnitude of $UF_{AH\ TK}$. This was achieved with the development of simplified algebraic equations that describe the toxicokinetics of chemicals at steady-state, and showed that to predict the $UF_{AH\text{-}TK}$ only the tissue:blood, blood:air partition coefficients (PTs & PBs), the extraction ratios (E), and cardiac output flowing to the liver (QLC) and the body weight-normalized alveolar ventilation rate (QPC) are required. Estimation of the magnitude of $UF_{AH\ TK}$ with algebraic equations that incorporate these parameters resulted in values that were identical to those obtained with the PBTK models.

The physiological model-based framework presented in this dissertation allows for the replacement of the default $UF_{AH\text{-}TK}$ with toxicokinetic data-derived values, provides an accurate estimate for its magnitude and suggests that the currently used $UF_{AH\text{-}TK}$ of 3.16 may result in inaccurate risk estimates. Furthermore, it shows that proper application of toxicokinetic theory can reduce uncertainties when establishing exposure limits for specific compounds and provide better assurance that established limits are adequately protective. Equally important, it has allowed for the identification of the mechanistic determinants that result in interspecies toxicokinetic differences and improves the scientific basis of the risk assessment process.

Even though this dissertation has advanced the quantitative evaluation of interspecies toxicokinetic uncertainty factors, and may help improve the

accuracy of risk estimates, the ultimate improvement will not occur until the foundation of the currently used dose-response methodologies is modified to account for the uncertainty/variability that surrounds the concept of risk and develop probabilistic estimates in accordance with the fundamental concept of risk.

Current noncancer dose-response assessment methodologies impart a deterministic character in risk, which by definition is a probability phenomenon. They utilize point value estimates to develop risk estimates, and in this context uncertainty arises from lack of knowledge. There is an answer, but because of weak theoretical considerations or because data are incomplete, inadequate, inconclusive, disputable or even non-existent, analytical methods and tools are not perfect and theories are based on assumptions, we know that the answer we have is not the right one. Risk estimates assessed in individuals are then applied to the population, which is characterized by both uncertainty and variability. Any available quantitative assessment on the uncertainty and variability of the inputs is ignored, which as shown by the results of this dissertation, may result in overestimation or underestimation of risk. Uncertainty factors are used to correct the lack of knowledge and additionally correct for variability, with the hope that the resulting estimate of risk will have a low probability of mistakenly stating that there is no effect when one is occurring. Although the uncertainty factors are intended to be conservative in the uncertainty dimension (giving risk

estimates that are usually expected to be higher than true risks for typical people) their arbitrary magnitude does not provide any assurances that this is accomplished. In fact, there is no way of knowing if they and the risk estimates are indeed conservative, and furthermore there is no way of quantitating their alleged conservative nature. Risk estimates are thus, limited by the selection of conservative and/or worst case scenarios, and risk managers and the public cannot assess the degree of conservatism of the risk assessment. Equally important, by setting the bias high enough (through the use of uncertainty factors) risk assessments may consider unrealistic scenarios.

The problem of deterministic approach arise not so much from the use of point value estimates, but with their inability to provide a means for selecting the proper point estimates. For example, it is difficult to argue that there are people who weigh 70 kg, but one could easily argue that a 70 kg individual is not a typical representative or average of the population. In other words, uncertainty analysis as used in the current dose-response assessment fails to account for variability in a quantitative way. The goal of uncertainty analysis should be not only to define as accurately as possible the weight of an individual, but also to describe the confidence with which it can be claimed that the use of a 70 kg person will produce a risk estimate that can be applied to the whole population or that it falls between defined range of values. In this context, uncertainty is a characteristic of the observer, which

can be reduced with further study and incorporates variability, which is a characteristic of the system we are studying and cannot be reduced by further study, it can only be characterized.

The weaknesses of the current dose-response assessment can be addressed by extending the use of physiological modeling techniques described in this dissertation to develop integrated toxicokinetic/toxico-dynamic (PBTK/TD) models that incorporate probabilistic methods (e.g., Monte Carlo) to estimate the propagation of uncertainty/variability in a population and derive risk estimates without the use of arbitrary uncertainty factors. The first step towards this goal will be the development of integrated PBTK/TD models. The advances of PBTK modeling, while satisfactory in determining the interspecies uncertainty factor of parent compound or its metabolite(s) at the target tissue in different species, is not sufficient for risk assessment purposes, because it is often limited by the need to make the assumption that the response to a given concentration of the chemical is the same in each species. Since toxicity has toxicokinetic and toxicodynamic components, the concept of equivalence must be seen as the sum of two components: toxicokinetic equivalence which deals with adjustment of the levels of the administered doses in animals and humans, and toxicodynamic equivalence which adjusts the response of animals and humans to an equivalent tissue dose. The development of integrated PBTK/TD models will enable the risk assessor to assess the potential health effects of human

exposure to environmental hazards based on the quantitative evaluation of tissue response in animal models, and evaluate accurately the overall UF_{AH}. More importantly, the development of human PBTK/TD models will make the use of UF_{AH} becomes redundant.

Probabilistic methods can then be applied to eliminate the problem of point estimates and determine the distribution of probable risk across a population. Monte Carlo simulation allows different parameters to be varied through their range of uncertainty simultaneously in one analytical effort. Instead of defining point estimates of parameters, distributed parameters are used which depict the frequency of occurrence of all expected values of that parameter in its "population". By distributed parameters it is meant that the parameter takes on different values at either different spatial co-ordinates or different times or both. Instead of point estimates for each parameter, a probability density function (PDF) describing the probability that the term has any specific numerical value is used. The distribution of risk is thereby determined as the result of the combined effects of multiple sources of variability or multiple sources of uncertainty. Since, each PDF depicts the frequency of occurrence of all expected values of that parameter in its "population", the need for the intrahuman uncertainty factor will be eliminated. The subchronic to chronic extrapolation can be carried out, by running the model over a long period of time, and thus a risk estimate (RfD, BMD) can be determined without using any uncertainty factor.

These extended techniques will make the analyses more informative to risk managers and members of the public by giving some perspective of the uncertainty behind point estimates. It may also contribute to the evaluation of the complexity of mechanistic models (a frequent criticism of physiological models), or it may be used to compare two different versions of the same model, and recommend use of the one with the least amount of uncertainty. Although probabilistic dose-response will add several steps to the risk assessment process, it will effectively implement EPA guidelines recommending quantification of the impact of uncertainty and variability in human health risk assessment (NAS, 1980; USEPA, 1986; NRC, 1994). The additional information concerning uncertainty and variability that is afforded by the new methodology will be potentially useful to the risk manager, for it necessarily increases the extent to which the efficiency of alternative risk management policy may be judged. The main restrain for general acceptance and use of this method, i.e., defining probability distributions for input parameters, can in some cases be reduced through sensitivity analysis or by approximation (triangular distributions). To improve the accuracy of probabilistic risk assessments, risk assessors will need to collect data to describe distributions for many currently undescribed input assumptions. Additionally, the extra information will help verify the assumption that the input parameters are distributed independently. Once appropriate probability distributions are selected as inputs to the PBTK/TD model, Monte Carlo simulation can provide a probabilistic RfD with no significant extra effort than

that required to determine a deterministic RfD. Then, by combining the proposed methodology with probabilistic exposure assessment, this approach promises to enhance the power of the overall risk assessment process. By doing so, risk assessment will allow for:

- greater understanding of the policy managers make
- reliable comparisons of alternative decisions, and
- increased understanding and acceptance of policy decisions by the public.

REFERENCES

Adolph, E.F., 1949, Quantitative relations in the physiological constituents of mammals, Science 109:579-585.

Altman, P.L., Dittmer, D.S., 1962, Growth including reproduction and morphological development, Fed. Proc. 337-366.

Andersen, M.E., 1987, Tissue dosimery in risk assessment, or what's the problem anyway? In "Pharmacokinetics in Risk Assessment, Drinking Water and Health, Vol. 8, National Academy Press, Washington, D.C.

Andersen, M.E., Krishnan, K., Conolly, R., McClellan, R.O., 1992, Mechanistic toxicology research and biologically-based modeling: partners for improving quantitative risk assessments, CITT Activities, 12:1-8.

Bekey, G.A, 1977, Models and reality: Some reflections on the art and science of simulation, Simulation 29(5),161-164).

Benedict, F.G.,1934, Die Oberflachenbestimmung verschiedener Tiergattungen, Ergeb. Physiol. 36:300-346.

Bigwood, E.J., 1973, The acceptable daily intake of food additives, CRC Crit. Rev. Toxicol., June, 41-93.

Boxenbaum, H. 1982a, Comparative toxicokinetics of benzodiazepines in dog and man, J. Pharmacokinet. Biopharmacol. 10:411-426.

Boxenbaum, H., 1982b, Interspecies scaling, allometry, physiological time, and the ground plan of toxicokinetics, J. Pharma. Biopharm. 10:201-227.

Brody, S., Procter, R.C., Ashworth, U.S.,1934, Basal metabolism, endogenous nitrogen, creatine and neutral sulfur excretions as functions of body weight, Univ. Missouri Agric. Exp. Sta. Res. Bull. 220:1-40.

Brody, S., 1945, Bioenergetics and Growth: With special reference to the efficiency complex in domestic animals, Reinold, New York.

Cannon, R.H., Jr. 1967, Dynamics of Physical Systems, McGraw-Hill, New York.

Clewell H.J., III and Jarnot, B. M., 1994, Incorporation of pharmacokinetics in noncancer risk assessment: example with chloropentafluorobenzene. *Risk Anal.* 14, 265-276.

Covello, V.T, Merkhofer M.W., 1993, Risk Assessment Methods, Approaches for assessing health and environmental; risks, Plenum Press, NY.

Crawford, J.D., Terry, M. E., Rourke, G.M., 1950, Simplification of drug dosage calculation by application of the surface area principle, Pediatrics 5:783-790.

Crump, K.S. 1984, A new method for determining allowable daily intakes, Fundam. Appl. Toxicol. 4:854-871.

Davidson, I.W.F., Parker, J.C., Beliles, R.P., 1986, Biological basis for extrapolation across mammalian species, Reg. Toxicol. Pharmacol. 6:211-237.

Dedrick, R.L., 1992, Toxicolgy lessons from cancer chemotherapy, CIIT Activities, 12:1-4.

Done, A.K., 1964, Developmental pharmacology, Clin. Pharmacol. Ther. 5:432-479.

Dourson, M.L., Stara, J.F., 1983, Regulatory history and experimental support of uncertainty (safety) factors, Reg. Toxicol. Pharmacol. 3:224-238.

Dourson, M.L., DeRosa, C.T., 1991, The use of uncertainty factors in establishing safe levels of exposure, In "Statistics in Toxicology", Krewski, D., Franklin, C., Eds., Gordon and Breach Science Publ., New York.

Edwards, N., 1975, Scaling of renal functions in mammals, Comp. Biochem. Physiol. 52A, 63-66.

Feldman, H.A., McMahon, T.A., 1983, The 3/4 mass exponent for energy metabolism is not a statistical artifact, Respir. Physiol. 52:149-163.

Food Safety Council, 1982, A proposed food safety evaluation process, The Nutrition Foundation, Inc. Washington, D.C.

Forbes, G.B., 1959, Body surface as a bases for dosage, Comment. Pediatrics 23:3-5.

Freireich, E.J., Gehan, E.A., Rall, D.P., Schimidt, L.H., and Scipper, H., 1966, Quantitative comparison of toxicity of anticancer agents in mouse, rat, hamster, dog, monkey and man. Cancer Chemotherap. Rep. 50: 219-224.

Gargas, M.L., Burgess, R.J., Voisard, D.E., Cason, G.H., Andersen, M.E., 1989, Partition coefficients of low molecular weight volatile chemicals in various liquids and tissues, Toxicol. Appl. Pharmacol., 98:87-99.

Gunther, B., 1975, Dimensional analysis and theory of biological similarity, Physiol. Rev. 55:659-699.

Guyton, A.C., 1947, Measurement of the respiratory volumes of laboratory animals, Am. J. Physiol. 150:70-77.

Guyton, A.C., 1971, Textbook of Medical Physiology, 4th ed., W.B. Saunders, Philadelphia.

Haefner, J.W., 1996, Modeling biological systems, Principles and applications, Chapman and Hall, N.Y.

Hemmingsen, A.M., 1950, The relation of standard (basal) energy metabolism to total fresh weight of living organisms, Rep. Steno. Mem. Hosp. (Copenhagen), 4:1-58.

Hill, T.A., Wands, R.C., 1989, Serial allometric factor extrapolation: compartmental and physiological toxicokinetic approaches, Health Phys. 57: Supp. 1, 395-401.

Hopkins, J.C., Leipold, R.J., 1996, On the dangers of adjusting the parameter values of mechanism-based mathematical models. Journal of Theoretical Biology, 183:417-427.

Huesner, A.A., 1982, Energy metabolism and body size. I. Is the 0.75 mass exponent of Kleiber's equation a statistical artifact, Respir. Physiol. 48:1-12.

Jarabek, A.M., 1994, Inhalation RfC methodology: dosimetric adjustments and dose-response estimation of noncancer toxicity of upper respiratory tract, Inhal. Toxicol. 6 (Supp): 301-325.

Kheir, N.A., 1988, Systems modeling and computer simulation, Marcel Dekker Inc, New York.

Klaasen, C.D. and Doull, J., 1980, Evaluation of safety: Toxicological evaluation, In "Toxicology", Klaasen, C.D. Amdur, Eds, MacMillan, New York.

Kleiber, M.,1932, Body size and metabolism, Hilgardia, 6:315-353.

Krishnan, K., Andersen, M.E., 1991, Interspecies scaling in toxicokinetics, In "New trends in toxicokinetics", Rescigno, A., Thakur, A.K., Eds. Plenum Press, New York.

Krishnan, K., Andersen, M.E., 1994, Physiologically based toxicokinetic modeling in toxicology, In "Principles and Methods of Toxicology" Hayes, A.W., Ed., Raven Press, N.Y.

Lehman, A.J., Fitzhugh, O.G., 1954, 100-fold margin of safety, Assoc. Food Drug Off. U.S. Q. Bull. 18:51-58.

Levins, R., 1966, The strategy of model building in population biology, American Scientist 54:421-431.

Leung, H.-W.,1993, Physiologically based toxicokinetic modeling in toxicology, In "General and Applied Toxicology", Ballantyne B. *et al.,* Eds, Stockton Press, New York.

Lindstedt, S.L., Calder, W.A., 1981, Body size and physiological time and longevity of homeothermic animals. Quart. Rev. Biol. 56:1-16.

Lu, F.C., 1985, Safety assessments of chemicals with threshold effects, Reg. Toxicol. Pharmacol. 5:460-464.

Luenberger, D.G., 1979, Introduction to Systems Dynamics, Wiley, New York.

Moore, B.,1909, The relationship of dosage of a drug to the size of the animal treated, especially in regard to the cause of the failures to cure trypanosomiasis, and other protozoan. Diseases in man and in large animals, Biochem. J. 4:323-330.

Mordenti, J., 1986a, Man vs beast: toxicokinetic scaling in mammals, J. Pharma. Sci. 75:1028-1040.

Mordenti, J., 1986b, Toxicokinetic scale-up: accurate prediction of human toxicokinetic profiles from animal data, J. Pharmacol. Sci. 74:1047-1099.

Mordenti, J., 1986c, Dosage regimen design for pharmaceutical studies conducted in animals, J. Pharm. Sci. 75:852-857.

NAS, National Academy of Sciences, 1977, Drinking water and health, Vol 1, Washington, D.C.

NRC, National Research Council, 1980, Problems in risk estimation, p. 25-65, in Drinking water and Health Vol. 3, Washington, DC National Academy Press.

NRC, National Research Council 1983, Risk assessment in the Federal Government: Managing the process, National Academy Press, Washington, D.C.

NRC, National Research Council, 1986, Drinking water and health, vol. 6, Washington, D.C., National Academy Press.

Perl, W.,1972, An extension of the diffusion equation to include clearance by capillary blood flow, In "Multicompartment analysis of tracer experiments" Whipple, H. E., Ed., 108:92-105, New York Academy of Sciences.

Pinkel, D., 1958, The use of body surface area as a criterion of drug dosage in cancer chemotherapy, Cancer Res. 18: 853-856.

Renwick, A.G., 1991, Safety factors and establishment of acceptable daily intakes, Food Addit. Contamin. 8:135-150.

Renwick, A.G., 1993, Data-derived safety factors for the evaluation of food additives and environmental contaminants, Food Addit. Contamin. 10:275-305.

Rubner, M.,1883, Ueber den Einfluss der Korpergross auf Stoffund Kraftwechsel, Z. Biol. 19:535-562.

Schmidt-Nielsen, K., 1984, Scaling: Why is animal size so important? Cambridge University Press, London.

Schlesinger, R.B., 1985, Comparative deposition of inhaled aerosols in experimental animals and humans: a review, J. Toxicol. Environ. Health 15:197-214.

Shearer, J.L., Murphy, A.T., Richardson, H.H., 1967, Introduction to Systems Dynamics, Addison Wesley, Reading, MA.

Stahl, W.R. ,1967, Scaling of respiratory variables in mammals, J. Appl. Physiol. 48:1038-1042.

Travis, C.C., White, R.K., Ward, R.C., 1990, Interspecies extrapolation of toxicokinetics, J.Theor. Biol.142:285-304.

USEPA, 1985, Principles of risk assessment: a nontechnical review. Environ Corporation.

USEPA, 1989, Interim methods for development of inhalation doses. EPA/600/ 888/066F.

USEPA, 1991, Guidelines for developmental toxicity risk assessment; Notice. Fed. Reg. 56, 63798-63826.

Vocci, F., Farber, T., 1988, Extrapolation of animal toxicity data to man, Regul. Toxicol. Pharmacol. 8:389-398.

ADDENDUM

Autres publications du candidat durant sa formation doctorale

Pelekis, M., and Krishnan, K. (1997). Assessing the relevance of rodent data on chemical interactions for health risk assessment purposes : A case study with dichloromethane-toluene mixture. *Regulatory Toxicology and Pharmacology* **25 :** 79-86.

Haddad, S., Pelekis, M., and Krishnan, K. (1996). A methodology for solving physiologically based pharmacokinetic models without the use of simulation softwares. *Toxicology Letters* **85**: 113-126.

Krishnan, K., and Pelekis, M., (1997). Hematotoxic interactions: occurrence, mechanisms and predictability. *Toxicology* **105**: 355-364.

Krishnan, K., Haddad, S., and Pelekis, M., (1997). A simple index for representing the discrepancy between simulations of physiological pharmacokinetic models and experimental data. *Toxicology and Industrial Health* **11**: 413-421.